Immunosuppression in breast cancer: a closer look at regulatory T cells

Kos, K.

Immunosuppression in breast cancer

A closer look at regulatory T cells

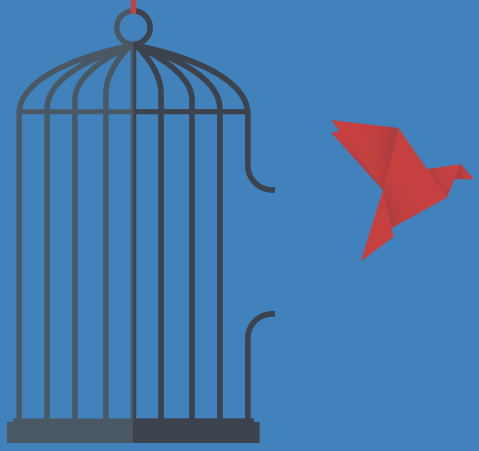

Kevin Kos

Immunosuppression in breast cancer:

a closer look at regulatory T cells

Kevin Kos

About the cover:
Immunosuppressive signals coming from the tumor microenvironment arrest successful anti-cancer immunity. Work in this thesis aims to understand how we can "break free" from specific components of tumor-associated immunosuppression to improve cancer treatment. This concept of "Breaking free" is illustrated on the cover, inspired by my passion for birds.

Cover concept: MaDedee & Kevin Kos
Layout: Ilse Modder, www.ilsemodder.nl
Printing: GildePrint Enschede, www.gildeprint.nl
ISBN: 978-94-6419-654-2

The research described in this thesis was performed at the division of Tumor biology and Immunology at the Netherlands Cancer Institute – Antoni van Leeuwenhoek hospital (NKI-AvL). The research was financially supported by the NWO Diamond Grant, KWF, and Oncode Institute. The printing of this thesis was financially supported by the NKI-AVL.

Immunosuppression in breast cancer:
a closer look at regulatory T cells

Proefschrift

ter verkrijging van
de graad van doctor aan de Universiteit Leiden,
op gezag van rector magnificus prof. dr. ir. H. Bijl,
volgens besluit van het college voor promoties
te verdedigen op woensdag 11 januari 2023
klokke 13:45 uur

door

Kevin Kos
geboren te Blaricum
in 1993

Promotor: Prof. Dr. K. E. de Visser
Co-promotor: Prof. Dr. J.G. Borst

Leden Promotiecommissie:
Prof. Dr. F. A. Ossendorp
Prof. Dr. S. H. van der Burg
Prof. Dr. M. Yazdanbakhsh
Prof. Dr. T. D. de Gruijl (Amsterdam UMC, location VUmc)
Dr. L. Akkari (Netherlands Cancer Institute)

TABLE OF CONTENTS

1

General introduction & Scope of the thesis

The mechanisms of mutation and selection that have driven the breath-taking diversity of multi-cellular life present an inherent danger to an individual: the development of cancer. This risk is particularly inflated in our species, as we are able to live far beyond our reproductive age[1]. As we age past our reproductive years, evolutionary investments in tumor suppression wane, and when combined with the accumulation of oncogenic mutations throughout our lives, the stage is set for malignant cell growth to occur. These fast growing, resilient, expansionistic cells, when left uncontrolled, give rise to a cellular mass that ultimately spreads throughout the body, asphyxiates healthy tissue and perturbs vital physiological systems. The magnitude of this problem is best illustrated in numbers, with nearly 10 million reported cancer-related deaths annually worldwide[2].

These cellular masses, or tumors, are highly heterogeneous. Besides cancer cells, tumors consist of a wide variety of non-malignant host cells that are densely packed in a framework of extracellular matrix, collectively known as the tumor microenvironment (TME). Within the TME, cells continuously interact with each other through direct- or indirect cellular crosstalk governed by receptor-ligand interactions, and paracrine molecules like cytokines, chemokines and extracellular vesicles. A rich variety of cell types is found in the TME including stromal-, endothelial- and immune cells, which can be further classified in numerous subsets. While cancer cells have the malignant, viral-like nature of replicating *ad infinitum* at expense of their host, the function of non-cancerous cells in the TME is ambiguous and plastic. The behaviour of an intratumoral non-cancerous cell is simultaneously dictated by many factors like cancer stage[3], anatomical location of the tumor[3], composition and molecular cues of the environment[4], genetic make-up of the malignant cells[5] and treatment status[6]. With this level of complexity it becomes clear that each tumor is unique, and that the cell types therein are not fixed into a certain state, but are continuously adapting to their chaotic environment. This has important implications for tumor development as a whole, as many cells in the TME can have both tumor-limiting, and tumor-promoting effects, depending on the context[7].

The dogma that cancer is not solely a result of alterations in oncogenes and tumor suppressor genes has only begun to shift in the past decades, due to studies that showed the importance of components from the TME for tumor initiation, progression, metastasis and therapy response[8]. Particularly the observation that tumors are infiltrated by virtually any immune cell subset[9–11] has slowly sparked an interest to understand the role of immune cells in cancer progression. Today, we are aware of the paradoxical relationship that our immune system has with cancer. On one hand, chronic inflammation and the associated endless cycle of cell death and repair is a major driver of carcinogenesis[12,13]. On the other hand, our immune system can be employed as a means to combat cancer. This idea is stooled on the basis that the immune system has evolved to deal with external threats that compromise tissue function and homeostasis. To tell friend from foe, several detection mechanisms are in place that can recognise threats of foreign nature. This can, amongst

others, be mediated by recognition of pathogen-derived immunogenic antigens, pathogen- and damage-associated molecules, or loss of antigen presentation machinery on host cells. Detection of these "red flags" enables the elimination of threats of pathogenic nature like viruses, bacteria and parasites, but similarly licenses the eradication of cancer cells that have acquired these abnormal features, by cytotoxic cells like $CD8^+$ T cells and NK cells, that have been properly educated and activated to do so.

Mounting a tumor-specific immune responses is not trivial, and requires an intricate interaction between both innate and adaptive arms of the immune system. In general, the process starts with the uptake of tumor-associated antigens by dendritic cells in the TME, which upon maturation, carry their load to nearby lymph nodes. There, dendritic cells process and present the cognate antigen to naïve $CD4^+$ T cells which, upon successful priming, activation and differentiation, further orchestrate the induction of tumor-specific effector programs. Under ideal circumstances, this drives the influx of activated anti-tumoral immune cells into tumors, which either directly engage in tumor cell killing through release of cytotoxic molecules and engagement of death receptors, or create supportive pro-inflammatory conditions that facilitate anti-tumoral polarization of myeloid cells. Excitingly, the development of immunotherapeutics aimed at removing important brakes that limit anti-tumor immunity has led to never-before-seen response rates in cancer types that are traditionally difficult to treat like melanoma, lung, and hereditary colorectal cancers[14–16], thereby demonstrating the potential of engaging the immune system for cancer treatment.

In reality, an effective anti-tumor immune response can be impaired in any of its stages[17]. One obvious bottleneck relates to the fact that cancers are in essence not consisting of foreign cells, resulting in limited recognition of tumor antigens as "non-self", and thus poor priming and recruitment of T cells[18]. In fact, this is amplified by the removal of highly immunogenic cancer clones during early tumorigenesis in a process called immunoediting, which drives the propagation of sub-clones that are "invisible" to immune recognition[19]. Tumors that have high mutational burden due to external mutagenic factors, such as melanomas and non-small cell lung cancers[20], can have high levels of tumor-specific neo-antigens, which correlate to immunotherapy response[21,22]. However, having high mutational burden is not unequivocally related to T cell infiltration[23], or immunotherapy response[24], suggesting additional mechanisms exist that affect the capacity of the immune system to eradicate malignancies. One such crucial mechanism is tumor-associated immunosuppression. Immunosuppression is an essential component of an organism in homeostasis, and has evolved to tightly regulate immune activation[25]. This is essential to prevent deleterious (auto)immune reactions to harmless self- and environmental antigens, to restrain excessive immune activation during infection, and to resolve inflammatory conditions after pathogen clearance.

Intriguingly, tumors are able to hijack immunoregulatory mechanisms to their own benefit to undermine anti-tumor immunity, highlighting the duality of the immune system in cancer. Through cancer-cell induced co-option of anti-inflammatory stromal- and immune cells that abundantly accumulate in the TME, multiple overlapping mechanisms of suppression can be stacked. This typically occurs in the chronically inflamed context of the TME, as the immune system fails to resolve the cancer[7,13]. Chronically stimulated immune cells produce molecules like IL-10, TGF-β, adenosine, iNOS and IL-6 which, although pleiotropic, contribute to an immunosuppressive environment that is characterized by tissue repair, regeneration, and exclusion and inhibition of cytotoxic cells, instead of effector cell activation and cancer cell killing. Furthermore, co-inhibitory ligands like PD-L1 become widely expressed in the TME, which further stall T cell activation and function[26]. Finally, the TME can become even more hostile to infiltrated effector cells through changes in the availability of nutrients and growth factors[27], increased acidity[28], hypoxia[29], and release of radical oxygen species[30]. Combined, this heavily compromises the efficacy of anti-cancer immunity, leading the immune system to completely lose its grasp on tumor development.

The dual role of the immune system in cancer progression is not limited to the local tumor site, but is also intertwined with the final and most deadly stage of cancer; its spread to distant sites in a process known as metastasis. As invasive cancer cells enter surrounding tissue and circulation, those with high immunogenicity have been shown to be eradicated by extrinsic immune pressure in an effort to limit metastatic disease[31]. However, this pressure likely shapes the evolution of poorly immunogenic variants, which disseminate to distant sites[31]. In addition, it is becoming increasingly clear that cancer cells do not take the metastatic journey alone, but succeed in corrupting immunoregulatory mechanisms to increase their chances of successful colonisation of distant organs[32]. The chronically inflamed conditions within the primary tumor resonate throughout the host, leading to systemic mobilisation of immunosuppressive myeloid cells that confer protection against elimination by tumor-specific effector cells[33,34]. Furthermore, tumor-associated factors have been shown to instruct immune cells in distant organs to “prepare” a permissive niche prior to cancer cell arrival[32,35]. Even tumor-draining lymph nodes, the strongholds of effector cell activation, can become severely immunosuppressed during tumor progression[36,37].

The mechanisms underlying systemic immunosuppression and the formation of a (pre-) metastatic niche are only beginning to be understood, in particular how the adaptive immune system is involved in these processes. Furthermore, it is currently unclear how systemic immunosuppression impacts organ-specific metastasis. Ultimately, improved understanding of these mechanisms is critical to devise novel treatment strategies for patients with metastatic cancer. To acquire this fundamental knowledge, genetically engineered mouse models (GEMMs) are an important tool to dissect the complex immunoregulatory mechanisms at play during metastasis formation. Importantly, these models can reflect

crucial aspects of human primary tumor development and the metastatic cascade, including tissue-tropism of metastasis, heterogeneity within the primary tumor, and the chronic and systemic inflammation that underlies *de novo* tumor development and progression[38,39].

SCOPE OF THE THESIS

Although astonishingly complex and intriguing at a cellular level, the manifestation of cancer imposes an enormous burden on patients, their families, and society as a whole. This results in severe physical and emotional distress, reduced quality of life, premature death and large economic costs. With 2,261,419 cases diagnosed worldwide in 2020, breast cancer is the most common form of cancer across both sexes, despite over 99% of cases occurring in women[40]. These data illustrate the Herculean task laid out in the field of oncology to be tackled, and provides the context in which the work in this thesis was performed. However, by standing on the shoulders of giants, our current understanding on the pathogenesis of breast cancer has massively increased over time. In stark contrast to the Egyptian medical writer Imhotep (~2600 BC) who, while describing the first documented case of breast cancer, noted that no therapy could be offered[41], we are currently amidst a revolution in the development of immunotherapeutic approaches. To fully harness the potential of these novel immunomodulatory drugs, it is essential to increase our understanding of immunoregulatory mechanisms at play in breast cancer, in particular in the context of metastasis. This thesis aims to provide further mechanistic insight into the role of a key regulator of immunosuppression: the FOXP3$^+$CD4$^+$ regulatory T cell (T_{reg}). While essential for maintaining immune homeostasis and tolerance[42], this adaptive immune cell has emerged as a valuable asset for malignant cell growth, through suppression of anti-tumor immunity[43,44]. However, it is largely unclear exactly how, when, and where T_{regs} contribute to the formation of metastases. Using GEMMs for primary- and metastatic breast cancer[45,46], the work in this thesis describes how tumors succeed in corrupting T_{regs} for their own benefit, and provides more details into the intricate relationship that T_{regs} hold with the TME, metastasis, and immunotherapy response.

In **chapter 2**, I introduce the biology of T_{regs} in the context of breast cancer, and review exciting clinical advancements that have improved the prognostic and predictive value of T_{regs} in breast cancer, and the therapeutic potential of targeting these cells. I propose that the use of GEMMs that closely mimic the diversity and stepwise progression of human breast cancer subtypes is necessary to propel our understanding of T_{reg} biology to a higher level and to deepen our knowledge of underlying mechanisms, which is important to take full advantage of novel immunomodulatory drugs that may take the stage in breast cancer treatment.

CD4$^+$ T cells are plastic cells that respond to environmental cues by adapting their gene expression and function to local tissue environments. In **chapter 3** we describe how tumors

exploit this feature to increase the intratumoral accumulation of immunosuppressive T_{regs}, with the help of tumor-associated macrophages (TAMs). By characterizing the cellular crosstalk between TAMs and $CD4^+$ T cells in spontaneous mammary tumors, we show that TAMs can drive the conversion of conventional $CD4^+$ T cells into T_{regs}. Mechanistic studies reveal that this is mediated via two distinct mechanisms. TAMs can drive T_{reg} conversion directly via production of TGF-β, but can also prepare conventional $CD4^+$ T cells for conversion through regulation of PD-1 expression.

Ever since their discovery, T_{regs} have been in the crosshair of cancer immunology research, and a great effort has been made to characterize the function of T_{regs} inside primary tumors and metastases. However, recent studies implicate that in particular T_{regs} in blood and lymph nodes of breast cancer patients may have important clinical value. In line with this notion, in **chapter 4**, we move the scope from T_{regs} in primary tumors, to those in distant organs of tumor-bearing hosts. Through extensive characterization of these cells we discovered that T_{regs} expand systemically and undergo tissue-specific phenotypic and functional alterations during primary mammary tumorigenesis. This elicits a tissue-specific effect on metastasis formation, as neoadjuvant targeting of T_{regs} using an Fc-optimized anti-CD25 antibody reduces cancer spread to axillary LNs, but not to the lungs. Mechanistically, we found that T_{regs} suppress the anti-metastatic potential of NK cells specifically in the lymph node niche. **Chapter 4** provides evidence that tissue-specific mechanisms of immunosuppression are instrumental in shaping organotropism of metastases. **Chapter 5** highlights this concept from the angle of another key player in immunosuppression: neutrophils. I discuss a mechanism by which breast cancer cells co-opt neutrophils to enhance neutrophil extracellular trap formation specifically in the lungs, thereby increasing lung metastasis.

Immune checkpoint blockade (ICB) like anti-PD1 and anti-CTLA4 provide important tools to boost T cell activation, and are increasingly used in the context of cancer to overcome immunosuppression and to induce anti-tumor immune responses. However, T_{regs} themselves can express high levels of PD-1 and CTLA4, posing the central question of **chapter 6**: how does checkpoint inhibition affect T_{regs}? By performing intervention studies with combinations of ICB and T_{reg} depletion in preclinical mouse models, we demonstrate that ICB induces systemic activation and proliferation of T_{regs}, but not conventional T cells. Depletion of ICB-activated T_{regs} unleashes strong immune activation in blood, and improves the response to immunotherapy in a model for metastatic breast cancer, that is otherwise unresponsive to ICB. This chapter proposes that T_{regs} should be more prominently considered when using therapeutic approaches that modulate T cell function.

As is evident from work in this thesis, functional analyses are helpful to fully uncover the role of T_{regs} in cancer. In **chapter 7** we describe the details of a standardized method for assessing the immunosuppressive potential of freshly isolated T_{regs} from tumors and lymphoid tissue,

which has been used in **chapter 3**, **4** and **6**.

Finally, the theoretical and clinical implications of the findings in this thesis are discussed in in context of current literature in **chapter 8**.

REFERENCES

1. Casás-Selves, M. & Degregori, J. How cancer shapes evolution, and how evolution shapes cancer. *Evolution (N. Y).* **4**, 624 (2011).
2. Global Cancer Observatory. https://gco.iarc.fr/.
3. Thorsson, V. *et al.* The Immune Landscape of Cancer. *Immunity* **48**, 812 (2018).
4. Wu, S. Z. *et al.* A single-cell and spatially resolved atlas of human breast cancers. *Nat. Genet.* **53**, 1334–1347 (2021).
5. Wellenstein, M. D. & de Visser, K. E. Cancer-Cell-Intrinsic Mechanisms Shaping the Tumor Immune Landscape. *Immunity* **48**, 399–416 (2018).
6. Benavente, S., Sánchez-García, A., Naches, S., LLeonart, M. E. & Lorente, J. Therapy-Induced Modulation of the Tumor Microenvironment: New Opportunities for Cancer Therapies. *Front. Oncol.* **10**, 2169 (2020).
7. Garner, H. & de Visser, K. E. Immune crosstalk in cancer progression and metastatic spread: a complex conversation. *Nat. Rev. Immunol.* 1–15 (2020) doi:10.1038/s41577-019-0271-z.
8. Witz, I. P. The Tumor Microenvironment: The Making of a Paradigm. *Cancer Microenviron.* **2**, 9 (2009).
9. Hersh, E. M., Mavligit, G. M., Gutterman, J. U. & Barsales, P. B. Mononuclear cell content of human solid tumors. *Med. Pediatr. Oncol.* **2**, 1–9 (1976).
10. Vose, B. M., Vánky, F., Argov, S. & Klein, E. Natural cytotoxicity in man: activity of lymph node and tumor-infiltrating lymphocytes. *Eur. J. Immunol.* **7**, 753–757 (1977).
11. Brubaker, D. B. & Whiteside, T. L. Localization of human T lymphocytes in tissue sections by a rosetting technique. *Am. J. Pathol.* **88**, 323 (1977).
12. De Visser, K. E., Eichten, A. & Coussens, L. M. Paradoxical roles of the immune system during cancer development. *Nature Reviews Cancer* vol. 6 24–37 (2006).
13. Shalapour, S. & Karin, M. Pas de Deux: Control of Anti-tumor Immunity by Cancer-Associated Inflammation. *Immunity* **51**, 15–26 (2019).
14. Blank, C. U. *et al.* Neoadjuvant versus adjuvant ipilimumab plus nivolumab in macroscopic stage III melanoma. *Nature Medicine* vol. 24 1655–1661 (2018).
15. Forde, P. M. *et al.* Neoadjuvant PD-1 blockade in resectable lung cancer. *N. Engl. J. Med.* **378**, 1976–1986 (2018).
16. Chalabi, M. *et al.* Neoadjuvant immunotherapy leads to pathological responses in MMR-proficient and MMR-deficient early-stage colon cancers. *Nat. Med. 2020 264* **26**, 566–576 (2020).
17. Chen, D. S. & Mellman, I. Oncology Meets Immunology: The Cancer-Immunity Cycle. *Immunity* **39**, 1–10 (2013).
18. Apavaloaei, A., Hardy, M. P., Thibault, P. & Perreault, C. The Origin and Immune Recognition of Tumor-Specific Antigens. *Cancers (Basel).* **12**, 1–13 (2020).
19. Mittal, D., Gubin, M. M., Schreiber, R. D. & Smyth, M. J. New insights into cancer immunoediting and its three component phases--elimination, equilibrium and escape. *Curr. Opin. Immunol.* **27**, 16–25 (2014).
20. Chalmers, Z. R. *et al.* Analysis of 100,000 human cancer genomes reveals the landscape of tumor mutational burden. *Genome Med.* **9**, 1–14 (2017).
21. Van Allen, E. M. *et al.* Genomic correlates of response to CTLA-4 blockade in metastatic melanoma. *Science (80-.).* **350**, 207–211 (2015).
22. Rizvi, N. A. *et al.* Mutational landscape determines sensitivity to PD-1 blockade in non-small cell lung cancer. *Science (80-.).* **348**, 124–128 (2015).
23. McGrail, D. J. *et al.* Multi-omics analysis reveals neoantigen-independent immune cell infiltration in copy-number driven cancers. *Nat. Commun.* **9**, (2018).
24. McGrail, D. J. *et al.* High tumor mutation burden fails to predict immune checkpoint blockade response across all cancer types. *Ann. Oncol.* **32**, 661–672 (2021).
25. Huntington, N. D., Gray, D. H. & Nicholas Huntington, C. D. Immune homeostasis in health and disease. *Immunol. Cell Biol.* **96**, 451–452 (2018).
26. Binnewies, M. *et al.* Understanding the tumor immune microenvironment (TIME) for effective therapy. *Nat. Med.* **24**, 541–550 (2018).
27. Lim, A. R., Rathmell, W. K. & Rathmell, J. C. The tumor microenvironment as a metabolic barrier to effector T cells and immunotherapy. *Elife* **9**, 1–13 (2020).
28. Wu, H. *et al.* T-cells produce acidic niches in lymph nodes to suppress their own effector functions. *Nat. Commun. 2020 111* **11**, 1–13 (2020).
29. Barsoum, I. B., Smallwood, C. A., Siemens, D. R. & Graham, C. H. A mechanism of hypoxia-mediated escape from adaptive immunity in cancer cells. *Cancer Res.* **74**, 665–674 (2014).
30. Weinberg, F., Ramnath, N. & Nagrath, D. Reactive Oxygen Species in the Tumor Microenvironment: An Overview. *Cancers (Basel).* **11**, (2019).
31. Angelova, M. *et al.* Evolution of Metastases in Space and Time under Immune Selection. *Cell* **175**, 751-765.e16 (2018).

32. Kitamura, T., Qian, B. Z. & Pollard, J. W. Immune cell promotion of metastasis. *Nat. Rev. Immunol.* **15**, 73–86 (2015).
33. Coffelt, S. B. *et al.* IL-17-producing γδ T cells and neutrophils conspire to promote breast cancer metastasis. *Nature* **522**, 345–348 (2015).
34. Wellenstein, M. D. *et al.* Loss of p53 triggers WNT-dependent systemic inflammation to drive breast cancer metastasis. *Nature* **572**, 538–542 (2019).
35. Doglioni, G., Parik, S. & Fendt, S. M. Interactions in the (pre)metastatic niche support metastasis formation. *Front. Oncol.* **9**, 219 (2019).
36. van Pul, K. M. *et al.* Selectively hampered activation of lymph node-resident dendritic cells precedes profound T cell suppression and metastatic spread in the breast cancer sentinel lymph node. *J. Immunother. Cancer* **7**, 133 (2019).
37. Rotman, J., Koster, B. D., Jordanova, E. S., Heeren, A. M. & de Gruijl, T. D. Unlocking the therapeutic potential of primary tumor-draining lymph nodes. *Cancer Immunol. Immunother.* **68**, 1681 (2019).
38. Gómez-Cuadrado, L., Tracey, N., Ma, R., Qian, B. & Brunton, V. G. Mouse models of metastasis: progress and prospects. *Dis. Model. Mech.* **10**, 1061–1074 (2017).
39. Kersten, K., de Visser, K. E., van Miltenburg, M. H. & Jonkers, J. Genetically engineered mouse models in oncology research and cancer medicine. *EMBO Mol. Med.* **9**, 137–153 (2017).
40. Ferlay, J. *et al.* Estimating the global cancer incidence and mortality in 2018: GLOBOCAN sources and methods. *Int. J. Cancer* **144**, 1941–1953 (2019).
41. Mukherjee, S. *The Emperor of All Maladies: A Biography of Cancer*. (Schribner, 2010).
42. Kim, J. M., Rasmussen, J. P. & Rudensky, A. Y. Regulatory T cells prevent catastrophic autoimmunity throughout the lifespan of mice. *Nat. Immunol.* **8**, 191–7 (2007).
43. Plitas, G. & Rudensky, A. Y. Regulatory T Cells in Cancer. *Annu. Rev. Cancer Biol.* **4**, 459–477 (2020).
44. Kos, K. & de Visser, K. E. The Multifaceted Role of Regulatory T Cells in Breast Cancer. *Annu. Rev. Cancer Biol.* **5**, (2021).
45. Derksen, P. W. B. *et al.* Somatic inactivation of E-cadherin and p53 in mice leads to metastatic lobular mammary carcinoma through induction of anoikis resistance and angiogenesis. *Cancer Cell* **10**, 437–449 (2006).
46. Doornebal, C. W. *et al.* A Preclinical Mouse Model of Invasive Lobular Breast Cancer Metastasis. *Cancer Res.* **73**, 353 LP – 363 (2013).

2

The multifaceted role of regulatory T cells in breast cancer

Kevin Kos[1] & Karin E. de Visser[1]

Affiliations
[1] Division of Tumor Biology & Immunology, Oncode Institute, Netherlands Cancer Institute, Amsterdam, The Netherlands

Annual Review of Cancer Biology. 2020*,* 5:291-310

ABSTRACT

The microenvironment of breast cancer hosts a dynamic cross-talk between diverse players of the immune system. While cytotoxic immune cells are equipped to control tumor growth and metastasis, tumor-corrupted immunosuppressive immune cells strive to impair effective immunity and promote tumor progression. Of these, T_{regs}, the gatekeepers of immune homeostasis, emerge as multifaceted players involved in breast cancer. Intriguingly, clinical observations suggest that blood and intratumoral T_{regs} can have strong prognostic value, dictated by breast cancer subtype. In line, emerging preclinical evidence shows that T_{regs} occupy a central role in breast cancer initiation and progression, and provide critical support to metastasis formation. Here, T_{regs} are not only important for immune escape, but also promote tumor progression independent of their immune regulatory capacity. Combining insights into T_{reg} biology with advances made across the rapidly growing field of immuno-oncology is expected to set the stage for the design of more effective immunotherapy strategies.

THE IMMUNE SYSTEM: A DOUBLE-EDGED SWORD IN CANCER

Tumors are complex entities consisting of not just cancer cells, but also a variety of non-malignant cell types. The local niche in and surrounding tumors is collectively described as the tumor microenvironment (TME), which can profoundly impact the development and progression of cancer[1–3]. It is now clear that the TME is not a static element of tumors, but its composition and functional state is highly diverse between cancer types, subtypes, and even individual tumors. In the past decades, particularly the immunological component of the TME has been studied extensively, with a focus on answering the central question: how can tumors develop in the context of a functional immune system? Addressing this fundamental question is essential to fully exploit the immune system for the treatment of cancer.

Breast cancer is perhaps one of the most studied cancer types in the context of the TME. Although survival rates for breast cancer patients are steadily increasing, it is still the leading cause of cancer-related deaths in women worldwide[4,5]. The vast majority of breast cancer-related mortality is due to the incurable metastatic stage of the disease. Clearly, understanding, preventing and treating metastatic breast cancer is an unmet need. As such, mechanistic insights into the complex interactions of key players in the TME could pave the way for novel innovative treatments and improved patient stratification.

Clinical studies have exposed a dual role of the immune system in breast cancer. For example, tumor-associated macrophages (TAMs) are associated with invasion, metastasis and a worse prognosis[6], while tumor infiltrating lymphocytes (TILs) are associated with a favorable prognosis[7]. To understand this duality, it is important to realise that cancers host a plethora of immune cell subsets, such as lymphocytes, various myeloid cells and innate lymphoid cells to which both pro- and anti-tumorigenic functions have been attributed[2]. Although immune cells such as $CD8^+$ T cells and NK cells have the molecular gear to recognize and eradicate malignant cells, they often encounter a highly immunosuppressive environment in tumors which blunts effective anti-tumor immunity. This milieu is characterized by widespread expression of immune checkpoint receptors, inhibitory cytokines, hypoxia and low levels of nutrients, all of which restrain the recruitment and function of cytotoxic immune cells[8]. Importantly, lymphocytes and tumor-associated myeloid cells including macrophages, neutrophils and monocytes profoundly contribute to the creation of this immune suppressive environment as well as to systemic immunosuppression that often accompanies primary tumor growth and which further potentiates cancer progression by facilitating immune escape[3].

A key orchestrator of immunosuppression is the $CD4^+$ regulatory T cell (T_{reg}), which has since its discovery been in the crosshairs of cancer immunology research[9,10]. T_{regs} can be abundantly

present in primary breast tumors and metastases[11]. Still, their exact impact and relevance to breast cancer progression has proven challenging to uncover, due to the complexities of immune cell cross-talk and metastatic disease. Recently, fundamental and preclinical research has provided exciting new insights into the biology of T_{regs} in breast cancer. This comes at an important time, as initial results of immune checkpoint inhibitors in breast cancer have been relatively disappointing[12]. The expanding use of these drugs for the treatment of breast cancer therefore necessitates a comprehensive understanding of immunosuppressive T_{regs}; are we pulling the right strings? In this review, we will therefore explore and discuss the current knowledge, challenges and clinical use of T_{regs} in breast cancer.

REGULATORY T CELLS: GATEKEEPERS OF IMMUNE HOMEOSTASIS

The immune system is a sophisticated defense network, evolved to withstand innumerable pathogenic challenges at any anatomical location. To do so, complex cellular interactions coordinate pathogen recognition, immune cell activation and the execution of effector programs. In order to return to, or maintain homeostasis, immunosuppressive signals are essential to dampen immune responses to prevent pathological immune responses such as chronic inflammation or auto-immunity. A key cell type involved in this process is the T_{reg}. The importance of T_{regs} in immune tolerance has become evident through characterization of so-called “scurfy mice” that suffer from a severe lethal auto-immune syndrome, characterized by inflamed skin, red eyes, enlarged lymphoid organs and early death[13]. Scurfy mice were first reported in 1949, but it was not until the early 2000’s that a mutation in the *Foxp3* gene, and consequential loss of T_{regs}, was identified as a direct cause for the severe immune pathology[14]. Further research showed that FOXP3 is the master transcription factor for the previously identified specialized immunosuppressive $CD4^+$ $CD25^+$ T lymphocytes, now known as T_{regs}[15,16]. Since then, it has become clear that reduced T_{regs} numbers and/or impaired T_{reg} functionality stands at the basis of autoimmune and inflammatory diseases, such as diabetes, multiple sclerosis and inflammatory bowel disease[17,18]. In contrast, their activation and accumulation in tumors is considered detrimental, as we will explore in depth.

T_{regs} utilize several strategies to antagonize both adaptive and innate immunity. Among these, the release of immunosuppressive mediators as IL-10, TGF-β and adenosine, and high expression of immunomodulatory receptors as CTLA-4, PD-L1 and LAG-3 are well established aspects of T_{reg} functionality which can interfere with the propagation of immune responses[9,19,20]. Scavenging of IL-2 from the environment and killing of effector T cells by the release of granzymes additionally contributes to immunosuppression[21,22]. Combined, these mechanisms can be employed to restrain dendritic cell (DC) function, or directly inhibit cytotoxic cells[21]. The exact effector program that is engaged is highly dependent on the tissue

and nature of the immune response[19,23]. Emerging evidence shows that T_{regs} can acquire expression of T_{helper} subset transcription factors (TFs), such as T-bet, GATA3 and RORγT which directs their function towards suppression of T_{helper} cells of that particular subset[19,23]. For example, T_{regs} expressing the Th1 TF T-bet are important for suppressing Th1 mediated inflammation, but cannot suppress Th2 or Th17 responses[24].

Two flavors of FOXP3$^+$ T_{regs}

In vivo*,* two distinct populations of FOXP3$^+$ T_{regs} are defined, based on their ontogeny and stability: thymically developed (natural) T_{regs} and extrathymically developed (peripheral or induced) T_{regs}. Thymic T_{regs} (tT_{regs}) represent a dedicated lineage with stable expression of FOXP3 and affinity for self-antigen. The generation of tT_{regs} occurs through a unique developmental program in the thymus, based on a delicate balance of T cell receptor (TCR) affinity and antigen specificity of CD4$^+$ progenitor cells[25–27]. Through this program, tT_{regs} are equipped with T cell receptors biased towards recognition of tissue restricted self-antigens, which enables the suppression of immune responses directed towards host peptides upon activation via their TCR[28–30].

Unlike tT_{regs}, peripheral T_{regs} (pT_{regs}) are extrathymically generated in the periphery from non-regulatory FOXP3$^-$ CD4$^+$ T cells. A crucial element of pT_{reg} differentiation is its dependence on TGF-β signalling, which in FOXP3$^-$ CD4$^+$ T cells, induces the interaction of SMAD2/3 with an intronic enhancer in the *Foxp3* locus, CNS1[31–33]. pT_{regs} have unstable FOXP3 expression, and miss the characteristic demethylation of the intronic element CNS2 observed in tT_{regs}, which is essential for T_{reg} stability during proliferation[31,34]. In addition, pT_{regs} display a TCR repertoire that recognizes foreign antigens, parallel to conventional CD4$^+$ T cells[35]. As such, pT_{regs} have been found to play important roles at barrier sites, including the gut, lungs and placenta to mitigate inflammatory responses in response to foreign, but harmless, environmental, dietary and microbial antigens[36–39].

The specific contributions of either tT_{regs} or pT_{regs} in cancer remain elusive, as to date no genuine phenotypic or functional marker has been discovered to distinguish both T_{reg} subtypes in vivo[40]. Instead, the ontogeny of T_{regs} in human cancer samples can be assessed ex vivo either via TCR repertoire sequencing, or via epigenetic analysis of the CNS2 element in the *Foxp3* gene, which is demethylated in tT_{regs}, but mostly methylated in pT_{regs}. As most studies on T_{regs} do not distinguish between tT_{regs} or pT_{regs}, we will refer to these cells as T_{regs}, unless stated otherwise.

Now, nearly two decades after their discovery, the extent of T_{reg} functionality appears astonishingly diverse. T_{regs} play critical roles in tissue regeneration and repair, intestinal regulation of the microbiome, hair morphogenesis, metabolic homeostasis, pregnancy and cancer[19,41]. However, it is less clear which mechanisms are engaged in the context of breast

cancer progression and metastasis. Therefore, we will first review the current clinical literature; what evidence exists that forms the basis for their clinical relevance in breast cancer?

CLINICAL SIGNIFICANCE OF T_{REGS} IN BREAST CANCER

The discovery in 2001 that $CD4^+$ $CD25^+$ immunosuppressive cells can be found in the blood of healthy individuals[42] kick-started research into the presence and behavior of these cells in cancer patients. In the following years, it was reported that $CD4^+$ $CD25^+$ T cells are increased in blood and tumors of patients with a variety of cancers, including breast-, pancreatic-, ovarian- and non-small cell lung cancer[43]. However, as CD25 expression is not restricted to T_{regs}, but can also be expressed by effector T cells, it was not until the discovery of FOXP3 as a unique marker of T_{regs}[15,16] and the development of reliable monoclonal antibodies that the presence of T_{regs} could be convincingly demonstrated in human cancers[44,45]. Since then, many studies have investigated the association between the presence of intratumoral T_{regs} and patient survival and therapy response in breast cancer (Table 1).

Despite an extensive body of literature, the clinical significance of T_{regs} in breast cancer remains controversial due to contrasting results between studies (Table 1). A key challenge in interpreting these studies is that the prognostic value of T_{regs} seems to differ per molecular breast cancer subtype. These subtypes are broadly defined on the basis of tumoral expression of the estrogen and progesterone hormone receptors (HR^+), the growth factor receptor HER2, or absence of these (triple-negative breast cancer, TNBC)[4]. Several meta-analyses published over the last few years showed that high FOXP3 TILs in HR^+ breast tumors correlate with poor survival, high grade and lymph node involvement[46–48]. However, multivariate Cox regression on patient outcome including adjustment for tumor size, grade and lymph node stage revealed that FOXP3 TILs are not an independent prognostic factor in HR^+ breast tumors[49,50]. Whether T_{regs} are causally involved in the differentiation of high grade tumors, lymph node metastasis and poor prognosis cannot be concluded from these descriptive analyses. In contrast to HR^+ breast cancer, FOXP3 TILs strongly correlate with a favorable prognosis in HR^- and TNBC subtypes[46,49,51,52]. Here, T_{reg} infiltration is strongly associated with high $CD8^+$- and T_{helper} cell infiltration, perhaps reflecting a T cell permissive environment[53]. This is further supported by the observation that T_{regs} are not associated with prognosis in triple-negative tumors with low CD8 infiltration[51]. In conclusion, T_{regs} correlate with disease outcome, in a subtype dependent manner, but future preclinical research is necessary to uncover the mechanistic link between T_{regs} and breast cancer subtypes.

TABLE 1. Prognostic significance of FOXP3 TILs across breast cancer subtypes

Subtype analysed	Patients (n)	Correlations with high FOXP3 TILs:			Reference
		Prognosis	Subtype	Clinical features	
DCIS	62	Poor (univariate)	DCIS[d]	ND[e]	(Bates et al. 2006)
ER-	77	No effect	ER-	High grade, LN met+[g]	
ER+	148	Poor (univariate)			
ER-	364	No effect	ER-; HER2+; basal	High grade, LN met+[g], large tumor size	(Mahmoud et al. 2011)
ER+	982	Poor (univariate)[a]			
MIXED	398	Poor (multivariate)	ER-; HER2+;basal	High grade	(Yan et al. 2011)
MIXED	1270	Poor (multivariate)	ER-; PR-; HER2+	High grade	(Liu et al. 2011)
MIXED	72	Poor (univariate)[a]	NS[f]	LN met+ [g], p53+, Ki67+	(Kim et al. 2013)
MIXED	90	Poor (multivariate)	ER-; HER2+	High grade	(Takenaka et al. 2013)
MIXED	90	Poor (univariate)[a]	HER2+	High grade, LN met+[g], large tumor size	(Maeda et al. 2014)
MIXED	498	Poor (univariate)[a]	HER2+; TNBC	High γδ T cell	(Allaoui et al. 2017)
MIXED	118	Poor (univariate)	ND[e]	High grade,LN met+[g], Ki67+, tumor nest	(Peng et al. 2019)
TNBC	86	Favorable (multivariate)	ND[e]	LN met+ [g]	(Lee et al. 2013)
ER- HER2-	175	Favorable (univariate)	NS[f]	High grade, high CD8+, young age	(West et al. 2013)
ER- HER2+		No effect			
ER+	2166	No effect (multivariate)[b]	ER-; HER2+; basal	High grade, LN met+[g], High CD8+, young age	(Liu et al. 2014)
ER- HER2+	250	No effect (multivariate)[c]			
BASAL	330	Favorable (multivariate)			
ER+	554	ND[e]	ER+	ND[e]	(Tsang et al. 2014)
ER- HER2+					
MIXED	218	No effect	ND[e]	High grade, high CD8+, high PD1+	(Sun et al. 2014)
TNBC	101	No effect	ND[e]	High CD8+	(Miyashita et al. 2015)
MIXED	207	No effect	ER-, HER2+; TNBC	High grade, Ki67+	(Papaioannou et al. 2019)

a. not significant in multivariate analysis
b. Poor prognosis in low $CD8^+$ tumors
c. favorable prognosis in high $CD8^+$ tumors
d. compared to normal breast
e. Abbreviation; ND, not determined
f. Abbreviation; NS, not significant differences
g. Abbreviation; LN met+; Lymph node involvement
Table references: [45], [49], [129], [130], [131], [132], [133], [134], [135] [136], [51], [50], [137], [138], [139], [140]

Predictive value of T_{regs} in cancer immunotherapy

Novel therapeutics targeting immune checkpoints as PD-1/PD-L1 and CTLA-4 are transforming the treatment landscape across cancer types[54]. In order to maximize efficacy, numerous studies are currently evaluating predictive biomarkers and novel treatment combinations[55]. Importantly, T_{regs} can be direct targets of these treatments, due to their high expression of immune checkpoint molecules[56]. While the use of immunotherapy in breast cancer is still in its infancy, research in other cancer types has revealed the potential predictive significance of T_{regs} in the context of PD-1/PD-L1 blockade. For example, PD-1 blockade has been associated with disease progression in gastric cancer patients, via the activation and expansion of intratumoral PD-1^+ T_{regs}[57]. Likewise, high intratumoral T_{reg} proliferation in response to anti-PD-1 has been linked to recurrence in melanoma[58]. Finally, PD-L1 mediated expansion of pT_{regs} is an important immune-suppressive axis in glioblastoma[59]. In recent years, the first trials investigating the efficacy of immune checkpoint blockade (ICB) in metastatic TNBC have been published, with a strong focus on PD-1/PD-L1 blockade[12,60–65]. Although clinical benefit is observed for a small proportion (approximately 5-20%) of breast cancer patients, emerging evidence shows that selecting patients based on immune parameters such as a high TIL score and high PD-L1 expression may modestly improve response rates[66]. Up until now, T_{regs} have not been specifically reported to be correlated with efficacy in these early studies. As such, research in the coming years should clarify whether T_{regs} are predictive for PD-1/PD-L1 based treatments in breast cancer.

Qualitative clinical assessment of T_{regs} in breast cancer

Besides quantification of intratumoral T_{regs}, there is a growing body of evidence indicating that a more in-depth qualitative assessment of T_{regs}, including information on phenotype, functional state and immune-cell crosstalk, may be important for disease outcome. For example, recent reports have shown that intratumoral T_{regs} from breast cancer patients display an activated phenotype with high expression of CD25, CTLA-4 and PD-1, and exert immunosuppressive activity[11,67,68]. In one of these studies, the transcriptome of T_{regs} from 105 treatment-naïve breast cancer patients was analysed[67]. The chemokine receptor CCR8 was identified to be uniquely expressed by intratumoral T_{regs}, but not by T_{regs} isolated from breast tissue and blood from healthy donors. CCR8^+ T_{regs} were found to be highly proliferative and enriched in high grade tumors. Strikingly, while intratumoral T_{reg} abundance based on *FOXP3* mRNA expression did not correlate with clinical features, stratifying patients based on the CCR8:*FOXP3* ratio in the tumor strongly correlated with poor survival in patients[67]. These findings illustrate that in-depth analysis of intratumoral T_{regs} provides important information. As the patients in this cohort predominantly had HR^+ tumors (74.3%), an important next step would be to validate these findings in $HER2^+$ and TNBC subtypes, in which T_{regs} are associated with good prognosis[51].

Many studies have reported increased frequencies of T_{regs} in the peripheral blood of breast cancer patients across subtypes[69–73], indicating that breast tumors can systemically engage T_{regs}. Still, their significance has remained elusive for a long time, until a recent report performed in-depth analyses on T_{regs} isolated from the blood and tumors of breast cancer patients[74]. It was found that a subpopulation of T_{regs} (Foxp3^{hi} CD45RA^{neg})[75], comprising approximately 19% of the total T_{reg} population in the peripheral blood of patients strongly resembles intratumoral T_{regs}, based on phenotype, TCR repertoire and CCR8 expression. This may suggest that intratumoral T_{regs} derive from Foxp3^{hi} CD45RA^{neg} T_{regs} in peripheral blood, or *vice versa*. These T_{regs} from blood had superior suppressive potential in vitro, compared to Foxp3^{low} CD45RA$^{pos/neg}$ T_{regs}. Foxp3^{hi} CD45RA^{neg} T_{regs} were found to be heterogeneous between patients in their signaling response to both immunosuppressive and inflammatory cytokines. High T_{reg} responsiveness to immunosuppressive cytokines correlated with poor survival, whereas high responsiveness to inflammatory cytokines had the opposite effect[74]. This exposes the potential clinical significance of T_{regs} in peripheral blood of breast cancer patients, but also highlights how T_{reg} heterogeneity may potentially influence disease outcome.

Over recent years, studies focusing on FOXP3 TILs are moving from basic quantification analyses towards sophisticated in-depth characterization, yielding exciting new insights with prognostic and potential therapeutic implications. As we are starting to discover the characteristics of T_{regs} with tumor-promoting capabilities, mechanistic studies should investigate their functional role in breast cancer progression, and whether their emergence can be therapeutically halted.

THE FUNCTIONAL ROLE OF T_{REGS} IN BREAST CANCER PROGRESSION AND METASTASIS

Preclinical animal models are key to mechanistically understand how T_{regs} impact breast cancer progression. An important tool to dissect T_{reg} function in these models is through their systemic depletion, which can be achieved via two strategies. Firstly, antibody-based approaches deplete T_{regs} through targeting of cell-surface receptors which are highly expressed on T_{regs}, including CD25, GITR and FR4[76–78]. Secondly, the development of transgenic mice that express the diphteria toxin receptor (DTR) under control of *Foxp3* either via direct knock-in (*Foxp3*^{DTR} mice), or by its introduction using a bacterial artificial chromosome (DEREG mice) has allowed for short-term inducible depletion upon injection of diphteria toxin (DT)[79,80]. A transgenic mouse model for mammary tumorigenesis that is regularly used to study the biology of T_{regs} in breast cancer is the MMTV-PyMT mouse model. T_{regs} have been shown to highly infiltrate mammary tumors of MMTV-PyMT mice, which is in part dependent on CCR2 expression on T_{regs}[81]. Ablation of T_{regs} in *Foxp3*^{DTR} mice with orthotopically transplanted MMTV-PyMT tumors drastically reduced tumor growth and

pulmonary metastases[82]. Mechanistically, IFNγ and $CD4^+$ conventional T cells were required for the observed anti-tumor effect, which was independent of $CD8^+$ T cells or NK cells. As pro-inflammatory signaling by myeloid cells was increased upon T_{reg} depletion, the authors speculated that IFNγ-activated macrophages may contribute to anti-tumoral inflammation[82]. The observation that T_{regs} constrain anti-tumor immunity in tumors has been reported by others. For example, anti-CD25 treatment in mice inoculated with 4T1 cancer cells strongly reduced tumor growth, which correlated with an increase in DCs and effector $CD8^+$ T cells in tumor draining lymph nodes, suggesting that T_{regs} modulate DC function[83]. Indeed, it has been reported that T_{regs} can inhibit the expression of co-stimulatory ligands on DCs thereby restraining CD8 activation and tumor clearance in a KRAS mutant model for pancreatic cancer[84]. It would be of interest to investigate whether similar mechanisms are at play in breast cancer. Elimination of T_{regs} is not always sufficient to drive strong anti-tumor responses. For example, immunosuppressive T_{regs} were found to be highly enriched in inoculated TNBC T-11 tumors, but DT-based T_{reg} ablation only slightly slowed tumor growth. T_{reg} ablation did potentiate PD-1/CTLA4 based immunotherapy which correlated with an increase in $IFN\gamma^+$ $CD8^+$ T cells[85]. These findings suggest that T_{regs} can form an important barrier for immunotherapy-induced anti-tumor immunity which has been reported before in preclinical inoculated melanoma and colon carcinoma tumors[76].

The studies above suggest that targeting T_{regs} in (breast) cancer models induces anti-tumoral inflammation which, sometimes in combination with immunotherapy, may have the potential to unleash anti-tumor immune responses. However, therapeutic elimination of T_{regs} may trigger auto-immunity in cancer patients, in particular in combination with ICB. Thus, an important next step would be to define the context-dependent molecular mechanisms engaged by T_{regs}, to enable precise targeting of relevant effector programs instead. A key challenge here is the apparent variability of the clinical significance of T_{regs} per breast cancer subtype, which necessitates the need to study these cells in clinically relevant mouse tumor models. Currently, the vast majority of murine breast cancer cell lines used for inoculation into mice and genetically engineered mouse models (GEMMs) for breast cancer give rise to ER^- mammary tumors[86], whereas ~75% of human invasive breast cancers are ER^+ [87]. As T_{regs} have been associated with a detrimental role particularly in HR^+ breast cancers, future research should ideally focus on the development and use of HR^+ breast tumor models to uncover the subtype dependent role of T_{regs} in breast cancer.

While in the context of established tumors, T_{regs} can interfere with anti-tumor immunity (Figure 1), recent findings in spontaneously developing tumor models suggest that at the onset of neoplastic progression T_{regs} may unexpectedly constrain pro-tumoral inflammation which promotes tumor initiation. One study reported that DT-based ablation of T_{regs} during the early, non-invasive neoplastic phase in the MMTV-PyMT model accelerated the progression of non-invasive lesions into invasive tumors[88]. The elimination of T_{regs} resulted in the

accumulation of macrophages in mammary glands and an induction of the Th2 cytokines IL-4 and IL-5, which have been reported to induce tumorigenic functions in macrophages[89]. The $CD44^+$ $CD24^-$ mammary stem cell compartment was also found to be expanded, with increased colony forming capacity in vitro. Whether T_{regs} directly control mammary stem cell proliferation or indirectly via the micro-environment remains to be addressed. In line with these findings, T_{regs} have also been reported to inhibit pancreatic carcinogenesis of neoplastic lesions in a KRAS mutant GEMM by repressing the recruitment of immunosuppressive myeloid cells[90]. These findings reinforce that T_{regs} are potent suppressors of inflammation in early stages of tumorigenesis, which has context dependent effects on tumor progression. As T_{regs} have been found to expand in ductal carcinoma in situ (DCIS)[45], more research is needed to uncover whether these cells play a protective or detrimental role in pre-cancerous breast cancer lesions.

Research on T_{regs} in other cancer types has revealed the versatile nature of these cells, and has uncovered novel mechanisms of immune cell crosstalk[84]. For example, T_{reg} derived IL-10 and IL-35 can promote $CD8^+$ T cell exhaustion in melanoma[91]. It is also becoming increasingly clear that T_{regs} can interact with a variety of myeloid cells including eosinophils, mast cells, macrophages, neutrophils and basophils, to hamper anti-tumor immunity[92,93]. T_{regs} were found to control intratumoral eosinophil and basophil infiltration, both of which can promote recruitment of $CD8^+$ T cells, leading to tumor rejection of melanoma cell lines[94,95]. In addition, T_{regs} indirectly maintain an immunosuppressive phenotype in TAMs by inhibiting the release of IFNγ in the TMEs of inoculated B16 and MC38 tumors[96]. Up until now, these interactions have not been investigated in the context of breast cancer, illustrating that we have perhaps only scratched the surface on T_{reg} effector functions in breast cancer. Promisingly, a transcriptional signature specific for tumor infiltrating T_{regs} has revealed remarkable similarity across tumor types in both human and mouse[97], suggesting that effector mechanisms may be shared across tumor types. In line, the chemokine receptor CCR8 was identified as part of this signature, endorsing previously discussed findings in human breast cancer[67].

Mechanisms of intratumoral accumulation of T_{regs} in breast tumors

Three main hypotheses have been postulated to explain the accumulation of T_{regs} in breast tumors. Firstly, T_{regs} that circulate in peripheral blood and lymph nodes may migrate into the TME following chemokine gradients upon activation. Secondly, it has been hypothesized that tissue-resident T_{regs} locally expand in the TME. Finally, intratumoral conversion of conventional $CD4^+$ T cells into T_{regs} may represent an important mechanism for T_{reg} accumulation. Although these hypotheses are non-mutually exclusive and may all contribute to T_{reg} accumulation, in particular the migration hypothesis has been supported with experimental evidence. Studies in human and mice have shown that T_{regs} express a wide range of chemokine receptors which may facilitate intratumoral homing, of which CCR2, CCR4, CCR5, CCR8, CXCR3 and

CXCR6 have been associated with breast cancer[9,67]. For example, $CCR2^+$ T_{regs} accumulate in multiple tumor models including the PyMT-MMTV model[81]. These cells display an activated phenotype, and were found to be tumor-antigen specific in an OVA-expressing sarcoma cell line inoculation model. Specific ablation of CCR2 on T_{regs} strongly reduced intratumoral T_{reg} accumulation[81]. CCR2 was also found to be expressed by intratumoral T_{regs} in human breast tumors[67]. Others have reported high expression of CCR4 by T_{regs} in the blood of breast cancer patients, with migratory capabilities to CCL22 and CCL17[68]. As discussed above, CCR8 has emerged as a chemokine receptor expressed uniquely by intratumoral T_{regs}[67,74], and has therefore gained attention as a potential therapeutic target. Anti-CCR8 mAb treatment of mice inoculated with CT26 colon carcinoma cells significantly reduced T_{regs} in tumors and enhanced intratumoral IFNγ expression[98]. In contrast, others have shown that CCR8 may be redundant for intratumoral T_{reg} homing, as injection of $CCR8^{KO}$ T_{regs} in mice inoculated with MC38 colon carcinoma cells did not interfere with their migration into tumors[97]. It has also been reported that autocrine production of CCL1, the ligand for CCR8, potentiates both T_{reg} proliferation and suppressive potential[99], suggesting that CCR8 may play an important role in maintaining T_{reg}-mediated immunosuppression, in addition to its chemotactic properties.

Accumulating evidence shows that intratumoral T_{regs} in breast cancer are transcriptionally distinct from T_{regs} in peripheral blood and lymph nodes, and share gene expression profiles with mammary tissue resident T_{regs}[67,100,101]. This suggests that either tissue resident cells expand in tumors, or that the local micro-environment drives transcriptional adaption of cells migrating into the TME. It has been reported that intratumoral and healthy breast T_{regs} within patients showed relatively little overlap of their TCR repertoire, suggesting that intratumoral T_{regs} do not derive from resident cells[67]. In addition, Ki67 expression in T_{regs} of healthy breast tissue was found to be drastically lower than in T_{regs} from tumor or blood. In line with the second notion, scRNA-seq of murine T_{regs} of naïve mice revealed that T_{reg} migration from lymphoid to non-lymphoid tissues indeed induces a transcriptional program specifically tailored to the destined tissue[102]. Furthermore, scRNA-seq of $CD45^+$ cells sorted from human breast tumors, blood and lymph nodes uncovered that intratumoral immune cells can acquire diverse phenotypes that are not found in circulation or normal tissue[100]. Here, five different T_{reg} clusters unique to the TME were identified, which were highly activated and expressed anti-inflammatory, exhaustion-, hypoxia-, and metabolism-related gene sets. Together, these studies suggest that transcriptional adaptation of migratory T_{regs} in the TME may explain the transcriptomic resemblance between intratumoral and mammary tissue resident T_{regs}, although further TCR profiling and genetic tracing studies are needed to definitively confirm this.

Research on the accumulation of tT_{regs} versus pT_{regs} in cancer has been rather limited due to the complexities of distinguishing both T_{reg} subsets in vivo. Yet, local induction of pT_{regs}

in the TME may in fact be an important mechanism of immunosuppression, as TGF-β is abundantly expressed in cancers[103]. However, analysis of T_{regs} in human glioma, melanoma and lung cancer samples did not reveal a substantial contribution of pT_{regs} to the total intratumoral T_{reg} pool[67,104–106]. For example, one study found that the overlap between TCR clonotypes of FOXP3$^+$ and FOXP3$^-$ CD4$^+$ T cells obtained from six melanoma tumors was 0.5-13.2%, indicating a relatively small proportion of T_{regs} may have been pT_{regs}. Yet, others have attributed important roles to pT_{regs} in murine cancer models[107–110]. One of these reports provided indications for their presence in the TME of breast cancer patients[110]. TCR repertoire analysis on CD4$^+$ T cells from tumor, blood and lymph nodes of five breast cancer patients revealed that tumor infiltrating T_{regs} are most similar to naïve CD4$^+$ T cells from tumor and blood, suggesting intratumoral conversion. By using the MDA-MB-231 TNBC cell line in humanized mice, it was further shown that TAM-secreted CCL18 specifically recruits naïve CD4$^+$ T cells, but not T_{regs}, via PITPNM3 into the TME. Here, these naïve CD4$^+$ T cells were capable of converting into FOXP3$^+$ T_{regs}, via unknown mechanisms. Blocking CCL18 in tumor bearing mice reduced intratumoral T_{reg} numbers and inhibited tumor growth[110]. As data on the role of pT_{regs} in breast cancer is still limited, future studies should focus on expanding these findings in a larger cohort of patients.

It is now well established that T_{regs} have various ways to accumulate into primary tumors. However, breast cancer survival is largely dictated by the extent of metastatic disease. Thus far, we have mostly discussed research on T_{regs} in breast cancer in the context of primary tumors, raising questions on the link between primary tumors and metastasis. Can T_{regs} impact metastasis formation from within the primary tumor? Or do circulating and/or tissue resident T_{regs} induce a systemic immunosuppressive axis which impacts metastasis formation?

Impact of T_{regs} on metastatic progression

Primary cancer cells have to progress through a multi-step process in order to successfully metastasize. This so-called metastatic cascade consists of tumor cell invasion, intravasation, survival in the circulation, extravasation, and outgrowth in a foreign, hostile environment, all while evading destruction by the immune system[2]. Prior to metastatic spread, tumor-derived systemic factors can even further potentiate metastasis by instructing (immature) myeloid cells to establish a pre-metastatic niche[111]. T_{regs} may potentially be involved in all steps of the metastatic cascade, through mechanisms both dependent and independent of their immune-regulatory function. However, progress into understanding their impact on the metastatic cascade is hampered by the limited availability of preclinical models that realistically recapitulate metastasis[112]. Cancer cell line-based mouse models fail to fully recapitulate the chronic and systemic inflammation that underlies *de novo* tumor development, progression and metastasis[113]. In addition, research in both 4T1 and PyMT models has shown that T_{reg} depletion reduces primary tumor growth which may obscure mechanisms at play during the

metastatic cascade[82,114]. Despite these shortcomings, several studies have revealed that tumor-induced (systemic) activation of T_{regs} can contribute to metastatic progression (Figure 1). This activation can be mediated via the release of various tumor-derived soluble factors, such as prostaglandins, complement factors and beta-galactoside-binding proteins[115–117]. For example, tumor-secreted galectin-1 was reported to enhance systemic T_{reg} expansion and their suppressive potential resulting in increased lung metastases in mice bearing inoculated 4T1 mammary tumors[115]. Others showed that overexpression of COX2 in inoculated TM40D mammary tumors enhanced bone metastasis, which correlated with increased recruitment of T_{regs} into the primary tumor[116]. In addition to factors released by the primary tumor, the local (pre)metastatic niche can also play an important role in the activation and recruitment of T_{regs}. For example, IL-33 and CCL17 have both been reported to be released in metastatic foci in the lungs of 4T1 tumor-bearing mice, leading to the recruitment of T_{regs} that express the receptor for these molecules, thereby promoting metastasis[118,119].

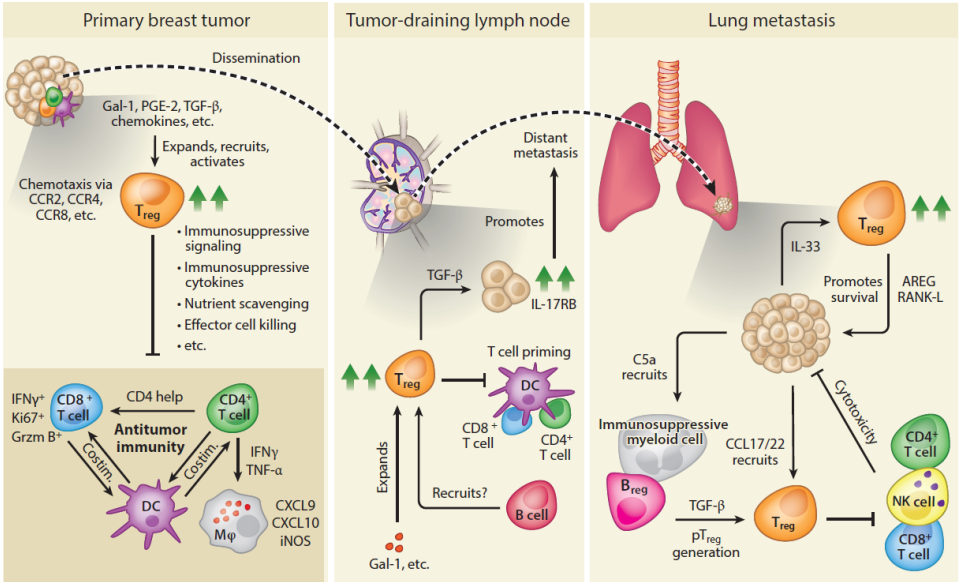

FIGURE 1. T_{regs} modulate their local environment to promote breast cancer progression. Tumor derived factors such as chemokines, cytokines and other mediators promote the accumulation and expansion of T_{regs} in primary breast tumors and metastatic niches. In the TME, T_{regs} constrain both innate and adaptive immune responses to counteract anti-tumor immunity. Mechanistically, T_{regs} can (among others) suppress the expression of co-stimulatory ligands on DCs, release inhibitory modulators that interfere with T cell activation, but are also equipped to induce apoptosis in effector cells. However, the effector mechanisms that are engaged in the context of the breast TME remain largely unknown. In addition, T_{regs} can enhance metastatic progression by promoting tumor cell survival and migration via secretion of TGF-β, AREG and RANK-L or by inhibition of cytotoxic effector cells. Abbreviations: Co-stim, co-stimulation; Gal-1, galectin-1; Grzm B, Granzyme B; Imm. suppr., immunosuppressive; Mϕ, macrophage.

Various tumor-driven pathways exist to systemically engage T_{regs} to the benefit of metastatic spread. An underlying question remains how T_{regs} mechanistically contribute to metastasis. Interestingly, T_{regs} have been found to directly contribute to metastasis of the 4T1 and MT2 cell lines in mice by promoting tumor cell survival via the release of RANK-L and AREG[118,120]. In addition, in line with their immunomodulatory properties, the pro-metastatic function of T_{regs} has been linked to inhibition of cytotoxic immune cells. To this regard, T_{reg} mediated inhibition of NK cells has been associated with increased pulmonary metastasis in the 4T1 model[121]. Others found that neoadjuvant ablation of T_{regs} in 4T1 bearing *Foxp3*^{DTR} mice almost completely abolished the formation of lung metastases, which was dependent on both $CD4^+$ and $CD8^+$ T cells, but not NK cells[114]. Of note, only neoadjuvant and not adjuvant T_{reg} depletion increased the systemic frequency and activation of tumor specific $CD8^+$ T cells[114]. It has not been addressed whether $CD4^+$ T cells directly engage in tumor-cell killing in the absence of T_{regs}, or perhaps provide essential help for $CD8^+$ T cell activation. The superiority of neoadjuvant over adjuvant targeting of T_{regs} suggests a role for T_{regs} in early stages of metastasis, which is supported by the clinical finding that T_{regs} associate with lymph node involvement[46].

Multiple clinical studies have reported associations between high T_{reg} infiltration in primary tumors and sentinel lymph nodes with lymph node (Table 1), but mechanistic data are limited. So far, one study has linked intranodal T_{regs} to breast cancer progression in mice. Here, using the 4T1 model, T_{reg}-derived TGF-β1 induced IL17RB in cancer cells in tumor draining lymph nodes (TDLN)[122]. IL17RB was found to potentiate the metastatic- and colony forming potential of cancer cells via NF-κb, which enhanced distant metastasis. Interestingly, analysis of IL17RB expression in lymph node metastasis and matched tumors of breast cancer patients confirmed that IL17RB is increased in lymph nodes, and correlates with FOXP3 frequency[122]. This study revealed that the TDLNs in breast cancer can function as a gateway to distant metastasis, with T_{regs} corrupted by the primary tumor. These findings raise the question whether T_{regs} are also involved in cancer cell dissemination to the draining lymph node. It has recently been reported that B cells promote metastasis to draining lymph nodes in the 4T1 and MMTV-PyMT models via the release of HSP4A-binding antibodies which directly promote tumor cell migration[123]. Interestingly, B cell depletion did significantly reduce tumor-induced T_{reg} accumulation in TDLNs. In line with these findings, it has previously been reported that regulatory B cells that accumulate in 4T1 tumor-bearing mice can induce pT_{regs} in a TGF-β dependent manner[109], revealing an interesting crosstalk between T_{regs} and B cells in breast cancer metastasis.

FUTURE PROSPECTS

T_{regs} have taken an increasingly important position in our understanding of the immune system in breast cancer. Preclinical research has revealed ingenious mechanisms employed by breast tumors to seize control of T_{regs} for their own benefit. In parallel, in-depth characterization of T_{regs} beyond traditional FOXP3 scoring in human samples is paving the way to advance their prognostic and predictive value in the clinic. Here, future efforts should focus on further defining the heterogeneity of T_{regs} and evaluate which features of T_{regs} are instrumental for disease progression, while also expanding current findings to HR^- subtypes of breast cancer where T_{regs} are associated with a good prognosis. As the use of immunomodulatory drugs is gaining momentum in the clinic, interrogating these observations in the context of immunotherapy is also an important next step.

The context dependency under which T_{regs} operate should also be increasingly taken into account in preclinical research. Until now the majority of research has been performed in a limited number of (cell line-based) breast cancer models, often with unclear translatability to human disease. An important challenge to address here is that breast cancer patients suffer from metastatic spread to a broad spectrum of anatomical locations, while experimental metastasis in animal models is often limited to the lungs. A crucial next step is therefore to validate preclinical findings in murine models that have increased translatability, both in terms of cancer subtype and metastasis formation. To achieve this, it is important to realize that the interaction between the immune system and cancer may even be more complex than initially assumed. We are only now beginning to understand that the genetic make-up of tumors may profoundly impact their accompanying micro-environment[124]. In addition, in-depth analyses of 168 metastatic and primary tumor samples from 10 breast cancer patients revealed that the composition of metastatic TMEs within patients was heterogeneous, even within particular organs. Moreover, the expression of immunomodulatory genes such as PD-1 and PD-L1 differed across metastases within individual patients[125]. These complexities of human metastatic disease illustrate the need for accurate models of metastasis.

Ultimately, these fundamental insights into the role of T_{regs} in breast cancer progression could form the basis for therapeutic intervention. As such, several early phase clinical trials have evaluated the FDA approved mAb daclizumab (anti-CD25) in combination with cancer vaccines in metastatic melanoma and breast cancer[126,127]. $FOXP3^+CD4^+$ T cells in peripheral blood were found to be reduced upon daclizumab treatment, but no significant clinical benefit was observed. However, daclizumab does not induce antibody-dependent cytotoxicity (ADCC), which others have suggested to be essential for intratumoral T_{reg} depletion and therapeutic efficacy[76,127]. Recently, an optimized ADCC inducing anti-CD25 antibody showed superior intratumoral T_{reg} depletion, and induced CD8-mediated tumor rejection in combination with anti-PD-1 in preclinical models. Alternatively, intratumoral injection of CD25 targeting immunotoxins also potently depletes intratumoral T_{regs}, leading to $CD8^+$ T

cell mediated tumor regression of inoculated 66c14 breast cancer tumors[128]. Importantly, these preclinical results suggest that effector T cell responses are not necessarily negatively impacted by CD25-based depletion, which may set the stage for clinical trials evaluating this new generation of T_{reg} targeting strategies. In addition to T_{reg} depletion, blocking of their intratumoral recruitment, conversion, or important effector mechanisms may be alternative future approaches to interfere with T_{reg}-mediated modulation of breast cancer[10].

In conclusion, recent research has exposed T_{regs} as important modulators of breast cancer progression and metastasis, while exciting advancements in clinical analysis improves the prognostic and predictive significance and potentially therapeutic targeting of these cells. The use of GEMMs that closely mimic the diversity and the step-wise progression of human breast cancer subtypes will propel our understanding of T_{reg} biology to a higher level and deepen our knowledge of underlying mechanisms. This knowledge could help to take full advantage of novel immunomodulatory drugs that may take the stage in breast cancer treatment.

ACKNOWLEDGEMENTS

We would like to thank Max Wellenstein and Wietske Pieters for insightful comments during the writing process. Research in the De Visser laboratory is funded by the Netherlands Organization for Scientific Research (grant NWO-VICI 91819616), the Dutch Cancer Society (KWF10083; KWF10623), European Research Council Consolidator award (InflaMet 615300) and Oncode Institute. K.K. is funded by the NWO Oncology Graduate School Amsterdam (OOA) Diamond Program.

REFERENCES

1. Hanahan, D. & Weinberg, R. A. Hallmarks of Cancer: The Next Generation. *Cell* **144**, 646–674 (2011).
2. Blomberg, O. S., Spagnuolo, L. & De Visser, K. E. Immune regulation of metastasis: Mechanistic insights and therapeutic opportunities. *Disease Models and Mechanisms* **11**, dmm036236 (2018).
3. Garner, H. & de Visser, K. E. Immune crosstalk in cancer progression and metastatic spread: a complex conversation. *Nature Reviews Immunology* 1–15 (2020) doi:10.1038/s41577-019-0271-z.
4. DeSantis, C. E. *et al.* Breast cancer statistics, 2019. *CA: A Cancer Journal for Clinicians* **69**, 438–451 (2019).
5. Bray, F. *et al.* Global cancer statistics 2018: GLOBOCAN estimates of incidence and mortality worldwide for 36 cancers in 185 countries. *CA: A Cancer Journal for Clinicians Cancer Journal for Clinicians* **68**, 394–424 (2018).
6. Qiu, S. Q. *et al.* Tumor-associated macrophages in breast cancer: Innocent bystander or important player? *Cancer Treatment Reviews* **70**, 178–189 (2018).
7. Denkert, C. *et al.* Tumour-infiltrating lymphocytes and prognosis in different subtypes of breast cancer: a pooled analysis of 3771 patients treated with neoadjuvant therapy. *The Lancet Oncology* **19**, 40–50 (2018).
8. Binnewies, M. *et al.* Understanding the tumor immune microenvironment (TIME) for effective therapy. *Nature Medicine* **24**, 541–550 (2018).
9. Yano, H., Andrews, L. P., Workman, C. J. & Vignali, D. A. A. Intratumoral regulatory T cells: markers, subsets and their impact on anti-tumor immunity. *Immunology* **157**, 232–247 (2019).
10. Plitas, G. & Rudensky, A. Y. Regulatory T Cells in Cancer. *Annual Review of Cancer Biology* **4**, 459–477 (2020).
11. Syed Khaja, A. S. *et al.* Preferential accumulation of regulatory T cells with highly immunosuppressive characteristics in breast tumor microenvironment. *Oncotarget* **8**, 33159–33171 (2017).
12. Planes-Laine, G. *et al.* PD-1/PD-l1 targeting in breast cancer: The first clinical evidences are emerging. a literature review. *Cancers* **11**, e1033 (2019).
13. Russell, W. L., Russell, L. B. & Gower, J. S. Exceptional inheritance of a sex-linked gene in the mouse explained on the basis that the X/O sex chromosome constitution is female. *PNAS* **45**, 554–560 (1959).
14. Brunkow, M. E. *et al.* Disruption of a new forkhead/winged-helix protein, scurfin, results in the fatal lymphoproliferative disorder of the scurfy mouse. *Nature Genetics* **27**, 68–73 (2001).
15. Hori, S., Nomura, T. & Sakaguchi, S. Control of Regulatory T Cell Development by the Transcription Factor Foxp3. *Science-* **299**, 1057–1061 (2003).
16. Fontenot, J. D., Gavin, M. A. & Rudensky, A. Y. Foxp3 programs the development and function of CD4+CD25+ regulatory T cells. *Nature Immunology* **4**, 330 (2003).
17. Bluestone, J. A., Bour-Jordan, H., Cheng, M. & Anderson, M. T cells in the control of organ-specific autoimmunity. *Journal of Clinical Investigation* **125**, 2250–2260 (2015).
18. John Leonard, A. D. *et al.* Identification of Natural Regulatory T Cell Epitopes Reveals Convergence on a Dominant Autoantigen. *Immunity* **47**, 107-117.e8 (2017).
19. Josefowicz, S. Z., Lu, L.-F. & Rudensky, A. Y. Regulatory T Cells: Mechanisms of Differentiation and Function. *Annual Review of Immunology* **30**, 531–564 (2012).
20. Lucca, L. E. & Dominguez-Villar, M. Modulation of regulatory T cell function and stability by co-inhibitory receptors. *Nature reviews. Immunology* (2020) doi:10.1038/s41577-020-0296-3.
21. Vignali, D. A. A., Collison, L. W. & Workman, C. J. How regulatory T cells work. *Nature Reviews Immunology* **8**, 523–532 (2008).
22. Loebbermann, J. *et al.* Regulatory T cells expressing granzyme B play a critical role in controlling lung inflammation during acute viral infection. *Mucosal Immunology* **5**, 161–172 (2012).
23. Koizumi, S. & Ishikawa, H. Transcriptional Regulation of Differentiation and Functions of Effector T Regulatory Cells. *Cells* **8**, 939 (2019).
24. Chinen, T. *et al.* An essential role for the IL-2 receptor in Treg cell function. *Nature Immunology* **17**, 1322–1333 (2016).
25. Moran, A. E. *et al.* T cell receptor signal strength in Treg and iNKT cell development demonstrated by a novel fluorescent reporter mouse. *Journal of Experimental Medicine* **208**, 1279–1289 (2011).
26. Legoux, F. P. *et al.* CD4$^+$ T Cell Tolerance to Tissue-Restricted Self Antigens Is Mediated by Antigen-Specific Regulatory T Cells Rather Than Deletion. *Immunity* **43**, 896–908 (2015).
27. Malhotra, D. *et al.* Tolerance is established in polyclonal CD4+ T cells by distinct mechanisms, according to self-peptide expression patterns. *Nature Immunology* **17**, 187–195 (2016).
28. Jordan, M. S. *et al.* Thymic selection of CD4+CD25+ regulatory T cells induced by an agonist self-peptide. *Nature Immunology* **2**, 301–306 (2001).
29. Sakaguchi, S., Yamaguchi, T., Nomura, T. & Ono, M. Regulatory T Cells and Immune Tolerance. *Cell* **133**,

775–787 (2008).
30. Kieback, E. *et al.* Thymus-Derived Regulatory T Cells Are Positively Selected on Natural Self-Antigen through Cognate Interactions of High Functional Avidity. *Immunity* **44**, 1114–1126 (2016).
31. Kanamori, M., Nakatsukasa, H., Okada, M., Lu, Q. & Yoshimura, A. Induced Regulatory T Cells: Their Development, Stability, and Applications. *Trends in Immunology* **37**, 803–811 (2016).
32. Marie, J. C., Letterio, J. J., Gavin, M. & Rudensky, A. Y. TGF-β1 maintains suppressor function and Foxp3 expression in CD4 +CD25+ regulatory T cells. *Journal of Experimental Medicine* **201**, 1061–1067 (2005).
33. Zheng, Y. *et al.* Role of conserved non-coding DNA elements in the Foxp3 gene in regulatory T-cell fate. *Nature* **463**, 808–812 (2010).
34. Lee, W. & Lee, G. R. Transcriptional regulation and development of regulatory T cells. *Experimental & Molecular Medicine* **50**, e456 (2018).
35. Curotto de Lafaille, M. A. & Lafaille, J. J. Natural and Adaptive Foxp3+ Regulatory T Cells: More of the Same or a Division of Labor? *Immunity* **30**, 626–635 (2009).
36. Josefowicz, S. Z. *et al.* Extrathymically generated regulatory T cells control mucosal TH2 inflammation. *Nature* **482**, 395–399 (2012).
37. Soroosh, P. *et al.* Lung-resident tissue macrophages generate Foxp3+ regulatory T cells and promote airway tolerance. *Journal of Experimental Medicine* **210**, 775–788 (2013).
38. Esterházy, D. *et al.* Compartmentalized gut lymph node drainage dictates adaptive immune responses. *Nature* **569**, 126–130 (2019).
39. Kalekar, L. A. *et al.* CD4(+) T cell anergy prevents autoimmunity and generates regulatory T cell precursors. *Nature immunology* **17**, 304–314 (2016).
40. Szurek, E. *et al.* Differences in expression Level of Helios and Neuropilin-1 do not distinguish thymus-derived from extrathymically-induced CD4+Foxp3+ Regulatory T Cells. *PLOS ONE* **10**, e0141161 (2015).
41. Sharma, A. & Rudra, D. Emerging Functions of Regulatory T Cells in Tissue Homeostasis. *Frontiers in Immunology* **9**, 883 (2018).
42. Baecher-Allan, C., Brown, J. A., Freeman, G. J. & Hafler, D. A. CD4+ CD25 high Regulatory Cells in Human Peripheral Blood. *The Journal of Immunology* **167**, 1245–1253 (2001).
43. Mougiakakos, D., Choudhury, A., Lladser, A., Kiessling, R. & Johansson, C. C. Regulatory T cells in cancer. *Advances in cancer research* **107**, 57–117 (2010).
44. Roncador, G. *et al.* Analysis of FOXP3 protein expression in human CD4+CD25+ regulatory T cells at the single-cell level. *European Journal of Immunology* **35**, 1681–1691 (2005).
45. Bates, G. J. *et al.* Quantification of Regulatory T Cells Enables the Identification of High-Risk Breast Cancer Patients and Those at Risk of Late Relapse. *Journal of Clinical Oncology* **24**, 5373–5380 (2006).
46. Jiang, D., Gao, Z., Cai, Z., Wang, M. & He, J. Clinicopathological and prognostic significance of FOXP3+ tumor infiltrating lymphocytes in patients with breast cancer: a meta-analysis. *BMC Cancer* **15**, 727 (2015).
47. Wang, Y., Sun, J. & Qu, X. Regulatory T cells are an important prognostic factor in breast cancer: a systematic review and meta-analysis. *Neoplasma* **63**, 789–798 (2016).
48. Zhou, Y. *et al.* Prognostic value of tumor-infiltrating Foxp3+ regulatory T cells in patients with breast cancer: a meta-analysis. *Journal of Cancer* **8**, 4098–4105 (2017).
49. Mahmoud, S. M. A. *et al.* An evaluation of the clinical significance of FOXP3+ infiltrating cells in human breast cancer. *Breast Cancer Research and Treatment* **127**, 99–108 (2011).
50. Liu, S. *et al.* Prognostic significance of FOXP3+ tumor-infiltrating lymphocytes in breast cancer depends on estrogen receptor and human epidermal growth factor receptor-2 expression status and concurrent cytotoxic T-cell infiltration. *Breast Cancer Research* **16**, (2014).
51. West, N. R. *et al.* Tumour-infiltrating FOXP3+ lymphocytes are associated with cytotoxic immune responses and good clinical outcome in oestrogen receptor-negative breast cancer. *British Journal of Cancer* **108**, 155–162 (2013).
52. Tsang, J. Y. S. *et al.* Lymphocytic infiltrate is associated with favorable biomarkers profile in HER2-overexpressing breast cancers and adverse biomarker profile in ER-positive breast cancers. *Breast Cancer Research and Treatment* **143**, 1–9 (2014).
53. Seo, A. N. *et al.* Tumour-infiltrating CD8+ lymphocytes as an independent predictive factor for pathological complete response to primary systemic therapy in breast cancer. *British Journal of Cancer* **109**, 2705–2713 (2013).
54. Wei, S. C., Duffy, C. R. & Allison, J. P. Fundamental mechanisms of immune checkpoint blockade therapy. *Cancer Discovery* **8**, 1069–1086 (2018).
55. Kim, I., Sanchez, K., McArthur, H. L. & Page, D. Immunotherapy in Triple-Negative Breast Cancer: Present and Future. *Current Breast Cancer Reports* **11**, 259–271 (2019).
56. Togashi, Y., Shitara, K. & Nishikawa, H. Regulatory T cells in cancer immunosuppression — implications

for anticancer therapy. *Nature Reviews Clinical Oncology* **16**, 356–371 (2019).
57. Kamada, T. *et al.* PD-1(+) regulatory T cells amplified by PD-1 blockade promote hyperprogression of cancer. *PNAS* **116**, 9999–10008 (2019).
58. Huang, A. C. *et al.* A single dose of neoadjuvant PD-1 blockade predicts clinical outcomes in resectable melanoma. *Nature Medicine* **25**, 454–461 (2019).
59. DiDomenico, J. *et al.* The immune checkpoint protein PD-L1 induces and maintains regulatory T cells in glioblastoma. *Oncoimmunology* **7**, e1448329–e1448329 (2018).
60. Schmid, P. *et al.* Atezolizumab and nab-paclitaxel in advanced triple-negative breast cancer. *New England Journal of Medicine* **379**, 2108–2121 (2018).
61. Adams, S. *et al.* Pembrolizumab monotherapy for previously untreated, PD-L1-positive, metastatic triple-negative breast cancer: Cohort B of the phase II KEYNOTE-086 study. *Annals of Oncology* **30**, 405–411 (2019).
62. Dirix, L. Y. *et al.* Avelumab, an anti-PD-L1 antibody, in patients with locally advanced or metastatic breast cancer: A phase 1b JAVELIN solid tumor study. *Breast Cancer Research and Treatment* **167**, 671–686 (2018).
63. Emens, L. A. *et al.* Long-term Clinical Outcomes and Biomarker Analyses of Atezolizumab Therapy for Patients with Metastatic Triple-Negative Breast Cancer: A Phase 1 Study. *JAMA Oncology* **5**, 74–82 (2019).
64. Nanda, R. *et al.* Pembrolizumab in patients with advanced triple-negative breast cancer: Phase Ib keynote-012 study. *Journal of Clinical Oncology* **34**, 2460–2467 (2016).
65. Voorwerk, L. *et al.* Immune induction strategies in metastatic triple-negative breast cancer to enhance the sensitivity to PD-1 blockade: the TONIC trial. *Nature Medicine* **25**, 920–928 (2019).
66. Emens, L. A. *et al.* Long-term Clinical Outcomes and Biomarker Analyses of Atezolizumab Therapy for Patients with Metastatic Triple-Negative Breast Cancer: A Phase 1 Study. *JAMA Oncology* **5**, 74–82 (2019).
67. Plitas, G. *et al.* Regulatory T Cells Exhibit Distinct Features in Human Breast Cancer. *Immunity* **45**, 1122–1134 (2016).
68. Gobert, M. *et al.* Regulatory T cells recruited through CCL22/CCR4 are selectively activated in lymphoid infiltrates surrounding primary breast tumors and lead to an adverse clinical outcome. *Cancer Research* **69**, 2000–2009 (2009).
69. Liyanage, U. K. *et al.* Prevalence of Regulatory T Cells Is Increased in Peripheral Blood and Tumor Microenvironment of Patients with Pancreas or Breast Adenocarcinoma. *The Journal of Immunology* **169**, 2756–2761 (2002).
70. Horlock, C. *et al.* The effects of trastuzumab on the CD4+CD25+FoxP3+ and CD4+IL17A+ T-cell axis in patients with breast cancer. *British Journal of Cancer* **100**, 1061–1067 (2009).
71. Wolf, A. M. *et al.* Increase of Regulatory T Cells in the Peripheral Blood of Cancer Patients. *Clinical Cancer Research* **9**, 606–612 (2003).
72. Perez, S. A. *et al.* CD4+CD25+ Regulatory T-Cell Frequency in HER-2/neu (HER)-Positive and HER-Negative Advanced-Stage Breast Cancer Patients. *Clinical Cancer Research* **13**, 2714–2721 (2007).
73. Decker, T. *et al.* Increased number of regulatory T cells (T-regs) in the peripheral blood of patients with Her-2/neu-positive early breast cancer. *Journal of Cancer Research and Clinical Oncology* **138**, 1945–1950 (2012).
74. Wang, L. *et al.* Connecting blood and intratumoral Treg cell activity in predicting future relapse in breast cancer. *Nature Immunology* **20**, 1220–1230 (2019).
75. Miyara, M. *et al.* Functional Delineation and Differentiation Dynamics of Human CD4+ T Cells Expressing the FoxP3 Transcription Factor. *Immunity* **30**, 899–911 (2009).
76. Arce Vargas, F. *et al.* Fc-Optimized Anti-CD25 Depletes Tumor-Infiltrating Regulatory T Cells and Synergizes with PD-1 Blockade to Eradicate Established Tumors. *Immunity* **46**, 577–586 (2017).
77. Coe, D. *et al.* Depletion of regulatory T cells by anti-GITR mAb as a novel mechanism for cancer immunotherapy. *Cancer Immunology, Immunotherapy* **59**, 1367–1377 (2010).
78. Yamaguchi, T. *et al.* Control of Immune Responses by Antigen-Specific Regulatory T Cells Expressing the Folate Receptor. *Immunity* **27**, 145–159 (2007).
79. Kim, J. M., Rasmussen, J. P. & Rudensky, A. Y. Regulatory T cells prevent catastrophic autoimmunity throughout the lifespan of mice. *Nature immunology* **8**, 191–7 (2007).
80. Lahl, K. *et al.* Selective depletion of Foxp3+ regulatory T cells induces a scurfy-like disease. *Journal of Experimental Medicine* **204**, 57–63 (2007).
81. Loyher, P. L. *et al.* CCR2 influences T regulatory cell migration to tumors and serves as a biomarker of cyclophosphamide sensitivity. *Cancer Research* **76**, 6483–6494 (2016).
82. Bos, P. D., Plitas, G., Rudra, D., Lee, S. Y. & Rudensky, A. Y. Transient regulatory T cell ablation deters oncogene-driven breast cancer and enhances radiotherapy. *The Journal of Experimental Medicine* **210**, 2435–2466 (2013).

83. Goudin, N. *et al.* Depletion of regulatory T cells induces high numbers of dendritic cells and unmasks a subset of anti-tumour CD8+CD11c+ PD-1lo effector T cells. *PLoS ONE* **11**, e0157822 (2016).
84. Jang, J. E. *et al.* Crosstalk between Regulatory T Cells and Tumor-Associated Dendritic Cells Negates Anti-tumor Immunity in Pancreatic Cancer. *Cell Reports* **20**, 558–571 (2017).
85. Taylor, N. A. *et al.* Treg depletion potentiates checkpoint inhibition in claudin-low breast cancer. *The Journal of clinical investigation* **127**, 3472–3483 (2017).
86. Özdemir, B. C., Sflomos, G. & Brisken, C. The challenges of modeling hormone receptor-positive breast cancer in mice. *Endocrine-Related Cancer* **25**, 319–330 (2018).
87. Bentzon, N., Düring, M., Rasmussen, B. B., Mouridsen, H. & Kroman, N. Prognostic effect of estrogen receptor status across age in primary breast cancer. *International Journal of Cancer* **122**, 1089–1094 (2007).
88. Martinez, L. M. *et al.* Regulatory T Cells Control the Switch From in situ to Invasive Breast Cancer. *Frontiers in Immunology* **10**, (2019).
89. DeNardo, D. G. *et al.* CD4+ T Cells Regulate Pulmonary Metastasis of Mammary Carcinomas by Enhancing Protumor Properties of Macrophages. *Cancer Cell* **16**, 91–102 (2009).
90. Zhang, Y. *et al.* Regulatory T cell depletion alters the tumor microenvironment and accelerates pancreatic carcinogenesis. *Cancer Discovery* CD-19-0958 (2020) doi:10.1158/2159-8290.cd-19-0958.
91. Sawant, D. V. *et al.* Adaptive plasticity of IL-10+ and IL-35+ Treg cells cooperatively promotes tumor T cell exhaustion. *Nature Immunology* **20**, 724–735 (2019).
92. Blatner, N. R. *et al.* In colorectal cancer mast cells contribute to systemic regulatory T-cell dysfunction. *PNAS* **107**, 6430–6435 (2010).
93. Zhou, J. *et al.* Exosomes released from tumor-associated macrophages transfer miRNAs that induce a Treg/Th17 cell imbalance in epithelial ovarian cancer. *Cancer Immunology Research* **6**, 1578–1592 (2018).
94. Carretero, R. *et al.* Eosinophils orchestrate cancer rejection by normalizing tumor vessels and enhancing infiltration of CD8 + T cells. *Nature Immunology* **16**, 609–617 (2015).
95. Sektioglu, I. M. *et al.* Basophils promote tumor rejection via chemotaxis and infiltration of CD8+ T cells. *Cancer Research* **77**, 291–302 (2017).
96. Liu, C. *et al.* Treg Cells Promote the SREBP1-Dependent Metabolic Fitness of Tumor-Promoting Macrophages via Repression of CD8+ T Cell-Derived Interferon-γ. *Immunity* **51**, 381-397.e6 (2019).
97. Magnuson, A. M. *et al.* Identification and validation of a tumor-infiltrating Treg transcriptional signature conserved across species and tumor types. *PNAS* **115**, E10672–E10681 (2018).
98. Villarreal, D. O. *et al.* Targeting CCR8 induces protective antitumor immunity and enhances vaccine-induced responses in colon cancer. *Cancer Research* **78**, 5340–5348 (2018).
99. Barsheshet, Y. *et al.* CCR8+ FOXP3+ Treg cells as master drivers of immune regulation. *PNAS* **114**, 6086–6091 (2017).
100. Azizi, E. *et al.* Single-Cell Map of Diverse Immune Phenotypes in the Breast Tumor Microenvironment. *Cell* **174**, 1293-1308.e36 (2018).
101. Szabo, P. A. *et al.* Single-cell transcriptomics of human T cells reveals tissue and activation signatures in health and disease. *Nature Communications* **10**, 4706 (2019).
102. Miragaia, R. J. *et al.* Single-Cell Transcriptomics of Regulatory T Cells Reveals Trajectories of Tissue Adaptation. *Immunity* **50**, 493-504.e7 (2019).
103. Batlle, E. & Massagué, J. Transforming Growth Factor-β Signaling in Immunity and Cancer. *Immunity* **50**, 924–940 (2019).
104. Lowther, D. E. *et al.* PD-1 marks dysfunctional regulatory T cells in malignant gliomas. *JCI insight* **1**, e85935 (2016).
105. Akimova, T. *et al.* Human lung tumor FOXP3+ Tregs upregulate four "Treg-locking" transcription factors. *JCI insight* **2**, e94075 (2017).
106. Ahmadzadeh, M. *et al.* Tumor-infiltrating human CD4 + regulatory T cells display a distinct TCR repertoire and exhibit tumor and neoantigen reactivity. *Science Immunology* **4**, eaao4310 (2019).
107. Alonso, R. *et al.* Induction of anergic or regulatory tumor-specific CD4+ T cells in the tumor-draining lymph node. *Nature Communications* **9**, 1–17 (2018).
108. Schreiber, T. H., Wolf, D., Bodero, M. & Podack, E. Tumor antigen specific iTreg accumulate in the tumor microenvironment and suppress therapeutic vaccination. *Oncoimmunology* **1**, 642–648 (2012).
109. Olkhanud, P. B. *et al.* Tumor-evoked regulatory B cells promote breast cancer metastasis by converting resting $CD4^+$ T cells to T-regulatory cells. *Cancer research* **71**, 3505–3515 (2011).
110. Su, S. *et al.* Blocking the recruitment of naive CD4+ T cells reverses immunosuppression in breast cancer. *Cell Research* **27**, 461–482 (2017).
111. Kitamura, T., Qian, B. Z. & Pollard, J. W. Immune cell promotion of metastasis. *Nature Reviews Immunology* **15**, 73–86 (2015).
112. Gómez-Cuadrado, L., Tracey, N., Ma, R., Qian, B. & Brunton, V. G. Mouse models of metastasis:

progress and prospects. *Disease models & mechanisms* **10**, 1061–1074 (2017).
113. Kersten, K., de Visser, K. E., van Miltenburg, M. H. & Jonkers, J. Genetically engineered mouse models in oncology research and cancer medicine. *EMBO Molecular Medicine* **9**, 137–153 (2017).
114. Liu, J. *et al.* Improved efficacy of neoadjuvant compared to adjuvant immunotherapy to eradicate metastatic disease. *Cancer Discovery* **6**, 1382–1399 (2016).
115. Dalotto-Moreno, T. *et al.* Targeting Galectin-1 Overcomes Breast Cancer-Associated Immunosuppression and Prevents Metastatic Disease. *Cancer Research* **73**, 1107–1117 (2013).
116. Karavitis, J. *et al.* Regulation of COX2 Expression in Mouse Mammary Tumor Cells Controls Bone Metastasis and PGE2-Induction of Regulatory T Cell Migration. *PLoS ONE* **7**, e46342 (2012).
117. Vadrevu, S. K. *et al.* Complement c5a receptor facilitates cancer metastasis by altering t-cell responses in the metastatic niche. *Cancer Research* **74**, 3454–3465 (2014).
118. Halvorsen, E. C. *et al.* IL-33 increases ST2+ Tregs and promotes metastatic tumour growth in the lungs in an amphiregulin-dependent manner. *OncoImmunology* **8**, e1527497 (2019).
119. Olkhanud, P. B. *et al.* Breast cancer lung metastasis requires expression of chemokine receptor CCR4 and regulatory T cells. *Cancer Research* **69**, 5996–6004 (2009).
120. Tan, W. *et al.* Tumour-infiltrating regulatory T cells stimulate mammary cancermetastasis through RANKL-RANK signalling. *Nature* **470**, 548–553 (2011).
121. Biragyn, A. *et al.* Inhibition of lung metastasis by chemokine CCL17-mediated in vivo silencing of genes in CCR4+ Tregs. *Journal of Immunotherapy* **36**, 258–267 (2013).
122. Huang, S. *et al.* TGF-β1 secreted by Tregs in lymph nodes promotes breast cancer malignancy via up-regulation of IL-17RB. *EMBO Molecular Medicine* **9**, 1660–1680 (2017).
123. Gu, Y. *et al.* Tumor-educated B cells selectively promote breast cancer lymph node metastasis by HSPA4-targeting IgG. *Nature Medicine* **25**, 312–322 (2019).
124. Wellenstein, M. D. & de Visser, K. E. Cancer-Cell-Intrinsic Mechanisms Shaping the Tumor Immune Landscape. *Immunity* **48**, 399–416 (2018).
125. De Mattos-Arruda, L. *et al.* The Genomic and Immune Landscapes of Lethal Metastatic Breast Cancer. *Cell Reports* **27**, 2690-2708.e10 (2019).
126. Jacobs, J. F. M. *et al.* Dendritic cell vaccination in combination with anti-CD25 monoclonal antibody treatment: A phase I/II study in metastatic melanoma patients. *Clinical Cancer Research* **16**, 5067–5078 (2010).
127. Rech, A. J. *et al.* CD25 blockade depletes and selectively reprograms regulatory T cells in concert with immunotherapy in cancer patients. *Science Translational Medicine* **4**, 134ra62 (2012).
128. Onda, M., Kobayashi, K. & Pastan, I. Depletion of regulatory T cells in tumors with an anti-CD25 immunotoxin induces CD8 T cell-mediated systemic antitumor immunity. *PNAS* **116**, 4575–4582 (2019).
129. Yan, M. *et al.* Recruitment of regulatory T cells is correlated with hypoxia-induced CXCR4 expression, and is associated with poor prognosis in basal-like breast cancers. *Breast Cancer Research* **13**, R47 (2011).
130. Liu, F. *et al.* CD8+ cytotoxic T cell and FOXP3+ regulatory T cell infiltration in relation to breast cancer survival and molecular subtypes. *Breast Cancer Research and Treatment* **130**, 645–655 (2011).
131. Kim, S. T. *et al.* Tumor-infiltrating lymphocytes, tumor characteristics, and recurrence in patients with early breast cancer. *American Journal of Clinical Oncology: Cancer Clinical Trials* **36**, 224–231 (2013).
132. Takenaka, M. *et al.* FOXP3 expression in tumor cells and tumor-infiltrating lymphocytes is associated with breast cancer prognosis. *Molecular and Clinical Oncology* **1**, 625–632 (2013).
133. Maeda, N. *et al.* Expression of B7-H3, a Potential Factor of Tumor Immune Evasion in Combination with the Number of Regulatory T Cells, Affects Against Recurrence-Free Survival in Breast Cancer Patients. *Annals of Surgical Oncology* **21**, 546–554 (2014).
134. Peng, G. L. *et al.* CD8+ cytotoxic and FoxP3+ regulatory T lymphocytes serve as prognostic factors in breast cancer. *American Journal of Translational Research* **11**, 5039–5053 (2019).
135. Allaoui, R. *et al.* Infiltration of γδ T cells, IL-17 + T cells and FoxP3 + T cells in human breast cancer. *Cancer Biomarkers* **20**, 395–409 (2017).
136. Lee, S., Cho, E. Y., Park, Y. H., Ahn, J. S. & Im, Y. H. Prognostic impact of FOXP3 expression in triple-negative breast cancer. *Acta Oncologica* **52**, 73–81 (2013).
137. Tsang, J. Y. S. *et al.* Lymphocytic infiltrate is associated with favorable biomarkers profile in HER2-overexpressing breast cancers and adverse biomarker profile in ER-positive breast cancers. *Breast Cancer Research and Treatment* **143**, 1–9 (2014).
138. Sun, S. *et al.* PD-1+ immune cell infiltration inversely correlates with survival of operable breast cancer patients. *Cancer Immunology, Immunotherapy* **63**, 395–406 (2014).
139. Miyashita, M. *et al.* Prognostic significance of tumor-infiltrating CD8+ and FOXP3+ lymphocytes in residual tumors and alterations in these parameters after neoadjuvant chemotherapy in triple-negative breast cancer: A retrospective multicenter study. *Breast Cancer Research* **17**, 124 (2015).
140. Papaioannou, E. *et al.* A standardized evaluation method for FOXP3+ Tregs and CD8+ T-cells in Breast

Carcinoma: Association with breast carcinoma subtypes, stage and prognosis. *Anticancer Research* **39**, 1217–1232 (2019).

3

Tumor-associated macrophages promote intratumoral conversion of conventional CD4+ T cells into regulatory T cells via PD-1 signalling

Kevin Kos[1,2,3], Camilla Salvagno[1,2,4], Max D. Wellenstein[1,2,5], Muhammad A. Aslam[1], Denize A. Meijer[1,2], Cheei-Sing Hau[1,2], Kim Vrijland[1,2], Daphne Kaldenbach[1,2], Elisabeth A.M. Raeven[1,2], Martina Schmittnaegel[6], Carola H. Ries[6], Karin E. de Visser[1,2,3*]

Affiliations
[1] Division of Tumor Biology & Immunology, Netherlands Cancer Institute, 1066 CX Amsterdam, The Netherlands
[2] Oncode Institute, Utrecht, The Netherlands
[3] Department of Immunology, Leiden University Medical Center, Leiden, The Netherlands.
[4] Current address: Department of Obstetrics and Gynecology, Weill Cornell Medicine, New York, NY, United States; Sandra and Edward Meyer Cancer Center, Weill Cornell Medicine, New York, NY, United States.
[5] Current address: Hubrecht Institute, Royal Netherlands Academy of Arts and Sciences (KNAW) and University Medical Center Utrecht, 3584 CT Utrecht, The Netherlands
[6] Roche Innovation Center Munich, Roche Pharma Research and Early Development, Penzberg, Germany
*Corresponding author. Email: k.d.visser@nki.nl

OncoImmunology. 2022, 11(1)

ABSTRACT

While regulatory T cells (T_{regs}) and macrophages have been recognized as key orchestrators of cancer-associated immunosuppression, their cellular crosstalk within tumors has been poorly characterized. Here, using spontaneous models for breast cancer, we demonstrate that tumor-associated macrophages (TAMs) contribute to the intratumoral accumulation of T_{regs} by promoting the conversion of conventional $CD4^+$ T cells (T_{convs}) into T_{regs}. Mechanistically, two processes were identified that independently contribute to this process. While TAM-derived TGF-β directly promotes the conversion of $CD4^+$ T_{convs} into T_{regs} *in vitro*, we additionally show that TAMs enhance PD-1 expression on $CD4^+$ T cells. This indirectly contributes to the intratumoral accumulation of T_{regs}, as loss of PD-1 on $CD4^+$ T_{convs} abrogates intratumoral conversion of adoptively transferred $CD4^+$ T_{convs} into T_{regs}. Combined, this study provides insights into the complex immune cell crosstalk between $CD4^+$ T cells and TAMs in the tumor microenvironment of breast cancer, and further highlights that therapeutic exploitation of macrophages may be an attractive immune intervention to limit the accumulation of T_{regs} in breast tumors.

INTRODUCTION

An important barrier for effective anti-tumor immunity in breast cancer is cancer-associated immunosuppression[1–3]. Within breast tumors, cancer cells and host cells including stromal cells, innate and adaptive immune cells, cooperate to limit the infiltration, proliferation and function of T cells with anti-tumor capacity[4]. A key cell type involved in cancer-associated immunosuppression is the $FOXP3^{+}CD4^{+}$ regulatory T cell (T_{reg}). Due to their immunosuppressive nature, T_{regs} play an essential role in immune homeostasis, but can be hijacked by tumors. Clinical studies in the context of breast cancer have shown that elevated levels of intratumoral T_{regs} correlate with high tumor grade and poor survival[5,6]. In line, preclinical data show that T_{regs} can interfere with anti-tumor immunity and immunotherapy response in mouse models for breast cancer[7–10]. Molecular insights into how T_{regs} accumulate inside tumors may set the stage for the development of novel therapeutic interventions aimed at reducing T_{reg} numbers in breast tumors.

Functional, immunosuppressive T_{regs} can develop via two distinct routes. The main route is through a specialised thymic developmental program that selects single positive $CD4^{+}$ thymocytes with a high affinity TCR recognising tissue-restricted self-antigen. These T_{reg} precursor cells further develop into mature, thymic-derived $FOXP3^{+}$ T_{regs} (tT_{regs}) under influence of cytokine stimulation of IL-2/IL-15[11], which coordinates the suppression of detrimental auto-immune responses directed towards self-antigen. In addition, peripherally induced T_{regs} (pT_{regs}) can arise in the periphery through induction of FOXP3 in non-regulatory $CD4^{+}$ conventional T cells (T_{convs})[12]. This latter process is mediated by TGF-β-induced SMAD3, which can bind an enhancer located in intron 2 (CNS1) of FOXP3, leading to its expression[13,14]. Preclinical research using $CNS1^{-/-}$ mice that lack these peripherally induced T_{regs} (pT_{regs}) have demonstrated a vital role for these cells in preventing excessive immune responses in the gut, by providing tolerance to commensal microbiota[12,15].

In addition to the indispensable role of TGF-β for the extrathymic differentiation of T_{regs}, this process can be fine-tuned by other factors, including PD-1 signalling[16]. Signalling through PD-1 in $CD4^{+}$ T cells can enhance TGF-β-mediated conversion of $CD4^{+}$ T_{convs} by inactivation of STAT1-mediated inhibition of FOXP3, or by improving the stability of FOXP3 in induced T_{regs} [17,18]. While PD-1-mediated conversion of $CD4^{+}$ T_{convs} into T_{regs} is critical for the prevention of graft rejection in a mouse model for graft versus host disease (GvHD)[18], the importance of PD-1 for the induction of T_{regs} within the tumor microenvironment, where PD-1 is often highly expressed on infiltrated T cells[19] , is unclear.

T_{regs} have been shown to accumulate in murine tumor models through chemotaxis-mediated recruitment, most notably via CCL2, CCL4, CCL8 and CCL17[20–22], but emerging data suggest that intratumoral conversion of $CD4^{+}$ T_{convs} into T_{regs} may additionally increase the

intratumoral presence of T_{regs} in breast cancer[23]. However, the underlying immune cell crosstalk that drives this process remains poorly understood. Interestingly, *in vitro* studies have shown that tumor-associated myeloid cells, such as dendritic cells and macrophages, induce the conversion of conventional $CD4^+$ T cells into T_{regs} [23–25], but the relevance of this crosstalk with myeloid cells in the context of spontaneous mammary tumors has not been characterized, despite the high abundance of particularly macrophages in human breast cancer[26].

In the current study, we used the transgenic *Keratin14 (K14)-cre;Cdh1$^{F/F}$;Trp53$^{F/F}$* (KEP) mouse model of invasive mammary tumorigenesis[27] to investigate the functional significance of crosstalk between tumor-associated macrophages (TAMs) and $CD4^+$ T cells in intratumoral accumulation of T_{regs}. We demonstrate that TAMs promote the intratumoral accumulation of immunosuppressive T_{regs} by driving the conversion of $CD4^+$ T cells into T_{regs} *in vivo. In vitro* studies showed that this process is dependent on TAM-derived TGF-β. In addition, we find that TAMs regulate PD-1 expression on intratumoral $FOXP3^-$ and $FOXP3^+CD4^+$ T cells. This facilitates T_{reg} conversion as genetic ablation of PD-1 on conventional T cells reduces their conversion into $FOXP3^+$ T_{regs} *in vivo.* Combined, this study reveals a novel interaction between TAMs and conventional $CD4^+$ T cells, that drives the intratumoral accumulation of T_{regs} in breast cancer, and thereby contributes to increased understanding of the immune interactions at play in breast cancer.

RESULTS

Regulatory T cells accumulate in *de novo* KEP mammary tumors and correlate with tumor-associated macrophages.

To study immune cell crosstalk between T_{regs} and TAMs in a model that closely recapitulates human breast tumor formation, we made use of the transgenic KEP mouse model, which spontaneously develops mammary tumors at 6-8 months of age[27]. Analysis of the infiltration of T_{regs}, identified by FOXP3 staining, showed that T_{regs} are more abundant in end stage KEP mammary tumors ($225mm^2$), as compared to healthy mammary gland (Fig. 1A-B). The immunosuppressive potential of intratumoral T_{regs} was determined by assessing their ability to suppress the proliferation of CD3/CD28-stimulated splenic $CD4^+$ and $CD8^+$ T cells *ex vivo*. T cell proliferation was significantly decreased in the presence of T_{regs} in an effector:target ratio-dependent manner (Fig. 1C), indicating that T_{regs} isolated from mammary KEP tumors have potent suppressor activity.

To investigate an association between T_{regs} and macrophages in breast tumors, we first characterized the infiltration of TAMs in end stage KEP tumors. As we have published previously[28], TAMs ($CD11b^+F4/80^{high}$, Fig. 1D) are the most abundant immune cell population

observed in KEP tumors (Fig. 1E), and orchestrate systemic immunosuppression via the release of IL-1β[29]. In line with this immunosuppressive character, TAMs in KEP tumors are negatively enriched for IFN-γ and IFN-α signaling compared to macrophages from healthy mammary glands, indicative of reduced immunostimulatory activity (Fig. S1A). Analysis of mRNA expression levels of FOXP3 (T_{regs}) and CSF1R (TAMs) in the human breast cancer cohort of The Cancer Genome Atlas using the Xena platform[30] revealed a positive correlation between FOXP3 and CSF1R (Fig. 1F). Likewise, this positive correlation between FOXP3 gene and CSF1R gene expression could be validated in a RNAseq dataset previously published by our lab, consisting of 120 tumors derived from 16 different GEMMs representing distinct subtypes of breast cancer[29] (Fig. 1G), thereby showing that these correlations exist across species and tumor models, raising the question whether T_{regs} and TAMs functionally interact in breast tumors.

TAMs promote T_{reg} accumulation in the tumor microenvironment by inducing the conversion of $CD4^+$ T_{convs} into T_{regs} *in vivo*

To elucidate whether TAMs are causally involved in the accumulation of T_{regs} in mammary tumors, we assessed the impact of macrophage depletion in tumor-bearing KEP mice on intratumoral T_{regs} (Fig. 2A). For this, a chimeric mouse IgG1 antagonistic antibody (clone 2G2) that binds to mouse CSF1R with high affinity was used[31], which blocks the interaction between CSF1 and CSF1R, thereby depleting macrophages which are dependent on CSF-1[28,32]. Indeed, in line with previous findings[28], anti-CSF1R treatment strongly reduced the $F4/80^{high}$ $CD11b^+$ macrophage population in KEP mammary tumors (Fig. 2B). In parallel, a strong reduction in the frequency and absolute counts of $FOXP3^+$ T_{regs} was observed in anti-CSF1R-treated mice compared to control-treated mice, which was limited to the TME, and not observed in other tissues (Fig. 2C-D, S1B). The phenotype of the remaining T_{regs}, as assessed by their expression of CD103, ICOS, CD25 and CD69, was not altered upon anti-CSF1R treatment (Fig. S1C). Of note, macrophage depletion did not significantly impact tumor burden or alter the frequency of conventional $CD4^+$ or $CD8^+$ T cells, (Fig. S1D-E). Together, these data indicate that TAMs play a role in the accumulation of T_{regs} in mammary tumors.

We then set out to assess how TAMs promote the intratumoral accumulation of T_{regs} in KEP mammary tumors. Since we previously reported that T_{regs} in KEP tumors show limited expression of Ki-67, similar to T_{regs} in healthy mammary glands where TAMs are not present, it is unlikely that TAMs facilitate intratumoral T_{reg} accumulation by enhancing their proliferation[10]. Others have reported that macrophages can release chemokines such as CCL17 and CCL22 that contribute to recruitment of T_{regs}[25,33,34], however, we did not observe altered gene expression of these chemokines, or other chemokines involved in T_{reg} recruitment into tumors[35–38], in tumors treated with control antibody or anti-CSF1R (Fig. S1F), suggesting that TAMs promote T_{reg} accumulation in KEP mammary tumors via a different mechanism.

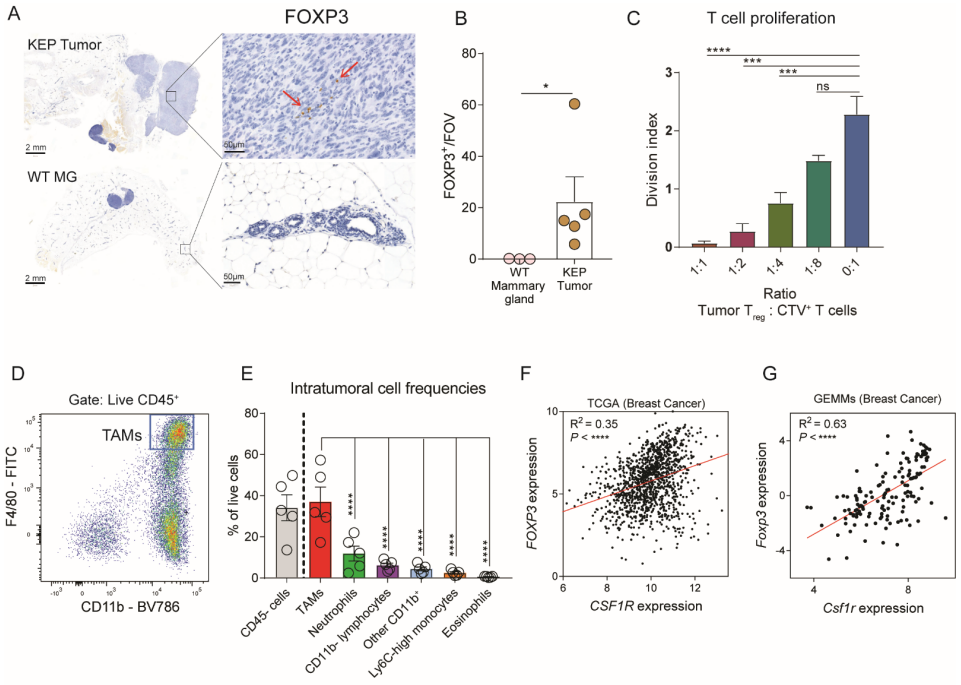

FIGURE 1. Characterization T_{regs} and TAMs in the TME of KEP tumors

A. Representative image of immunohistochemical staining of FOXP3 in mammary tumors (225mm^2) of KEP mice (top), or healthy mammary glands of WT littermates (bottom). Red arrows indicate FOXP3$^+$ cells. **B.** Quantification of data shown in (A). n = 3-5 mice/group. Per sample, 5 times 40x fields of view were averaged. **C.** Division index of CTV labelled CD4$^+$CD25$^-$ and CD8$^+$ splenic T cells isolated from WT mice, co-cultured with various numbers of CD4$^+$CD25$^+$ T_{regs} isolated from mammary tumors (225mm^2) of KEP mice in indicated ratios for 96 hours (data pooled from 3 independent experiments, mean ± SEM shown). **D.** Representative dot plot depicting TAMs (CD11b$^+$, F4/80^{high}) gated on CD45$^+$ cells in mammary (225m^2) tumors of KEP mice. **E.** Frequencies of intratumoral CD45$^-$ and CD45$^+$ immune cell subpopulations of total live cells in (225m^2) mammary tumors of KEP mice (n=5). Percentage of TAMs (CD45$^+$CD11b$^+$F4/80^{high}), neutrophils (CD45$^+$CD11b$^+$Ly6G$^+$Ly6C^{int}), CD11b$^-$ lymphocytes (CD45$^+$CD11b$^-$), Ly6C^{high} monocytes (CD45$^+$CD11b$^+$F4/80$^-$Ly6G$^-$Ly6C^{high}SSC-a^{low}), eosinophils (CD45$^+$CD11b$^+$F4/80$^{low/int}$Ly6G$^-$SiglecF$^+$SSC-A^{high}, other CD11b$^+$ (% CD11b$^+$ - % TAMs, neutrophils, Ly6C^{high} monocytes, eosinophils) are quantified. **F.** Scatter plot depicting correlation between *FOXP3* versus *CSF1R* mRNA expression log2(norm_count+1) in tumors of the TCGA human breast cancer cohort (n=1218 patient samples). **G.** Scatter plot depicting correlation between *Foxp3* versus *Csf1r* mRNA expression (normalised read counts) in mammary tumors obtained from 16 different GEMMs for mammary tumor formation, as previously described[29] (n = 145). Data in B,C,E depict mean ± SEM. P-values are determined by Mann-Whitney test (B) One-way ANOVA (C,E) Pearson's correlation (F,G). * P < 0.05, ** P < 0.01, *** P < 0.001, **** P < 0.0001.

We hypothesized that TAMs may promote T_{reg} accumulation by inducing the conversion of $CD4^+$ T_{convs} into T_{regs}. To test this hypothesis, gene expression profiles of T_{regs} isolated from end stage mammary tumors, WT mammary glands or WT spleen were compared with the gene expression profiles of $CD4^+$ T_{convs} ($CD4^+CD25^-$) isolated from end-stage mammary tumors. Correlation analysis suggests that intratumoral T_{regs} are transcriptionally more similar to intratumoral $CD4^+$ T_{convs} than to T_{regs} isolated from WT mammary gland or spleen (Fig. 2E), perhaps suggesting that there might be a relationship between intratumoral T_{regs} and $CD4^+$ T_{convs}, that may arise through conversion of $CD4^+$ T_{convs} into T_{reg} cells.

To test whether TAMs are functionally involved in conversion of $CD4^+$ T_{convs} into T_{regs}, $CD4^+CD25^-$ T_{convs} isolated from spleen and lymph nodes of tumor-bearing mice were cultured with or without TAMs FACS-sorted from KEP tumors (Fig. S1E). After 72 hours of co-culture, we found a significant increase in FOXP3 expression in $CD4^+CD25^-$ T_{convs} cultured with TAMs compared to $CD4^+CD25^-$ T_{convs} cultured without TAMs, indicating that TAMs have the potential to drive conversion of $CD4^+$ T_{convs} into T_{regs} under *in vitro* conditions (Fig. 2F-G, S1H). In these cultures, we also observed increased viability of $CD4^+$ T cells co-cultured with TAMs, suggesting TAMs might also support $CD4^+$ T cell survival (Fig. S1I).

Next, we set out to investigate whether TAMs also mediate T_{conv}-T_{reg} conversion *in vivo*, and thus might explain the observed reduction of intratumoral T_{regs} in anti-CSF1R-treated KEP mice (Fig. 2B). $CD4^+$ T_{convs} ($CD4^+CD25^-$) cells were FACS-sorted from naïve mTmG mice, which have continuous and ubiquitous expression of TdTomato, allowing for their *in vivo* tracing. Following *in vitro* activation to improve $CD4^+$ T_{convs} homing into tumors, $CD4^+$ T_{convs} (~98% purity post activation, S1J) were adoptively transferred into KEP mice bearing *de novo* mammary tumors (Fig. 2H). Analysis of tumor-bearing mice, 7 days after adoptive transfer, revealed that $TdTomato^+$ cells could be retrieved from blood and multiple tissues, including spleen, draining lymph nodes and tumors (Fig. 2I). Transferred $CD4^+CD25^-$ $TdTomato^+$ cells in non-tumor tissues lowly expressed FOXP3 (~7% in draining lymph node, <5% in blood and spleen), whereas ~33% of transferred cells found in KEP tumors expressed FOXP3, indicating that $TdTomato^+$ conventional $CD4^+$ T cells undergo conversion into T_{regs} *in vivo* (Fig. 2I-J). Strikingly, macrophage depletion in parallel to adoptive transfer of $FOXP3^-$ $CD4^+$ $TdTomato^+$ cells into tumor-bearing KEP mice (Fig. 2H) significantly reduced the frequency of $FOXP3^+$ cells within the transferred $TdTomato^+$ population in tumors but not in draining lymph nodes, spleen or blood when compared to control antibody-treated mice (Fig. 2J). Combined, these data indicate that TAMs promote the intratumoral accumulation of T_{regs}, which can at least partly be explained through the potential of TAMs to drive the conversion of $CD4^+$ T_{convs} into T_{regs}.

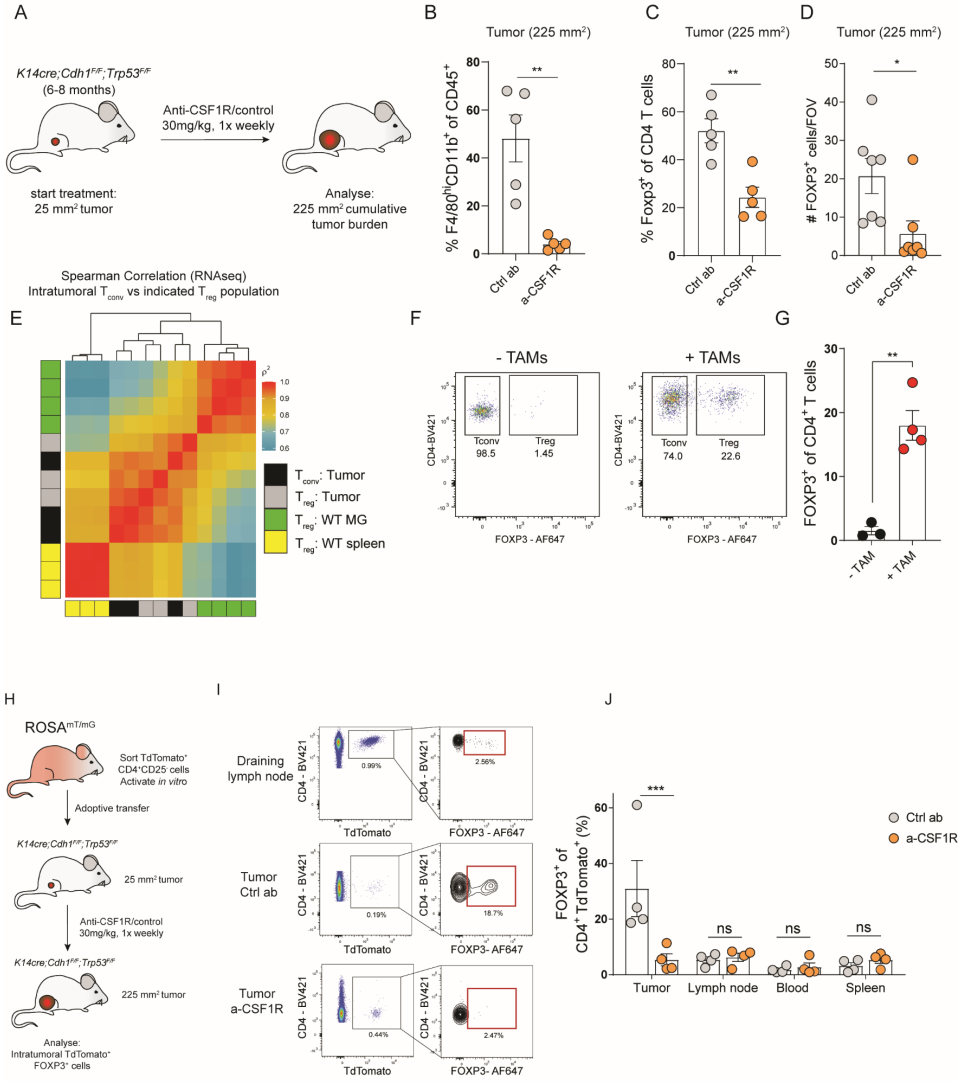

FIGURE 2. TAMs promote the conversion of CD4⁺ T_{convs} into T_{regs}

A. Schematic overview of study. KEP mice bearing 25mm² mammary tumors received weekly treatment of anti-CSF1R or control, until analysis at a cumulative tumor size of 225mm². **B.** Frequency of F4/80^{high}CD11b⁺ cells of CD45⁺ cells in mammary tumors of KEP mice treated with anti-CSF1R or control (n=5 mice/group). **C.** Frequency of FOXP3⁺ cells of CD4⁺ cells in mammary tumors of KEP mice treated with anti-CSF1R or control (n=5 mice/group). **D.** Immunohistochemical quantification of FOXP3⁺ cells in mammary tumors of mice treated with anti-CSF1R or control (n=7 mice/group). **E.** Correlation plot matrix plot showing Spearman coefficient between transcriptional profiles of T_{regs} and T_{convs} (n = 3) isolated from indicated tissue of KEP mice bearing end-stage mammary tumors and healthy mammary glands of WT littermates (n = 4). **F.** Representative dot plots of FOXP3 expression in live CD4⁺CD25⁻ T cells isolated from spleens of tumor-bearing KEP mice after co-culture with, or without TAMs (CD3⁻F4/80^{high}) for 72 hours. **G.** Percentage of FOXP3⁺ cells in CD4⁺ T_{convs} (CD45⁺CD3⁺CD4⁺CD25⁻) isolated from spleens of tumor-bearing KEP mice after co-culture with, or without TAMs (CD3⁻F4/80^{high}) for 72 hours (data pooled from 3-4 independent *in vitro* experiments). **H.** Schematic overview of study.

TdTomato$^+$ CD4$^+$CD25$^-$ T cells were FACS sorted from spleens of ROSA$^{mT/mG}$ mice, activated *in vitro* for 96 hours, and subsequently adoptively transferred into KEP mice bearing 25mm^2 mammary tumors that received weekly treatment of anti-CSF1R or control. 7 days later, mice were analysed. **I.** Representative dot plots depicting FOXP3 expression on adoptively transferred TdTomato$^+$ CD4$^+$ T_{convs} in draining lymph nodes and tumors of control and anti-CSF1R-treated mice. **J.** Frequencies of FOXP3$^+$ cells within adoptively transferred TdTomato$^+$ CD4$^+$ T_{convs} in draining lymph node, blood, spleen and tumors of control, and anti-CSF1R-treated mice (n=4/mice group). Data in B-D, G, J depict mean ± SEM. P-values are determined by Student's T test (B-D, G), Two-way ANOVA (J). * P < 0.05, ** P < 0.01, *** P < 0.001, **** P < 0.0001.

TAM-mediated *in vitro* conversion of CD4$^+$ T_{convs} into T_{regs} is mediated by TGF-β.

Next, we set out to explore the underlying mechanism of TAM-mediated induction of T_{regs}. We first focussed on the potential role of TAM-derived TGF-β, as TGF-β is well known to be indispensable for the conversion of CD4$^+$ T_{convs} into T_{regs} [13]. Gene set enrichment analysis (GSEA) of macrophages isolated from mammary tumors of KEP mice and healthy mammary glands of WT littermates using a previously published dataset[39] revealed that TAMs are enriched (FDR < 0.05) for genes involved in TGF-β signalling, compared to macrophages from healthy mammary glands (Fig. 3A). To test whether TAM-derived TGF-β might contribute to conversion of CD4$^+$ T_{convs} into T_{regs}, CD4$^+$CD25$^-$ T cells isolated from spleen and lymph nodes were co-cultured with TAMs isolated from KEP tumors in the presence or absence of anti-TGF-β. Indeed, blockade of TGF-β significantly reduced TAM-mediated induction of T_{regs}, indicating that TAMs can promote the conversion of CD4$^+$ T_{convs} into T_{regs} *in vitro* in a TGF-β-dependent manner (Fig. 3B-C, S2A). This process did not require an antigen-specific interaction, as *in vitro* blockade of MHC-II did not modulate T_{reg} induction (Fig. S2B). Furthermore, *in vitro* exposure of splenic CD4$^+$ T_{convs} to conditioned medium obtained from TAMs did not induce FOXP3 (Fig. S2C), suggesting close proximity of both CD4$^+$ T_{convs} and TAMs is required for TGF-β-mediated induction of FOXP3 in CD4$^+$ T_{convs}.

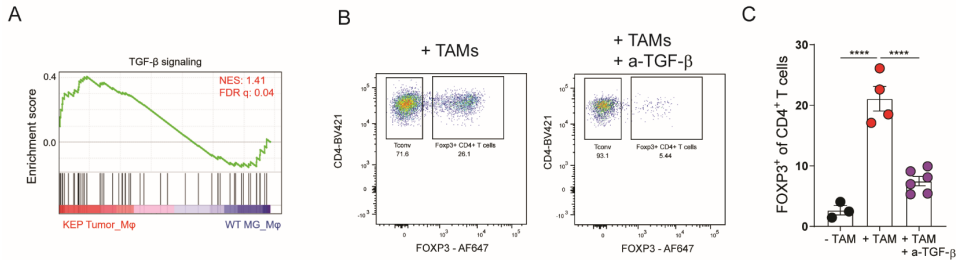

FIGURE 3. TAM-derived TGF-β promotes T_{conv}-T_{reg} conversion

A. GSEA comparing gene expression of KEP TAMs and WT mammary gland macrophages [39] with TGF-β signalling gene set from [62]. Normalized enrichment score (NES) and false discovery rate (FDR) indicated. Data obtained using a previously published dataset [39]. **B.** Representative dot plot of FOXP3 expression in CD4$^+$ T_{convs} isolated from spleens of tumor-bearing KEP mice after co-culture with TAMs (CD3$^-$F4/80^{high}) and 50 µg/mL anti-TGF-β for 72 hours. **C.** Percentage of FOXP3$^+$ cells in CD4$^+$ T_{convs} (CD45$^+$CD3$^+$CD4$^+$CD25$^-$) isolated from spleens of tumor-bearing KEP mice after co-culture with TAMs (CD3$^-$F4/80^{high}) and 50 µg/mL anti-TGF-β for 72 hours (data pooled from 3-6 independent *in vitro* experiments). Data in C depict mean ± SEM. P-values determined by One-way ANOVA (C), * P < 0.05, ** P < 0.01, *** P < 0.001, **** P < 0.0001.

TAMs promote PD-1 expression on intratumoral CD4$^+$ T cells

The peripheral conversion of CD4$^+$ T_{convs} into T_{reg} cells is dependent on TGF-β, but can be additionally enhanced by various contact-dependent mechanisms, such as PD-1 signalling, which has become clear from *in vitro* studies and studies using murine models for experimental colitis and experimental graft versus host disease[17,18,40]. However, in breast cancer, it is largely unclear whether PD-1/PD-L1 signalling in tumors contributes to the conversion of intratumoral CD4$^+$ T_{convs} into T_{regs}, even though high expression of PD-1 has been observed on intratumoral T cells in breast cancer patients[19]. To gain insight into this, we analysed PD-L1 expression in the TME and found that PD-L1 is most highly expressed by TAMs (Fig. 4A-B). Furthermore, analysis of PD-1 expression on CD4$^+$ T cells that were co-cultured with TAMs revealed that TAM-induced FOXP3$^+$ T_{regs} have significantly higher expression of the co-inhibitory molecule PD-1 as compared to non-converted FOXP3$^-$ CD4$^+$ T cells (Fig. 4C), which was also observed in the context of anti-TGF-β (Fig. S2D). Interestingly, by assessing the intratumoral distribution of TAMs, identified by Iba1 staining, T_{regs}, CD4$^+$ T cells and PD-1, we identified that these populations can cluster together in KEP tumors (Fig. S2E). Combined, these observations raise the question whether TAMs can modulate PD-1 expression on CD4$^+$ T cells that convert into T_{regs}.

To investigate a potential link between TAMs and PD-1 that may impact the conversion of CD4$^+$ T_{convs} into T_{regs} *in vivo*, we characterized PD-1 expression on FOXP3$^-$ and FOXP3$^+$ CD4$^+$ T cells in tumor-bearing KEP mice and WT littermates. This revealed that PD-1 was significantly increased on both CD4$^+$ subtypes in mammary tumors as compared to healthy mammary glands of WT littermates (Fig. 4D-E). Increased PD-1 expression in tumor-bearing KEP mice was specific to the TME, and not observed in blood, spleens, lungs or draining lymph nodes on T_{regs} and CD4$^+$ T_{convs} in KEP versus WT mice. Next, PD-1 expression on T cells in KEP tumors treated with anti-CSF1R or control antibody was analysed. Strikingly, macrophage depletion reduces PD-1 expression on both FOXP3$^-$ and FOXP3$^+$ intratumoral CD4$^+$ T cells (Fig. 4F-G), but not on CD8$^+$ T cells (Fig. S2F). To investigate whether PD-1 expression on intratumoral conventional CD4$^+$ T cells could be directly modulated by TAMs, PD-1^{neg} and PD1^{pos} CD4$^+$CD25$^-$ T cells isolated from KEP tumors were cultured with or without FACS-sorted TAMs (Fig. S1G, S2G). After 72 hours of culture, TAMs were found to significantly induce PD-1 on PD-1^{neg} sorted cells (Fig. S2H). PD-1 expression of PD-1^{pos} sorted CD4$^+$CD25$^-$ T cells was reduced to 64% after 72 hours, which was partially abrogated by addition of TAMs (Fig. 4H), indicating that TAMs can induce and maintain PD-1 expression on intratumoral CD4$^+$ T cells. In line with these findings, a positive correlation between *CSF1R* and *PDCD1* was identified in both the TCGA breast cancer dataset (Fig. 4I)[30], and our GEMM RNAseq dataset (Fig. 4J)[29]. Together, these data indicate that TAMs can positively regulate PD-1 expression on CD4$^+$ T cells in breast tumors.

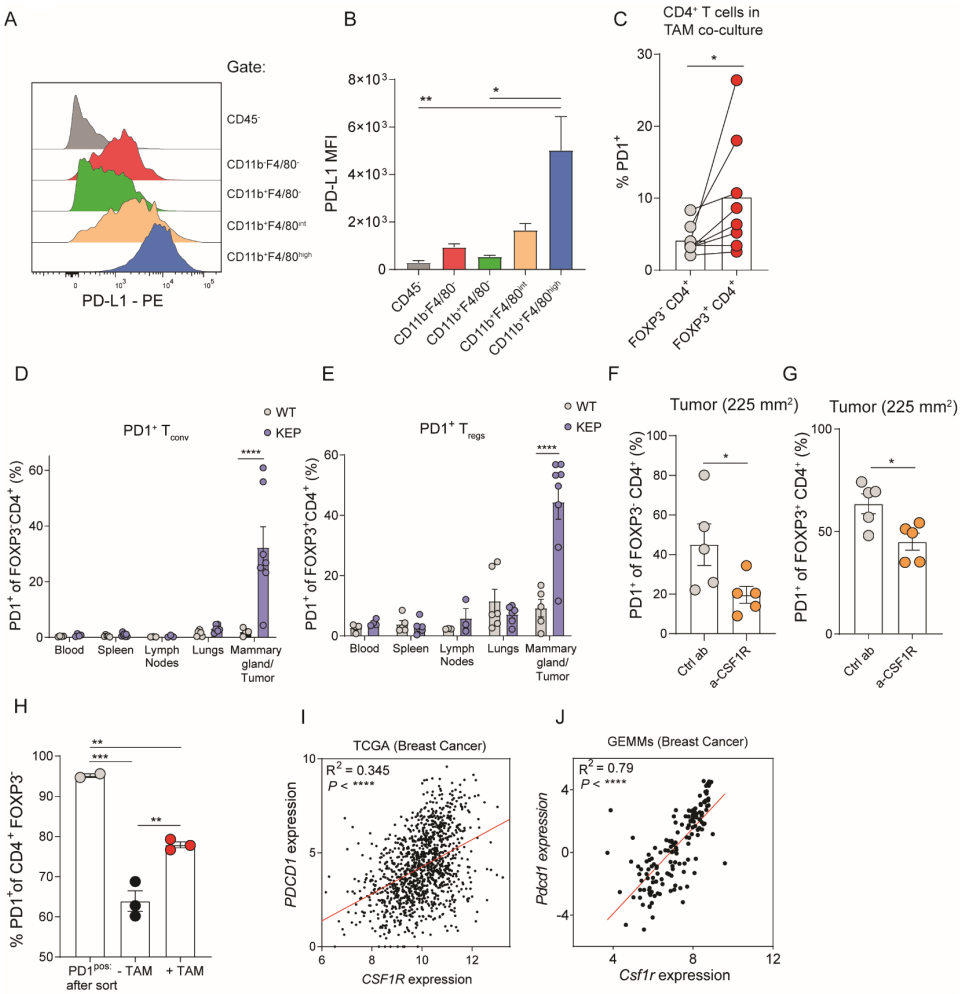

FIGURE 4. TAMs modulate PD-1 expression of CD4+ T cells.

A. Representative histogram depicting PD-L1 expression on indicated cell populations in mammary tumors (225m^2) of KEP mice. **B.** Quantification of PD-L1 MFI in indicated populations depicted in A (n=3 mice/group). **C.** Quantification of PD-1 expression in FOXP3$^-$ and FOXP3$^+$ sorted CD4$^+$ T_{convs} isolated from spleens of tumor-bearing KEP mice that were co-cultured with TAMs for 72h with 300U/mL IL-2 and 20ng/mL M-CSF. Data pooled from 8 independent *in vitro* experiments. **D-E.** Frequencies of PD-1 expression gated on FOXP3$^-$ (D) and FOXP3$^+$ (E) CD4$^+$ T cells in indicated tissues of KEP mice bearing (225m^2) mammary tumors versus WT littermates (n=3-8 mice/group). **F-G.** Frequency of PD-1$^+$ cells of CD4$^+$FOXP3$^-$ (F) CD4$^+$FOXP3$^+$ (G) T cells in mammary tumors of mice treated with anti-CSF1R or control (n=5 mice/group). **H.** Quantification of PD-1 expression in PD-1^{pos}CD4$^+$CD25$^-$ T cells isolated from KEP mammary tumors cultured with CD45$^+$ F4/80^{high} macrophages for 72h with 300U/mL, IL-2 and 20ng/mL M-CSF. Data pooled from 2-3 independent *in vitro* experiments. **I.** Scatter plot depicting correlation between *PDCD1* versus *CSF1R* mRNA expression log2(norm_count+1) in tumors of the TCGA human breast cohort (n=1218 patient samples). **J.** Scatter plot depicting correlation between *Pdcd1* versus *Csf1r* mRNA expression (normalised read counts) in mammary tumors obtained from 16 different GEMMs for mammary tumor formation, as previously described[29] (n = 145).

Data in B-H depict mean ± SEM. P-values determined by unpaired Student's T test (F-G), Wilcoxon signed rank test (C), Two-way ANOVA (D,E), One-way ANOVA (B,H), Pearson's Correlation (I,J),* P < 0.05, ** P < 0.01, *** P < 0.001, **** P < 0.0001.

PD-1 expression on CD4$^+$ T_{convs} contributes to their intratumoral conversion into $T_{regs,}$ independent of tumor-associated macrophages.

Our findings show that TAMs promote the intratumoral conversion of CD4$^+$ T_{convs} in T_{regs} via release of TGF-β (Fig. 2), and also promote PD-1 expression on intratumoral CD4$^+$ T cells (Fig. 4F-G). To gain insight into the hypothesis that increased PD-1 signalling might promote the conversion of intratumoral CD4$^+$ T_{convs} into T_{regs} *in vivo*, we first explored the relationship between PD-1 and FOXP3 in the TME of breast cancer. Analysis of PDCD1 and FOXP3 gene expression in the TCGA breast cancer cohort[30] and our previously described breast cancer GEMM RNAseq dataset[29] identified a positive correlation between these two genes (Fig. 5A-B). In addition, PD-1 protein expression on intratumoral CD4$^+$ T_{convs} positively correlates with T_{reg} accumulation in KEP tumors (Fig. 5C), further suggesting that PD-1 expression on CD4$^+$ T_{convs} might be linked to T_{reg} accumulation.

Next, we set out to investigate whether PD-1 plays a functional role in the conversion of CD4$^+$ T_{convs} into T_{regs} *in vivo*. For this, we first treated tumor-bearing KEP mice with PD-L1 blocking antibodies until end-stage tumor size was reached, but we did not find an effect on intratumoral T_{reg} accumulation (Fig. S3A). Notably, previous studies have shown that antibody-mediated blockade of PD-1/PD-L1 signalling can reinvigorate PD1$^+$ T_{regs}, thereby inducing their proliferation[41–44]. To circumvent this potential confounding mechanism of antibody-induced T_{reg} proliferation as a result of broadly targeting PD-1/PD-L1 signalling, we next applied an approach specifically targeting CD4$^+$ T_{convs} instead. For this, a CRISPR-Cas9 based approach was used to edit PD-1 in CD4$^+$ T_{convs} isolated from splenocytes of ROSA$^{GFP\text{-}CAS9}$ mice, which have constitutive and ubiquitous expression of CAS9[45]. CD4$^+$CD25$^-$ were purified from splenocytes by magnetic bead isolation, reaching a purity of 98% CD4$^+$CD25$^-$ FOXP3$^-$ cells of total live cells (Fig. S3B). Following *in vitro* activation for 48 hours using CD3/CD28 coated beads, CD4$^+$ T_{convs} were transduced with a modified pRubic retroviral vector encoding mCherry and a guideRNA targeting exon 2 of *PDCD1*, or control vector. Successful editing of the *PDCD1* gene in pRubic-sgPD-1 transduced CD4$^+$ T_{convs} was confirmed by TIDE analysis[46] on pRubic-sgPD-1 and pRubic-Ctrl transduced cells (Fig. S3C). In line, PD-1 protein expression was strongly reduced on pRubic-sgPD-1 CD4$^+$ T_{convs} as compared to pRubic-Ctrl CD4$^+$ T_{convs}, analysed 4 days after transduction (Fig. 5D-E). To evaluate the function of PD-1 in the intratumoral conversion of CD4$^+$ T_{convs} into T_{regs} *in vivo*, CD4$^+$ T_{convs} were transduced with pRubic-sgPD-1 and pRubic-Ctrl and adoptively transferred into mice bearing orthotopically injected KEP cell-line tumors (Fig. 5F). Of note, PD-1 was lowly expressed on both pRubic-sgPD-1 and pRubic-Ctrl CD4$^+$ T_{convs} prior to adoptive transfer (Fig. S3D). Analysis of tumors by flow cytometry 7 days after transfer showed similar infiltration of both sgPD-1, and sgEmpty mCherry$^+$ CD4$^+$ T_{convs} cells (Fig. S3E), but revealed that control CD4$^+$ T_{convs} upregulate PD-1 in the TME, which was not observed for PD-1 edited CD4$^+$ T_{convs}, confirming that successful editing of the PD-1 gene is maintained *in vivo* (Fig. 5G).

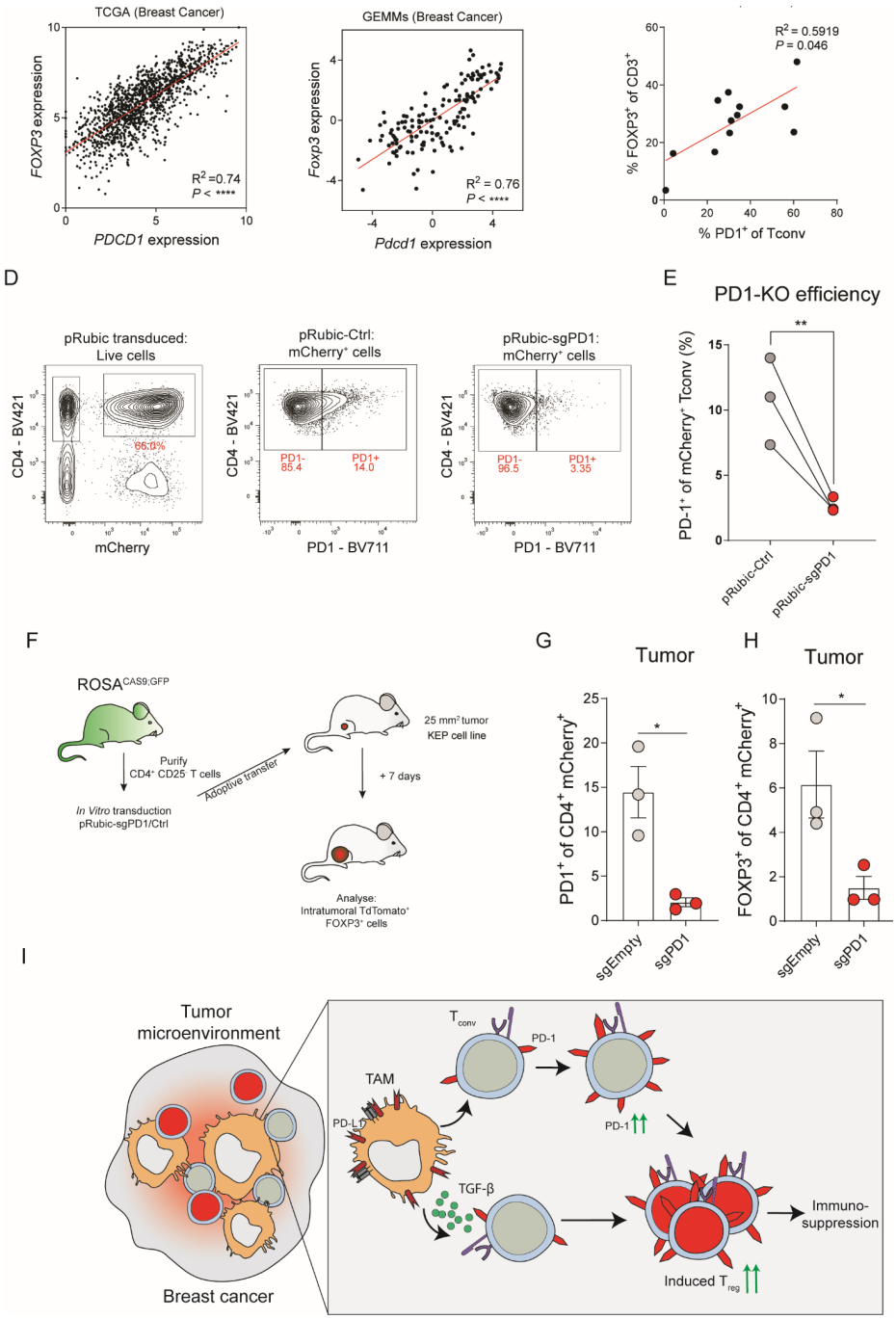

FIGURE 5. PD-1 promotes intratumoral conversion of CD4+ T_{convs} into T_{regs}
A. Scatter plot depicting correlation between *FOXP3* versus *PDCD1* mRNA expression log2(norm _count+1) in tumors of the TCGA human breast cohort (n=1218 patient samples). **B.** Scatter plot depicting correlation between *Foxp3* versus *Pdcd1* mRNA expression (normalised read counts) in mammary tumors obtained from 16 different GEMMs for breast cancer (n = 145). **C.** Scatter plot

depicting correlation between PD-1 expression on $CD4^+$ T_{convs} and % $CD4^+FOXP3^+$ of total T cells in KEP mammary tumors (n=12 mice). **D.** Representative dot plot of mCherry (left) and PD-1 (middle, right) expression in $CD4^+$ T_{convs} transduced with indicated pRubic vector, after 4 days of culture with IL-2. **E.** Quantification of PD-1 expression on $CD4^+$ T_{convs} transduced with indicated pRubic vector (data pooled from 3 *in vitro* independent experiments). **F.** Schematic overview of study. $CD4^+CD25^-$ cells from $ROSA^{CAS9\text{-}GFP}$ mice were purified, activated and transduced with pRubic-sgPD-1 or pRubic-Ctrl and adoptively transferred into mice bearing 25mm^2 KEP cell line tumors. After 7 days, mice were analysed. **G.** Quantification of PD-1 expression on $CD4^+$ $mCherry^+$ cells in KEP cell line tumors of mice receiving adoptive transfer of pRubic-sgPD-1 or pRubic-Ctrl $CD4^+$ T_{convs} (n=3 mice/group). **H.** Quantification of FOXP3 expression on $CD4^+$ $mCherry^+$ cells in KEP cell line tumors of mice receiving adoptive transfer of pRubic-sgPD-1 or pRubic-Ctrl $CD4^+$ T_{convs} (n=3 mice/group). **I.** Graphical representation describing findings presented in this study. TAMs can directly promote T_{reg} conversion by release of TGF-β but can also, in a distinct fashion, "prepare" $CD4^+$ T_{convs} for conversion through induction of PD-1. Data in G,H depict mean ± SEM. P-values determined by Pearson's correlation (A-C), Paired students T-test (E), Unpaired Student's T Test (G-H). * $P < 0.05$, ** $P < 0.01$, *** $P < 0.001$, **** $P < 0.0001$.

Strikingly, PD-1 edited $CD4^+$ T_{convs} showed reduced conversion into T_{regs}, as indicated by a significant lower expression of FOXP3 as compared to control $CD4^+$ T_{convs} in tumors (Fig. 5H). No differences were observed in PD-1 or FOXP3 expression in non-tumor tissues including blood, spleen or draining LN or blood (S3F). Combined, these data confirm that PD-1 expression on conventional $CD4^+$ T cells promotes intratumoral conversion into T_{regs}.

Finally, we studied whether TAMs are directly involved in promoting conversion of $CD4^+$ T_{convs} into T_{regs} via PD-1 signaling, or whether this is primarily mediated by TGF-β. Despite high expression of PD-L1 by TAMs in the TME of KEP tumors (Fig 4A-B), blockade of PD-L1 *in vitro* did not reduce TAM-mediated conversion of $CD4^+$ T_{convs} into T_{regs} (Fig. S3G) This indicates that TAMs can directly promote T_{reg} conversion by release of TGF-β, but can also, in a distinct fashion, "prepare" $CD4^+$ T_{convs} for TAM-indepent conversion through induction of PD-1 (Fig. 5I).

DISCUSSION

High intratumoral infiltration of immunosuppressive T_{regs} is associated with poor prognosis of breast cancer patients[47]. Insights into the mechanisms underlying the intratumoral accumulation of T_{regs} may set the stage for the development of novel therapeutic interventions. In the current study, we demonstrate that TAMs play a critical role in the accumulation of immunosuppressive T_{regs} in primary mammary tumors of the preclinical KEP mouse model. By studying the fate of endogenous $CD4^+$ T cells and adoptively transferred $CD4^+$ T_{convs} in spontaneous mammary tumors in the context of anti-CSF1R, we show that TAMs support the intratumoral conversion of $CD4^+$ T_{convs} into $FOXP3^+$ T_{regs} *in vivo.* Mechanistically, two independent processes were identified that contribute to this process (Fig. 5I). Firstly, *in vitro* co-culture studies with TAMs and $CD4^+$ T_{convs} revealed that TAM-derived TGF-β

promotes the conversion of $CD4^+$ T_{convs} into T_{regs}. Secondly, analysis of $CD4^+$ T_{convs} in the context of anti-CSF1R revealed that TAMs promote PD-1 expression on intratumoral $CD4^+$ T cells. By studying adoptively transferred PD-1^{KO} $CD4^+$ T_{convs} in mammary tumors *in vivo,* we demonstrate that PD-1^{KO} $CD4^+$ T_{convs} have reduced potential to convert into T_{regs} in tumors *in vivo*, showing that PD-1 further augments the conversion of $CD4^+$ T_{convs} into T_{regs}. Combined, this study reveals the importance of TAMs for the intratumoral conversion of $CD4^+$ T_{convs} into immunosuppressive T_{regs} in *de novo* mammary tumors, highlighting the importance of myeloid-lymphoid immune cell crosstalk in the tumor microenvironment.

Despite their distinct precursors, distinguishing thymic derived-, from peripheral T_{regs} has been obscured by the lack of a protein-based marker to differentiate between tT_{regs} and pT_{regs} *in vivo*. Instead, their identification has relied on epigenetic analysis of regions in the FOXP3 gene that are uniquely demethylated and accessible in tT_{regs} but not pT_{regs}, and analysis of TCR repertoire overlap in suspected pT_{regs} with $CD4^+$ T_{convs}. Due to the complexity of these analyses, it has been poorly characterized whether conversion of $FOXP3^-$ $CD4^+$ T cells in the tumor microenvironment (TME) substantially contributes to intratumoral accumulation of T_{regs}. Nonetheless, being able to differentiate tT_{regs} from pT_{regs} in tumors is important, as preclinical studies have suggested that pT_{regs} have specific properties that may prove valuable for clinical exploitation to alleviate intratumoral immunosuppression. For example, pT_{regs} have been shown to be unstable in inflammatory milieus that lack TGF-β, resulting in loss of FOXP3 and immunosuppressive function[48,49], suggesting that targeting TGF-β might affect pT_{regs}. In addition, tT_{regs} and $CD4^+$ T_{convs}, the precursor cells of pT_{regs}, are recruited into tumors through different chemotactic signals[50], suggesting that independent therapeutic approaches are required to both block the intratumoral recruitment of tT_{regs}, and the intratumoral conversion of pT_{regs}. In the current study, we show that intratumoral conversion of $CD4^+$ T_{convs} into T_{regs} in spontaneous KEP mammary tumors is supported by TAMs, suggesting that therapeutic targeting of TAMs may be an alternative approach to reducing intratumoral T_{regs}. One potential limitation of this study is that despite careful isolation of highly pure T_{regs} and Tconvs, cells were not isolated using a Foxp3-reporter system which would, by definition, be a more pure approach for isolation of Tconvs and T_{regs}. Important to note here is that anti-CSF1R treatment reduced intratumoral T_{regs}, but did not increase $CD8^+$ T cells or reduce tumor burden, despite the potent suppressor function of T_{regs} *in vitro*. This suggests that additional layers of immunosuppression may be present in the microenvironment of KEP mammary tumors. In line with this, previous research in our lab has shown that neutrophils additionally suppress anti-tumor immunity in absence of TAMs[28]. Thus, it is likely that combination strategies are necessary to alleviate the multiple immunosuppressive pathways at play in the tumor microenvironment. Although we have not deeply explored the anti-tumor effects of combination treatments in the current study, the fundamental insights gained from dissecting separate layers of intratumoral immunosuppression could form the basis for novel treatment combinations.

TAMs make up an important part of breast tumors, which has both been observed in human breast cancers, as well as in preclinical models of breast cancer[26,39]. It is important to realise that TAMs have high plasticity, characterized by diverse phenotypes, activation states and biological functions[51]. Despite this diversity, TAMs are often associated with suppression of anti-tumor immune responses, and poor prognosis in cancer[52]. In line with this, preclinical research using the KEP model has shown that targeting macrophages with anti-CSF1R enhances chemotherapy efficacy of platinum-based drugs by unleashing type I interferon response[28]. Interestingly, *in vitro* studies using human monocyte-derived macrophages reported that macrophages contribute to conversion of human $CD4^+$ T_{convs} into T_{regs} through their release of TGF-β[24]. Vice versa, T_{regs} have also been shown to promote TAM infiltration in the context of indoleamine 2,3-dioxygenase-expressing murine B16 cell line tumors[53]. Furthermore, macrophages have been described to release a plethora of chemokines[51,54,55], including CCL4, CCL22, and CCL17 which have been implicated in the recruitment of T_{regs} in tumors[25]. In light of this, we here investigated the importance of TAMs for intratumoral T_{reg} accumulation in breast tumors *in vivo*. We show that TAMs play a pivotal role in the accumulation of T_{regs} in a transgenic mouse model for spontaneous mammary tumorigenesis. Mechanistically, we found that TAMs promote $CD4^+$ T_{conv} conversion into T_{regs} via release of TGF-β, but also by enhancing PD-1 expression on conventional $CD4^+$ T cells. These data are in line with two recent studies that also identified a link between macrophages and T_{regs} in the context of non-small cell lung cancer (NSCLC). Lung tissue-resident macrophages (TRM) were found to promote T_{reg} accumulation in a murine model for NSCLC[25]. TRMs were shown to express high levels of *Ccl17* and *Tgfb1*, which were hypothesized to contribute to the recruitment and expansion of T_{regs} in this model. Secondly, antiangiogenic therapy in NSCLC was shown to facilitate the infiltration of PD-1^+ T_{regs} into the TME, which were further supported by TAMs that created a TGF-β rich environment[56].

Previous studies have shown a role for PD-1 in the extrathymic differentiation of T_{regs} in non-tumor tissue[17,18,40,57,58]. In mice, PD-1 deficiency did not impact thymic development of T_{regs}, nor their suppressive potential *in vitro*, but PD-1 deficiency on $CD4^+$ T_{convs} specifically reduced their differentiation into T_{regs} in lymphopenic $Rag^{-/-}$ mice[58]. In line, others showed that PD-L1-coated beads synergized with TGF-β to promote T_{reg} conversion *in vitro*[40]. Mechanistically, PD-1/PD-L1 signalling in $CD4^+$ T cells can promote T_{reg} conversion by inactivation of STAT1-mediated inhibition of FOXP3, and by improving the stability of FOXP3 in induced T_{regs}[17,18]. Despite these findings, the role of PD-1-mediated induction of T_{regs} in the context of cancer has been unclear, whereas PD-1 is highly expressed on intratumoral T cells in breast cancer patients[19]. We here show that PD-1 expression on $CD4^+$ T cells, is directly involved in intratumoral conversion of $CD4^+$ T_{convs} into T_{regs} *in vivo*. Importantly, we found that TAMs primarily support the initial step of PD-1-mediated T_{reg} conversion by inducing PD-1 on $CD4^+$ T_{convs}, but are not further supporting conversion of $PD1^+$ $CD4^+$ T_{convs} via PD-L1 signalling *in vitro*. Since we found PD-L1 to be widely expressed in the TME of

KEP tumors, an important topic of future research is to identify which PD-L1$^+$ cell type drives PD-1 mediated conversion in KEP tumors, and whether additional signals from these cells are facilitating this conversion process.

Since PD-1 blockade is becoming increasingly standardized for the treatment of cancers, future studies should further address whether therapeutic blockade of PD-1 indeed reduces T_{conv}-T_{reg} conversion in human tumors, and its relevance for treatment efficacy. One important aspect to consider is that several recent studies have shown that blockade of PD-1 or PD-L1 leads to reinvigoration of T_{regs} thereby inducing their activation and proliferation, like observed on effector T cells[42–44]. This opposing effect of PD-1/PD-L1 blocking strategies, which decreases conversion of CD4$^+$ T_{convs} into T_{regs}, but increases proliferation of PD-1$^+$ and PD-L1$^+$ T_{regs}, further complicates clinical assessment of T_{reg} conversion, and suggests that future PD-1 blocking strategies should be optimally targeted at CD4$^+$ T_{convs}, but not T_{regs}.

Taken together, this study reveals a novel relationship between TAMs, PD-1 expression on CD4$^+$ T cells and T_{reg} conversion in breast cancer. These data provide insight into the interdependency between different members of the TME that cooperate to establish immunosuppression, but also highlight that therapeutic targeting of macrophages affects the immunosuppressive tumor microenvironment beyond macrophages itself, making it an attractive immune intervention strategy for cancer treatment.

MATERIALS AND METHODS

Mice

Mice were kept in individually ventilated cages at the animal laboratory facility of the Netherlands Cancer Institute under specific pathogen free conditions. Food and water were provided *ad libitum.* All animal experiments were approved by the Netherlands Cancer Institute Animal Ethics Committee, and performed in accordance with institutional, national and European guidelines for Animal Care and Use. The study is compliant with all relevant ethical regulations regarding animal research.

The following genetically engineered mice have been used in this study: *Keratin14 (K14)-cre;Cdh1$^{F/F}$;Trp53$^{F/F}$*, *ROSA$^{mT/mG}$,* and *ROSA$^{CAS9\text{-}GFP}$*. The generation and characterization of the *Keratin14 (K14)-cre;Cdh1$^{F/F}$;Trp53$^{F/F}$* model for spontaneous mammary tumorigenesis has been described before[27]. All mouse models were on FVB/n background, and genotyping was performed by PCR analysis on toe clips DNA as described[27]. Starting at 6-7 weeks of age, female mice were monitored twice weekly for the development of spontaneous mammary tumor development in all mammary glands. Upon mammary tumor formation, perpendicular tumor diameters were measured twice weekly using a calliper. In KEP mice,

sizes of individual mammary gland tumors in one animal were summed to determine cumulative tumor burden. End-stage was defined as cumulative tumor burden of 225mm^2. Age-matched WT littermates were used as controls.

Intervention studies

Antibody treatments in tumor-bearing KEP mice were initiated at a tumor size of 25mm^2. Mice were randomly allocated to treatment groups and were intraperitoneally injected with chimeric (hamster/mouse) anti-CSF-1R antibody (clone 2G2, Roche Innovation Center Munich; single loading dose of 60 mg/kg followed by 30 mg per kg once a week); control antibody (IgG1, MOPC21, Roche Innovation Center Munich; single loading dose of 60 mg per kg followed by 30 mg per kg once a week); Rat anti-mouse PD-L1 (Clone 10F.9G2; 200 µg once a week). Treatments were discontinued at cumulative tumor burden of 225mm^2 unless indicated otherwise.

Flow cytometry analysis and cell sorting

Draining lymph nodes, spleens, tumors and lungs were collected in ice-cold PBS, and blood was collected in heparin-containing tubes. Draining lymph nodes, spleens, tumors were processed as previously described[59]. Lungs were perfused with ice-cold PBS *post mortem* to flush blood. Next, lungs were cut into small pieces and mechanically chopped using the McIlwain tissue chopper. Lungs were enzymatically digested in 100 µg/mL Liberase Tm (Roche) under continuous rotation for 30 minutes at 37 °C. Enzyme activity was neutralized by addition of cold DMEM/8% FCS and suspension was dispersed through a 70 µm cell strainer. Blood was obtained via cardiac puncture for end-stage analyses. Erythrocyte lysis for blood and lungs was performed using NH_4Cl erythrocyte lysis buffer for 2x5 and 1x1 minutes respectively. Single cell suspensions were incubated in anti-CD16/32 (2.4G2, BD Biosciences) for 5 minutes to block unspecific Fc receptor binding. Next, cells were incubated for 20 minutes with fluorochrome conjugated antibodies diluted in FACS buffer (2.5% FBS, 2 mM EDTA in PBS). For analysis of FOXP3, cells were fixed and permeabilized after surface and live/dead staining using the FOXP3 Transcription buffer set (Thermofisher), according to manufacturer's instruction. Fixation, permeabilization and intracellular FOXP3 staining was performed for 30 minutes. Single cell suspensions of mice that received adoptive transfer of pRubic-mCherry CD4$^+$ T_{convs} were additionally fixed in 2% PFA (ThermoFisher) for 30 minutes, prior to fixation using the FOXP3 Transcription buffer set to enhance simultaneous detection of FOXP3 and mCherry as previously described[60]. Cell suspensions were analysed on a BD LSR2 SORP or sorted on a FACS ARIA II (4 lasers), or FACS FUSION (5 lasers). Single cell suspensions for cell sorting were prepared under sterile conditions. Sorting of CD4$^+$ T_{convs} (Live, CD45$^+$CD3$^+$CD4$^+$CD25$^-$PD-1$^{pos/neg}$ from indicated tissues and TAMs (Live, CD45$^+$CD3$^-$F4/80^{high}) isolated from spontaneous mammary KEP tumors (>100mm^2) was performed as previously described[59]. Gating strategies depicted in Figure S1+2. See supplementary table 1 for antibodies used.

mTmG CD4$^+$ T_{convs} adoptive transfer studies

For adoptive transfer studies, naïve CD4$^+$ T_{convs} (Live, CD3$^+$CD4$^+$CD25$^-$CD44$^-$) were FACS sorted from ROSA$^{mT/mG}$ mice, and activated *in vitro* using CD3/CD28 dynabeads (ThermoFisher) in a 1:2 bead:cell and 300U/mL IL-2 (PeproTech) ratio in 24-wells plates. After 96 hours, Dynabeads were magnetically removed, cells were washed and resuspended in HBSS and intravenously injected into KEP mice bearing 25mm^2 mammary tumors (1.5-2.5*10^6 cells/mouse). After 7 days, mice were sacrificed, single cell suspensions were prepared and adoptively transferred cells were analysed by flow cytometry as described above.

CD4$^+$ T_{convs} – macrophage co-culture *in vitro* assays

3*10^3-1.0*10^4 CD4$^+$ T_{convs} (PD-1$^{pos/neg}$ as indicated for intratumoral CD4$^+$ T_{convs}) obtained from indicated source were co-cultured with 1.5*10^4- 5.0*10^4 (1:5 T cell:TAM ratio) TAMs in a round bottom, tissue culture treated 96-wells plate in cIMDM supplemented with 300U/mL IL-2 and 20 ng/mL M-CSF, and 50 µg/mL anti-TGF-β, 50 µg/mL anti-PD-L1 or 100 µg/mL anti-MHC-II as indicated. After 72 hours, cells were washed with FACS buffer, and prepared for flow-cytometric analysis as described above. Conditioned medium was collected from 1-2*10^5 TAMs cultured for 48h in cIMDM supplemented with 20 ng/mL M-CSF in flat-bottom, tissue culture treated 12-wells plate. CD4$^+$ T_{conv} culture with TAM conditioned medium were additionally supplemented with CD3/CD28 Dynabeads (1:5 bead:cell ratio).

Cloning of pRubic-PD-1 retroviral vector

Transduction of CD4$^+$ T_{convs} isolated from splenocytes of ROSA$^{CAS9\text{-}GFP}$ mice was carried out using a modified retroviral pRubic-T2A-Cas9-mCherry vector (**https://www.addgene.org/75347/)** containing sgRNA targeting exon 2 of *Pdcd1*. sgRNA-PD-1 was assembled by annealing complementary oligonucleotides 5'-CACCGCAGCTTGTCCAACTGGTCGG-3' and 5'-AAACCCGACCAGTTGGACAAGCTGC-3', with BbsI overhangs. Annealed oligo's were subsequently ligated into the BbsI-digested PxL vector, which provided U6 promotor and gRNA scaffold. Then, gRNA-PD-1, U6 promotor and gRNA scaffold were cloned into pRubic vector using BstBI isoschizomer SfuI and PacI, resulting in pRubic-PD-1 or control pRubic vector, without gRNA. Successful insertion of gRNA into pRubic backbone was confirmed by sanger sequencing on purified DNA using hU6-Forward primer (5'-GAGGGCCTATTTCCCATGATT-3').

Generation of pRubic Retrovirus

For generation of pRubic-retrovirus, 2*10^6 HEK cells were plated in 10cm^2 dishes. 24 hours later, HEK cells were transfected with 1.5µg vector pRubic-PD-1/pRubic-empty vector, and 1.0µg pCL-ECO vector, using X-tremeGENE 9 DNA Transfection Reagent (06365787001, Roche). Retroviral supernatants were harvested after 48 and 72 hours. Viral particles were concentrated by spinning at 20,000 rpm for 2 hours at 4°C using the Avanti J-30I centrifuge

(Beckman Coulter). pRubic-PD-1 and pRubic-empty retroviral titers were determined by using the qPCR Retrovirus Titration kit according to manufacturer's instruction.

CD4$^+$ T_{convs} transduction and adoptive transfer

For adoptive transfer studies of pRubic transduced T_{convs}, T_{convs} were purified from single cell suspensions prepared from splenocytes of ROSA$^{CAS\text{-}GFP}$ mice. To specifically purify T_{conv} from splenocytes, the magnetic based EasySep CD4$^+$ T cell isolation kit (StemCell Technologies) was used to obtain CD4$^+$ T cells through negative selection. Next, enriched CD4$^+$ T cells were used as input for the Miltenyi CD4$^+$CD25$^+$ regulatory T cell isolation kit (Miltenyi Biotec) to separate CD25$^+$ from CD25$^-$ cells. Purity of negatively selected CD4$^+$CD25$^-$ cells was confirmed by flow cytometry, and used for transduction. Retroviral transduction of T_{conv} was performed as previously described by Kurachi et al[45]. In brief, T_{conv} cells were activated *in vitro* using CD3/CD28 dynabeads (1:5 bead:cell ratio) and 300U/mL IL-2 for 48 hours. Activated cells were harvested and enriched using a 30-60% Percoll gradient, in which activated, blasting cells accumulate at the interface layer of the centrifuged Percoll gradient. Cells derived from the interface layer were washed, and transferred to a 96-wells plate coated with 20 µg/mL Retronectin (Takara) and supplemented with 600U/mL of IL-2 and CD3/CD28 dynabeads (1:2 bead:cell ratio) and retroviral vectors (100 multiplicity of infection, pRubic-mCherry-sgPD-1 and pRubic-mCherry-Ctrl). Cells were spin-transduced at 2000g, 30°C for 60 minutes. After spin-transduction, cells were incubated at 37°C, 5% CO2 overnight, and further used for *in vitro* analyses or adoptive transfer experiments.

TIDE analysis

The TIDE webtool[46] was used to assess Crispr-CAS9 editing efficiency of PDCD1 gene in pRubic transduced CD4$^+$ T_{convs}. After transduction, pRubic-sgPD-1 and pRubic-Ctrl transduced CD4$^+$ T_{convs} were cultured in cIMDM supplemented with 300U/ml of IL-2. After 96 hours, DNA was isolated using QIAamp DNA Micro kit (56304, QIAGEN) according to the manufacturer's instructions followed by PCR amplification of exon 2 of *PDCD1* gene (forward 5'-TCAGTTATGCTGAAGGAAGAGC-3', reverse 5'-GGCAGAGAGCCTAAGAGGTC-3') using 2µl 10x High Fidelity PCR Buffer (P/N 52045, Thermofisher), 0.6µl (50mM) MgSO4 (P/N 52044, Thermofisher), 0.4µl (10mM) dNTP mix (P/N y02256, Thermofisher), 0.25µl Platinum Taq (DNA Polymerase High Fidelity; 11304-011, Thermofisher) and 1µL of each primer. Amplified DNA was purified from an 1% agarose gel using Illustra GFX PCR DNA and Gel Band Purification kit. Next, DNA was sequenced by Sanger sequencing (PDCD1 exon 2 forward primer 5'-TCAGTTATGCTGAAGGAAGAGC-3' and samples were analyzed using the TIDE webtool using gRNA sequence targeting PDCD1 exon 2 ('5-CAGCTTGTCCAACTGGTCGG-3') (http://tide.nki.nl), using DNA from pRubic-Ctrl as control sample. Default parameters were used and decomposition window was set form 304-450bp.

Adoptive transfer of pRubic-mCherry transduced CD4$^+$ T_{convs}

For adoptive transfer, CD3/CD28 Dynabeads were magnetically removed, cells were washed and resuspended in HBSS and intravenously injected into mice bearing 25mm^2 mammary tumors of orthotopically injected KEP cell-line (2*10^6 cells/mouse). After 7 days, mice were sacrificed, single cell suspensions were prepared and adoptively transferred cells were analysed by flow cytometry as described above.

The Cancer Genome Atlas (TCGA) and breast cancer GEMM gene expression correlation analysis

Gene expression data of *FOXP3, PDCD1* and *CSF1R (*log2(norm_count+1)) were obtained from the TCGA breast cancer cohort (n=1218, version 2017-10-13, accessible through https://tcga-xena-hub.s3.us-east 1.amazonaws.com/download/TCGA.BRCA.sampleMap%2FHiSeqV2.gz. Correlation analysis was performed using University of California Santa Cruz's XenaBrowser.net. *Foxp3*, *Pdcd1* and *Csf1r* gene expression data from Breast cancer GEMMs were obtained and analysed as previously described[29].

KEP TAM gene expression analysis

GSEA[61] was performed using GSEA software (v. 4.0.3) on mSigDB Hallmark gene sets[62] using normalized gene expression data of "WT-MG-KEP" and "TAM-KEP" datasets obtained from GSE126268, as previously described[39]. Permutations for each gene set was conducted 1000 times to obtain an empirical null distribution.

Immunohistochemistry

Immunohistochemical analyses were performed by the Animal Pathology facility at the Netherlands Cancer Institute. Formalin-fixed tissues were processed, sectioned and stained as described[63]. In brief, tissues were fixed for 24h in 10% neutral buffered formalin and embedded in paraffin. Slides were digitally processed using the Panoramic P1000 slidescanner, and analysed in QuPath (V.03.0).

RNAseq of T_{regs} and CD4$^+$ T_{convs}

For transcriptome analysis of T_{regs} from end-stage (225mm^2) KEP tumors, WT mammary gland and spleen, single cell suspensions were prepared as described before[9]. A minimum of 70.000 T_{regs} (Live, CD45$^+$, CD3$^+$, CD4$^+$, CD25^{high}) or CD4$^+$ T_{convs} (Live, CD45$^+$, CD3$^+$, CD4$^+$, CD25$^-$) were sorted in RLT buffer with 1% β-mercapto ethanol. Due to low abundance of T_{regs} in WT mammary glands, tissue of 3 mice was pooled for each WT T_{reg} sample prior to sorting. Library preparation was performed as previously described[64]. Total RNA was extracted using RNAeasy mini kit (Qiagen). RNA quality and quantity control was performed using Agilent RNA 6000 Pico Kit and 2100 Bioanalyzer System. RNA samples with an RNA Integrity Number > 8 were subjected to library preparation. The strand-specific reads (65bp single-end) were sequenced with the HiSeq 2500 machine. Demultiplexing of the

reads was performed with Illumina's bcl2fastq. Demultiplexed reads were aligned against the mouse reference genome (build 38) using TopHat (version 2.1.0, bowtie 1.1). TopHat was supplied with a known set of gene models (Ensembl version 77) and was guided to use the first-strand as the library-type. As additional parameters --prefilter-multihits and --no coverage were used. Normalized counts from DESeqDataSet from the DESeq2 package were subjected to calculate correlation among the samples by using 'cor' function using spearman method in R language (version 4.0.2).

T_{reg} suppression assays

T_{reg}-T cell suppression assays were performed as previously described[59]. In brief, T_{regs} (Live, $CD45^{+,}$ $CD3^{+}$, $CD8^{-}$ $CD4^{+}$, $CD25^{high}$) sorted from freshly isolated KEP mammary tumors ($225mm^2$) were activated overnight in IMDM containing 8% FCS, 100 IU/ml penicillin, 100 µg/ml streptomycin, 0.5% β-mercapto-ethanol, 300U/mL IL-2, 1:5 bead:cell ratio CD3/CD28 coated beads (Thermofisher). Per condition, $5.0*10^5$ cells were seeded in 96-wells plate, which were further diluted to appropriate ratios (1:1 – 1:8). Responder cells (Live, $CD45^{+,}$ $CD3^{+}$, $CD4^{+}$, $CD25^{-}$ and Live, $CD45^{+,}$ $CD3^{+}$, $CD8^{+}$) were rested overnight. Next, responder cells were labelled with CellTraceViolet, and co-cultured with T_{regs} in cIMDM supplemented with CD3/CD28 beads (1:5 bead cell ratio) for 96 hours (without exogenous IL-2).

Statistical analysis

Data analyses were performed using GraphPad Prism (version 8). The statistical tests used are described in figure legends. All tests were performed two-tailed. P-values < 0.05 were considered statistically significant. Sample sizes for mouse intervention experiments were pre-determined using G*Power software (version 3.1). Asterisks indicate statistically significant differences compared to WT. * $P < 0.05$, ** $P < 0.01$, *** $P < 0.001$, **** $P < 0.0001$.

Acknowledgements

Research in the De Visser laboratory is funded by the Netherlands Organization for Scientific Research (grant NWO-VICI 91819616), the Dutch Cancer Society (KWF10083; KWF10623, KWF13191), European Research Council Consolidator award (InflaMet 615300) and Oncode Institute. K.K. is funded by the NWO Oncology Graduate School Amsterdam (OOA) Diamond Program. We acknowledge members of the Tumor Biology & Immunology Department, NKI for their insightful input. We thank the flow cytometry facility, genomics core facility, animal laboratory facility, transgenesis facility and animal pathology facility of the Netherlands Cancer Institute for technical assistance.

Data availability

Available from the authors upon reasonable request.

Contributions

K.K. and K.E.d.V. conceived the ideas and designed the experiments. K.K., C.S. performed experiments and data analysis. M.D.W., D.A.M, provided technical assistance. M.A. performed bioinformatical analysis. K.K., D.K., K.V., C.-S.H., and L.R. performed animal experiments. C.H.R. and M.S. provided the anti-CSF-1R antibody and control antibody. K.E.d.V. supervised the study, K.E.d.V and K.K. acquired funding, K.K. and K.E.d.V. wrote the paper and prepared the figures with input from all authors.

Conflict of interest statement

K.E.d.V. reports research funding from Roche/Genentech and is consultant for Macomics. C.R is an employee of Roche and owns intellectual property for the use of CSF1R-inhibitors. M.S. is an employee of Roche.

REFERENCES

1. Vonderheide, R. H., Domchek, S. M. & Clark, A. S. Immunotherapy for breast cancer: What are we missing? *Clin. Cancer Res.* **23**, 2640–2646 (2017).
2. Garner, H. & de Visser, K. E. Immune crosstalk in cancer progression and metastatic spread: a complex conversation. *Nat. Rev. Immunol.* 1–15 (2020) doi:10.1038/s41577-019-0271-z.
3. Binnewies, M. *et al.* Understanding the tumor immune microenvironment (TIME) for effective therapy. *Nat. Med.* **24**, 541–550 (2018).
4. Bates, J. P., Derakhshandeh, R., Jones, L. & Webb, T. J. Mechanisms of immune evasion in breast cancer. *BMC Cancer* **18**, 1–14 (2018).
5. Bates, G. J. *et al.* Quantification of regulatory T cells enables the identification of high-risk breast cancer patients and those at risk of late relapse. *J. Clin. Oncol.* **24**, 5373–5380 (2006).
6. Jiang, D., Gao, Z., Cai, Z., Wang, M. & He, J. Clinicopathological and prognostic significance of FOXP3+ tumor infiltrating lymphocytes in patients with breast cancer: A meta-analysis. *BMC Cancer* **15**, (2015).
7. Bos, P. D., Plitas, G., Rudra, D., Lee, S. Y. & Rudensky, A. Y. Transient regulatory T cell ablation deters oncogene-driven breast cancer and enhances radiotherapy. *J. Exp. Med.* **210**, 2435–2466 (2013).
8. Liu, J. *et al.* Improved efficacy of neoadjuvant compared to adjuvant immunotherapy to eradicate metastatic disease. *Cancer Discov.* **6**, 1382–1399 (2016).
9. Kos, K. & de Visser, K. E. The Multifaceted Role of Regulatory T Cells in Breast Cancer. *Annu. Rev. Cancer Biol.* **5**, (2021).
10. Kos, K. *et al.* Tumor-educated Tregs drive organ-specific metastasis in breast cancer by impairing NK cells in the lymph node niche. *Cell Rep.* **38**, 110447 (2022).
11. Lee, W. & Lee, G. R. Transcriptional regulation and development of regulatory T cells. *Exp. Mol. Med.* **50**, e456 (2018).
12. Josefowicz, S. *et al.* Extrathymically generated regulatory T cells control mucosal TH2 inflammation. *Nature* **482**, 395–399 (2012).
13. Zheng, Y. *et al.* Role of conserved non-coding DNA elements in the Foxp3 gene in regulatory T-cell fate. *Nature* **463**, 808–812 (2010).
14. Xu, L., Kitani, A. & Strober, W. Molecular mechanisms regulating TGF-B-induced Foxp3 expression. *Mucosal Immunology* vol. 3 230–238 (2010).
15. Campbell, C. *et al.* Extrathymically Generated Regulatory T Cells Establish a Niche for Intestinal Border-Dwelling Bacteria and Affect Physiologic Metabolite Balance. *Immunity* **48**, 1245–1257 (2018).
16. Kanamori, M., Nakatsukasa, H., Okada, M., Lu, Q. & Yoshimura, A. Induced Regulatory T Cells: Their Development, Stability, and Applications. *Trends Immunol.* **37**, 803–811 (2016).
17. Knight, D. *et al.* PD-1 Inhibitory Receptor Downregulates Asparaginyl Endopeptidase and Maintains Foxp3 Transcription Factor Stability in Induced Regulatory T Cells. *Immunity* **49**, 247-263.e7 (2018).
18. Amarnath, S. *et al.* The PDL1-PD1 Axis Converts Human T_H1 Cells into Regulatory T Cells. *Sci. Transl. Med.* **3**, 111ra120 LP-111ra120 (2011).
19. Du, H. *et al.* The co-expression characteristics of LAG3 and PD-1 on the T cells of patients with breast cancer reveal a new therapeutic strategy. *Int. Immunopharmacol.* **78**, 106113 (2020).
20. Plitas, G. *et al.* Regulatory T Cells Exhibit Distinct Features in Human Breast Cancer. *Immunity* **45**, 1122–1134 (2016).
21. Sugiyama, D. *et al.* Anti-CCR4 mAb selectively depletes effector-Type FoxP3+CD4+ regulatory T cells, evoking antitumor immune responses in humans. *Proc. Natl. Acad. Sci. U. S. A.* **110**, 17945–17950 (2013).
22. Olkhanud, P. B. *et al.* Breast cancer lung metastasis requires expression of chemokine receptor CCR4 and regulatory T cells. *Cancer Res.* **69**, 5996–6004 (2009).
23. Kaplanov, I. *et al.* Blocking IL-1β reverses the immunosuppression in mouse breast cancer and synergizes with anti–PD-1 for tumor abrogation. *Proc. Natl. Acad. Sci. U. S. A.* **116**, 1361–1369 (2019).
24. Schmidt, A. *et al.* Human macrophages induce CD4 + Foxp3 + regulatory T cells via binding and re-release of TGF-β. *Immunol. Cell Biol.* **94**, 747–762 (2016).
25. Casanova-Acebes, M. *et al.* Tissue-resident macrophages provide a pro-tumorigenic niche to early NSCLC cells. *Nat. 2021 5957868* **595**, 578–584 (2021).
26. Qiu, S. Q. *et al.* Tumor-associated macrophages in breast cancer: Innocent bystander or important player? *Cancer Treat. Rev.* **70**, 178–189 (2018).
27. Derksen, P. W. B. *et al.* Somatic inactivation of E-cadherin and p53 in mice leads to metastatic lobular mammary carcinoma through induction of anoikis resistance and angiogenesis. *Cancer Cell* **10**, 437–449 (2006).
28. Salvagno, C. *et al.* Therapeutic targeting of macrophages enhances chemotherapy efficacy by unleashing type I interferon response. *Nat. Cell Biol.* **21**, 511–521 (2019).

29. Wellenstein, M. D. *et al.* Loss of p53 triggers WNT-dependent systemic inflammation to drive breast cancer metastasis. *Nature* **572**, 538–542 (2019).
30. Goldman, M. *et al.* Visualizing and interpreting cancer genomics data via the Xena platform. *Nat. Biotechnol.* **38**, 675–678 (2020).
31. Ries, C. H. *et al.* Targeting tumor-associated macrophages with anti-CSF-1R antibody reveals a strategy for cancer therapy. *Cancer Cell* **25**, 846–859 (2014).
32. Hume, D. A. & MacDonald, K. P. A. Therapeutic applications of macrophage colony-stimulating factor-1 (CSF-1) and antagonists of CSF-1 receptor (CSF-1R) signaling. *Blood* vol. 119 1810–1820 (2012).
33. Ushio, A. *et al.* CCL22-Producing Resident Macrophages Enhance T Cell Response in Sjögren's Syndrome. *Front. Immunol.* **9**, 2594 (2018).
34. Mizukami, Y. *et al.* CCL17 and CCL22 chemokines within tumor microenvironment are related to accumulation of Foxp3+ regulatory T cells in gastric cancer. *Int. J. cancer* **122**, 2286–2293 (2008).
35. Loyher, P. L. *et al.* CCR2 influences T regulatory cell migration to tumors and serves as a biomarker of cyclophosphamide sensitivity. *Cancer Res.* **76**, 6483–6494 (2016).
36. Mailloux, A. W. & Young, M. R. I. Regulatory T-cell trafficking: from thymic development to tumor-induced immune suppression. *Crit. Rev. Immunol.* **30**, 435–447 (2010).
37. Wang, L. *et al.* Connecting blood and intratumoral Treg cell activity in predicting future relapse in breast cancer. *Nat. Immunol.* **20**, 1220–1230 (2019).
38. Wang, D. *et al.* Colorectal cancer cell-derived CCL20 recruits regulatory T cells to promote chemoresistance via FOXO1/CEBPB/NF-κB signaling. *J. Immunother. Cancer* **7**, 215 (2019).
39. Tuit, S. *et al.* Transcriptional Signature Derived from Murine Tumor-Associated Macrophages Correlates with Poor Outcome in Breast Cancer Patients Article Transcriptional Signature Derived from Murine Tumor-Associated Macrophages Correlates with Poor Outcome in Breast Cancer Patients. *Cell Rep.* **29**, (2019).
40. Francisco, L. M. *et al.* PD-L1 regulates the development, maintenance, and function of induced regulatory T cells. *J. Exp. Med.* **206**, 3015–3029 (2009).
41. Huang, A. C. *et al.* A single dose of neoadjuvant PD-1 blockade predicts clinical outcomes in resectable melanoma. *Nat. Med.* **25**, 454–461 (2019).
42. Kamada, T. *et al.* PD-1(+) regulatory T cells amplified by PD-1 blockade promote hyperprogression of cancer. *PNAS* **116**, 9999–10008 (2019).
43. Kumagai, S. *et al.* The PD-1 expression balance between effector and regulatory T cells predicts the clinical efficacy of PD-1 blockade therapies. *Nat. Immunol.* **21**, 1346–1358 (2020).
44. Peligero, C. *et al.* PD-L1 Blockade Differentially Impacts Regulatory T Cells from HIV-Infected Individuals Depending on Plasma Viremia. *PLoS Pathog.* **11**, (2015).
45. Kurachi, M. *et al.* Optimized retroviral transduction of mouse T cells for in vivo assessment of gene function. *Nat. Protoc.* **12**, 1980–1998 (2017).
46. Brinkman, E. K., Chen, T., Amendola, M. & Van Steensel, B. Easy quantitative assessment of genome editing by sequence trace decomposition. *Nucleic Acids Res.* **42**, e168–e168 (2014).
47. Jiang, D., Gao, Z., Cai, Z., Wang, M. & He, J. Clinicopathological and prognostic significance of FOXP3+ tumor infiltrating lymphocytes in patients with breast cancer: a meta-analysis. *BMC Cancer* **15**, 727 (2015).
48. Koenecke, C. *et al.* Alloantigen-specific de novo-induced Foxp3+ Treg revert in vivo and do not protect from experimental GVHD. *Eur. J. Immunol.* **39**, 3091–3096 (2009).
49. Ghali, J. R., Alikhan, M. A., Holdsworth, S. R. & Kitching, A. R. Induced regulatory T cells are phenotypically unstable and do not protect mice from rapidly progressive glomerulonephritis. *Immunology* **150**, 100–114 (2017).
50. Su, S. *et al.* Blocking the recruitment of naive CD4+ T cells reverses immunosuppression in breast cancer. *Cell Res.* **27**, 461–482 (2017).
51. DeNardo, D. G. & Ruffell, B. Macrophages as regulators of tumour immunity and immunotherapy. *Nature Reviews Immunology* vol. 19 369–382 (2019).
52. Tan, Y. *et al.* Tumor-Associated Macrophages: A Potential Target for Cancer Therapy. *Front. Oncol.* **0**, 2201 (2021).
53. Campesato, L. F. *et al.* Blockade of the AHR restricts a Treg-macrophage suppressive axis induced by L-Kynurenine. *Nat. Commun. 2020 111* **11**, 1–11 (2020).
54. Sanin, D. E., Prendergast, C. T. & Mountford, A. P. IL-10 Production in Macrophages Is Regulated by a TLR-Driven CREB-Mediated Mechanism That Is Linked to Genes Involved in Cell Metabolism. *J. Immunol.* **195**, 1218–1232 (2015).
55. Ceci, C., Atzori, M. G., Lacal, P. M. & Graziani, G. Targeting tumor-associated macrophages to increase the efficacy of immune checkpoint inhibitors: A glimpse into novel therapeutic approaches for metastatic melanoma. *Cancers* vol. 12 1–32 (2020).
56. Amaia, M.-U. *et al.* Overcoming microenvironmental resistance to PD-1 blockade in genetically

engineered lung cancer models. *Sci. Transl. Med.* **13**, eabd1616 (2021).
57. DiDomenico, J. *et al.* The immune checkpoint protein PD-L1 induces and maintains regulatory T cells in glioblastoma. *Oncoimmunology* **7**, e1448329–e1448329 (2018).
58. Chen, X. *et al.* PD-1 regulates extrathymic regulatory T-cell differentiation. *Eur. J. Immunol.* **44**, 2603–2616 (2014).
59. Kos, K., van Baalen, M., Meijer, D. A. & de Visser, K. E. Flow cytometry-based isolation of tumor-associated regulatory T cells and assessment of their suppressive potential. in *Methods in Enzymology* (2019). doi:10.1016/bs.mie.2019.07.035.
60. Heinen, A. P. *et al.* Improved method to retain cytosolic reporter protein fluorescence while staining for nuclear proteins. *Cytom. Part A* **85**, 621–627 (2014).
61. Subramanian, A. *et al.* Gene set enrichment analysis: A knowledge-based approach for interpreting genome-wide expression profiles. *Proc. Natl. Acad. Sci. U. S. A.* **102**, 15545–15550 (2005).
62. Liberzon, A. *et al.* The Molecular Signatures Database Hallmark Gene Set Collection. *Cell Syst.* **1**, 417–425 (2015).
63. Doornebal, C. W. *et al.* A Preclinical Mouse Model of Invasive Lobular Breast Cancer Metastasis. *Cancer Res.* **73**, 353 LP – 363 (2013).
64. Aslam, M. A. *et al.* The Ig heavy chain protein but not its message controls early B cell development. *Proc. Natl. Acad. Sci. U. S. A.* **117**, 31343–31352 (2020).

SUPPLEMENTARY MATERIAL

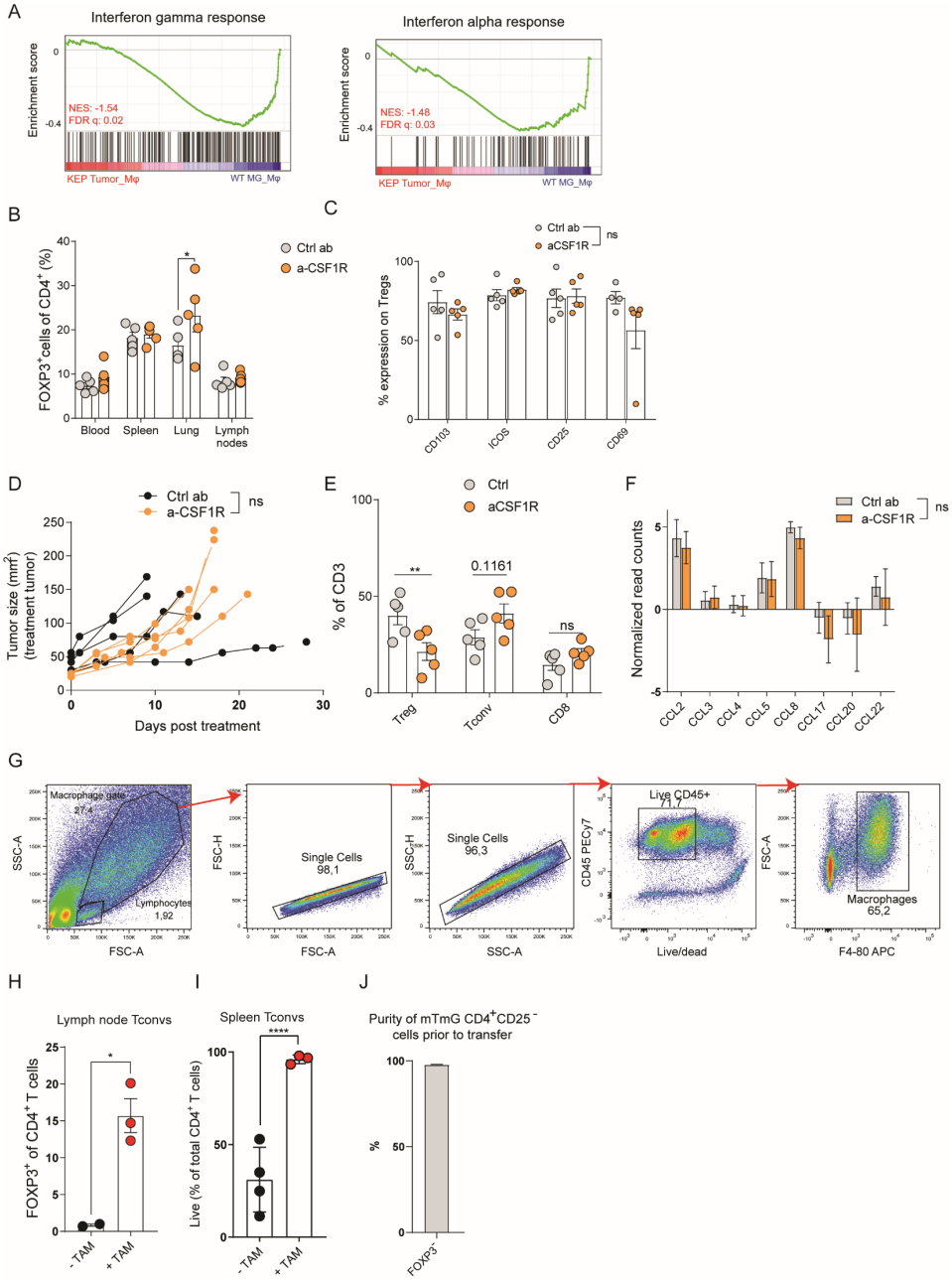

SUPPLEMENTARY FIGURE 1.

A. GSEA comparing gene expression of KEP TAMs and WT mammary gland macrophages[39]. IFN-γ and IFN-α gene sets from[62] are shown. Normalized enrichment score (NES) and false discovery rate (FDR) indicated. Data obtained using a previously published dataset[39]. **B.** Frequency of $FOXP3^+$ cells of $CD4^+$ cells in indicated tissues of KEP tumor-bearing mice treated with anti-CSF1R or control antibody (n=5 mice/group). **C.** Quantification of CD103, ICOS, CD25 and CD69 on $CD4^+$ $FOXP3^+$ T cells in KEP mammary tumors of KEP mice treated with control antibody, or anti-CSF1R (n=4-5 mice/group), as determined by flow cytometry. **D.** Tumor growth curves of mice treated with anti-CSF1R or control antibody. Treatment tumor is shown. Treatment was stopped when cumulative tumor burden reached $225mm^2$ (n=5 mice/group). **E.** Frequencies of T_{regs} ($CD4^+FOXP3^+$), $CD4^+$ T_{convs} ($CD4^+FOXP3^-$) and $CD8^+$ T cells of total $CD3^+$ T cells in mammary tumors of KEP mice treated with control antibody, or anti-CSF1R (n=5 mice/group). **F.** Quantification of mRNA expression (normalised read counts) of indicated chemokines in mammary tumors mice treated with anti-CSF1R or control (n=5 mice/group). **G.** Gating strategy for sorting live, $CD45^+$, $F4/80^+$ macrophages from spontaneous KEP mammary tumors. **H.** Percentage of $FOXP3^+$ cells in $CD4^+$ T_{convs} ($CD45^+CD3^+CD4^+CD25^-$) isolated from draining lymph nodes of tumor-bearing KEP mice after co-culture with, or without TAMs ($CD3^-F4/80^{high}$) for 72 hours (data pooled from 2 independent experiments). **I.** Percentage of live (negative for live/dead marker) cells, gated on total $CD4^+$ T cells in co-cultures of sorted $CD4^+$ t cell populations from indicated tissues with TAMs, after 72 hours. **J.** Purity, ($FOXP3^-$), of $CD4^+$ T_{convs} ($CD45^+CD3^+CD4^+CD25^-$) sorted from spleens of mTmG mice, after activation with CD3/CD28 beads for 96 hours (n=2 mice). Data in B,C,E,F,H-J depict mean ± SEM. P-values determined by Two-way ANOVA (B,C,E,F), Student's T test (H,I), Area under curve calculation (D). * $P < 0.05$, ** $P < 0.01$.

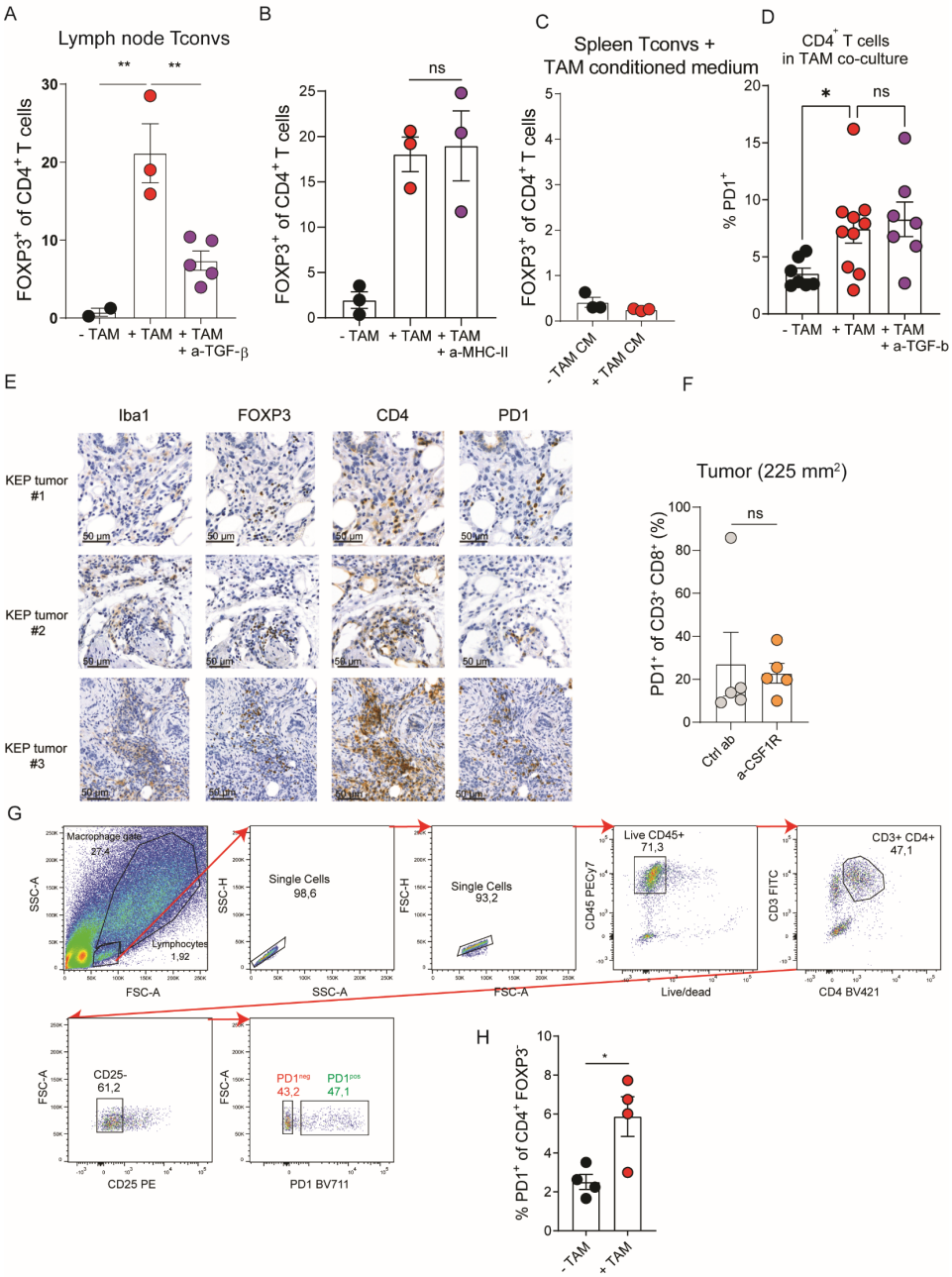
A
Lymph node Tconvs
FOXP3+ of CD4+ T cells
- TAM
+ TAM
+ TAM + a-TGF-β
B
FOXP3+ of CD4+ T cells
ns
- TAM
+ TAM
+ TAM + a-MHC-II
C
Spleen Tconvs + TAM conditioned medium
FOXP3+ of CD4+ T cells
- TAM CM
+ TAM CM
D
CD4+ T cells in TAM co-culture
% PD1+
ns
- TAM
+ TAM
+ TAM + a-TGF-b
E
Iba1
FOXP3
CD4
PD1
KEP tumor #1
KEP tumor #2
KEP tumor #3
50 µm
F
Tumor (225 mm2)
PD1+ of CD3+ CD8+ (%)
ns
Ctrl ab
a-CSF1R
G
Macrophage gate 27,4
Lymphocytes 1,92
SSC-A
FSC-A
Single Cells 98,6
SSC-H
SSC-A
Single Cells 93,2
FSC-H
FSC-A
Live CD45+ 71,3
CD45 PECy7
Live/dead
CD3+ CD4+ 47,1
CD3 FITC
CD4 BV421
CD25- 61,2
FSC-A
CD25 PE
PD1neg 43,2
PD1pos 47,1
FSC-A
PD1 BV711
H
% PD1+ of CD4+FOXP3-
- TAM
+ TAM

SUPPLEMENTARY FIGURE 2.

A. Percentage of FOXP3$^+$ cells in CD4$^+$ T_{convs} (CD45$^+$CD3$^+$CD4$^+$CD25$^-$) isolated from draining lymph nodes of tumor-bearing KEP mice after co-culture with TAMs (CD3$^-$F4/80^{high}) and 50 µg/mL anti-TGF-β for 72 hours (data pooled from 3-6 independent *in vitro* experiments). **B.** Percentage of FOXP3$^+$ cells in CD4$^+$ T_{convs} (CD45$^+$CD3$^+$CD4$^+$CD25$^-$) isolated from spleens of tumor-bearing KEP mice after co-culture with TAMs (CD3$^-$F4/80^{high}) and 100 µg/mL anti-MHC-II for 72 hours (data pooled from 2 independent *in vitro* experiments with 3 biological replicates). **C.** Percentage of FOXP3$^+$ cells in CD4$^+$ T_{convs} (CD45$^+$CD3$^+$CD4$^+$CD25$^-$) isolated from spleens of tumor-bearing KEP mice after culture in conditioned medium obtained from TAMs that were cultured for 48h and supplemented with 20ng/mL M-CSF and CD3/CD28 beads (data pooled from 2 independent *in vitro* experiments, n=3 mice/group). **D.** Quantification of PD-1 expression gated on total CD4$^+$ T cells in CD4$^+$ T_{convs} isolated from spleens of tumor-bearing KEP mice that were co-cultured with TAMs for 72h with 300U/mL IL-2 and 20ng/mL M-CSF and 50 µg/mL anti-TGF-β. (n=7-10 mice/group). **E.** immunohistochemical staining of Iba1, FOXP3, CD4, PD-1 on serial sections of mammary tumors (225mm^2) of three independent KEP mice. Representative images of Iba1, CD4 and PD1 surrounding clusters of FOXP3$^+$ cells are shown. **F.** Frequency of PD-1$^+$ cells of CD8$^+$ T cells in mammary tumors of mice treated with anti-CSF1R or control (n=5 mice/group). **G.** Gating strategy for sorting live, CD45$^+$, CD3$^+$, CD4$^+$, CD25$^-$, PD-1$^{pos/neg}$ cells from spontaneous KEP mammary tumors. **H.** Quantification of PD-1 expression in PD-1^{neg}CD4$^+$CD25$^-$ T cells isolated from KEP mammary tumors cultured with CD45$^+$ F4/80^{high} macrophages for 72h with 300U/mL IL-2 and 20ng/mL M-CSF. Data pooled from 4 independent *in vitro* experiments. Data in A-D, F,H depicts mean ± SEM. P-value determined by One-way ANOVA (A,D) Unpaired Student's T test (B-C, F,H).

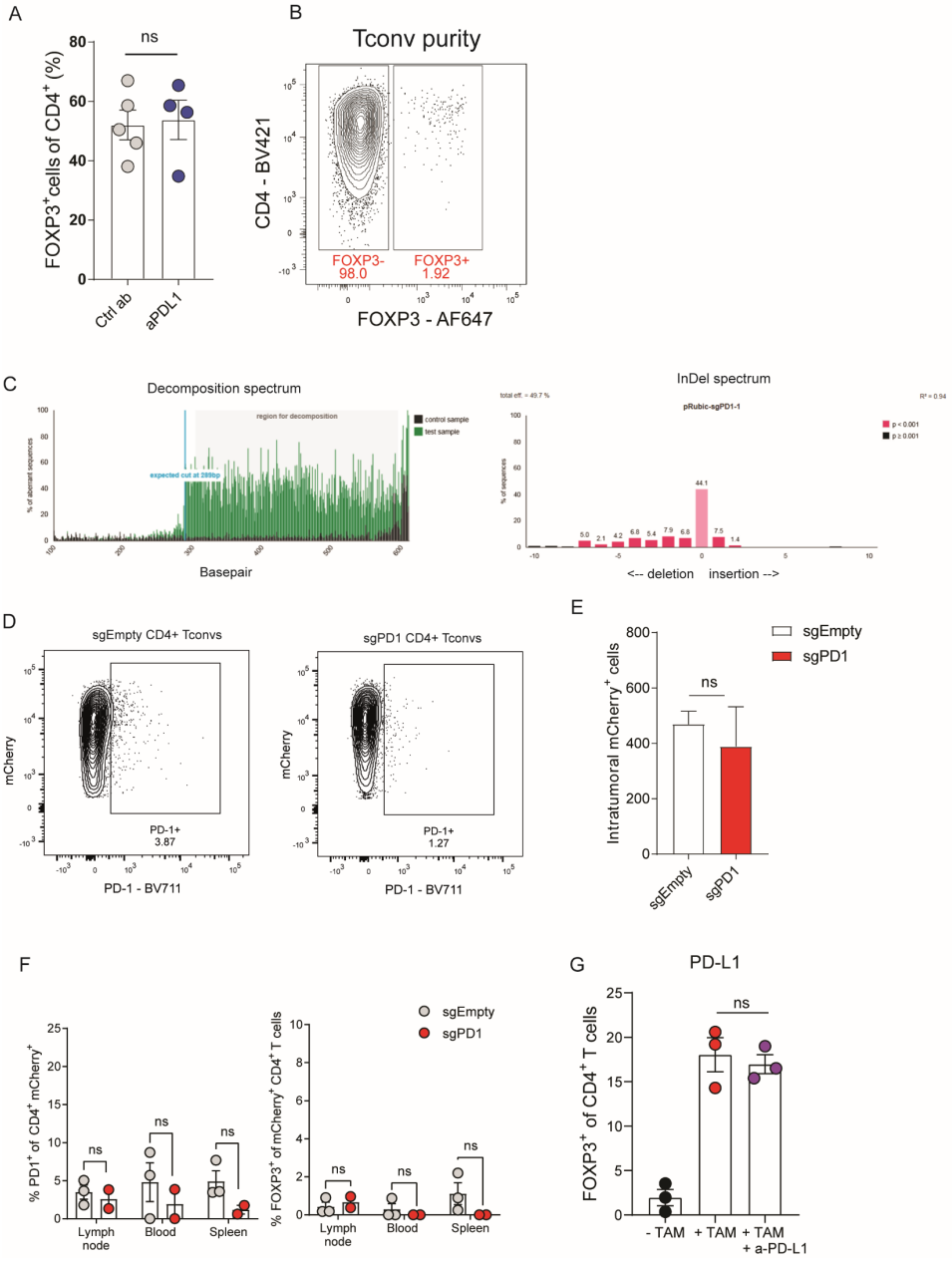
A
ns
FOXP3+cells of CD4+ (%)
Ctrl ab
aPDL1
B
Tconv purity
CD4 - BV421
FOXP3- 98.0
FOXP3+ 1.92
FOXP3 - AF647
C
Decomposition spectrum
region for decomposition
control sample
test sample
expected cut at 289bp
% of aberrant sequences
Basepair
InDel spectrum
pRubic-sgPD1-1
p < 0.001
p ≥ 0.001
% of sequences
<-- deletion insertion -->
D
sgEmpty CD4+ Tconvs
sgPD1 CD4+ Tconvs
mCherry
PD-1+ 3.87
PD-1+ 1.27
PD-1 - BV711
E
sgEmpty
sgPD1
Intratumoral mCherry+ cells
ns
sgEmpty
sgPD1
F
% PD1+ of CD4+ mCherry+
% FOXP3+ of mCherry+ CD4+ T cells
sgEmpty
sgPD1
ns
Lymph node
Blood
Spleen
G
PD-L1
FOXP3+ of CD4+ T cells
ns
- TAM
+ TAM
+ TAM + a-PD-L1

SUPPLEMENTARY FIGURE 3.

A. Frequency of $FOXP3^+$ cells of $CD4^+$ cells in mammary tumors of KEP mice treated with anti-PD-L1 or control (n=4-5 mice/group). These mice were treated in the cohort shown in figure 2C, therefore, data in the control group are the same as shown in 2C. **B.** Dot plot depicting CD4 and FOXP3 expression of total live cells of $CD4^+CD25^-$ T_{convs} purified from splenocytes of $ROSA^{CAS9\text{-}GFP}$ mice after *in vitro* activation and transduction. **C.** TIDE analysis performed depicting decomposition (left) and InDel (right) spectrum performed on DNA isolated from purified $CD4^+CD25^-$ T_{convs} transduced with pRubic-sgPD-1, using pRubic-Ctrl transduced cells as control. **D.** Dot plots depicting mCherry and PD1 expression of live cells of $CD4^+CD25^-$ T_{convs} purified from splenocytes of $ROSA^{CAS9\text{-}GFP}$ mice after *in vitro* activation and transduction with indicated vectors. **E.** Number of $mCherry^+$ cells recorded in flow-cytometric analysis of KEP cell-line tumors of mice receiving adoptive transfer of pRubic-sgPD-1 or pRubic-Ctrl $CD4^+$ T_{convs} (n=3 mice/group). **F.** Quantification of PD-1 (left) and FOXP3 (right) expression on $CD4^+$ $mCherry^+$ cells in draining lymph nodes, blood and spleen of mice receiving adoptive transfer of pRubic-sgPD-1 or pRubic-Ctrl T_{convs} (n=2-3 mice/group). **H.** Percentage of $FOXP3^+$ cells in $CD4^+$ T_{convs} ($CD45^+CD3^+CD4^+CD25^-$) isolated from spleens of tumor-bearing KEP mice after co-culture with TAMs ($CD3^-F4/80^{high}$) and 50 µg/mL anti-PD-L1 for 72 hours (data pooled from 2 independent *in vitro* experiments, with 3 biological replicates). Data in A, B, E-G depict mean ± SEM. P-value determined by Unpaired Student's T test (A, E, G), Two-way ANOVA (F).

4

Tumor-educated T_{regs} drive organ-specific metastasis in breast cancer by impairing NK cells in the lymph node niche

Kevin Kos[1,2], Muhammad A. Aslam[1,3,11], Rieneke van de Ven[4,9,11], Max D. Wellenstein[1,2,10], Wietske Pieters[1], Antoinette van Weverwijk[1,2], Danique E.M. Duits[1,2], Kim van Pul[4], Cheei-Sing Hau[1,2], Kim Vrijland[1,2], Daphne Kaldenbach[1,2], Elisabeth A.M. Raeven[1,2], Sergio A. Quezada[5], Rudi Beyaert[6,7], Heinz Jacobs[1], Tanja D. de Gruijl[4], Karin E. de Visser[1,2,8,12]

Affiliations
[1] Division of Tumor Biology & Immunology, Netherlands Cancer Institute; 1066 CX Amsterdam, The Netherlands
[2] Oncode Institute, Utrecht; The Netherlands
[3] Institute of Molecular Biology and Biotechnology, Bahauddin Zakariya University; 60800 Multan, Pakistan
[4] Department of Medical Oncology, Amsterdam UMC, Vrije Universiteit Amsterdam, Cancer Center Amsterdam and Amsterdam Institute for Infection and Immunity;1081 HV Amsterdam, The Netherlands
[5] Cancer Immunology Unit, University College London Cancer Institute; WC1E 6DD London, UK
[6] Center for Inflammation Research, Unit of Molecular Signal Transduction in Inflammation, VIB; 9052 Ghent, Belgium
[7] Department of Biomedical Molecular Biology, Ghent University; 9052 Ghent, Belgium
[8] Department of Immunology, Leiden University Medical Center; Leiden, The Netherlands.
[9] Current address: Department of Otolaryngology/Head-Neck Surgery, Amsterdam UMC, Vrije Universiteit Amsterdam, Cancer Center Amsterdam and Amsterdam Institute for Infection and Immunity; 1081 HV Amsterdam, The Netherlands
[10] Current address: Hubrecht Institute, Royal Netherlands Academy of Arts and Sciences (KNAW) and University Medical Center Utrecht; 3584 CT Utrecht, The Netherlands
[11] These authors contributed equally
[12] Corresponding author: k.d.visser@nki.nl

Cell Reports. 2022, 38(9):110447

ABSTRACT

Breast cancer is accompanied by systemic immunosuppression which facilitates metastasis formation, but how this shapes organotropism of metastasis is poorly understood. Here, we investigate the impact of mammary tumorigenesis on T_{regs} in distant organs and how this impacts multi-organ metastatic disease. Using a preclinical mouse mammary tumor model that recapitulates human metastatic breast cancer, we observe systemic accumulation of activated, highly immunosuppressive T_{regs} during primary tumor growth. Tumor-educated T_{regs} show tissue-specific transcriptional rewiring in response to mammary tumorigenesis. This has functional consequences for organotropism of metastasis, as T_{reg} depletion reduces metastasis to tumor-draining lymph nodes, but not to lungs. Mechanistically, we find that T_{regs} control NK cell activation in lymph nodes, thereby facilitating lymph node metastasis. In line, an increased T_{reg}/NK cell ratio is observed in sentinel lymph nodes of breast cancer patients compared to healthy controls. This study highlights that immune regulation of metastatic disease is highly organ dependent.

Graphical Abstract

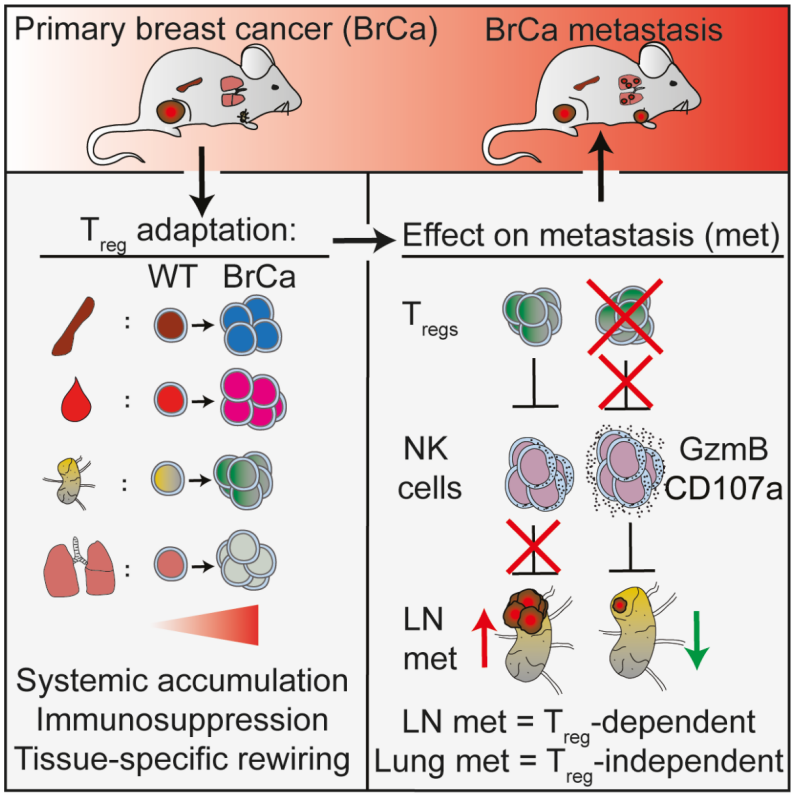

INTRODUCTION

The main cause of breast cancer-related mortality is metastatic disease. Over the past decades, breast cancer survival has improved through detection and intervention in early stages of breast cancer, but preventing and treating metastasis remains an unmet clinical need[1]. Disseminated cancer cells progress through a multistep cascade, which involves complex interactions between cancer- and host cells, including immune cells[2]. The immune system plays a dual role in metastasis formation. While properly activated cytotoxic immune cells are equipped to control metastasis, tumor-induced immunosuppressive immune cells exploit a diversity of mechanisms to promote metastasis[3]. Emerging data indicate that tissue tropism of metastasis may be influenced by the immune contexture in distant organs, suggesting an additional layer of complexity in metastasis formation[4]. However, how immunosuppressive mechanisms differ per metastatic site, and how this shapes tissue tropism of metastasis, is poorly understood.

An important cell type involved in immunosuppression in cancer is the $CD4^+FOXP3^+$ regulatory T cell (T_{reg})[5–7]. In breast cancer, immunosuppressive T_{regs} densely populate human tumors, and high levels of intratumoral T_{regs} correlate with high tumor grade and poor survival[6,8]. Intriguingly, clinical data suggest that primary breast tumors impact T_{regs} beyond the tumor micro-environment. T_{regs} in peripheral blood have been reported to be increased in breast cancer patients[9–12], and their responsiveness to cytokine stimulation is predictive of breast cancer relapse[13]. In addition, recent studies have shown that T_{regs} accumulate in sentinel lymph nodes (LNs) of breast cancer patients, which correlates with cancer spread to these LNs[14–18], suggesting a potential role for T_{regs} in modulating metastasis to tumor-draining LNs.

Despite these intriguing clinical observations, and the attention that tumor-associated T_{regs} have received in the context of breast cancer in recent years[7,19], the lack of preclinical models that closely recapitulate human multi-organ metastatic disease has limited our understanding of the importance of T_{regs} in cancer spread to different distant organs[20]. Preclinical studies performed with mouse models based on orthotopic inoculation of breast cancer cell lines have shown that ablation of T_{regs} can attenuate primary tumor growth and subsequent metastasis formation to the lungs[21–23]. However, research on T_{regs} in the context of cancer is mostly focused on their role in the micro-environment of primary tumors or metastases. The systemic impact of primary tumors on T_{regs} in distant organs, and their functional significance for metastasis formation in different tissue contexts has remained largely unclear. Additionally, the role of T_{regs} in hallmarks of metastatic disease such as systemic immunosuppression and the development of a pre-metastatic niche is understudied[3], and therefore remains elusive.

Here we describe how mammary tumors systemically rewire T_{regs}, and how this impacts metastatic disease to different organs. To achieve this, we utilized models that allow for interrogation of tissue-specific metastasis, *i.e.* the transgenic *Keratin14 (K14)-cre;Cdh1$^{F/F}$;Trp53$^{F/F}$* (KEP) mouse model of invasive mammary tumorigenesis[24], and the KEP-based mastectomy model for spontaneous multi-organ metastatic disease[25]. We observed systemic accumulation of activated, highly immunosuppressive T_{regs} during primary tumor growth. These T_{regs} showed striking tissue-specific transcriptional rewiring in response to mammary tumorigenesis, and elicited a tissue-specific effect on metastasis formation, as neoadjuvant depletion of T_{regs} reduced cancer spread to axillary (Ax.) LNs, but not to the lungs. Mechanistically, we demonstrate that T_{regs} promote LN metastasis formation through inhibition of NK cells in the lymph node niche. These findings add another mechanism to the emerging body of literature that immune regulation of metastatic disease is highly organ dependent, warranting a more personalized approach in the fight against metastatic disease.

RESULTS

Primary mammary tumors induce systemic expansion and activation of T_{regs}

To assess whether *de novo* mammary tumor formation exerts a systemic impact on T_{regs}, we examined the abundance, phenotype and activation status of T_{regs} in tumors, blood, and distant organs of the KEP mouse model, which spontaneously develops mammary tumors at 6-8 months of age resembling human invasive lobular carcinomas (ILC)[24]. We observed that mammary KEP tumors are highly infiltrated by FOXP3$^+$CD4$^+$ T cells, as compared to healthy mammary glands of age-matched wild-type (WT) littermate controls (Fig. 1A, 1B). Interestingly, increased frequencies and absolute counts of T_{regs} were also observed in blood and in loco-regional or distant organs that are conducive to metastatic spread such as tumor draining LNs (TDLNs, axillary and inguinal, dependent on the location of the primary mammary tumor), spleen, lungs and non-draining LNs (NDLNs) of KEP mice bearing end-stage mammary tumors (225mm^2) (Fig. 1A, C, S1A-B). Notably, we did not find a relative increase in CD4$^+$FOXP3$^-$, or CD8$^+$ T cells (with the exception of CD8$^+$ T cells in TDLNs) in tumor-bearing KEP mice (Fig. 1D, S1C-D). An increase in absolute cell counts was also observed for CD4$^+$FOXP3$^-$ and CD8$^+$ T cells in LNs and tumors (Fig. S1E-G), due to expansion of these tissue compartments in KEP mice versus WT controls. However, comparing the ratio of FOXP3$^+$/CD8$^+$ and FOXP3$^+$/FOXP3$^-$ cells in different tissues of tumor-bearing KEP mice and WT controls (Fig. S1H-I) confirmed that mammary tumorigenesis specifically and systemically expands T_{regs} amongst the adaptive immune cell compartment. We then assessed whether T_{reg} expansion is explained by their increased proliferation or survival in tumor-bearing KEP mice. Ki67 expression on T_{regs} in tumor-bearing KEP mice was found to be uniquely increased in LNs, compared to WT controls (Fig. S1J). Notably,

no difference was observed between TDLNs and NDLNs showing T_{reg} proliferation is systemically increased in LNs of tumor-bearing KEP mice (Fig. S1K). Furthermore, KEP T_{regs} showed increased viability when exposed to serum obtained from tumor-bearing KEP mice, as opposed to serum obtained from WT mice (Fig. S1L). Combined, these data suggest that LNs may be an important site for T_{reg} proliferation in KEP mice, and that a soluble factor in KEP serum may contribute to increased T_{reg} survival.

To investigate whether this systemic increase of T_{regs} is consistently observed across pre-clinical mouse models of breast cancer, we analyzed T_{reg} frequency in five different transgenic mouse models that represent different subsets of human breast cancers (Fig. 1E). Indeed, we found T_{regs} to be significantly increased in the blood of tumor-bearing mice of all five models compared to WT controls, indicating systemic T_{reg} expansion is a prevalent feature of mammary tumorigenesis.

Using high-dimensional flow cytometry, we observed that T_{regs} both in- and outside of mammary tumors, have increased expression of surface proteins associated with T_{reg} activation and suppressor function including CTLA4, ICOS, and CD103 in KEP tumor-bearing mice compared to WT controls, showing that these cells undergo a profound phenotypic change during mammary tumor progression (Fig. 1F, S1M-N). To address whether the enhanced activation state of KEP T_{regs} impacts their functionality throughout the tumor-bearing host, we FACS sorted T_{regs} from TDLNs, spleen and tumors from KEP mice and WT controls to assess their suppressive activity on the proliferation of $CD4^+$ and $CD8^+$ T cells *in vitro*. Regardless of the tissue of origin, T_{regs} from tumor-bearing mice were significantly more potent in suppressing T cell proliferation compared to T_{regs} isolated from WT mice (Fig. 1G-J), indicating that tumor-educated T_{regs} have enhanced immunosuppressive potential, both intratumorally, as well as in TDLNs and spleen.

We next determined the dynamics of T_{reg} accumulation and education by following T_{reg} frequency and phenotype in aging KEP mice (from 2 to 8 months of age). Around 3 months of age, most KEP mice display microscopic neoplastic lesions in their mammary glands which over time progress into palpable mammary tumors, with a median latency of 6-8 months[24]. T_{reg} frequency in blood gradually increased during neoplastic progression in KEP mice, and was significantly increased in KEP mice of 7 months and older prior to the onset of palpable mammary tumors, as compared to age-matched controls (Fig. 1K). Further analysis of these T_{regs} showed that the impact of mammary tumorigenesis on T_{reg} phenotype showed different kinetics per protein. Whereas the expression of CTLA4 increased prior to the development of palpable tumors, the expression of ICOS and CD103 was exclusively increased in tumor-bearing KEP mice (Fig. 1L, S1O-P). Together, these data demonstrate that primary mammary tumorigenesis engages T_{regs} beyond the tumor microenvironment, leading to their systemic expansion and activation.

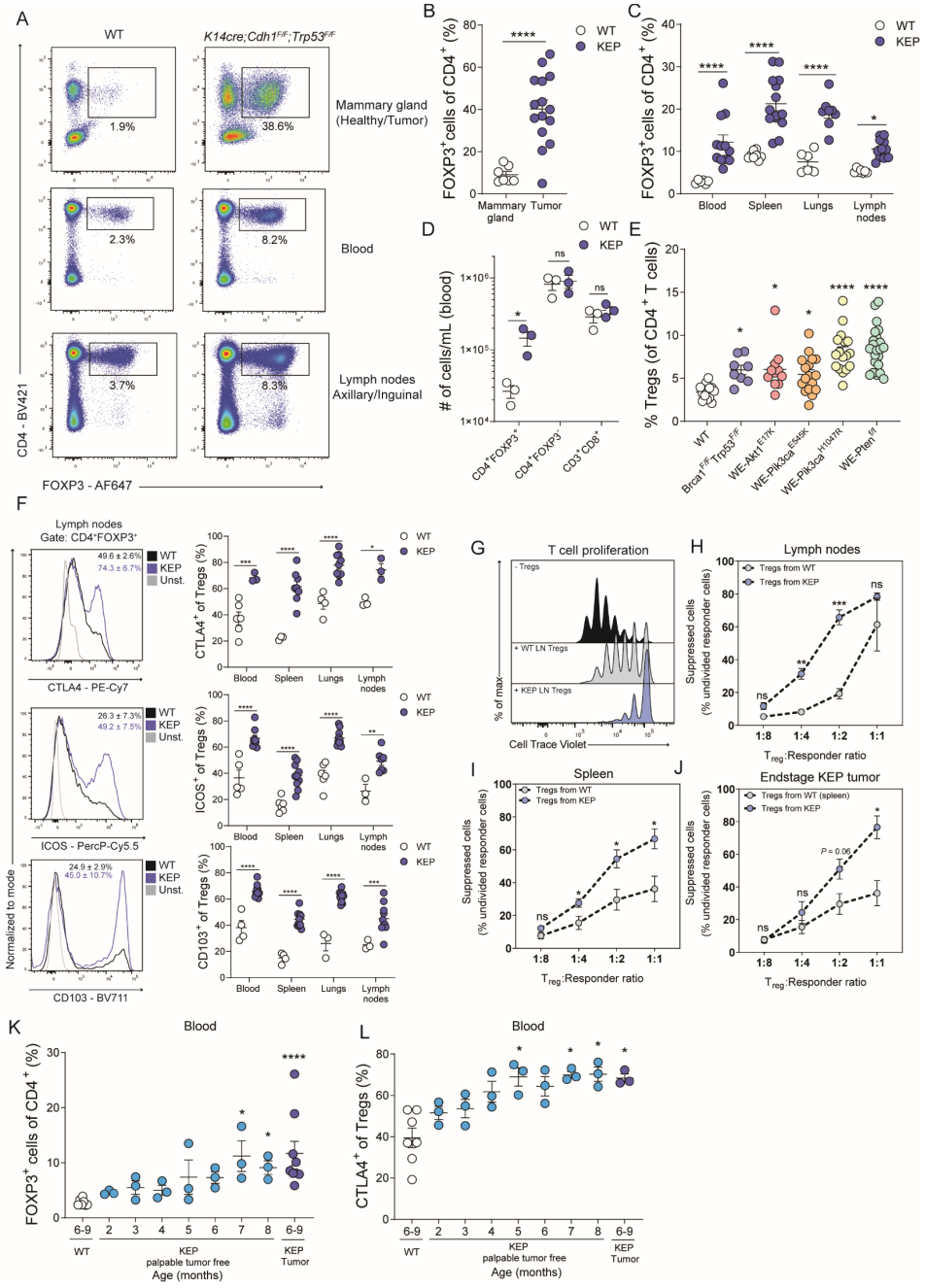

FIGURE 1. Primary mammary tumors induce systemic expansion and activation of CD4⁺FOXP3⁺ T cells.

A. Representative dot plots depicting the CD4⁺FOXP3⁺ T_{reg} population (%) gated on live, CD45⁺CD3⁺ cells in indicated tissues of *K14cre;Cdh1$^{F/F}$;Trp53$^{F/F}$* (KEP) mice bearing (225mm^2) mammary tumors versus WT controls. **B-C**. Frequencies of FOXP3⁺ cells of CD4⁺ T cells in indicated tissues of KEP

mice bearing mammary tumors (225mm^2) versus WT controls (n=6-15 mice/group) as determined by flow cytometry. **D**. Quantification of absolute cell counts of indicated adaptive immune cell populations per mL of blood of KEP mice bearing mammary tumors (225mm^2) versus WT controls (n=3 mice/group). **E**. Frequencies of FOXP3$^+$ cells of CD4$^+$ T cells in blood of mice bearing end-stage tumors of indicated transgenic mouse models for mammary tumorigenesis compared to age-matched WT mice (n=8-22 mice/group). **F**. Representative histograms depicting expression (left) and quantification (right) of CTLA4, ICOS and CD103 gated on CD4$^+$ FOXP3$^+$ T cells, in indicated tissues of KEP mice (blue) bearing (225mm^2) tumors versus WT littermates (black) by flow cytometry (n=3-11 mice/group) **G**. Representative histogram plots of CTV expression in activated CD4/CD8 T cells alone (black) or upon co-culture with CD4$^+$CD25$^+$ cells (grey and blue) obtained from indicated tissues at 1:2 T_{reg}:responder ratio. **H-J**. Quantification of undivided responder cells (CD8$^+$ and CD4$^+$ T cells) based on CTV expression, upon co-culture with CD4$^+$CD25$^+$ isolated from indicated tissues at various ratios (data pooled from 3-4 independent experiments, with 2 technical replicates per experiment). **K**. Frequencies of FOXP3$^+$ cells of CD4$^+$ T cells in blood of tumor-free, tumor-bearing (225mm^2) KEP mice and WT controls. (n=3-9 mice/group). **L**. Frequencies of CTLA4$^+$ cells of FOXP3$^+$CD4$^+$ T cells in blood of tumor-free, tumor-bearing (225mm^2) KEP mice and WT controls (n=3-7 mice/group). Data in B-F, H-L show mean ± S.E.M. P-values determined by unpaired Student's t-test (B, D, H, I, J), One-way ANOVA with Dunnett's multiple comparison test (E), Two-way ANOVA with Sidak's multiple comparison test (C,F), and Kruskal-Wallis test with Dunn's multiple comparison test (K,L). Asterisks indicate statistically significant differences compared to WT. * $P < 0.05$, ** $P < 0.01$, *** $P < 0.001$, **** $P < 0.0001$.

Mammary tumors alter the transcriptome of T_{regs} in tumors and distant organs

To delineate the impact of mammary tumor progression on T_{regs} in distant organs, RNA sequencing was performed on T_{regs} (CD4$^+$CD25^{high}) isolated from blood, TDLNs, lungs, spleens, healthy mammary glands, and mammary tumors (225mm^2) from tumor-bearing KEP mice and WT controls (Fig. 2A). Importantly, CD4$^+$CD25^{high} cells isolated from these tissues showed high and equal FOXP3 expression (Fig. S2A). Principal Component Analysis (PCA) showed distinct clustering of T_{regs}, based on their residence in either lymphoid tissue (spleen and LNs) and blood, or residence in peripheral tissue (lungs, tumor, mammary gland) (Fig. 2B). Furthermore, T_{regs} residing in distant organs cluster together independent of tumor status, whereas the gene expression profiles of tumor- and mammary gland T_{regs} appear very distinct. Indeed, differential gene expression analysis comparing intratumoral KEP T_{regs} and mammary tissue-resident T_{regs} revealed 3707 differentially expressed genes (Fig. 2C). Ingenuity Pathway Analysis (IPA) showed the significantly changed pathways between T_{regs} from tumors and mammary glands to pertain to cell migration and extravasation (Fig. 2D), which is underscored by some of the most differentially expressed genes, including *Mmp10*, *Mmp13* and *Ccr8* (data file S1). We confirmed by gene set enrichment analysis (GSEA) that intratumoral KEP T_{regs} are significantly enriched for a clinically relevant cross-species and cross-tumor model tumor-infiltrating T_{regs} (TIT_{regs}) signature[26] (Fig. 2E).

Next, we sought to explore how mammary tumorigenesis affects T_{regs} in distant organs by comparing gene expression profiles of KEP versus WT T_{regs} from matched tissues. This comparison identified differential gene regulation in T_{regs} in all organs tested, indicating that mammary tumors induce systemic transcriptional changes in T_{regs} (Fig. 2F). To further map

these differentially regulated genes and their occurrence across different tissues, we analyzed their distribution in KEP versus WT T_{regs} across tissues (Fig. 2G). Doing so, we identified a set of 31 core genes to be significantly different (27 upregulated, 3 downregulated, 1 bi-directional dependent on tissue) in KEP T_{regs} regardless of tissue residence, suggesting a certain level of convergent, tissue-independent transcriptional rewiring in response to mammary tumorigenesis (Fig. 2H). Among those upregulated, we found genes encoding proteins important for T cell activation and the immunosuppressive features of T_{regs}, such as *Icos*, *Klrg1, Havcr2*, *Tigit* and *Tnfrsf9*. KEP T_{regs} were also found to have enhanced gene expression of *Gzmb*, which is known for its cytolytic function in NK and $CD8^+$ T cells, but has been shown to contribute to immunosuppression when expressed by T_{regs}[27]. Combined, these data suggest that mammary tumorigenesis enhances systemic immunosuppression through transcriptional rewiring of T_{regs} in distant organs.

We additionally identified *Il1rl1,* a gene encoding the IL-33 receptor ST2 to be systemically increased in KEP T_{regs} compared to WT T_{regs}, which was confirmed by FACS analysis (Fig. S2B-C). IL-33/ST2 signaling on T_{regs} has recently been described to induce a pro-tumorigenic phenotype in intratumoral T_{regs}[28–30] and has also been shown to drive expansion of T_{regs} *in vitro* and *in vivo*[31]. In KEP mice, IL-33 was found to be significantly increased in TDLNs compared to WT LNs, which was not observed in blood, tumor or lungs (Fig. S2D). Nevertheless, short-term neutralization of IL-33 in tumor-bearing KEP mice utilizing two independent approaches *i.e.* treatment of mice with anti-IL-33 or with an IL-33 antagonist (IL-33 Trap[32]) (Fig. S2E) did not alter systemic T_{reg} accumulation, proliferation, or phenotype (Fig. S2F-I), suggesting that in mice with established mammary tumors, the presence of the $ST2^+$ T_{reg} population is maintained independent of endogenous IL-33.

Taken together, these data demonstrate that mammary tumorigenesis induces systemic transcriptional rewiring of T_{regs}, sharing a core set of genes associated with T_{reg} function and activation.

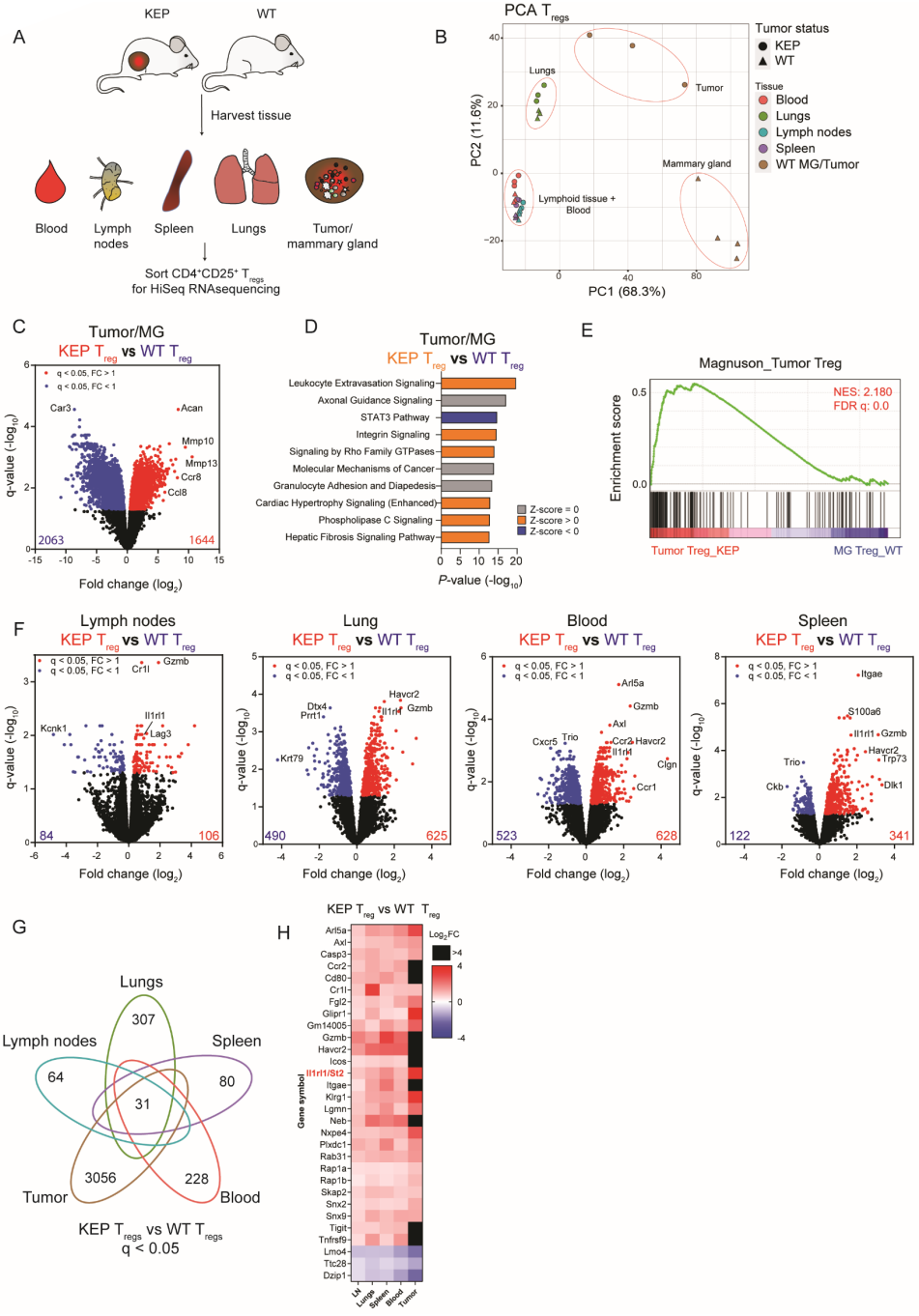

FIGURE 2. Mammary tumor formation impacts T_{reg} gene expression in distant sites. **A.** Schematic overview of experiment. **B.** PCA plot of transcriptomic profiles of T_{regs}. Each symbol represents one sample of sequenced T_{regs}. **C.** Volcano plots showing differentially expressed genes (q<0.05) comparing T_{regs} isolated from tumors of KEP mice versus healthy mammary gland of WT controls. **D.** IPA on differentially expressed genes (q<0.05) comparing T_{regs} isolated from tumors of

KEP mice versus healthy mammary gland of WT controls. Top 10 statistically significant pathways are shown. **E**. GSEA comparing KEP/WT T_{regs} isolated from tumors and healthy mammary gland with TIT_{reg} gene set (Magnuson et al., 2018). Normalized enrichment score (NES) and false discovery rate (FDR) indicated. **F**. Volcano plots showing differentially expressed genes ($q<0.05$) from T_{regs} isolated from indicated tissues of tumor-bearing KEP mice versus WT controls. Red indicates upregulated in KEP, blue indicates upregulated in WT. **G**. Venn diagram showing distribution of differentially expressed genes ($q<0.05$) identified by comparing gene expression of T_{regs} isolated of tumor-bearing KEP mice versus WT controls for each tissue. **H.** Heatmap depicting Log_2FC change of 30 shared KEP T_{reg} genes up/down regulated in KEP T_{regs} across tissue ($q<0.05$, KEP T_{reg} versus WT T_{reg} per tissue).

The impact of mammary tumorigenesis on T_{regs} is dictated by the tissue context

In addition to transcriptional commonalities observed in KEP T_{regs} in distant organs, we identified a large number of tumor-induced genes in KEP T_{regs} that were not shared across multiple tissues, but rather dependent on the tissue-context (Fig. 2G), indicating that the local environment shapes the response of T_{regs} to mammary tumorigenesis. Therefore, we continued our characterization of T_{regs} in distant organs of tumor-bearing KEP mice by exploring the impact of the tissue-context. To do so, we omitted tumors and mammary glands from the dataset and re-analyzed the T_{reg} transcriptome. PCA analysis revealed that T_{regs} derived from the same tissues cluster together, indicating that tissue residence is a more dominant factor for the transcriptional state of T_{regs} than the presence or absence of a primary mammary tumor (Fig. 3A). To elaborate the relationship between T_{regs} in different tissues, we performed correlation analysis, and found T_{regs} from LNs, spleen and blood to be relatively closely correlated, whereas lung T_{regs} were very distinct (Fig. 3B). Interestingly, visualization of differentially regulated genes of matched tissues in a force-directed graph (KEP vs WT T_{regs}, $q < 0.05$)[33] revealed complex relationships between clusters of genes dependent on the tissue context (Fig. 3C). Among these, roughly 30% of differentially regulated genes in KEP T_{regs} versus WT T_{regs} were found to be tissue specific (74/183 genes in LN, 379/1100 genes in lung, 417/1129 genes in blood, 107/462 genes in spleen), indicating that KEP T_{regs} in distant organs acquire a unique tissue-specific transcriptional profile (Fig. 3C, data file S1). We next performed IPA to interrogate which molecular pathways are associated with the differentially expressed genes between KEP and WT T_{regs} in distant organs. Notably, we identified several pathways related to T cell effector states (Th1 pathway, Th2 pathway, T helper cell differentiation, Th1 and Th2 Activation Pathway) to be shared among KEP T_{regs} in multiple distant organs (Fig. 3D). In addition to shared pathways, we also found several pathways that were only observed for specific tissues, such as “Integrin Signaling” in blood T_{regs} and “Apoptosis Signaling” in lung T_{regs}, highlighting the differential impact of mammary tumorigenesis on T_{regs} in distant organs.

Taken together, these data demonstrate that the mammary tumor-induced changes in T_{regs} are strongly influenced by their tissue context, raising the question whether these site-specific differences may have functional consequences for the progression of breast cancer.

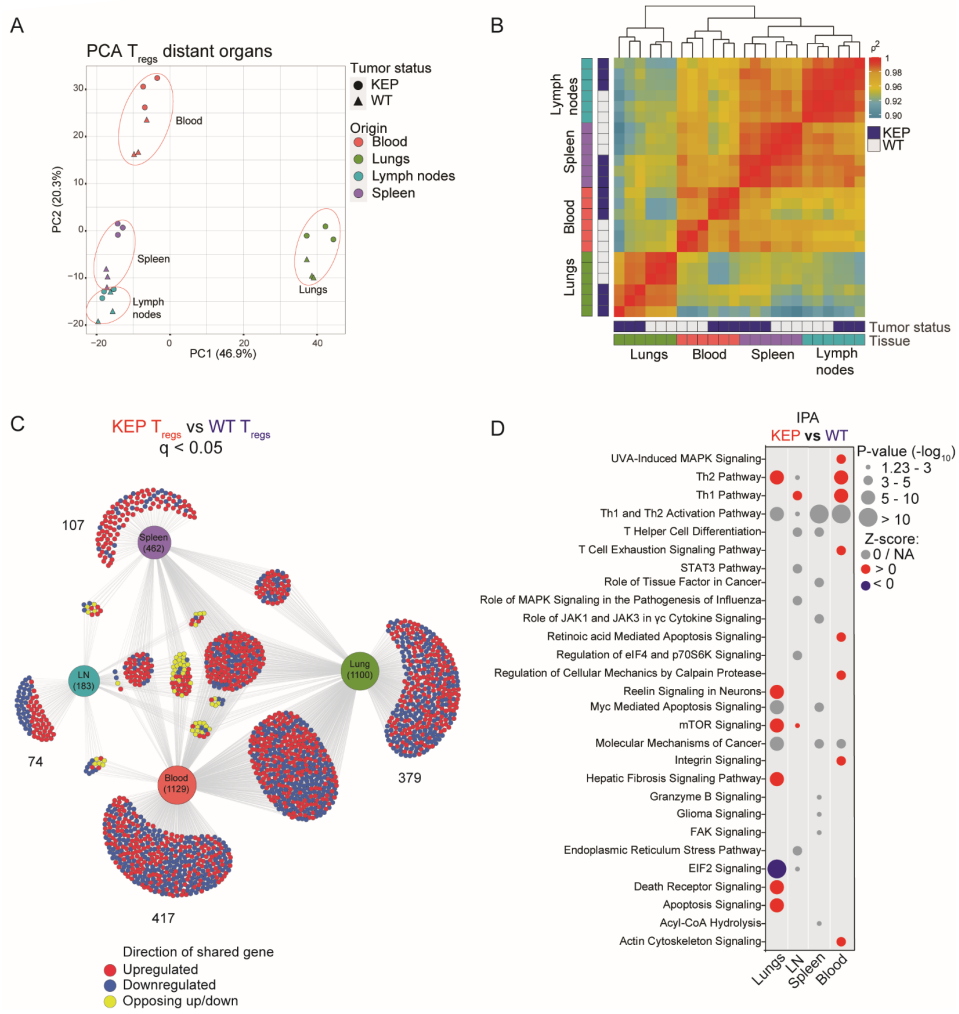

FIGURE 3. Tissue-dependent transcriptional changes in KEP T_{regs}.
A. PCA plot of transcriptional profiles of T_{regs} isolated from distant organs and blood of KEP mice bearing end-stage tumors versus healthy mammary gland of WT controls. **B**. Correlation plot matrix plot showing Spearman coefficient between transcriptional profiles of T_{regs} isolated from distant organs and blood of KEP mice bearing end-stage tumors and WT controls. **C.** Force-directed graph depicting differentially expressed genes between KEP T_{regs} vs WT T_{regs} (q<0.05). Genes identified by comparing gene expression of T_{regs} isolated from distant organs and blood of tumor-bearing KEP mice versus WT controls for each tissue, depicted by Divenn[33]. **D**. IPA on differentially expressed genes (q<0.05) comparing T_{regs} isolated from indicated tissues of KEP mice bearing end-stage tumors versus WT controls. Top 10 significant pathways are shown for each tissue.

Tumor-educated T_{regs} promote lymph node metastasis but not lung metastasis

As we observed systemic and organ-specific mammary tumor-induced alterations of T_{regs}, we set out to explore the impact of T_{regs} on multi-organ metastatic disease utilizing the KEP-based mastectomy model of spontaneous breast cancer metastasis (Fig. 4A)[25,34]. In this model, after orthotopic transplantation of a KEP-derived tumor fragment followed by surgical removal of the outgrown tumor, mice develop overt multi-organ metastatic disease, mainly in Ax. TDLNs and lungs. Like primary tumor formation, metastatic disease is also accompanied by the accumulation of T_{regs}, with elevated expression of ICOS, CTLA4 and ST2, as compared to non-transplanted naïve controls (Fig. S3A-E).

To assess the functional significance of T_{regs} during early metastasis formation, we treated mice in the neoadjuvant setting with a recently developed Fc-modified antibody, targeting the IL2Rα receptor, CD25 (anti-CD25-M2a), which has been described to efficiently and specifically deplete T_{regs} in tumors and peripheral tissue[35]. Indeed, anti-CD25-M2a treatment efficiently depleted $FOXP3^{+}CD4^{+}$ T cells from tumors, spleen, lymph nodes, lungs and circulation in mice bearing transplanted KEP tumors (Fig. 4B-C, S3F-G). Depletion of T_{regs} was observed for up to 10 days after start of treatment in blood. Although anti-CD25-M2a treatment resulted in increased IFNy expression in both intratumoral $CD4^{+}$ and $CD8^{+}$ T cells (Fig. 4D), consistent with the concept that tumor-induced T_{regs} are immunosuppressive, we did not observe an effect on primary tumor growth (Fig. 4E). Similarly, depletion of T_{regs} in mammary tumor-bearing transgenic KEP mice did not affect primary tumor growth or survival (Fig. S3H).

After mastectomy, mice were monitored for the development of overt metastases. While neoadjuvant T_{reg} depletion did not improve metastasis-related survival or reduce the number of lung metastases (Fig. 4F, S3I), micro- and macroscopic analysis of Ax. TDLNs (Fig. S3J) revealed that anti-CD25-M2a treated mice developed significantly fewer LN metastases as compared to controls (Fig. 4G). The incidence of LN metastasis of control mice was 93% (14/15), which was reduced to 56% (9/16) upon anti-CD25-M2a treatment. No difference was observed in the size of LN metastases that did develop in both groups (Fig. S3K). The observation that T_{reg} depletion reduces the incidence of LN metastasis by ~50%, but does not affect lung metastasis, was consistent across four independent experimental KEP tumor donors, even though LN metastasis incidence of control groups varied between 41.67%-93.3% in a donor-dependent fashion (Fig. 4H-I). These findings indicate that T_{regs} promote metastasis formation, leading to increased incidence of LN metastasis, but also reveals that the impact of T_{regs} on metastasis formation is dependent on the tissue context since lung metastases remain unaffected.

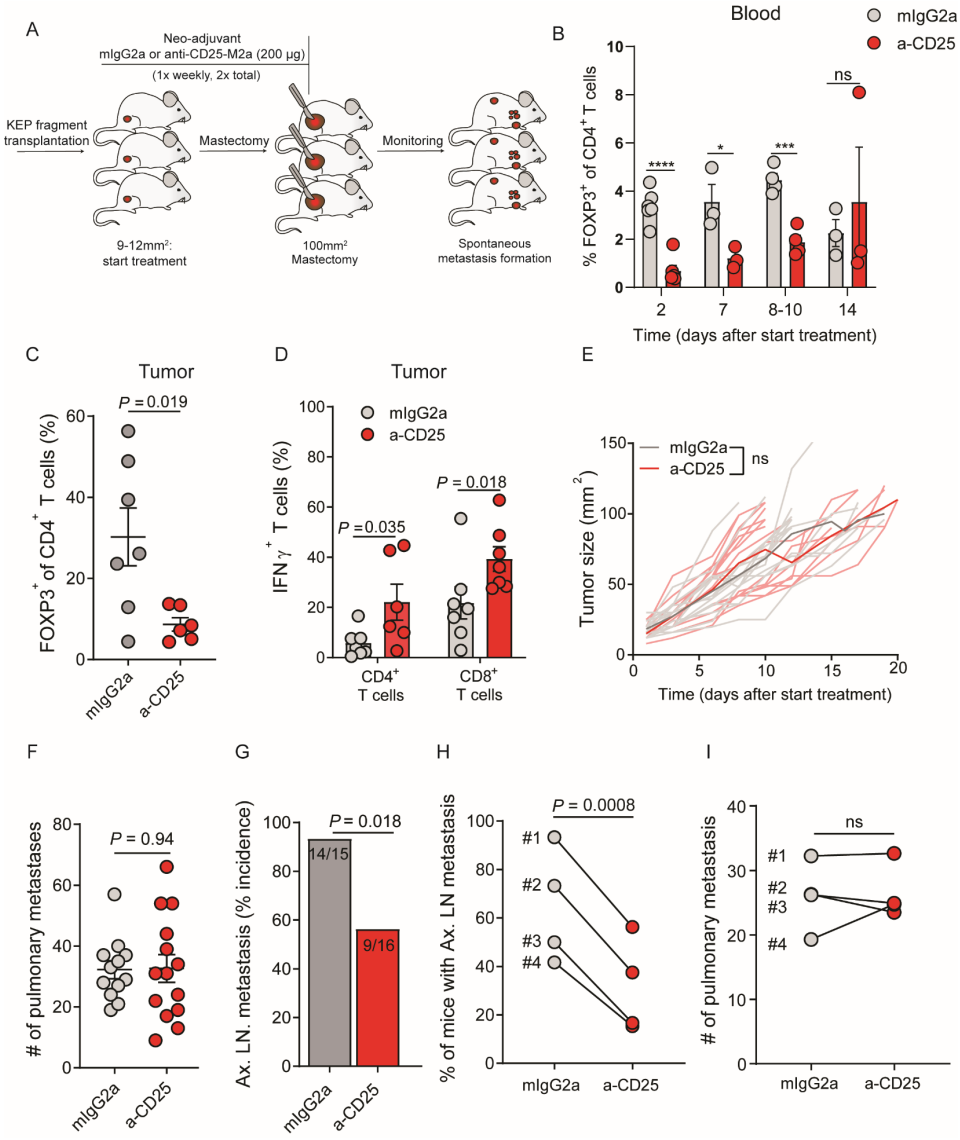

FIGURE 4. Tumor-educated T_{regs} promote lymph node metastasis but not lung metastasis **A**. Schematic overview of study. (n=15-16 mice/group). **B**. Frequency of FOXP3⁺ cells of CD4⁺ T cells in mice bearing transplanted KEP tumors, treated with mIgG2a or anti-CD25 at indicated timepoints after start of treatment. (n=3-6 mice/group) **C**. Intratumoral frequency of FOXP3⁺ cells in mastectomized tumors, gated on live, CD45⁺, CD3⁺,CD4⁺ T cells as determined by flow cytometry (n=6-7 mice/group). **D**. Frequency of IFNγ⁺ cells of CD4⁺ and CD8⁺ T cells, in 100mm² mastectomized KEP tumors of mice treated with neoadjuvant mIgG2a and anti-CD25 as determined by flow cytometry (n=6-7 mice/group) following a 3 hour ex vivo stimulation. **E**. Primary tumor growth kinetics of mice bearing transplanted KEP tumors, treated with mIgG2a or anti-CD25. **F**. Number of pulmonary metastases in mice treated with neoadjuvant mIgG2a and anti-CD25. (n=15-16 mice/group). **G**. % and number of mice with detectable micro/macroscopic metastases in Ax. TDLNs, in mice treated with neoadjuvant mIgG2a and anti-CD25. (n=15-16 mice/group). **H-I**. Ax. TDLN metastasis incidence (**H**) and # of lung metastases (**I**) of each independent experimental donor is shown, in mice receiving weekly neoadjuvant treatment of 200 µg mIgG2a or anti-CD25. Symbol indicates an experimental group (mIgG2a/a-CD25), each line

connects an independent experimental (donor #1 used in Fig. 4G,I n=15-16 mice/group, donor #2 used in Fig. 5A n=15-16, donor 3+4 used in Fig. 6A n=30-31 mice/group). Data in B-D, F show mean ± S.E.M. P-values are determined by Unpaired Student's T-test (B,C,F), Mann-Whitney test (D), area under curve (AUC) calculation (E), Fisher's exact test (G), and Paired Student's T-test (H,I)

T_{regs} differentially modulate NK cell activation in the lymph node and lung niche.

To gain more insight into how T_{regs} promote metastasis formation in Ax. LNs, we first explored the potential role of $CD8^+$ T cells in controlling LN metastasis formation upon T_{reg} depletion, as we found that T_{regs} suppress IFNγ expression by $CD8^+$ T cells in the primary tumor microenvironment (Fig. 4D). To do so, we co-depleted $CD8^+$ T cells (Fig. S4A) and T_{regs} in the KEP metastasis model, but did not find a difference in LN metastasis incidence between anti-CD25 and anti-CD25/CD8 treatment (Fig. 5A), suggesting that the reduced LN metastasis incidence upon depletion of T_{regs} is not linked to intratumoral activation of $CD8^+$ T cells (Fig. 4D). Since we observed systemic activation and rewiring of highly immunosuppressive T_{regs} in response to tumorigenesis, we next hypothesized that T_{regs} may differentially facilitate metastasis formation through tissue-specific interactions in the local metastatic niche, independent of their activity in the primary tumor.

To study this as close to the *in vivo* situation as possible, we assessed the impact of tumor-educated T_{regs} on immune cells with potential anti-tumor activity in Ax. TDLNs *in vivo*, instead of using traditional *in vitro* suppression assays in which cells may lose their functionality imposed by their respective tissue-microenvironment. *In vitro* suppression assays therefore fail to reproduce the complex interactions that exist *in vivo,* rendering these assays of limited value for studying metastatic niche-dependent processes. Instead, we depleted T_{regs} in mice bearing transplanted KEP tumors and analyzed the phenotype and function of T- and NK cells in Ax. TDLNs compared to control treated and naïve mice when primary tumors reached a size of 100mm^2 *ex vivo*. We also analyzed T- and NK cells in tumors, blood and lungs, to gain insights into the tissue-specific impact of tumor-educated T_{regs} on these cells. Interestingly, increased expression of the cytotoxic molecule granzyme B by NK cells ($CD3^-$, $NKp46^+$, $DX5^+$) was observed in the Ax. TDLNs of tumor-bearing mice upon T_{reg} depletion (Fig. 5B-C, S4B). Increased granzyme B expression was not observed in NK cells in lungs, blood and tumor upon T_{reg} depletion despite higher baseline expression compared to Ax. TDLNs (Fig. S4C-E), indicating that tumor-activated T_{regs} interfere with granzyme B expression of NK cells specifically in the Ax. LN niche. Next, we analyzed the surface expression of CD107a on NK cells as a readout for their degranulation, which is an important mechanism for NK cell cytotoxicity[36]. This showed that NK cells in Ax. TDLNs, but not lungs or Ax. NDLNs, from T_{reg}-depleted mice cells have increased surface expression of CD107a compared to control treatment (Fig. 5D, S4F), showing that Ax. TDLN NK cells increase the release of intracellular granules upon T_{reg} depletion *in vivo*. In *in vitro* stimulated NK cells, CD107a expression was not significantly affected by T_{reg} depletion (Fig. S4G), suggesting that the impact of T_{regs} on NK cell degranulation is not affecting their intrinsic capacity to degranulate under highly

stimulatory conditions, but is rather a result of T_{reg}/NK cell interactions *in vivo*. In contrast, we did not find a significant effect of T_{reg} depletion on T cells in terms of granzyme B, CD107a, IFNγ, TNFα expression or IFNγ by NK cells in Ax. TDLNs and lungs (Fig. S4H-L).

To further dissect the differential impact of T_{regs} on NK cells in the LN and lung niche *in vivo*, we conducted bulk RNAseq analysis on FACS-sorted NK cells isolated from T_{reg}-depleted and T_{reg}-proficient tumor-bearing mice (Fig. 5E). Notably, anti-CD25 induces depletion of T_{regs} via antibody-dependent cell-mediated cytotoxicity (ADCC) through engagement of Fc receptors[35] on innate effector cells, including NK cells[37]. To confirm that the observed activation of NK cells upon antibody-mediated depletion of T_{regs} is independent of their role in ADCC, we now utilized *Foxp3*$^{DTR\text{-}GFP}$ mice in which FOXP3^{+} cells are efficiently depleted upon injection of diphtheria toxin (DT) (Fig. S5A). NK cells were obtained from lungs and Ax. TDLNs of PBS or DT treated *Foxp3*$^{DTR\text{-}GFP}$ mice bearing transplanted KEP tumors. Gene expression analysis of NK cells from T_{reg}-depleted versus T_{reg} non-depleted mice identified 1036 and 646 genes to be differentially expressed in the LNs and lungs respectively, showing that the influence –directly, indirectly, or due to NK cell intrinsic differences- of T_{regs} on the NK cell transcriptome, is more pronounced in Ax. TDLNs than in lungs (Fig. 5F-G, data file S2).

To identify which molecular pathways are controlled by T_{regs} in NK cells in tumor-bearing mice, we performed GSEA analysis on the differentially expressed genes of both lung and Ax. TDLN NK cells from T_{reg}-depleted versus T_{reg} non-depleted mice using the MSigDB Hallmark Gene sets, which represent 50 well-defined biological processes[38] (Fig. 5H, S5B). We found that the depletion of T_{regs} induces the upregulation of molecular pathways related to DNA replication (G2M checkpoint, E2F targets, mitotic spindle) and inflammation (inflammatory response, IFNγ response) in both Ax. TDLN and lung NK cells, suggesting a common role of T_{regs} in curbing NK cell proliferation and activation. However, we also identified pathways that were uniquely upregulated in either Ax. TDLN NK cells (IL6-JAK-STAT3 signaling, IL2-STAT5 signaling) or lung NK cells (Interferon alpha response, TNFα signaling via NF-κB). Although both Ax. TDLN and lung NK cells show signs of activation upon depletion of T_{regs} based on GSEA, we identified 676 genes to be uniquely upregulated in Ax. TDLN NK cells of T_{reg}-depleted versus T_{reg}-non-depleted mice, compared to 326 in lung NK cells (Fig. 5I). Interestingly, a subset of genes found specifically upregulated in Ax. TDLN NK cells of T_{reg}-depleted mice encodes for proteins with immunomodulatory properties that were not found in lung NK cells of T_{reg}-depleted animals, including *Gzmb*, which we had previously identified in our FACS-based analyses of NK cells (Fig. 5B-C). Furthermore, we identified other genes encoding for proteins involved in cytotoxicity (*Gzma, Serpinb9b),* migration (*Ccl4, Ccl8, Ccl22, Cxcr6*), co-stimulatory receptors (*Icosl, Tnfrsf4),* and co-inhibitory receptors (*Tigit, Lag3, Ctla4, Klrg1*), which are indicative of activated NK cells. In summary, these data show that T_{regs} regulate NK cells in a tissue-specific manner, and suggest that tissue-context does not only drive T_{reg} phenotype, but also impacts their interactions with target cells such as NK cells.

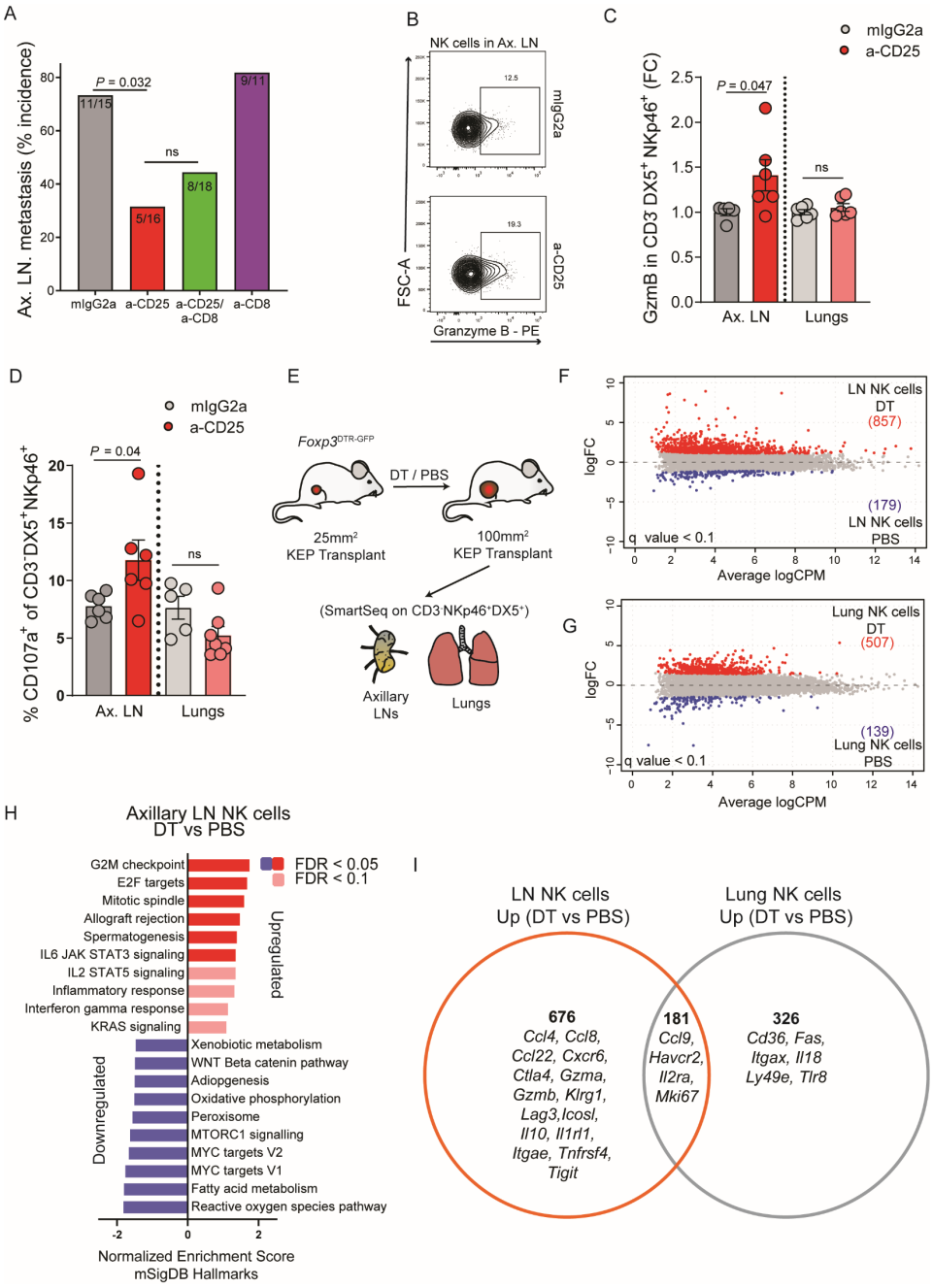

FIGURE 5. T_{regs} differentially impact NK cells in LN and lungs

A. % and number of mice with detectable micro/macroscopic metastases in Ax. TDLNs, in mice treated with neoadjuvant indicated treatments. (n11-18 mice/group). **B.** Representative dot plot of granzyme B expression by NK cells in Ax. TDLNs of mice bearing 100mm^2 KEP tumors, treated with neoadjuvant mIgG2a or anti-CD25. **C**. Relative granzyme B expression by NK cells (CD3$^-$DX5$^+$NKp46$^+$) in Ax. TDLNs and lungs of mice bearing 100mm^2 KEP tumors, treated with neoadjuvant mIgG2a or anti-CD25,

following a 3 hour ex vivo stimulation (n=6 mice/group). Data are normalized to % GzmB$^+$ of NK cells of control mIgG2a treated mice. **D.** CD107a expression of NKp46$^+$ DX5$^+$ NK cells from Ax. TDLNs and lungs of mice bearing transplanted KEP tumors (100mm^2) receiving weekly neoadjuvant treatment of 200µg anti-CD25 or mIgG2a (n=6/group). **E**. Schematic overview of study. Mice received treatment at t=0 and t=7. (n=4 mice/group). **F-G** MA plot of differentially regulated transcripts for Ax. TDLN NK cells (**F**), and lung NK cells (**G**) DT versus PBS treatment. Significantly different transcripts are labelled in red (up), and blue (down). **H**. GSEA analysis of Ax. TDLN NK cells, DT vs PBS, using hallmark gene sets. Top 10 enriched up- and downregulated pathways are shown. **I**. Venn diagram depicting distribution of upregulated genes ($q < 0.1$) between Ax. TDLN and lung NK cells DT versus PBS treatment. Data in C-D show mean ± S.E.M. P-values are determined by Mann-Whitney Test (C-D) and Fisher's Exact test (A).

T_{regs} promote metastasis through inhibition of NK cells in the lymph node niche

We next assessed whether the inhibitory effect of T_{regs} on Ax. TDLN NK cells impacts their capacity to control LN metastasis formation. We performed neoadjuvant co-depletion of T_{regs} using anti-CD25-M2a and NK cells using anti-NK1.1 in the KEP metastasis model. Anti-NK1.1 efficiently depleted NKp46$^+$DX5$^+$ NK cells in the blood of KEP tumor-bearing mice (Fig. S5C). Strikingly, whereas depletion of T_{regs} significantly reduced the incidence of Ax. LN metastasis, combined depletion of T_{regs} and NK cells completely restored LN metastasis formation (Fig. 6A). Anti-NK1.1 alone did not alter LN metastasis incidence and none of the treatments affected the number of lung metastases (Fig. 6B). Combined, our findings show that tumor-educated T_{regs} repress NK cell activation in Ax. TDLNs, thereby curbing their anti-metastatic potential, leading to an increased incidence of LN metastasis. This T_{reg}-mediated immune escape mechanism is specific to the Ax. LN, as T_{regs} did not control lung metastasis in this model. Because we did observe some activation of lung NK cells at the transcriptional level in T_{reg}-depleted versus non-depleted mice (Fig. 5I), we hypothesized that additional layers of immunosuppression in the lung microenvironment that are independent of T_{regs} may hinder the anti-metastatic potential of lung NK cells. In support of this hypothesis, we found that lung NK cells are mostly terminally differentiated (CD27$^-$ CD11b$^+$) in tumor-free mice, but undergo a partial shift towards a non-cytotoxic immature phenotype (CD27$^-$CD11b$^-$) in tumor-bearing mice, independent of T_{regs} (Fig. S5D). In contrast to lungs, and in line with previous literature [39,40], Ax. TDLN NK cells were found to be mostly in CD27$^+$CD11b$^-$ (immature) and CD27$^+$CD11b$^+$ (cytotoxic) states (Fig. S5E), highlighting the differences between NK cells in LNs and lung. Importantly, maturation status in Ax. TDLN NK cells was not affected in tumor-bearing mice, suggesting this mechanism is specific to lungs, and potentially contributes to observed differences between lung and LN.

Reduced NK cells versus increased T_{regs} in sentinel lymph nodes of breast cancer patients

Finally, we validated our preclinical findings on T_{reg} and NK cell interactions in the lymph node niche of breast cancer patients. To do so, we analyzed the accumulation of T_{regs} (CD4$^+$CD25^{high}FOXP3$^+$) and NK cells (CD56$^+$CD16$^-$ and CD56^{low}CD16$^+$) in tumor-free and tumor-positive sentinel LNs of breast cancer patients (BrCa SLN-/SLN+), and in Ax. LNs from

healthy controls (HLNs), using a previously described flow cytometry dataset[14]. In line with previous analyses of this unique dataset[14] and consistent with our preclinical data (Fig. 1C), T_{reg} levels are significantly elevated in BrCa SLNs as compared to HLNs (Fig. 6C). We also observed a statistically significant reduction of $CD56^{low}CD16^{+}$, but not $CD56^{+}CD16^{-}$ NK cells in BrCa SLN-, and a similar trend in BrCa SLN+ (Fig. 6D-E). Notably, in particular $CD56^{low}CD16^{+}$ have been described to have cytotoxic activity[41]. Combined, this shifts the T_{reg}/NK cell ratio strongly towards T_{regs} in both tumor-free and tumor-positive BrCa SLNs compared to HLNs (Fig. 6F). Despite the low number of BrCa SLN+ samples, we also observed a non-significant trend of a higher T_{reg}/NK cell ratio in SLN+ versus SLN- samples. A rise in T_{regs} in conjunction with a reduction of potentially cytotoxic NK cells in the SLN niche is in accordance with our preclinical finding that LN NK cells have reduced expression of CD107a and the cytotoxic molecule granzyme B under control of T_{regs} in tumor-bearing mice (Fig. 5B-D).

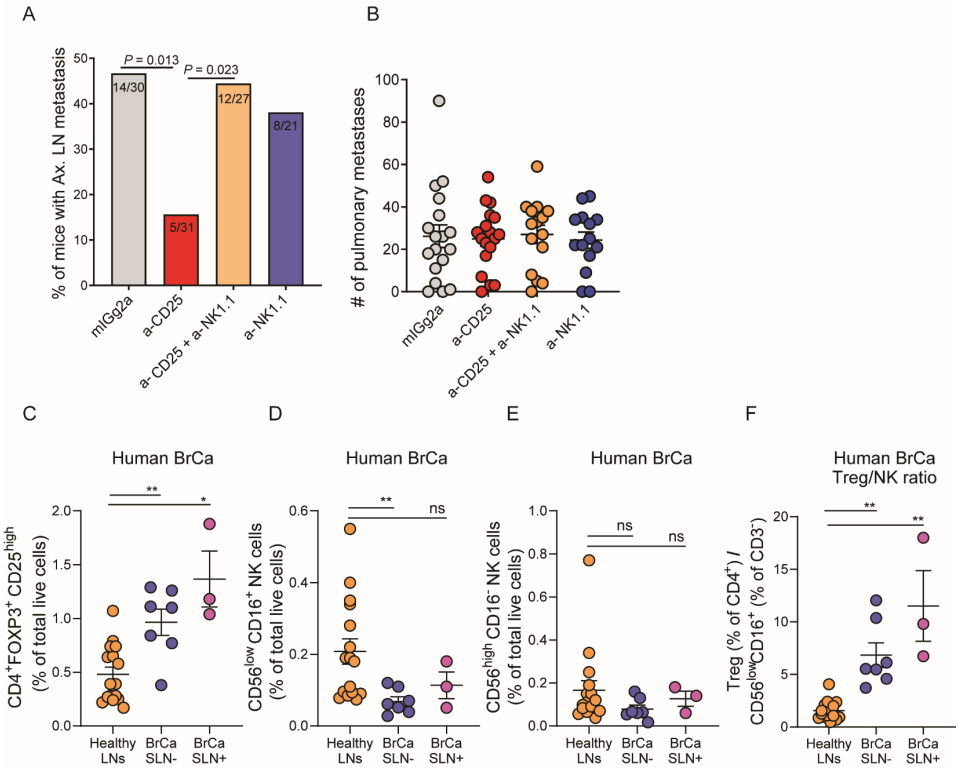

FIGURE 6. T_{regs} promote axillary LN metastasis through inhibition of NK cells.
A. % and number of mice with detectable micro/macroscopic metastases in Ax. TDLNs, in mice receiving neoadjuvant treatment as indicated. (n=21-31 mice/group, data pooled from two independent experiments). **B**. Number of pulmonary metastases in mice receiving indicated neoadjuvant treatment. (n=14-16 mice/group). **C.** Frequencies of $CD3^{+}CD4^{+}CD25^{+}FOXP3^{+}$ cells of total live cells in human HLNs (n=16), BrCa tumor-negative (n=7) and tumor-positive (n=3) SLNs. **D-E.** Frequencies of indicated subset of NK cells of total live cells in human HLNs (n=16), BrCa tumor-negative (n=7) and tumor-positive (n=3) SLNs. **F.** Ratio of T_{reg} (% of $CD4^{+}$) versus $CD56^{low}CD16^{+}$ (% of $CD3^{-}$) in human HLNs

(n=16), BrCa tumor-negative (n=7) and tumor-positive (n=3) SLNs. Data in B-F show mean ± S.E.M. P-values are determined by Kruskal-Wallis test with Dunn's correction for multiple comparisons (C-F), Fishers Exact test (A). ** P < 0.01, *** P < 0.001, **** P < 0.0001

DISCUSSION

Understanding the nature of cancer-associated systemic immunosuppression and its impact on different (pre-)metastatic niches is essential to ultimately design effective therapeutic strategies that prevent or fight metastatic disease. Here, we show that mammary tumorigenesis has an extensive impact on T_{regs}, both intratumorally and in distant organs. Tumor-educated T_{regs} are highly activated and immunosuppressive, and display tissue-specific adaptation to tumor development. This has functional relevance for metastasis formation, as T_{regs} selectively promote LN metastasis, but not lung metastasis, through inhibition of NK cells. These data highlight the importance of the tissue-context for immune escape mechanisms, and reveal a causal role for T_{regs} in the development of LN metastasis. An extensive number of clinical studies has reported that high infiltration of $FOXP3^+$ TILs in either primary breast tumors or Ax. LNs is associated with an increased incidence of LN metastasis, across breast cancer subtypes[14–18,42]. As five-year survival of breast cancer patients with LN involvement is up to 40% lower than node-negative patients[43,44], it is of crucial importance to understand the potential role of T_{regs} in the development of LN metastasis. Interestingly, one study of which we have further explored the dataset here, showed that T_{regs} are not only increased in sentinel LNs with metastatic involvement, but also accumulate in non-invaded sentinel LNs compared to LNs from healthy women, suggesting T_{reg} accumulation precedes LN metastasis formation[14]. Recently, others have studied the phenotype of T_{regs} in LNs of breast cancer patients and showed that T_{regs} acquire an increased effector-like phenotype in tumor cell-invaded versus non-invaded LNs[17]. These data are in line with our observations that T_{regs} in LNs are increased and activated in the context of mammary tumorigenesis. So far, clinical correlations between T_{regs} and breast cancer metastasis to other anatomical sites have not been reported, which suggest that T_{regs} may play a unique role in the formation of LN metastasis, as supported by our data.

NK cells are a well-recognized key element of the anti-tumor response[45,46], but the role and cellular crosstalk of NK cells in the context of lymph node metastasis has remained unclear. Here, we show that NK cells in Ax. TDLNs have anti-metastatic potential, provided they are relieved from the immunosuppressive pressure by T_{regs}. The relevance of these findings for human breast cancer is supported by our observation that the T_{reg}/NK cell ratio strongly shifts towards T_{regs} in SLNs of BrCa patients compared to healthy LNs. In addition, an explorative study using metastatic LNs from melanoma patients showed that *ex vivo* depletion of T_{regs} enhanced cytolytic activity of LN NK cells *in vitro*, suggesting T_{regs} can also inhibit LN NK cells in melanoma[47]. For breast cancer specifically, the expression

of granzyme B within tumor-infiltrating NK cells was found to negatively correlate to T_{reg} accumulation [48]. Furthermore, another recent study identified that clearance of Ax. LN metastasis in breast cancer patients treated with neoadjuvant chemotherapy significantly correlated with increased cytotoxic potential of NK cells in peripheral blood as well as with decreased intratumoral CTLA4 gene expression[49], which is well known to be important for T_{reg} immunosuppression[50].

Our findings demonstrate that T_{regs} show tissue-dependent rewiring in response to mammary tumorigenesis, which may either be explained through tissue-specific upstream regulators, or is reflective of the distinct inherent differences between tissue-resident T_{regs}, in particular in lymphoid versus non-lymphoid organs. Tissue-context does not only drive T_{reg} phenotype in tumor-bearing hosts, but also dictates the interaction between T_{regs} and one of their cellular targets, NK cells. Specifically, we found T_{reg} depletion to differentially affect lung and LN NK cells at both the transcriptional and the protein level (Fig. 5). Although transcriptomic analyses revealed that LN and lung NK cells acquire a more activated phenotype upon T_{reg} depletion, we found this to unleash NK-cell mediated anti-metastatic activity only in the lymph node niche, but not the lungs. We speculate that this may occur through the induction of an effector mechanism observed specifically in LN- but not lung- NK cells, such as increased expression of; the cytotoxic molecules granzyme A and B, NK cell co-stimulatory receptors, or chemokine receptors (Fig. 5I). Whether these specific phenotypic alterations observed in LN NK cells upon T_{reg} depletion are intrinsic to LN NK cells, or due to a unique feature of tumor-educated T_{regs} in TDLNs, remains to be elucidated. Alternatively, NK cells may be functionally repressed through other immunosuppressive mechanisms that are independent of $T_{regs,}$ and specific to the lung niche. For example, we observed that lung, but not LN NK cells undergo a shift towards a more immature state in tumor-bearing mice (Fig. S5D-E). This occurs independent of $T_{regs,}$ and potentially impacts their anti-metastatic potential. In line with this hypothesis, a recent study revealed that lung NK cells are suppressed by IL-33 activated innate lymphoid type 2 cells, which stunts their ability to control pulmonary metastasis of intravenously injected B16F10 cells[51]. This shows that NK cells can be suppressed beyond the control of T_{regs} in the lungs, highlighting the importance of local, tissue-specific mechanisms of immunosuppression and cancer immune surveillance during metastasis formation. Finally, NK cells may be functionally irrelevant for lung metastasis formation in this model independent of their activation status, through cancer cell-intrinsic differences between lymph- and lung metastasizing cancer cells that impacts their likelihood to be killed by NK cells[45,52], which we have not explored in this study.

The lack of T_{reg}-mediated promotion of lung metastasis formation is seemingly in contrast with studies in the 4T1 breast cancer model where T_{regs} have been shown to promote lung metastasis[22,23]. An important difference between these studies and our study is that 4T1 primary mammary tumors respond to T_{reg} depletion, resulting in attenuation of tumor

growth[22,23], while both spontaneous- and transplanted primary KEP mammary tumors do not respond to T_{reg} depletion (Fig. 4E, S3H). It was recently reported that the reduction in lung metastasis upon T_{reg} depletion in 4T1-bearing mice is a consequence of the primary tumor responding to T_{reg} depletion, and not an effect of T_{regs} on metastatic colonies in the lung niche[23]. In fact, an important conclusion from this study was that lung metastases are not effectively controlled after T_{reg} depletion[23], in line with our findings that metastasis to the lungs is not influenced by T_{regs}. Furthermore, syngeneic cell lines like 4T1 poorly reflect the immunogenicity of human tumors of the same origin[53]. Recent research has shown that syngeneic cell lines derived from GEMMs show key differences in their immune landscape, with increased frequencies of T_{regs}, $CD8^+$ T cells and NK cells, as compared to primary tumors in GEMMs[54]. These differences in immune landscape may critically impact the outcome of immunological studies, and thereby reduce their clinical value as compared to GEMM-based models such as the KEP model.

Despite observations that exogenous IL-33 can induce acute peripheral accumulation of $ST2^+$ T_{regs}[55] we find that blockade of endogenous IL-33 does not affect tumor-induced systemic T_{reg} accumulation or proliferation (Fig. S2F-I), suggesting that T_{reg} expansion in mammary tumor-bearing mice is regulated independent of IL-33, and thus remains an avenue of future research. Our *in vitro studies* (Fig S1L) suggest that a soluble factor in KEP serum can promote T_{reg} survival. An important cytokine involved in T_{reg} proliferation and survival[56] that we did not study here is IL-2. Therefore, future studies may analyze whether IL-2 is differentially expressed or regulated in tumor-bearing hosts, and might contribute to T_{reg} expansion, as has been observed in tumor-bearing mice treated with recombinant IL-2[56].

In conclusion, these findings reveal a causal role for T_{regs} in the formation of LN metastasis through local suppression of NK cells, and may form the basis for the design of neoadjuvant therapeutic strategies aimed to reduce nodal metastasis in breast cancer patients.

Limitations of the study

Although the use of a spontaneous GEMM-derived metastasis model increases the translational value of our findings, the absence of similar models for multi-organ spontaneous metastasis pose the experimental limitation of validation in comparable models. It will be relevant to extend our findings to similar models, when these are generated in the future. Another possible limitation is the analysis of T_{reg} populations by bulk RNAseq. This technique provides limited insight into changes occurring in different T_{reg} subpopulations within one tissue. Future studies may explore the distant impact of tumors on T_{regs} more deeply using single-cell RNAseq or related techniques. Finally, we have not uncovered the molecular basis of tumor-induced T_{reg} expansion, or precise T_{reg}-NK cell interactions in the TDLN. Thus, a deeper investigation in this direction is an important avenue of future research.

Acknowledgements

We acknowledge Alexander Rudensky for providing the IRES-DTR-GFP construct, Dr. Emiel J. Th. Rutgers and Dr. Petrousjka van den Tol for provision of clinical samples, and members of the Tumor Biology & Immunology Department, NKI for their insightful input. We thank the flow cytometry facility, genomics core facility, animal laboratory facility, transgenesis facility and animal pathology facility of the Netherlands Cancer Institute for technical assistance. This research was funded by NWO Oncology Graduate School Amsterdam (OOA) Diamond Program (KK), Netherlands Organization for Scientific Research grant NWO-VICI 91819616 (KEdV), Dutch Cancer Society grant KWF10083; KWF10623; KWF13191 (KEdV), KWF VU2015-7864 (RvdV, TDdG, KEdV) Oncode Institute (KEdV), and A Sister's Hope (TDdG). Components of the graphical abstract were prepared using Servier Medical Art, licensed under Creative Commons Attribution 3.0 Unported License.

Author contributions

KK and KEdV conceived the ideas and designed the experiments. KK performed experiments and data analysis. MAA performed bioinformatical analyses. MDW, WP, AvW, DD generated data. KK, DK, KV, C-SH, and LR performed animal experiments. SAQ and RB provided a-CD25-M2A and IL33Trap respectively. RvdV, KvP, TDdG collected samples and generated human data. KEdV supervised the study, KEdV and KK acquired funding, KK and KEdV wrote the paper and prepared the figures with input from all authors.

Declaration of Interests

KEdV reports research funding from Roche/Genentech and is consultant for Macomics outside the scope of this work. RvdV reports research funding from Genmab. TDdG received research support from Idera Pharmaceuticals, advisory/consultancy fees from LAVA Therapeutics, Parner Therapeutics, and Immunicum, and owns stock from LAVA Therapeutics.

MATERIAL AND METHODS

RESOURCE AVAILABILITY

Lead contact

Further information and requests for resources and reagents should be directed to and will be fulfilled by the lead contact, Karin. E. de Visser (K.d.visser@nki.nl).

Materials availability

All reagents generated in this study are available upon request with a completed material transfer agreement.

Data and code availability

Bulk T_{reg} and NK RNA-sequencing data have been deposited in the GEO and are publicly available as of the date of publication. Accession numbers are listed in the key resources table.

This paper does not report original code.

Any additional information required to reanalyze the data reported in this paper is available from the lead contact upon request.

EXPERIMENTAL MODEL AND SUBJECT DETAILS

Mice

The generation and characterization of genetically engineered mouse models for spontaneous mammary tumorigenesis has been described before [24,57–60]. The following mice have been used in this study: *Keratin14 (K14)-cre;Cdh1$^{F/F}$;Trp53$^{F/F}$, Whey Acidic Protein (Wap)-cre;Cdh1$^{F/F}$;Pik3ca^{E545K}, (Wap)-cre;Cdh1$^{F/F}$;Pik3ca^{H1047R}, Wap-cre;Cdh1$^{F/F}$;Pten$^{F/F}$, Wap-cre;Cdh1$^{F/F}$;Akt^{E17K}, Brca1$^{F/F}$;Trp53$^{F/F}$* (generous gift of Jos Jonkers, NKI) and *Cdh1$^{F/F}$;Trp53$^{F/F}$;Foxp3$^{GFP\text{-}DTR}$* mice (further referred to as *Foxp3$^{GFP\text{-}DTR}$*). All mouse models were on FVB/n background, and genotyping was performed by PCR analysis on toe clips DNA as described [24]. Starting at 6-7 weeks of age, female mice were monitored twice weekly for the development of spontaneous mammary tumor development. Tumors in *Brca1$^{F/F}$;Trp53$^{F/F}$* mice were somatically induced through intraductal delivery of lentiviral-Cre as described before[58,59]. Mice were monitored twice weekly for spontaneous mammary tumor development starting 6 weeks after intraductal delivery of lenti-viral Cre. Upon mammary tumor formation, perpendicular tumor diameters were measured twice weekly using a caliper. In all models, end-stage was defined as cumulative tumor burden of 225mm^2. Age-matched WT littermates were used as controls.

Mice were kept in individually ventilated cages a the animal laboratory facility of the Netherlands Cancer Institute under specific pathogen free conditions. Food and water were provided *ad libitum.* All animal experiments were approved by the Netherlands Cancer Institute Animal Ethics Committee, and performed in accordance with institutional, national and European guidelines for Animal Care and Use. The study is compliant with all relevant ethical regulations regarding animal research.

Patients

The mean age of the ten female patients at the time of SLN procedure was 56.3 years. Patients had either lobular (n=2) or ductal (n=6) carcinoma of the breast, one patient had a tumor that was classified as ductal/lobular and one patient a tumor that was classified as mucinous adenocarcinoma. One patient, who was diagnosed with two invasive breast

tumors (ductal), had both a luminal A (Her2-, ER+, PR+) and a luminal B Her2+ (Her2+, ER-, PR-) tumor. All other patients were diagnosed with hormone receptor expressing (Her2-, ER+, PR+) tumors, of which six were classified as luminal A and three as luminal B. The study was approved by the Institutional Review Board (IRB) of the VU University medical center and SLN samples were collected and handled according to guidelines described in the Code of Conduct for Proper Use of Human Tissue of the Dutch Federation of Biomedical Scientific Societies with written informed consent from the patients prior to SLN sampling.

METHOD DETAILS

Generation of Foxp3$^{GFP\text{-}DTR}$ mice

Cdh1$^{F/F}$;*Trp53*$^{F/F}$;*Foxp3*$^{GFP\text{-}DTR}$ mice (further referred to as *Foxp3*$^{GFP\text{-}DTR}$) were generated using the previously described IRES-DTR-GFP targeting construct[61] (generous gift of Prof. Alexander Rudensky, MSKCC). Notably, Cre-recombinase is not expressed in *Foxp3*$^{GFP\text{-}DTR}$ mice, and generation of *Foxp3*$^{GFP\text{-}DTR}$ mice within the *Cdh1*$^{F/F}$;*Trp53*$^{F/F}$ background matches the background of control (*Cdh1*$^{F/F}$;*Trp53*$^{F/F}$) mice used throughout the manuscript. The linearized IRES-DTR-GFP construct was introduced in the 3′ untranslated region of Foxp3 upstream of the polyadenylation signal in *Cdh1*$^{F/F}$;*Trp53*$^{F/F}$ (FVB) embryonic stem cells (ESC) by electroporation as described before[61,62]. Neomycin-resistant clones were screened by PCR across the 3' arm. Correct targeting of the construct was confirmed by Southern blot. Correctly targeted clones were transfected with a FLP-deleter plasmid for excision of the PGK-Neo cassette. Transfected clones were selected by puromycin, and loss of the PGK-Neo cassette was confirmed by PCR. Selected ESCs were injected into C57BL/6N blastocysts and chimeric male offspring were mated to *Cdh1*$^{F/F}$;*Trp53*$^{F/F}$ mice. Homozygous *Cdh1*$^{F/F}$;*Trp53*$^{F/F}$;*Foxp3*$^{GFP\text{-}DTR}$ females were used for experiments.

KEP metastasis model

The KEP metastasis model has been applied as previously described[25]. Tumors from KEP mice (100mm^2) were fragmented into small pieces (~1 mm^2) and stored at -150 °C in Dulbecco's Modified Eagle's Medium F12 containing 30% fetal calf serum and 10% dimethyl sulfoxide. Selection of mouse invasive lobular carcinomas (mILC) donor tumors was based on high cytokeratin 8 and absence of vimentin and E-cadherin expression as determined by immunohistochemistry. Donor KEP tumor pieces were orthotopically transplanted into the 4th mammary fat pad of female recipient 9-12 week old WT FVB/n mice (Janvier). Upon tumor outgrowth to a size of 100mm^2, donor tumors were surgically removed. Following mastectomy, mice were monitored for development of overt multi-organ metastatic disease by daily palpation and observation of physical health, appearance, and behavior. Lungs, liver, spleen, intestines, mesenterium, kidneys, adrenal glands, and tumor-draining (subiliac, proper axillary and accessory axillary) and distant LNs (mesenteric, renal, and caudal) were collected and analyzed microscopically for the presence of metastatic foci by immunohistochemical cytokeratin 8 staining. Macroscopically overt metastases were

collected separately for further analysis. Mice were excluded from analysis due to following predetermined reasons: No outgrowth of tumors upon transplantation, mice sacrificed due to surgery-related complications, mice sacrificed due to development of end-stage (225mm^2) local recurrent tumors prior to presentation of metastatic disease.

Murine intervention studies

Antibody treatments were initiated at tumor sizes of 25-45mm^2 (as indicated) in spontaneous mammary tumor-bearing KEP and *Foxp3*$^{GFP\text{-}DTR}$ mice, and at 12-20mm^2 in the KEP metastasis model (neoadjuvant setting). Mice were randomly allocated to treatment groups upon presentation of mammary tumors of indicated size. Tumor development in KEP mice prevented full blinding to genotypes during mouse handling, but researchers were blinded to treatment and genotype during cell, tissue and immunohistological analysis. Mice were intraperitoneally injected with: Fc-receptor optimized anti-CD25 (Clone M2a [35] 200 µg weekly for 2 weeks; mIgG2a control antibody 200 µg weekly for 2 weeks (C1.18.4, BioXcell); anti-mouse CD8α single loading dose of 400 µg, followed by 200 µg thrice a week (2.43, BioXcell); anti-mouse NK1.1, single loading dose of 400 µg, followed by 200 µg twice a week (PK136, BioXcell); Difteria Toxin (Sigma) 25 µg twice total (t = 0, t = 7 days); anti-mouse IL-33 (R&D systems) 3.75 µg thrice a week for 2 weeks; IL-33Trap[32] 50 µg daily for 1 week. Animal sample size for intervention studies was determined by power analysis using G*power software, using effect sizes obtained from historical experiments or preliminary data. Due to the spontaneous nature of the used animal models for primary tumor formation and metastasis, cohorts were sequentially completed and analyzed in succession, similar in set up to clinical trials. In the KEP metastasis model, treatments were discontinued upon mastectomy. For survival curve experiments and end-stage analyses in KEP mice, antibody treatment continued until the tumor or the cumulative tumor burden reached 225mm^2. For KEP intervention and KEP metastasis experiments, the following end points were applied according to the Code of Practice Animal Experiments in cancer research: (metastatic) tumor size > 225mm^2, >20% weight loss since start of experiment, respiratory distress upon fixation, severe lethargy, (metastatic) tumor causing severe clinical symptoms as a result of location, invasive growth or ulceration.

Preparation of single cell suspensions

For flow cytometry based analysis and cell sorting for *in vitro* assays and RNA sequencing, single cell suspensions were prepared from freshly isolated mouse tissues. Mice were sacrificed at indicated time points. KEP tumors, healthy mammary glands spleens and LNs were prepared as previously described [63]. In brief, tumors and mammary glands were mechanically chopped using the McIlwain tissue chopper (Mickle Laboratory Engineering) and enzymatically digested with 3 mg ml−1 collagenase type A (Roche) and 25 µg ml−1 DNase I (Sigma) in serum-free medium for 1 h at 37°C in a shaking water bath. Enzyme activity was neutralized by addition of cold DMEM/8% FCS and suspension was dispersed

through a 70 µm cell strainer. Lungs were perfused with ice-cold PBS *post mortem* to flush blood. Next, lungs were cut into small pieces and mechanically chopped using the McIlwain tissue chopper. Lungs were enzymatically digested in 100 µg/mL Liberase Tm (Roche) under continuous rotation for 30 minutes at 37 °C. Enzyme activity was neutralized by addition of cold DMEM/8% FCS and suspension was dispersed through a 70 µm cell strainer. Spleens and lymph nodes were collected in ice-cold PBS, and dispersed through a 70 µm cell strainer. Blood was obtained via cardiac puncture for end-stage analyses, and via tail vein puncture for time point analyses and collected in tubes containing heparin. Erythrocyte lysis for blood, spleen and lungs was performed using NH_4Cl erythrocyte lysis buffer for 2x5 (blood) and 1x1 (spleen, lungs) minutes.

Flow cytometry: analysis and cell sorting

Single cell suspensions of human and murine samples were incubated in anti-CD16/32 (2.4G2, BD Biosciences) to block unspecific Fc receptor binding for 5 minutes. Next, cells were incubated for 20 minutes with fluorochrome conjugated antibodies diluted in FACS buffer (2.5% FBS, 2 mM EDTA in PBS). For analysis of nuclear transcription factors, cells were fixed and permeabilized after surface and live/dead staining using the FOXP3 Transcription buffer set (Thermofisher), according to manufacturer's instruction. Fixation permeabilization and intracellular FOXP3 staining was performed for 30 minutes. For analysis of granzyme B, TNFα and IFNγ, single cell suspensions were incubated in cIMDM (IMDM containing 8% FCS, 100 IU/ml penicillin, 100 µg/ml streptomycin, 0.5% β-mercapto-ethanol), 50 ng/ml PMA, 1 µM ionomycin and Golgi-Plug (1:1000; BD Biosciences) for 3 h at 37 °C prior to surface staining. For analysis of T_{reg} proliferation *in vivo*, mice were injected with the thymidine analog EdU (200 µg) 24 and 48h prior to sacrifice. DNA incorporation of EdU was measured using Click-iT™ EdU Cell Proliferation Kit for Imaging according to manufacturer's instruction. Cell suspensions were analyzed on a BD LSR2 SORP or BD Symphony SORP, or sorted on a FACS ARIA II (4 lasers), or FACS FUSION (5 lasers). Single cell suspensions for cell sorting were prepared under sterile conditions. Gating strategies for T_{reg} sorting as previously described[63]. See Key Resources Table for antibodies used. Absolute cell counts were determined using 123count eBeads (ThermoFisher) according to manufacturer's instruction.

T_{reg} suppression assays

T_{reg}-T cell suppression assays were performed as previously described[63]. Briefly, T_{regs} (Live, $CD45^{+,}$ $CD3^{+}$, $CD8^{-}$ $CD4^{+}$, $CD25^{high}$) sorted from freshly isolated samples were activated overnight in IMDM containing 8% FCS, 100 IU/ml penicillin, 100 µg/ml streptomycin, 0.5% β-mercapto-ethanol, 300U/mL IL-2, 1:5 bead:cell ratio CD3/CD28 coated beads (Thermofisher). Per condition, $5.0*10^5$ cells were seeded in 96-wells plate, which were further diluted to appropriate ratios (1:1 – 1:8). Responder cells (Live, $CD45^{+,}$ $CD3^{+}$, $CD4^{+}$, $CD25^{-}$ and Live, $CD45^{+,}$ $CD3^{+}$, $CD8^{+}$) were rested overnight. Next, responder cells were

labelled with CellTraceViolet, and co-cultured with T_{regs} in cIMDM supplemented with CD3/CD28 beads (1:5 bead cell ratio) for 96 h (without exogenous IL-2).

NK cell degranulation assay

Single cell suspensions of murine LN and lung samples were plated in a 96-wells plate, and incubated in IMDM containing 8% FCS, 100 IU/ml penicillin, 100 µg/ml streptomycin, 0.5% β-mercapto-ethanol, Golgi-Plug and Golgi-Stop (1:1,000; BD Biosciences) and anti-CD107a (clone LAMP-1, 1:200, Biolegend) for 4 h at 37 °C. For stimulation, cells were additionally supplemented with 50 ng ml^{-1} PMA, 1 mM ionomycin.

T_{reg}- KEP serum co-culture assay

$5.0*10^4$ splenic KEP T_{regs} sorted from freshly isolated samples were incubated for 96 h in 96-wells plated coated with 5 µg/mL anti-CD3 in IMDM containing 100 IU/ml penicillin, 100 µg/ml streptomycin, 0.5% β-mercapto-ethanol supplemented with 20% serum obtained from end-stage tumor-bearing KEP mice, or naïve littermates. Next, absolute cell counts were determined by flow cytometry as described above.

IL-33 protein analysis

To quantify IL-33 protein in different tissues of KEP mice and littermates, LegendPlex BioAssay (BioLegend) was used according to manufacturers' instruction. Protein lysates from snap frozen tissue were prepared by pulverizing small tissue fragments (1-$2mm^2$), which were incubated in RIPA buffer (50 mM Tris-HCl, pH 7.4, 150 mM NaCl, 1% NP40, 0.5% DOC, 0.1% SDS, 2 mM EDTA) complemented with protease and phosphatase inhibitors (Roche) for 30 minutes at 4 °C. Protein concentration was quantified using the BCA protein assay kit (Pierce). Samples were diluted to 4 mg/mL protein of which 40uL was used as input for IL-33 LegendPlex Bioassay according to manufacturers' instruction. Protein content (pg/mL) was determined using BioLegend LegendPlex analysis software.

Immunohistochemistry

Immunohistochemical analyses were performed by the Animal Pathology facility at the Netherlands Cancer Institute. Formalin-fixed tissues were processed, sectioned and stained as described[25]. In brief, tissues were fixed for 24 h in 10% neutral buffered formalin, embedded in paraffin, sectioned at 4 µm and stained with haematoxylin and eosin (H&E) for histopathological evaluation. H&E slides were digitally processed using the Aperio ScanScope (Aperio). For immunohistochemical analysis, 5 µm paraffin sections were cut, deparaffinized and stained. To score pulmonary metastasis, lung sections were stained for cytokeratin-8 and metastatic nodules were counted by two independent researchers. To score axillary LN metastasis incidence, draining axillary (proper and accessory) LN of mice that did not develop macroscopic LN metastasis were stained for cytokeratin-8. Presence of cytokeratin-8^+ cells (≥1) within LNs was indicative of micro metastatic disease. Stained

tissue slides were digitally processed using the Aperio ScanScope. Brightness and contrast for representative images were adjusted equally among groups.

RNAseq sample preparation: T_{regs}

For transcriptome analysis of T_{regs} from end-stage (225mm^2) tumor-bearing KEP mice and WT controls, single cell suspensions were prepared from spleens, mammary LNs, lungs, blood, tumor and naïve WT mammary glands as described above. A minimum of 70.000 T_{regs} (Live, CD45$^+$, CD3$^+$, CD4$^+$, CD25^{high}) were sorted in RLT buffer with 1% b-mercapto ethanol. Due to low abundance of T_{regs} in WT mice, tissue of 3 mice was pooled for each WT T_{reg} sample prior to sorting. Library preparation was performed as previously described[64].

RNAseq sample preparation: NK cells

For transcriptome analysis of NK cells of DT/PBS treated tumor-bearing (100mm^2) *Foxp3*$^{GFP\text{-}DTR}$ mice, single cells suspensions were prepared from axillary LNs and lungs, as described above. A minimum of 5000 NK cells (Live, CD45$^+$, CD3$^-$, NKp46$^+$, DX5$^+$) were sorted in RLT buffer with 1% β-mercapto-ethanol. Library preparation was performed as previously described[65], using 2100 Bioanalyzer System for library quality control.

RNAseq of T_{reg} and NK cells

Sorted T_{reg} and NK cells were resuspended in RLT buffer + 1% β -mercapto-ethanol. Total RNA was extracted using RNAeasy mini kit (Qiagen). RNA quality and quantity control was performed using Agilent RNA 6000 Pico Kit and 2100 Bioanalyzer System. RNA samples with an RNA Integrity Number > 8 were subjected to library preparation. The strand-specific reads (65bp single-end) were sequenced with the HiSeq 2500 machine. Demultiplexing of the reads was performed with Illumina's bcl2fastq. For T_{reg} RNAseq, demultiplexed reads were aligned against the mouse reference genome (build 38) using TopHat (version 2.1.0, bowtie 1.1). TopHat was supplied with a known set of gene models (Ensembl version 77) and was guided to use the first-strand as the library-type. As additional parameters --prefilter-multihits and --no coverage were used. For NK cell RNAseq, demultiplexed reads were aligned against the mouse reference genome (build 38) using Hisat2. Hisat2 was supplied with a known set of gene models (Ensembl version 87).

RNAseq analysis

In order to count the number of reads per gene, a custom script, itreecount (https://github.com/NKI-GCF/itreecount), has been used. This script is based on the same concept as HTSeq-count. A list of the total number of uniquely mapped sequencing reads for each gene that is present in the provided Gene Transfer Format (GTF) file was generated. For T_{reg} RNAseq, differential expression was performed using the R package Limma/Voom on normalized counts. Resulting p-values are corrected for multiple testing. A gene was considered differentially expressed if the p-value <0.05, and read counts >30 in all samples of a group.

For PCA the genes that have no expression across all samples within the dataset were removed. Furthermore, the analysis was restricted to only those genes that have at least two counts per million (CPM) value, calculated via edgeR package (3.30.3) using 'cpm' function in all samples from the included conditions and in this way lowly abundant genes were excluded. PCA was performed using the `prcomp` function on variance stabilizing transformed data with the `vst` function from the DESeq2 package with default arguments and plotted by using ggplot2 package (3.3.3) in R language (version 4.0.2).

Hierarchical cluster analysis for the samples was performed using 'hclust' function with default arguments. Dendrogram was made by using 'dendro_data' function from ggdendro package (0.1.22). Sample to sample distances obtained using 'dist' function on variance stabilizing transformed data were subjected to hierarchical cluster analysis and dendrogram preparation. Normalized counts from DESeqDataSet from the DESeq2 package were subjected to calculate correlation among the samples by using 'cor' function using spearman method in R language (version 4.0.2).

Differential gene expression analysis of NK cells was performed in R language (version 4.0.2) only on relevant samples using edgeR package (3.30.3) and default arguments with the design set either to PBS or DT-treatment group. Lowly abundant genes (< 2 CPM) from all the samples in a specific contrast were excluded. Furthermore, to avoid any biasness due to the variation among the replicates within a group, the analysis was confined to the genes which have read counts (> 2 CPM) among all the replicates from either of the two groups in a specific contrast. Genes were considered to be differentially expressed when the False discovery rate (FDR) was below 0.1 after the Benjamini–Hochberg multiple testing correction. MA plots were generated after differential expression analysis in R language (version 4.0.2).

IPA and GSEA analysis

Pathway enrichment analysis of KEP/WT T_{regs} RNAseq data was performed using Ingenuity Pathway Analysis software (QIAGEN), analyzing differentially expressed genes with q value < 0.05 for KEP/WT T_{regs}. Gene Set Enrichment Analysis (GSEA)[66] was performed using GSEA software (v. 4.0.3) on RNAseq data (transcripts for which read count > 30 included) of KEP/WT T_{reg} of indicated tissues, on gene sets obtained from[26], and mSigDB Hallmark gene sets[38]. Permutations for each gene set was conducted 1000 times to obtain an empirical null distribution.

Human sentinel LN sampling

Viable cells were collected from SLN from ten female patients diagnosed with clinically node negative BrC scheduled to undergo a SLN procedure between February and July 2014, as previously described[14]. None of the patients received neoadjuvant chemo- or hormone

therapy prior to the SLN procedure. These ten patients were part of a previously described larger cohort[14], and were selected based on availability of (previously unpublished) NK cell flow cytometry data. Axillary healthy LN were retrieved after written informed consent from prophylactic mastectomy specimens (n=16) in the Antoni van Leeuwenhoek Hospital between 2012-2014. The collection of these samples was also previously described and approved by the local IRB[14].

Preparation of human LN samples

Viable cells were scraped from the cutting surface of a bisected SLN before routine histopathological examination and after confirmation by the pathologist that the SLN was suitable for cell harvesting (i.e. >0.5 cm), as described[14,67]. SLN cells were subsequently washed twice in IMDM supplemented with 10% FCS, 100 I.E./ml sodium penicillin, 100 µg/ml streptomycin sulfate, 2 mM L-glutamine (P/S/G), and 0.01 mM β-mercapto-ethanol, counted, and used for immune phenotyping. FACS staining for surface and intracellular proteins was performed as described[14] and data were acquired on a FACSCalibur flow cytometer (Becton Dickinson). NK cell and T_{reg} frequencies were determined using FlowJo software (version 10.7). See Key Resources Table for antibodies used.

Statistical analysis

Data analyses were performed using GraphPad Prism (version 8). Data show means ± SEM unless stated otherwise. The statistical tests used are described in figure legends. For comparison of two groups of continuous data, Student's T-test and Mann Whitney's T Test were used as indicated. For comparison of a single variable between multiple groups of normally distributed continuous data, we used one-way ANOVA, followed by indicated post-hoc analyses. For comparison of ≥2 variables between multiple groups, two-way ANOVA was used, with Sidak's post-hoc analysis. Fisher's exact test was used to assess significant differences between categorical variables obtained from lymph node metastasis incidence experiments. All tests were performed two-tailed. P-values < 0.05 were considered statistically significant. Sample sizes for mouse intervention experiments were predetermined using G*Power software (version 3.1). *In vivo* interventions and RNAseq experiments were performed once with indicated sample sizes, unless otherwise indicated. In vitro experiments were repeated independently as indicated, with at least three biological replicates per condition. Asterisks indicate statistically significant differences compared to WT. * $P < 0.05$, ** $P < 0.01$, *** $P < 0.001$, **** $P < 0.0001$.

REFERENCES

1. DeSantis, C. E. *et al.* Breast cancer statistics, 2019. *CA. Cancer J. Clin.* **69**, 438–451 (2019).
2. Lambert, A. W., Pattabiraman, D. R. & Weinberg, R. A. Emerging Biological Principles of Metastasis. *Cell* **168**, 670–691 (2017).
3. Garner, H. & de Visser, K. E. Immune crosstalk in cancer progression and metastatic spread: a complex conversation. *Nat. Rev. Immunol.* 1–15 (2020) doi:10.1038/s41577-019-0271-z.
4. Angelova, M. *et al.* Evolution of Metastases in Space and Time under Immune Selection. *Cell* **175**, 751-765.e16 (2018).
5. Plitas, G. & Rudensky, A. Y. Regulatory T Cells in Cancer. *Annu. Rev. Cancer Biol.* **4**, 459–477 (2020).
6. Plitas, G. *et al.* Regulatory T Cells Exhibit Distinct Features in Human Breast Cancer. *Immunity* **45**, 1122–1134 (2016).
7. Kos, K. & de Visser, K. E. The Multifaceted Role of Regulatory T Cells in Breast Cancer. *Annu. Rev. Cancer Biol.* **5**, (2021).
8. Liu, S. *et al.* Prognostic significance of FOXP3+ tumor-infiltrating lymphocytes in breast cancer depends on estrogen receptor and human epidermal growth factor receptor-2 expression status and concurrent cytotoxic T-cell infiltration. *Breast Cancer Res.* **16**, (2014).
9. Decker, T. *et al.* Increased number of regulatory T cells (T-regs) in the peripheral blood of patients with Her-2/neu-positive early breast cancer. *J. Cancer Res. Clin. Oncol.* **138**, 1945–1950 (2012).
10. Liyanage, U. K. *et al.* Prevalence of Regulatory T Cells Is Increased in Peripheral Blood and Tumor Microenvironment of Patients with Pancreas or Breast Adenocarcinoma. *J. Immunol.* **169**, 2756–2761 (2002).
11. Perez, S. A. *et al.* CD4+CD25+ Regulatory T-Cell Frequency in HER-2/neu (HER)-Positive and HER-Negative Advanced-Stage Breast Cancer Patients. *Clin. Cancer Res.* **13**, 2714–2721 (2007).
12. Wolf, A. M. *et al.* Increase of Regulatory T Cells in the Peripheral Blood of Cancer Patients. *Clin. Cancer Res.* **9**, 606–612 (2003).
13. Wang, L. *et al.* Connecting blood and intratumoral Treg cell activity in predicting future relapse in breast cancer. *Nat. Immunol.* **20**, 1220–1230 (2019).
14. van Pul, K. M. *et al.* Selectively hampered activation of lymph node-resident dendritic cells precedes profound T cell suppression and metastatic spread in the breast cancer sentinel lymph node. *J. Immunother. Cancer* **7**, 133 (2019).
15. Faghih, Z. *et al.* Immune profiles of CD4+ lymphocyte subsets in breast cancer tumor draining lymph nodes. *Immunol. Lett.* **158**, 57–65 (2014).
16. Mansfield, A. S. *et al.* Simultaneous Foxp3 and IDO expression is associated with sentinel lymph node metastases in breast cancer. *BMC Cancer* **9**, (2009).
17. Núñez, N. G. *et al.* Tumor invasion in draining lymph nodes is associated with Treg accumulation in breast cancer patients. *Nat. Commun.* **11**, 1–15 (2020).
18. Jiang, D., Gao, Z., Cai, Z., Wang, M. & He, J. Clinicopathological and prognostic significance of FOXP3+ tumor infiltrating lymphocytes in patients with breast cancer: A meta-analysis. *BMC Cancer* **15**, (2015).
19. Clark, N. M. *et al.* Regulatory T Cells Support Breast Cancer Progression by Opposing IFN-γ-Dependent Functional Reprogramming of Myeloid Cells. *Cell Rep.* **33**, 108482 (2020).
20. Gómez-Cuadrado, L., Tracey, N., Ma, R., Qian, B. & Brunton, V. G. Mouse models of metastasis: progress and prospects. *Dis. Model. Mech.* **10**, 1061–1074 (2017).
21. Bos, P. D., Plitas, G., Rudra, D., Lee, S. Y. & Rudensky, A. Y. Transient regulatory T cell ablation deters oncogene-driven breast cancer and enhances radiotherapy. *J. Exp. Med.* **210**, 2435–2466 (2013).
22. Liu, J. *et al.* Improved efficacy of neoadjuvant compared to adjuvant immunotherapy to eradicate metastatic disease. *Cancer Discov.* **6**, 1382–1399 (2016).
23. Hughes, E. *et al.* Primary breast tumours but not lung metastases induce protective anti-tumour immune responses after Treg-depletion. *Cancer Immunol. Immunother.* 1–11 (2020) doi:10.1007/s00262-020-02603-x.
24. Derksen, P. W. B. *et al.* Somatic inactivation of E-cadherin and p53 in mice leads to metastatic lobular mammary carcinoma through induction of anoikis resistance and angiogenesis. *Cancer Cell* **10**, 437–449 (2006).
25. Doornebal, C. W. *et al.* A Preclinical Mouse Model of Invasive Lobular Breast Cancer Metastasis. *Cancer Res.* **73**, 353 LP – 363 (2013).
26. Magnuson, A. M. *et al.* Identification and validation of a tumor-infiltrating Treg transcriptional signature conserved across species and tumor types. *PNAS* **115**, E10672–E10681 (2018).
27. Cao, X. *et al.* Granzyme B and Perforin Are Important for Regulatory T Cell-Mediated Suppression of Tumor Clearance. *Immunity* **27**, 635–646 (2007).
28. Pastille, E. *et al.* The IL-33/ST2 pathway shapes the regulatory T cell phenotype to promote intestinal cancer. *Mucosal Immunol.* **12**, 990–1003 (2019).

29. Li, A. *et al.* IL-33 Signaling Alters Regulatory T Cell Diversity in Support of Tumor Development. *Cell Rep.* **29**, 2998-3008.e8 (2019).
30. Son, J. *et al.* Tumor-Infiltrating Regulatory T Cell Accumulation in the Tumor Microenvironment is Mediated by IL33/ST2 Signaling. *Cancer Immunol. Res.* **8**, canimm.0828.2019 (2020).
31. Matta, B. M. & Turnquist, H. R. Expansion of regulatory T cells in vitro and in vivo by IL-33. in *Methods in Molecular Biology* vol. 1371 29–41 (Humana Press Inc., 2016).
32. Holgado, A. *et al.* IL-33trap is a novel IL-33–neutralizing biologic that inhibits allergic airway inflammation. *J. Allergy Clin. Immunol.* **144**, 204–215 (2019).
33. Sun, L. *et al.* Divenn: An interactive and integrated web-based visualization tool for comparing gene lists. *Front. Genet.* **10**, 421 (2019).
34. Coffelt, S. B. *et al.* IL-17-producing γδ T cells and neutrophils conspire to promote breast cancer metastasis. *Nature* **522**, 345–348 (2015).
35. Arce Vargas, F. *et al.* Fc-Optimized Anti-CD25 Depletes Tumor-Infiltrating Regulatory T Cells and Synergizes with PD-1 Blockade to Eradicate Established Tumors. *Immunity* **46**, 577–586 (2017).
36. Paul, S. & Lal, G. The Molecular Mechanism of Natural Killer Cells Function and Its Importance in Cancer Immunotherapy. *Front. Immunol.* **0**, 1124 (2017).
37. Duhan, V. *et al.* NK cell–intrinsic FcεRIγ limits CD8+ T-cell expansion and thereby turns an acute into a chronic viral infection. *PLoS Pathog.* **15**, e1007797 (2019).
38. Liberzon, A. *et al.* The Molecular Signatures Database Hallmark Gene Set Collection. *Cell Syst.* **1**, 417–425 (2015).
39. Chiossone, L. *et al.* Maturation of mouse NK cells is a 4-stage developmental program. *Blood* **113**, 5488–5496 (2009).
40. Hayakawa, Y. & Smyth, M. J. CD27 Dissects Mature NK Cells into Two Subsets with Distinct Responsiveness and Migratory Capacity. *J. Immunol.* **176**, 1517–1524 (2006).
41. Poli, A. *et al.* CD56bright natural killer (NK) cells: An important NK cell subset. *Immunology* vol. 126 458–465 (2009).
42. Kim, S. T. *et al.* Tumor-infiltrating lymphocytes, tumor characteristics, and recurrence in patients with early breast cancer. *Am. J. Clin. Oncol. Cancer Clin. Trials* **36**, 224–231 (2013).
43. Dings, P. J. M., Elferink, M. A. G., Strobbe, L. J. A. & de Wilt, J. H. W. The Prognostic Value of Lymph Node Ratio in Node-Positive Breast Cancer: A Dutch Nationwide Population-Based Study. *Ann. Surg. Oncol.* **20**, 2607–2614 (2013).
44. Beenken, S. W. *et al.* Axillary Lymph Node Status, But Not Tumor Size, Predicts Locoregional Recurrence and Overall Survival After Mastectomy for Breast Cancer. *Ann. Surg.* **237**, 732–739 (2003).
45. López-Soto, A., Gonzalez, S., Smyth, M. J. & Galluzzi, L. Control of Metastasis by NK Cells. *Cancer Cell* vol. 32 135–154 (2017).
46. Huntington, N. D., Cursons, J. & Rautela, J. The cancer–natural killer cell immunity cycle. *Nature Reviews Cancer* vol. 20 437–454 (2020).
47. Ghiringhelli, F. *et al.* CD4+CD25+ regulatory T cells inhibit natural killer cell functions in a transforming growth factor-β-dependent manner. *J. Exp. Med.* **202**, 1075–1085 (2005).
48. Mamessier, E. *et al.* Human breast cancer cells enhance self tolerance by promoting evasion from NK cell antitumor immunity. *J. Clin. Invest.* **121**, 3609–3622 (2011).
49. Kim, R. *et al.* A potential role for peripheral natural killer cell activity induced by preoperative chemotherapy in breast cancer patients. *Cancer Immunol. Immunother.* **68**, 577–585 (2019).
50. Wing, K. *et al.* CTLA-4 control over Foxp3+ regulatory T cell function. *Science (80-.).* **322**, 271–275 (2008).
51. Schuijs, M. J. *et al.* ILC2-driven innate immune checkpoint mechanism antagonizes NK cell antimetastatic function in the lung. *Nat. Immunol.* **21**, 998–1009 (2020).
52. Reiter, J. G. *et al.* Lymph node metastases develop through a wider evolutionary bottleneck than distant metastases. *Nat. Genet.* **52**, 692–700 (2020).
53. Zhong, W. *et al.* Comparison of the molecular and cellular phenotypes of common mouse syngeneic models with human tumors. *BMC Genomics* **21**, 2 (2020).
54. Gutierrez, W. R. *et al.* Divergent immune landscapes of primary and syngeneic Kras-driven mouse tumor models. *Sci. Rep.* **11**, 1098 (2021).
55. Hemmers, S., Schizas, M. & Rudensky, A. Y. T reg cell-intrinsic requirements for ST2 signaling in health and neuroinflammation. *J. Exp. Med.* **218**, (2021).
56. Sun, Z. *et al.* A next-generation tumor-targeting IL-2 preferentially promotes tumor-infiltrating CD8+ T-cell response and effective tumor control. *Nat. Commun.* **10**, (2019).
57. Wellenstein, M. D. *et al.* Loss of p53 triggers WNT-dependent systemic inflammation to drive breast cancer metastasis. *Nature* **572**, 538–542 (2019).
58. Annunziato, S. *et al.* Modeling invasive lobular breast carcinoma by CRISPR / Cas9-mediated somatic genome editing of the mammary gland. *Genes Dev.* **30**, 1470–1480 (2016).

59. Annunziato, S. *et al.* Comparative oncogenomics identifies combinations of driver genes and drug targets in BRCA1-mutated breast cancer. *Nat. Commun.* **10**, (2019).
60. Boelens, M. C. *et al.* PTEN Loss in E-Cadherin-Deficient Mouse Mammary Epithelial Cells Rescues Apoptosis and Results in Development of Classical Invasive Lobular Carcinoma. *Cell Rep.* **16**, 2087–2101 (2016).
61. Kim, J. M., Rasmussen, J. P. & Rudensky, A. Y. Regulatory T cells prevent catastrophic autoimmunity throughout the lifespan of mice. *Nat. Immunol.* **8**, 191–7 (2007).
62. Huijbers, I. J. *et al.* Using the GEMM-ESC strategy to study gene function in mouse models. *Nat. Protoc.* **10**, 1755–1785 (2015).
63. Kos, K., van Baalen, M., Meijer, D. A. & de Visser, K. E. Flow cytometry-based isolation of tumor-associated regulatory T cells and assessment of their suppressive potential. in *Methods in Enzymology* (2019). doi:10.1016/bs.mie.2019.07.035.
64. Aslam, M. A. *et al.* The Ig heavy chain protein but not its message controls early B cell development. *Proc. Natl. Acad. Sci. U. S. A.* **117**, 31343–31352 (2020).
65. Picelli, S. *et al.* Full-length RNA-seq from single cells using Smart-seq2. *Nat. Protoc.* **9**, 171–181 (2014).
66. Subramanian, A. *et al.* Gene set enrichment analysis: A knowledge-based approach for interpreting genome-wide expression profiles. *Proc. Natl. Acad. Sci. U. S. A.* **102**, 15545–15550 (2005).
67. Vuylsteke, R. J. C. L. M. *et al.* Sampling tumor-draining lymph nodes for phenotypic and functional analysis of dendritic cells and T cells. *Am. J. Pathol.* **161**, 19–26 (2002).

SUPPLEMENTARY MATERIALS

Data file S1: Differentially expressed genes KEP/WT T_{regs} for indicated tissues, and distribution across tissue. Related to Figure 2 and 3.

Data file S2: Differentially expressed genes of DT/PBS treated NK cells for indicated tissues, and distribution across tissue. Related to Figure 5. These files are available in the online version of the paper.

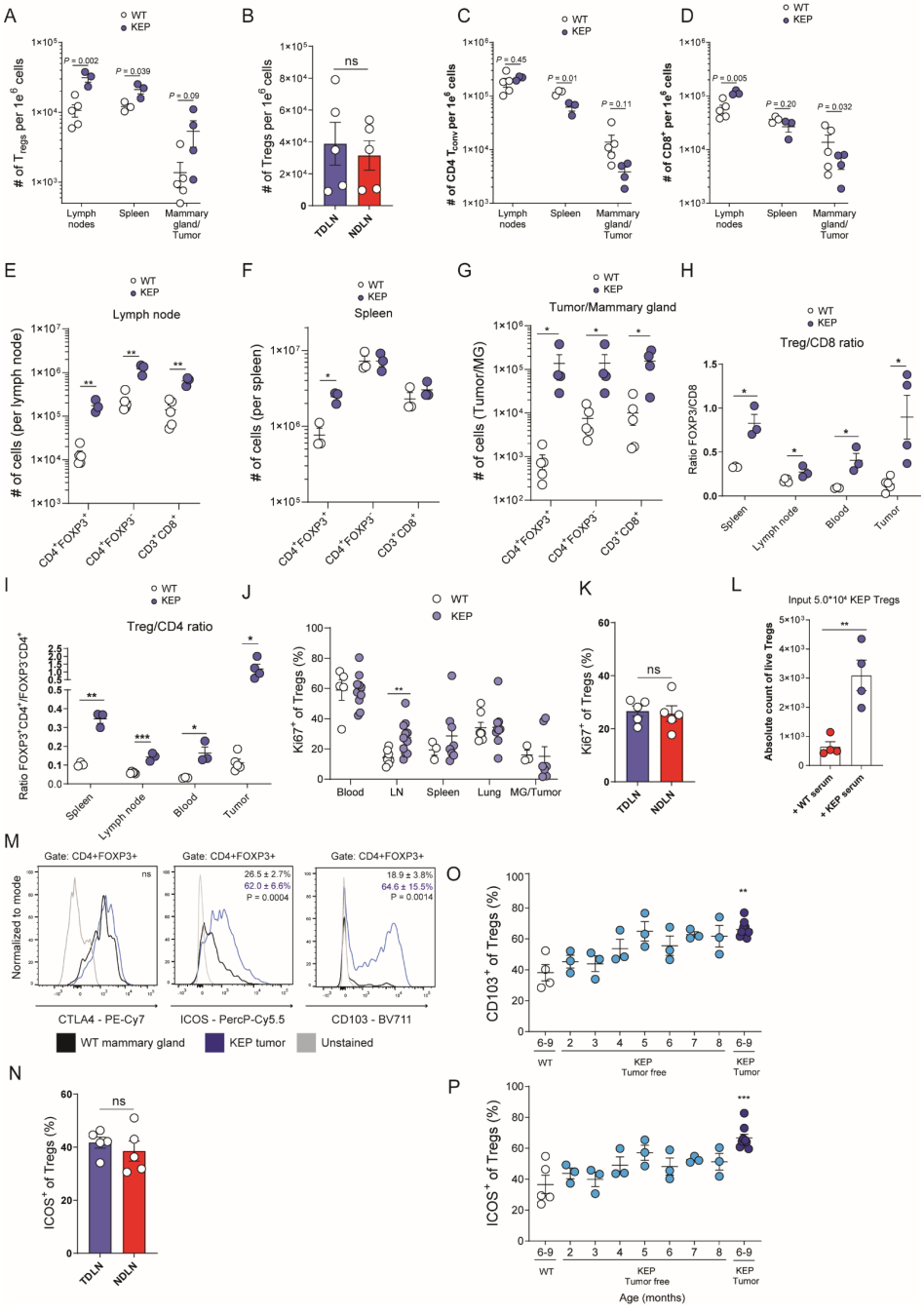
A
WT
KEP
# of Tregs per 1e6 cells
P = 0.002
P = 0.039
P = 0.09
Lymph nodes
Spleen
Mammary gland/ Tumor
B
# of Tregs per 1e6 cells
ns
TDLN
NDLN
C
# of CD4 Tconv per 1e6 cells
P = 0.45
P = 0.01
P = 0.11
D
# of CD8+ per 1e6 cells
P = 0.005
P = 0.20
P = 0.032
E
Lymph node
# of cells (per lymph node)
CD4+FOXP3+
CD4+FOXP3-
CD3+CD8+
F
Spleen
# of cells (per spleen)
G
Tumor/Mammary gland
# of cells (Tumor/MG)
H
Treg/CD8 ratio
Ratio FOXP3/CD8
Spleen
Lymph node
Blood
Tumor
I
Treg/CD4 ratio
Ratio FOXP3+CD4+/FOXP3-CD4+
J
Ki67+ of Tregs (%)
Blood
LN
Spleen
Lung
MG/Tumor
K
Ki67+ of Tregs (%)
L
Input 5.0*10⁴ KEP Tregs
Absolute count of live Tregs
+WT serum
+KEP serum
M
Gate: CD4+FOXP3+
Normalized to mode
ns
26.5 ± 2.7%
62.0 ± 6.6%
P = 0.0004
18.9 ± 3.8%
64.6 ± 15.5%
P = 0.0014
CTLA4 - PE-Cy7
ICOS - PercP-Cy5.5
CD103 - BV711
WT mammary gland
KEP tumor
Unstained
N
ICOS+ of Tregs (%)
O
CD103+ of Tregs (%)
WT
KEP Tumor free
KEP Tumor
P
ICOS+ of Tregs (%)
Age (months)

FIGURE S1. T_{regs} selectively expand in mammary tumor-bearing mice. Related to figure 1.
A-**D**. Absolute cell counts of T_{regs} (**A,B**), T_{conv} (**C**) and $CD8^+$ T cells (**D**) per $1e^6$ cells in indicated tissues (n=3 mice/group) of tumor-bearing ($225mm^2$) KEP mice and WT controls (n=3-5 mice/group). **E-G**. Total absolute cell counts of indicated T cell population per lymph node (**E**), spleen (**F**) and tumor/mammary gland (**G**) of tumor-bearing ($225mm^2$) KEP mice and WT controls (n=3-5 mice/group). **H-I**. Ratio (based on data in **A**,**C**,**D**) of $FOXP3^+CD4^+/CD8^+$ T cells (**H**) and $FOXP3^+CD4^+/FOXP3^-CD4^+$ (**I**) in indicates tissue of tumor-bearing ($225mm^2$) KEP mice and WT controls. **J**. Quantification of Ki67 expression on T_{regs} in tumor-bearing KEP mice ($100\text{-}225mm^2$) and WT controls in indicated tissues as determined by flow cytometry (n=3-10 mice/group). **K.** Quantification of Ki67 expression on T_{regs} in TDLN and NDLN of tumor-bearing KEP mice ($225mm^2$) by flow cytometry (n=5 mice/group). **L**. $5*10^4$ KEP T_{regs} ($CD4^+CD25^+$) were cultured for 96 hours with 5 µg/mL anti-CD3 and 20% serum obtained from WT controls or tumor-bearing KEP mice ($225mm^2$). Quantification of live KEP T_{regs} is shown (data pooled from 2 independent experiment with 2 biological replicates per experiment). **M**. Representative histograms depicting expression of intracellular CTLA4, ICOS and CD103 gated on $CD4^+$ $FOXP3^+$T cells, in ($225m^2$) tumors of KEP (blue) mice versus WT controls (black) by flow cytometry. % represent mean frequency (n=3-7 mice/group). **N.** Quantification of ICOS expression on T_{regs} in TDLN and NDLN of tumor-bearing KEP mice ($225mm^2$) by flow cytometry (n=5 mice/group). **O**-**P**. Frequencies of $CD103^+$ cells (**O**) and ICOS (**P**) of $FOXP3^+CD4^+$ T cells in blood of tumor-free, and tumor-bearing ($225mm^2$) KEP mice and WT controls (n=3-10 mice/group). Data in A-L, N-P show mean ± S.E.M. P-values are determined by Unpaired Students T-test (A-F,K,M,N), Unpaired Students T-test with Holm-Sidak correction for multiple testing (H-I,J), Mann-Whitney Test (G,L) and Kruskal-Wallis test with Dunn's multiple comparison test (O,P).

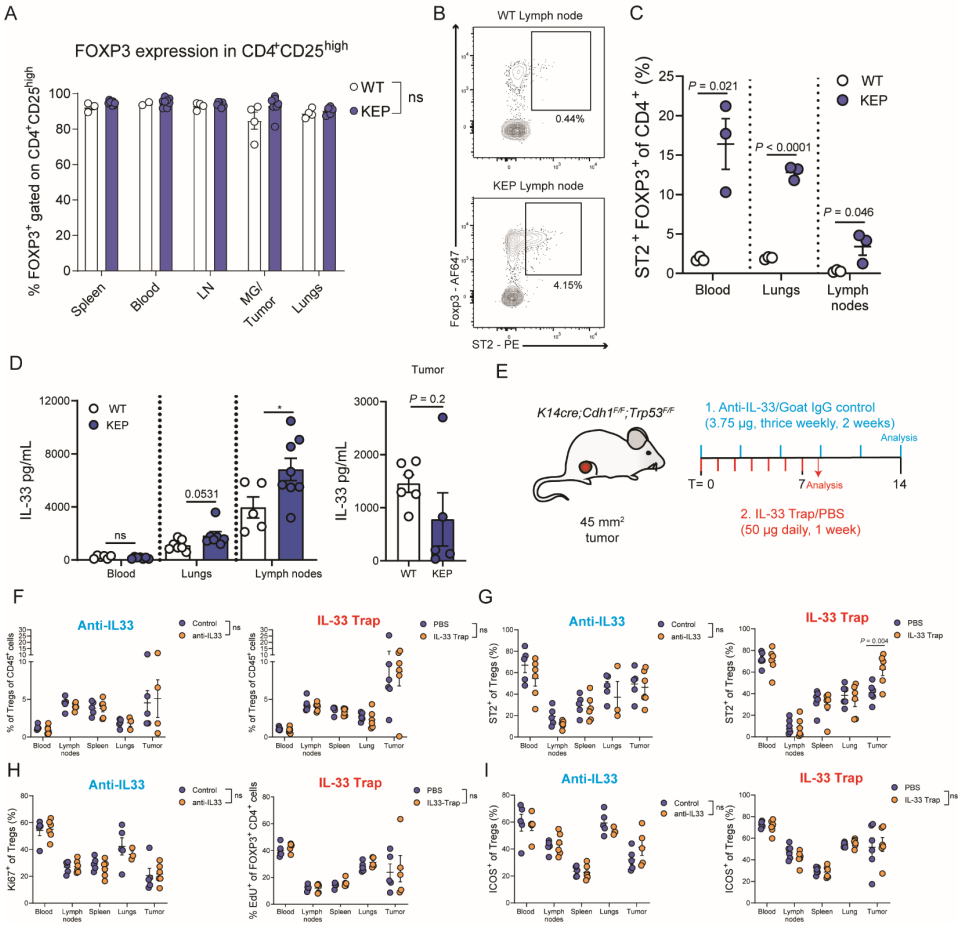
A
FOXP3 expression in CD4+CD25high
% FOXP3+ gated on CD4+CD25high
WT
KEP
ns
Spleen
Blood
LN
MG/ Tumor
Lungs
B
WT Lymph node
0.44%
KEP Lymph node
4.15%
Foxp3 - AF647
ST2 - PE
C
ST2+ FOXP3+ of CD4+ (%)
P = 0.021
P < 0.0001
P = 0.046
Blood
Lungs
Lymph nodes
D
IL-33 pg/mL
ns
0.0531
*
Blood
Lungs
Lymph nodes
Tumor
P = 0.2
WT
KEP
E
K14cre;Cdh1F/F;Trp53F/F
45 mm2 tumor
1. Anti-IL-33/Goat IgG control
(3.75 µg, thrice weekly, 2 weeks)
Analysis
T= 0
7
14
2. IL-33 Trap/PBS
(50 µg daily, 1 week)
F
Anti-IL33
Control
anti-IL33
IL-33 Trap
PBS
IL-33 Trap
% of Tregs of CD45+ cells
G
ST2+ of Tregs (%)
P = 0.004
H
Ki67+ of Tregs (%)
% EdU+ of FOXP3+ CD4+ cells
I
ICOS+ of Tregs (%)
Blood
Lymph nodes
Spleen
Lungs
Lung
Tumor

FIGURE S2. Role of IL-33 for T_{regs} in KEP tumor-bearing mice. Related to figure 2.
A. Quantification of FOXP3 expression in $CD4^+CD25^{high}$ T cells in indicated tissues of WT and tumor-bearing KEP mice (n=4-8 mice/group). **B**. Representative dot plot depicting ST2 expression on $CD4^+$ cells in TDLNs of 100mm^2 tumor-bearing KEP mice and WT controls. Gated on Live, $CD45^+$, $CD3^+CD4^+$ cells. **C**. Quantification of data shown in (**B**), for indicated tissues (n=3 mice/group). **D**. Legendplex analysis of IL-33 protein content in serum, lung, LN and KEP tumor lysates. Tissue samples obtained from tumor-bearing (225mm^2) KEP mice and WT controls (n=5-8 biological replicates per group). **E.** Schematic overview of IL-33 blockade strategies. Tumor-bearing KEP mice were treated with either anti-IL-33 (n=6 mice/group) /goat IgG control (n=5 mice/group) (3.75 µg, thrice weekly), or with IL-33Trap/PBS (n=6/group 50 µg/daily) for indicated timepoints starting at a tumor size of ~45mm^2. Il-33Trap/PBS treated mice received 200 µg EdU 48h and 24h prior to sacrifice to analyse cell proliferation. **F-I** Analysis of % T_{regs} of $CD45^+$ cells (**F**), ST2 expression on T_{regs} (**G**), Ki67 expression on T_{regs} (left panel), or EdU^+ T_{regs} (right panel) (**H**), ICOS expression on T_{regs} (**I**) in indicated tissue of mice receiving treatments as indicated in (n=3 for lungs anti-IL-33, n=5-6 for other comparison). Data in A, C-D, F-I show mean ± S.E.M. P-values are determined by Unpaired Students T-test (C-D). Unpaired Students T-test with Holm-Sidak correction for multiple testing (A), 2-way ANOVA with Holm-Sidak's multiple comparison test (F-I).

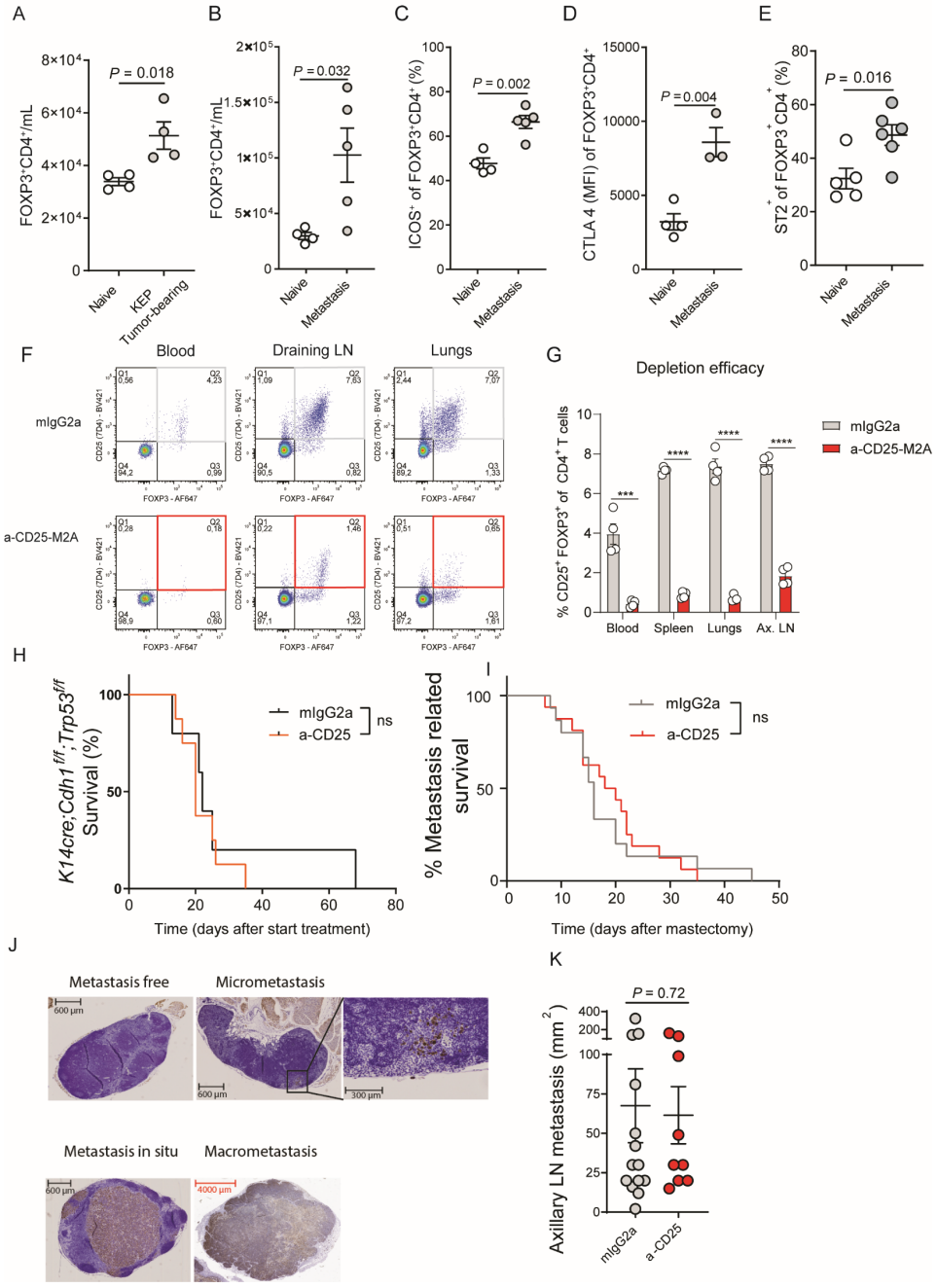
A
FOXP3+CD4+/mL
P = 0.018
Naive
KEP Tumor-bearing
B
FOXP3+CD4+/mL
P = 0.032
Naive
Metastasis
C
ICOS+ of FOXP3+CD4+ (%)
P = 0.002
Naive
Metastasis
D
CTLA 4 (MFI) of FOXP3+CD4+
P = 0.004
Naive
Metastasis
E
ST2+ of FOXP3+ CD4+ (%)
P = 0.016
Naive
Metastasis
F
Blood
Draining LN
Lungs
mIgG2a
a-CD25-M2A
CD25 (7D4) - BV421
FOXP3 - AF647
G
Depletion efficacy
% CD25+ FOXP3+ of CD4+ T cells
mIgG2a
a-CD25-M2A
Blood
Spleen
Lungs
Ax. LN
H
K14cre;Cdh1f/f;Trp53f/f
Survival (%)
mIgG2a
a-CD25
ns
Time (days after start treatment)
I
% Metastasis related survival
mIgG2a
a-CD25
ns
Time (days after mastectomy)
J
Metastasis free
Micrometastasis
Metastasis in situ
Macrometastasis
600 µm
300 µm
4000 µm
K
P = 0.72
Axillary LN metastasis (mm2)
mIgG2a
a-CD25

FIGURE S3. Systemic T_{reg} activation in mice bearing breast cancer metastasis. Related to figure 4.

A-B. Absolute cell count of T_{reg} ($CD4^+FOXP3^+$ T cells) in blood of naïve mice, versus mice bearing orthotopically transplanted primary KEP tumors prior to mastectomy (80-100mm^2) (**A**), or end-stage metastatic disease (**B**) (n=4-5 mice/group). **C-E**. Analysis of ICOS (**C**) and CTLA4 (**D**) and ST2 (**E**) expression on T_{regs} in blood of mice with end-stage metastatic disease, versus naïve controls (n=4-6 mice/group). **F**. Representative dot plots of CD25 and FOXP3 expression, gated on live $CD4^+$ T cells in blood, draining axillary lymph node and lungs of KEP tumor-bearing mice treated with mIgG2a or anti-CD25. Mice were sacrificed 3 days after start treatment (n=4 mice/group). **G**. Quantification of $CD25^+FOXP3^+$ of $CD4^+$ T cell gate (Q2) shown in (**F**) in indicated tissues of KEP tumor-bearing mice treated with mIgG2a or anti-CD25. Mice were sacrificed 3 days after start treatment (n=4 mice/group).**H.** Kaplan-Meier plot of tumor-specific survival of KEP mice treated with mIgG2a or anti-CD25. Treatment (weekly injection of 200 µg antibody) was initiated at tumor size of 25mm^2, and continued until end-stage (225mm^2) (n=5-7 mice/group). **I**. Metastasis related survival after mastectomy of KEP tumor-bearing mice receiving weekly neoadjuvant treatment of 200 µg mIgG2a or anti-CD25. **J**. Representative immunohistochemical keratin 8 staining depicting axillary TDLNs in mice with end-stage metastatic disease with, and without metastatic infiltration of keratin 8^+ cancer cells. **K**. LN tumor size (mm^2) upon sacrifice in mice with LN metastasis, treated with mIgG2a or anti-CD25-M2a (n=9-14 mice/group). Data in A-E, G, K show mean ± S.E.M. P-value was determined by Mann Whitney test (A-E, K), Unpaired Students T-test with Holm-Sidak correction for multiple testing (G) log-rank test (H,I).

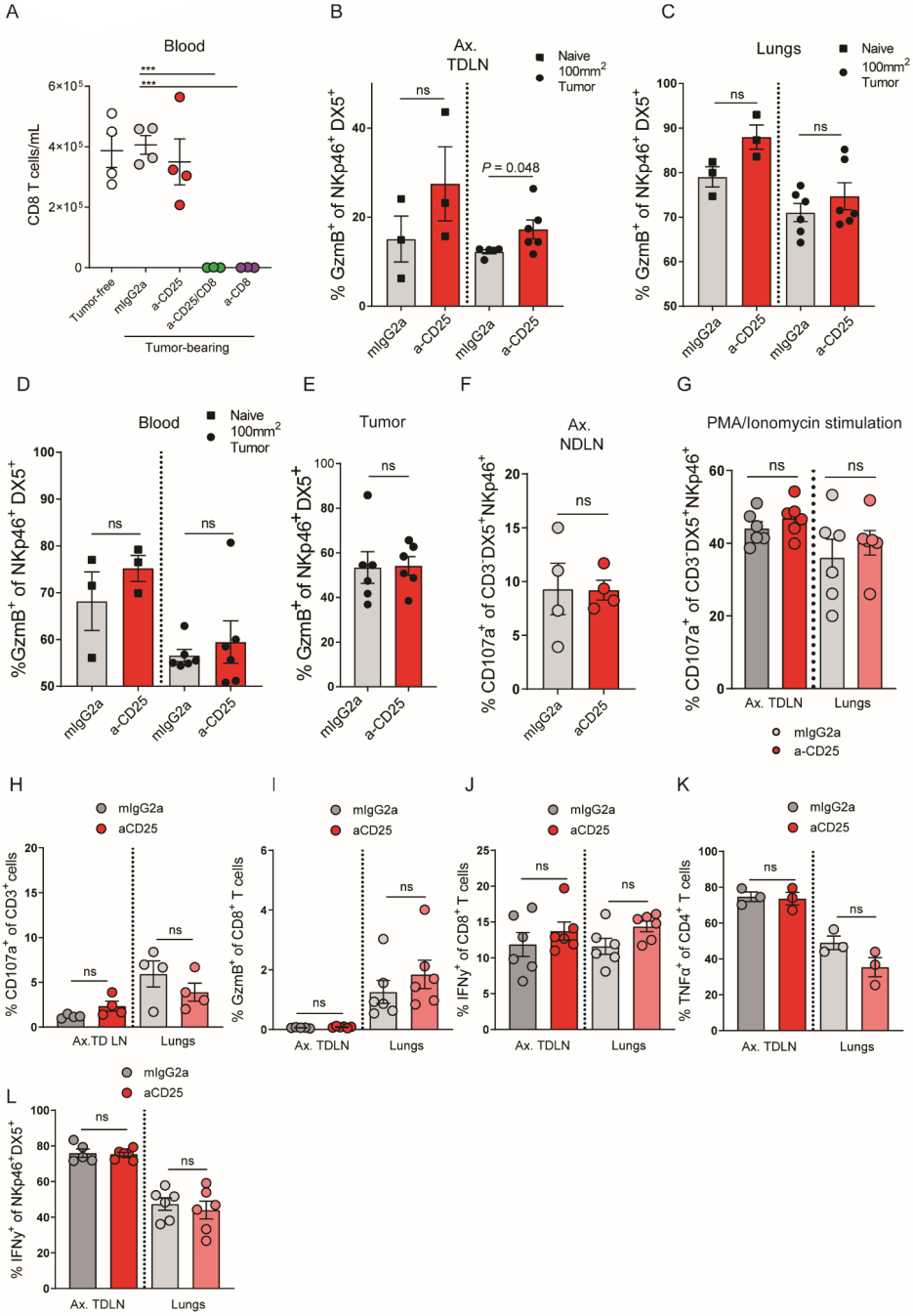
A
Blood
CD8 T cells/mL
Tumor-free
mIgG2a
a-CD25
a-CD25/CD8
a-CD8
Tumor-bearing
B
Ax. TDLN
Naive
100mm2 Tumor
% GzmB+ of NKp46+ DX5+
P = 0.048
C
Lungs
D
Blood
%GzmB+ of NKp46+ DX5+
E
Tumor
F
Ax. NDLN
% CD107a+ of CD3-DX5+NKp46+
G
PMA/Ionomycin stimulation
Ax. TDLN
Lungs
H
% CD107a+ of CD3+ cells
I
% GzmB+ of CD8+ T cells
J
% IFNγ+ of CD8+ T cells
K
% TNFα+ of CD4+ T cells
L
% IFNγ+ of NKp46+DX5+
ns

FIGURE S4. Tissue-specific impact of T_{reg} depletion on T- and NK cell activation. Related to figure 5.

A. Absolute count of $CD8^+$ T cells/mL of blood in tumor-free and mice bearing orthotopically transplanted KEP tumors treated with indicated treatments, 8-10 days after start of treatment (n=3-4 mice/group). **B-E**. Granzyme B expression 3h after ex vivo stimulation of $NKp46^+DX5^+$ NK cells from axillary TDLNs (**B**), lungs (**C**), blood (**D**) tumor (**E**) of mice bearing orthotopically transplanted KEP tumors ($100mm^2$) and WT controls (n=3/group), receiving weekly neoadjuvant treatment of 200 µg anti-CD25 or mIgG2a (n=6/group). **F.** *Ex vivo* CD107a expression of unstimulated $NKp46^+DX5^+$NK cells from contralateral Ax. NDLN of mice bearing orthotopically transplanted KEP tumors ($100mm^2$) receiving weekly neoadjuvant treatment of 200 µg anti-CD25 or mIgG2a (n=6/group). **G.** CD107a expression 4h after *ex vivo* stimulation of $NKp46^+DX5^+$NK cells with PMA/ionomycin from Ax. TDLNs and lungs of mice bearing orthotopically transplanted KEP tumors ($100mm^2$) receiving weekly neoadjuvant treatment of 200 µg anti-CD25 or mIgG2a (n=6/group). **H**. *Ex vivo* CD107a expression of unstimulated $CD45^+CD3^+$ cells from Ax. TDLNs of mice bearing orthotopically transplanted KEP tumors ($100mm^2$) receiving weekly neoadjuvant treatment of 200 µg anti-CD25 or mIgG2a (n=4/group). **I**-**L**. Expression of GzmB (**I**), and IFNγ by $CD8^+$ T cells (**J**), TNFα by $CD4^+$ T cells (**K**), IFNγ by NK cells (**L**) following a 3 hour *ex vivo* stimulation in Ax. TDLNs and lungs of mice bearing orthotopically transplanted KEP tumors ($100mm^2$) Receiving weekly neoadjuvant treatment of 200 µg anti-CD25 or mIgG2a (n=3-6 mice/group). Data in A-L show mean ± S.E.M. P-value was determined by Mann-Whitney test (B-L), One-way ANOVA (A). *** $P < 0.001$.

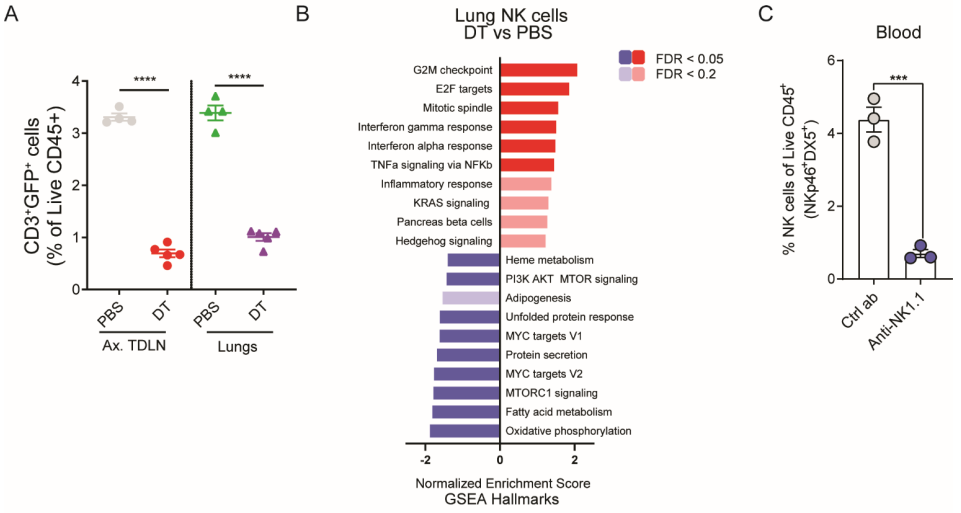
A
CD3+GFP+ cells
(% of Live CD45+)
****
****
PBS
DT
PBS
DT
Ax. TDLN
Lungs
B
Lung NK cells
DT vs PBS
FDR < 0.05
FDR < 0.2
G2M checkpoint
E2F targets
Mitotic spindle
Interferon gamma response
Interferon alpha response
TNFa signaling via NFKb
Inflammatory response
KRAS signaling
Pancreas beta cells
Hedgehog signaling
Heme metabolism
PI3K AKT MTOR signaling
Adipogenesis
Unfolded protein response
MYC targets V1
Protein secretion
MYC targets V2
MTORC1 signaling
Fatty acid metabolism
Oxidative phosphorylation
Normalized Enrichment Score
GSEA Hallmarks
C
Blood
% NK cells of Live CD45+
(NKp46+DX5+)
***
Ctrl ab
Anti-NK1.1

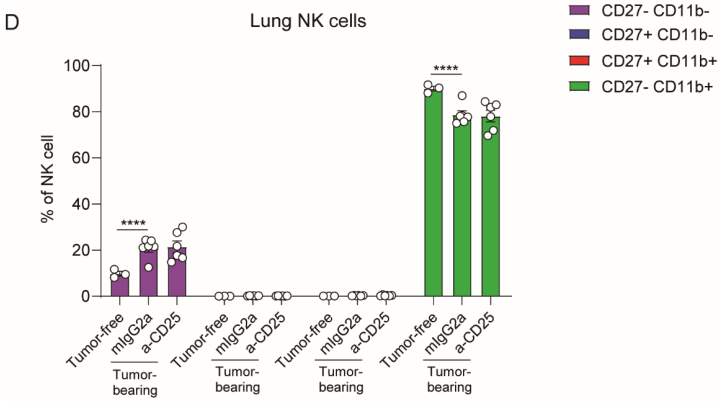
D
Lung NK cells
CD27- CD11b-
CD27+ CD11b-
CD27+ CD11b+
CD27- CD11b+
% of NK cell
****
****
Tumor-free
mIgG2a
a-CD25
Tumor-bearing

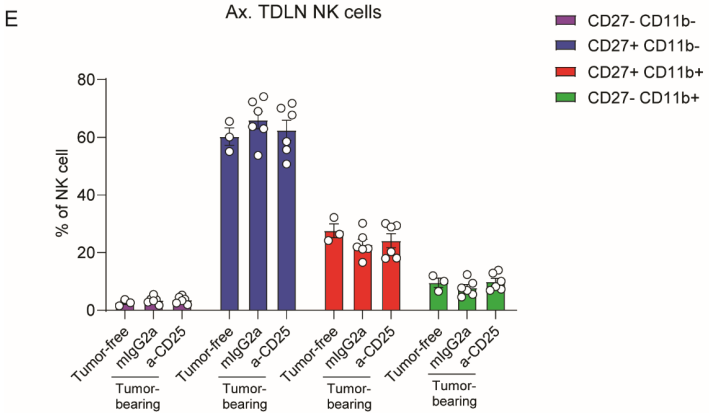
E
Ax. TDLN NK cells
CD27- CD11b-
CD27+ CD11b-
CD27+ CD11b+
CD27- CD11b+
% of NK cell
Tumor-free
mIgG2a
a-CD25
Tumor-bearing

FIGURE S5. Kinetics of NK cells in KEP tumor-bearing mice. Related to figure 5 and 6.
A. Frequency of $CD3^+GFP^+$ cells of total live $CD45^+$ cells in Ax. TDLNs and lungs of *Foxp3*$^{GFP\text{-}DTR}$ mice bearing orthotopically transplanted KEP tumors ($100mm^2$), receiving weekly treatment of PBS or 25 µg DT (n=5/group). **B**. GSEA analysis of lung NK cells, DT vs PBS, using hallmark gene sets. Top 10 enriched up- and downregulated pathways are shown. **C**. Frequency of $CD3^-NKp46^+DX5^+$ NK cells of total live $CD45^+$cells in blood of mice bearing orthotopically transplanted KEP tumors, 8-10 days after start of indicated treatment (n=3/group). **D-E**. Frequency of NK cells in different maturation states based on expression of CD27 and CD11b in lungs (**D**) and Ax. TDLNs (**E**) in tumor-free (n=3/group), or tumor-bearing mice treated with mIgG2a or anti-CD25 (n=6/group). Data in A,C-E show mean ± S.E.M. P-value was determined by Unpaired Student's T-test (A, C), Two-way ANOVA with Dunnett's correction for multiple testing (D-E). *** $P < 0.001$, **** $P < 0.0001$.

5

Neutrophils create a fertile soil for metastasis

Kevin Kos[1] & Karin E. de Visser[1,*]

Affiliations
[1] Division of Tumor Biology & Immunology, Oncode Institute, Netherlands Cancer Institute, Amsterdam, The Netherlands

Cancer Cell. 2021, 8;39(3):301-303

ABSTRACT

Neutrophils can facilitate the metastatic spread of cancer; however, how neutrophils are activated at metastatic sites remains poorly understood. In this issue of *Cancer Cell*, Xiao *et al.* demonstrate that the protease Cathepsin C secreted by breast cancer cells triggers neutrophils to form neutrophil extracellular traps in the metastatic niche, thereby promoting lung metastasis.

Upon arrival in distant organs, disseminated cancer cells can only form metastases when they succeed in creating a permissive environment that fosters their survival and outgrowth. While some members of the immune system can be harnessed to prevent metastatic spread, the role of others has proven to be context dependent, or even pro-metastatic. Among these immune cells are neutrophils. These granulocytic myeloid cells are well known for their key role in acute inflammation and immune regulation, and have recently gained much attention in the context of metastatic disease.

Neutrophil diversity, function and fate are shaped by environmental cues, enabling their quick and effective adaptation to a great diversity of homeostatic and pathological conditions[1]. During homeostasis, the phenotype and activity of these short-lived cells are mainly regulated by their tissue location, circadian oscillations and cellular aging[2]. Disruption of homeostasis, for instance during tumor development, can induce a drastic systemic mobilization of (partly immature) neutrophils from the bone marrow. Importantly, neutrophil accumulation in cancer patients has been associated with a worse prognosis[3]. In line with these clinical observations, preclinical studies have revealed that neutrophils can enhance metastasis formation through a variety of effector functions, including systemic suppression of T cells, preparation of the pre-metastatic niche, or promotion of cancer cell survival. In some preclinical settings, however, cancer-induced neutrophils inhibit metastasis, highlighting their functional plasticity [1]. As such, it is of vital importance to understand the molecular mechanisms that drive the functional adaptations of neutrophils towards a metastasis-supporting phenotype, as this may uncover novel therapeutic opportunities. In this issue, Xiao *et al.* describe an intriguing pathway exploited by breast cancer cells to enhance their metastatic potential through the co-option of neutrophils in the metastatic lung niche[4].

An important cause of breast cancer-related mortality is lung metastasis, which has limited treatment options, in part due to poor understanding of critical interactions between disseminated cancer and host cells that foster their outgrowth. Xiao *et al.* set out to profile the secretome of breast cancer cell lines with varying degrees of lung metastatic potential to identify secreted factors that are potentially involved in creating a permissive metastatic niche. They discovered that Cathepsin C (CTSC), a lysosomal cysteine protease, is consistently elevated in lung-tropic breast cancer cell lines. Cysteine cathepsin proteases are multifunctional proteolytic enzymes that act in a wide range of biological processes, and can exert their enzymatic activity both intracellularly (most notably in the lysosome) and extracellularly. Cathepsins are often dysregulated in cancer, and experimental evidence has specifically implicated CTSB, CTSK, CTSL, CTSS and CTSZ in breast cancer metastasis[5], whereas the role of CTSC has remained less clear, due to its context dependent role in carcinogenesis[6].

By using a variety of intravenously injected and orthotopically transplanted breast cancer cell lines in mice, Xiao et al. showed that CTSC overexpression in cancer cells exacerbates lung metastasis, whereas knock-down of CTSC reduces the metastatic burden in lungs. While modulation of CTSC has no direct effect on primary tumor outgrowth, CTSC critically increases cancer cell proliferation early upon their colonization of the lungs, thus suggesting that CTSC improves the adaptation of disseminated cancer cells to their new micro-environment. The authors observed that tumor-derived CTSC induces the recruitment of neutrophils into the lungs through paracrine communication. Strikingly, antibody-mediated depletion of neutrophils completely abrogates the pro-metastatic effect of CTSC, uncovering a crucial interaction between CTSC-expressing cancer cells and neutrophils.

Also in breast cancer patients, an association between high intratumoral CTSC expression and poor survival was observed, and CTSC expression levels are particularly high in lung metastases versus primary tumors. These data are in line with previous clinical studies that have linked high CTSC expression to increased incidence of both brain- and lung metastasis in breast cancer patients[5]. The current study from Xiao *et al.* provides insight into the pro-metastatic role of CTSC, and warrants further research into whether the same axis is relevant for metastasis formation in the brain.

In an impressive set of mechanistic studies, Xiao and colleagues showed that cancer cell-derived CTSC enzymatically activates the serine protease PR3 expressed on the membrane of neutrophils (Figure 1). This process induces the activation of IL-1β in lung neutrophils, which kick-starts an inflammatory cascade involving the secretion of IL-6 and CCL3 resulting in the recruitment of additional neutrophils from the circulation. In parallel, IL-1β activation also initiates intracellular production of reactive oxygen species (ROS) in neutrophils, which promotes the formation of neutrophil extracellular traps (NETs). NETs are extracellular web-like chromatin structures made of DNA fibres, histones and granule proteins, that are released from neutrophils primarily through an alternative cell death process called NETosis. These DNA traps play an important role in the defence against large pathogens by trapping microbes in place, but have recently also been observed in the microenvironment of various human cancer types including pancreatic, breast, lung, and liver cancer[7]. Notably, the authors demonstrated that the *in vivo* destruction of NETs through treatment of mice with DNAse I is sufficient to prevent the metastatic outgrowth of CTSC-expressing cancer cells in the lungs, highlighting a causal role for NETs in CTSC-enhanced metastasis formation. But how do these neutrophil-derived DNA traps enhance the metastatic potential of breast cancer cells?

Several mechanisms have been reported by which NETs can promote metastasis, including direct induction of cancer cell chemotaxis to the liver[8], and the awakening of dormant cancer cells in lungs [9]. Xiao and colleagues add a new mechanism to the list by demonstrating

that NETs induce the degradation of the matricellular protein thrombospondin-1 (TSP-1), which has been shown to be important for tumor spheroid outgrowth *in vitro*. Combined, this study reveals an intriguing novel pathway by which tumoral CTSC expression dictates metastatic potential by exploiting neutrophils in the metastatic lung niche (Figure 1).

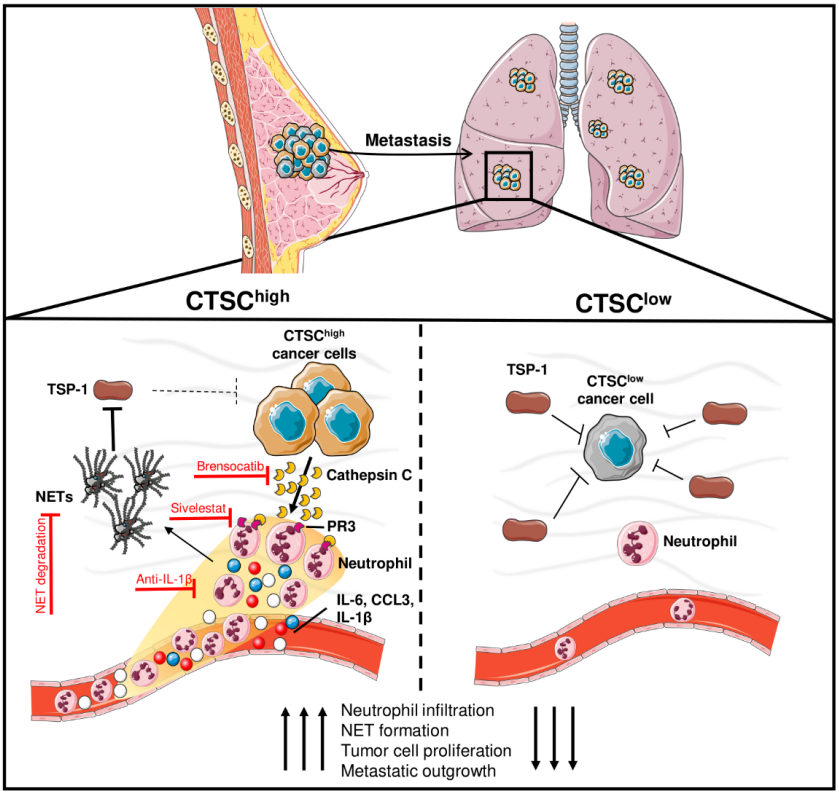

FIGURE 1. Breast cancer cells gain metastatic potential through expression of CTSC
In the metastatic lung niche, cancer cell-derived CTSC activates PR3 on neutrophils, leading to a signalling cascade that promotes the recruitment of neutrophils from circulation, and enhances NET formation via IL-1β. In turn, cancer cells gain a proliferative advantage through the NET-mediated degradation of TSP-1, resulting in enhanced metastatic outgrowth. This figure was created using Servier Medical Art templates, which are licensed under a Creative Commons Attribution 3.0 Unported License; https://smart.servier.com.

These novel findings raise the question whether targeting the CTSC-PR3-IL1β-NET axis represents a viable therapeutic strategy to prevent metastatic spread of CTSC-expressing breast cancer. Excitingly, the authors showed that a small molecule inhibitor of CTSC, brensocatib, suppresses experimental lung metastasis. Besides CTSC, IL-1β might be an attractive actionable therapeutic target (Figure 1). Indeed, a recent clinical study has revealed that inhibition of IL-1β in patients with atherosclerosis reduces lung cancer

incidence, which associates with a reduction of tumor promoting inflammation[10]. As of yet, it is unclear whether the efficacy of targeting the CTSC-PR3-IL1β-NET pathway will be limited to preventing lung metastasis, or whether it may also prevent metastases in other tissues. This may be dependent on the tissue-specific expression levels of TSP-1, thereby highlighting a clinically relevant direction for future research.

The clinical relevance of this work is supported by complementary findings in samples of several human breast cancer cohorts, showing that tumoral CTSC expression strongly correlates with neutrophil and NET markers, as well as with lung metastasis. Interestingly, by analysing these cohorts, Xiao *et al.* found substantial interpatient heterogeneity of CTSC expression, and showed that CTSC is highest expressed in triple-negative breast cancer. It is unclear how CTSC is regulated in different subtypes of breast cancer, and looking forward, an important next step would therefore be to identify the patient population that is most likely to benefit from therapeutic exploitation of these findings. Taken together, this study reveals a novel mechanism that confers breast cancer cells with enhanced metastatic potential through co-option of the immune system. Importantly, these insights open new avenues for the future design of therapeutic strategies aimed at blocking a cancer cell's ability to create a permissive metastatic niche.

Acknowledgments
Research in the De Visser laboratory is funded by the Netherlands Organization for Scientific Research (grant NWO-VICI 91819616), the Dutch Cancer Society (KWF10083, KWF10623),and Oncode Institute. K.K. is funded by the NWO Oncology Graduate School Amsterdam (OOA) Diamond Program.

REFERENCES

1. Jaillon, S. *et al.* Neutrophil diversity and plasticity in tumour progression and therapy. *Nat. Rev. Cancer* **20**, 485–503 (2020).
2. Ballesteros, I. *et al.* Co-option of Neutrophil Fates by Tissue Environments. *Cell* **183**, 1282-1297.e18 (2020).
3. Gentles, A. J. *et al.* The prognostic landscape of genes and infiltrating immune cells across human cancers. *Nat. Med.* **21**, 938–945 (2015).
4. Xiao, Y., Cong, M., Jiatao, L. & Guogong, H. Cathepsin C Promotes Breast Cancer Lung Metastasis by Modulating Neutrophil Infiltration and Neutrophil Extracellular Trap Formation. *Cancer Cell*.
5. Olson, O. C. & Joyce, J. A. Cysteine cathepsin proteases: Regulators of cancer progression and therapeutic response. *Nat. Rev. Cancer* **15**, 712–729 (2015).
6. Ruffell, B. *et al.* Cathepsin C is a tissue-specific regulator of squamous carcinogenesis. *Genes Dev.* **27**, 2086–2098 (2013).
7. Papayannopoulos, V. Neutrophil extracellular traps in immunity and disease. *Nat. Rev. Immunol.* **18**, 134–147 (2018).
8. Yang, L. *et al.* DNA of neutrophil extracellular traps promotes cancer metastasis via CCDC25. *Nature* **583**, 133–138 (2020).
9. Albrengues, J. *et al.* Neutrophil extracellular traps produced during inflammation awaken dormant cancer cells in mice. *Science (80-.).* **361**, (2018).
10. Ridker, P. M. *et al.* Effect of interleukin-1β inhibition with canakinumab on incident lung cancer in patients with atherosclerosis: exploratory results from a randomised, double-blind, placebo-controlled trial. *Lancet* **390**, 1833–1842 (2017).

6

Immune checkpoint blockade triggers T_{reg} activation which blunts therapeutic response in metastatic breast cancer

Kevin Kos[1,2,3,†], Lorenzo Spagnuolo[1,2†], Olga Blomberg[1,2,3†], Kelly Kersten[1], Cheei-Sing Hau[1,2], Kim Vrijland[1,2], Daphne Kaldenbach[1,2], Elisabeth A.M. Raeven[1,2], Karin E. de Visser[1,2*]

Affiliations
[1] Division of Tumor Biology & Immunology, Netherlands Cancer Institute, 1066 CX Amsterdam, The Netherlands
[2] Oncode Institute, Utrecht, The Netherlands
[3] Department of Immunology, Leiden University Medical Center, Leiden, The Netherlands.
[†] These authors contributed equally
[*] Corresponding author. Email: k.d.visser@nki.nl

Unpublished

ABSTRACT

Immune checkpoint inhibitors such as anti-PD-1 and anti-CTLA4 are aimed at activating anti-tumoral effector cells, but their effect on immunosuppressive regulatory T cells that express high levels of immune checkpoint molecules is unclear. Using mouse models for spontaneous primary and metastatic breast cancer, we studied how immune checkpoint blockade (ICB) influences T_{regs} and how this impacts the therapeutic benefit of ICB. We observed that ICB drives intratumoral and systemic accumulation of T_{regs}, but not $CD8^+$ T cells. Neoadjuvant depletion of T_{regs} combined with ICB changes the immune landscape of mammary tumors into a state favourable for ICB response, characterised by increased T-cell activation, more eosinophils, and elevated PD-L1 and MHC-II expression on myeloid cells. Systemically, depletion of T_{regs} during ICB resulted in the accumulation of $CD8^+$ T cells and NK cells, and induces durable T cell activation. Consequently, depletion of T_{regs} in the context of ICB prolongs metastasis-related survival, which is not observed upon T_{reg} depletion or ICB alone. Combined, this study shows that T_{regs} are inadvertently activated by ICB and pose a barrier for ICB efficacy in breast cancer.

INTRODUCTION

The development of immune checkpoint inhibitors that block immunoregulatory receptors like PD-1 and CTLA4 have ushered in a new era of cancer treatment. In particular patients with immunogenic tumors, such as melanoma[1], non-small cell lung cancer (NSCLC)[2], or microsatellite instable cancers[3], have shown impressive responses upon treatment with anti-PD1/PD-L1 and anti-CTLA4 antibodies. However, despite these successes, an important fraction of those patients does not respond to anti-PD1 and/or anti-CTLA4 immunotherapy (ICB), or acquires treatment resistance[4]. Moreover, the efficacy of ICB in other cancer types, such as breast cancer, is limited[5,6], highlighting the need to understand the obstacles of immunotherapy response.

The main rationale of ICB is to improve the capacity of tumor-specific $CD8^+$ T cells to expand, recognize and clear cancer cells[7]. To achieve this, anti-CTLA4 blocks the interaction between the co-inhibitory molecule CTLA4 expressed on T cells and CD80/CD86 expressed on mature, antigen presenting dendritic cells thereby improving T cell priming and activation. Anti-PD1 blocks the interaction of PD-1 with PD-L1, which can be widely expressed on tumor-, stromal, and immune cells and is a negative regulator of T cell function through inhibition of co-stimulation and TCR signalling[8]. PD-1 and CTLA-4 expression is not limited to cytotoxic $CD8^+$ T cells, but is also found on intratumoral $CD4^+FOXP3^+$ regulatory T cells (T_{regs})[9,10]. T_{regs} are important regulators of immune homeostasis endowed with a plethora of immunoregulatory features, making them key orchestators of cancer-associated immunosuppression[11,12]. T_{regs} can negatively impact anti-tumor immunity in breast cancer mouse models through inhibition of both innate and and adaptive immune cell function[11], thereby contributing to primary tumor growth[13,14] and metastases[15].

Recent evidence indicates that anti-PD1 and anti-CTLA4 may inadvertently lead to the activation of T_{regs}. Anti-PD1 has been shown to induce the proliferation of T_{regs} in tumors of melanoma patients, which correlates to poor prognosis[16]. Moreover, high PD-1 expression on T_{regs} versus $CD8^+$ T cells strongly correlates with non-responsiveness to anti-PD1 in NSCLC, gastric cancer and melanoma patients[17], and has been linked to hyper progression in gastric cancer patients[18]. Anti-CTLA4 was found to induce proliferation of tumor-associated T_{regs} in MC38 tumor-bearing mice[19]. In cancer patients, anti-CTLA4 treatment has been shown to expand immunosuppressive T_{regs} in blood and tumors[20,21], although it is unclear how this impacts therapy response. These data suggest that activation of T_{regs} might be an unintended effect of ICB, raising the question how this impacts the anti-cancer efficacy of ICB.

Here, we set out to study whether interactions between T_{regs} and dual anti-PD1 and anti-CTLA4 blockade form a hurdle for anti-tumor immunity. To study this, we made use of the transgenic *K14cre;Cdh1*$^{F/F}$*;Trp53*$^{F/F}$ (KEP) mouse model of invasive mammary tumorigenesis[22], and the KEP-based mastectomy model for spontaneous multi-organ metastatic disease[23]. Primary

tumors and metastases arising in these models are unresponsive to ICB. We observed that ICB fails to induce $CD8^+$ T cell activation or proliferation, but instead enhance T_{reg} proliferation and activation in tumor-bearing mice. Neoadjuvant ablation of T_{regs} using the *Foxp3*$^{DTR\text{-}GFP}$ model in the context of ICB led to the accumulation of $CD8^+$ T cells, eosinophils and NK cells in blood. Strikingly, ICB synergizes with T_{reg} depletion to curb metastatic disease. Combined, this study provides experimental evidence that T_{regs} impair the efficacy of ICB in spontaneous models for breast cancer.

RESULTS

ICB drives T_{reg} accumulation in ICB-unresponsive spontaneous mammary tumors

To investigate the mpact of T_{regs} on immunotherapy response, we first assessed the efficacy of dual anti-PD1 anti-CTLA4 immune checkpoint blockade in controlling tumor growth of transgenic KEP mice bearing spontaneous mammary tumors. Treatment with ICB was initiated at a tumor size of 25mm^2 and continued until end-stage tumor size (225mm^2) was reached (Fig. 1A). Consistent with poor ICB response in breast cancer patients, ICB treatment did not enhance survival of tumor-bearing KEP mice compared to control treatment (Fig. 1B). Characterisation of T cell populations in tumors of KEP mice showed that ICB treatment does not alter the intratumoral infiltration of $CD8^+$ and $CD4^+$ T cells (Fig. S1A), but instead increased the intratumoral accumulation of $FOXP3^+$ cells (Fig. 1C, D). As a result, the intratumoral ratio of CD8/FOXP3 cells decreased upon ICB treatment (Fig. S1B), whereas a high CD8/FOXP3 ratio has been associated with improved survival in breast cancer patients[24]. In line with increased intratumoral accumulation of $FOXP3^+$ cells, we found increased expression of the proliferation marker Ki-67 on T_{regs} in KEP mice treated with ICB compared to untreated mice (Fig. 1E). Next, we investigated whether the observed increase in T_{regs} in ICB-treated mice was limited to the TME by analysing blood and lymph nodes of ICB-treated KEP mice bearing end-stage tumors. This showed that T_{regs}, but not $CD8^+$ T cells, are also increased in blood of tumor-bearing KEP mice receiving ICB (Fig. 1G, S1C). In tumor-draining lymph nodes, T_{reg} frequency was not significantly altered, but these T_{regs} did express higher levels of Ki-67 (Fig. S1D).

To study the impact of T_{regs} on immunotherapy response in the context of metastasis, we first set out to validate our findings in the orthotopic KEP transplantation model, based on transplantation of tumor fragments (Fig. 1G). Similar to the spontaneous KEP model, ICB treatment does not enhance the survival of mice bearing orthotopically transplanted KEP tumors compared to control treatment (Fig. 1H). Furthermore, T_{regs}, but not conventional T cells, were increased in frequency and showed enhanced Ki-67 expression in tumors of ICB-treated mice, compared to control-treated mice (Fig. 1I-J, S1E). Finally, in these mice, T_{regs} in blood were found to be increased upon ICB treatment (Fig. 1K), in line with observations in the spontaneous KEP model (Fig. 1F). To evaluate whether ICB, besides T_{reg} accumulation, also influences T_{reg} functionality *in*

vitro, a suppression assay was performed. T_{regs} isolated from draining lymph nodes of control-, or ICB-treated KEP tumor-bearing mice were co-cultured with *in vitro* activated splenic T cells to assess the impact of either T_{reg} population on T cell proliferation. Both T_{reg} populations similarly inhibited the proliferation of responder T cells, demonstrating that ICB does not enhance the suppressive capacity of T_{regs} in this *ex vivo* context (Fig. 1L). Combined, these data show that ICB induces systemic accumulation of T_{regs} in tumor-bearing mice, raising the question how this impacts immune cell crosstalk in ICB-treated mice.

Neoadjuvant depletion of T_{regs} in the context of ICB remodels systemic and tumor immune landscapes

To gain insight into the function of T_{regs} in the context of ICB, we utilized *Foxp3*$^{DTR\text{-}GFP}$ mice that we generated on the FVB genetic background in which T_{regs} can be transiently depleted upon short-term diphtheria toxin (DT) treatment[25]. *Foxp3*$^{DTR\text{-}GFP}$ mice were transplanted with KEP tumor fragments, and upon tumor take, mice were treated with combinations of ICB, ICB control antibody (rat IgG2a clone 2A3), DT, or PBS (DT vehicle control), until tumors reached a size of ~120mm^2 (Fig. 2A). At this time point, mastectomy was performed to remove the primary tumor. Analysis of blood and resected tumors showed that T_{regs} were efficiently depleted from mice treated with DT and ICB + DT (Fig. S2A, 2G).

First, we investigated whether depletion of T_{regs} in the context of ICB changes the composition and activation of circulating immune cells, measured 1-2 days before mastectomy (pre-mastectomy). Interestingly, besides their effect on T_{regs}, both ICB and DT monotherapy do not significantly impact the immune cell abundance in blood compared to control-treated mice, with the exception of increased eosinophil counts upon DT treatment (Fig. 2B, S2B). In contrast, the combination of ICB and DT induced a significant increase in both $CD8^+$ T cells and NK cells compared to monotherapies (Fig. 2C-D), both of which are important effector cells for anti-tumor immunity. Notably, we also observed a strong increase in $CD4^+CD8^+$ T cells (Fig. 2E), which have been described to be enriched in patients with auto-immune disease[26,27] and cancer[28,29], and have been shown to display reactivity towards autologous melanoma cell lines *in vitro*[29]. As genetic ablation of T_{regs} is associated with the development of autoimmune-related pathology[30,31], we performed a preliminary analysis to investigate whether combining ICB with T_{reg} depletion exacerbates inflammation-related pathology compared to T_{reg}-depleted mice. Histopathological assessment of various tissues obtained from mice that were sacrificed after mastectomy at indicated time points was performed blindly by a trained animal pathologist. This revealed no differences in inflammation-related pathology between control + DT and ICB + DT treatment groups (Fig. S2C, Table 1). In addition, no differences were observed in sizes of spleen, and small intestine (S2D). Due to the preliminary nature of this investigation, further analysis in tumor- and non-tumor bearing mice with matched duration of control-, ICB- and DT treatment, should clarify to what extent the observed pathology is explained by cancer-related inflammation as opposed to T_{reg} depletion-induced inflammation.

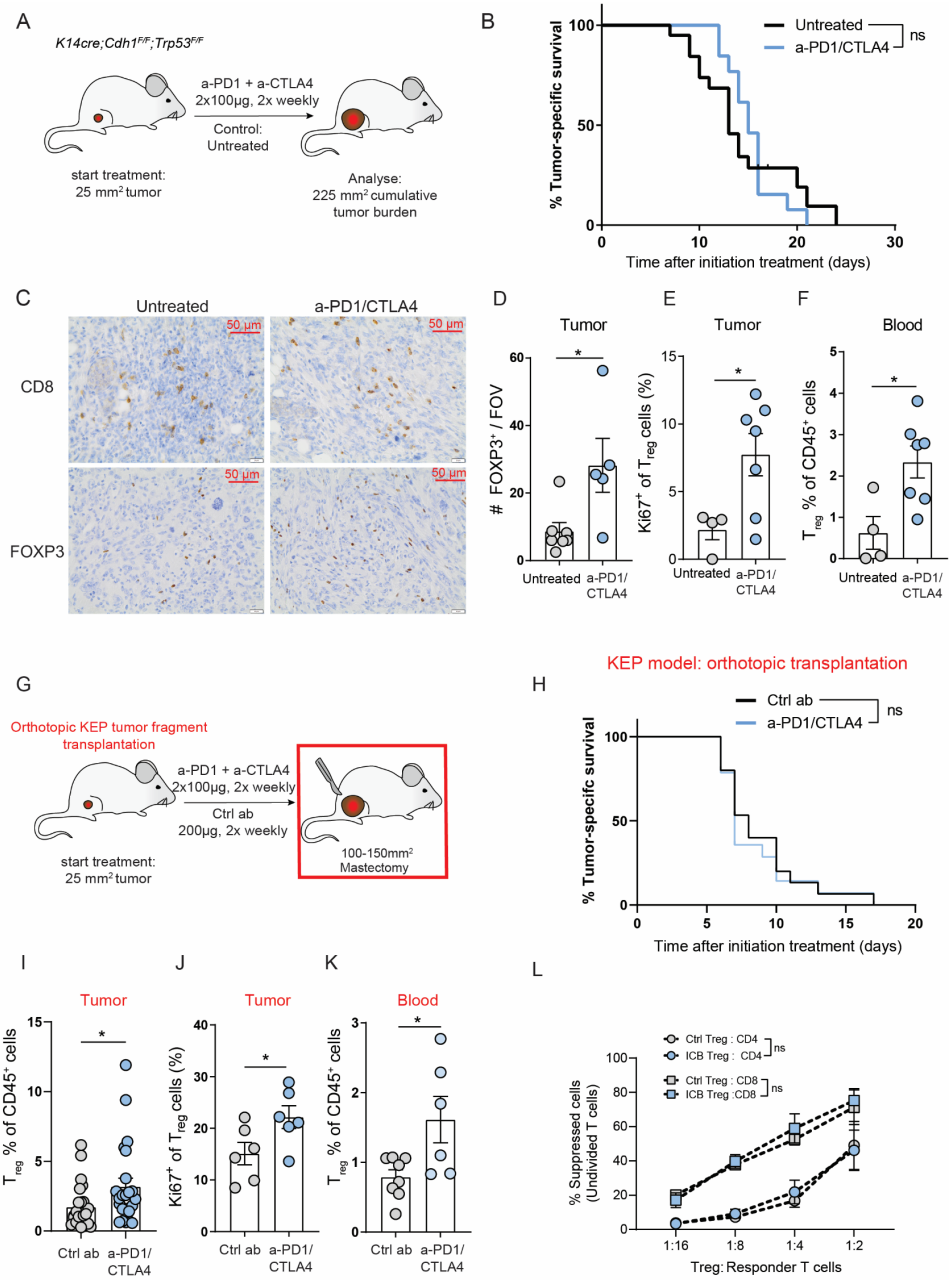

FIGURE 1. ICB fails to inhibit mammary tumor outgrowth and activates intratumoral and systemic T_{reg} accumulation in transgenic KEP mice

A. Schematic overview of study: tumor-bearing KEP mice either did not receive treatment, or were treated with a combination of anti-PD-1 and anti-CTLA4 (ICB) starting at a tumor size of 25mm^2 until end stage tumor size of 225mm^2. **B.** Kaplan-Meier survival curves of KEP mice treated as indicated (n= 12-15 mice/group). Censored cases indicate mice that were sacrificed due to tumor-unrelated causes. **C.** Representative images of immunohistochemical staining of CD8 and FOXP3 in mammary tumors (225mm^2) of KEP mice, treated as indicated. Scale bar of 50 µm is shown. **D.** FOXP3 counts in spontaneous mammary tumors

($225mm^2$) of KEP mice treated as indicated, as determined by immunohistochemical analysis (counts per 40x field of view, average of five randomly selected areas) (n=5-7 mice/group). **E.** Frequency of Ki-67 expression on T_{regs} ($CD4^+CD25^+$) in mammary tumors ($225mm^2$) of untreated or anti-PD-1/CTLA4-treated KEP mice, analysed by flow cytometry (n=4-7 mice/group). **F.** Frequency of T_{regs} ($CD4^+CD25^+$) as % of total live $CD45^+$ cells in blood of untreated or anti-PD-1/CTLA4-treated KEP mice bearing mammary tumors ($225mm^2$) as determined by flow cytometry (n=4-7 mice group). **G.** Schematic overview of study: mice bearing orthotopically transplanted KEP tumors fragments ($1mm^2$) were treated twice weekly with control antibody or a combination of anti-PD-1 and anti-CTLA4 (ICB) starting at a tumor size of $25mm^2$. **H.** Kaplan-Meier survival curve of mice bearing orthotopically transplanted KEP tumors that were treated with control antibody (n=15) or ICB (n=14). Endpoint was defined as tumor size of $12x12mm^2$. **I.** Frequency of T_{regs} as % of total live $CD45^+$ cells in orthotopically transplanted KEP tumors ($100\text{-}150mm^2$) of mice treated with control antibody, or anti-PD-1/CTLA4, as analysed by flow cytometry (n=23-24 mice/group). **J.** Frequency of Ki-67 expression on T_{regs} in orthotopically transplanted KEP tumors ($100\text{-}150mm^2$) of mice treated with control antibody, or anti-PD-1/CTLA4, as analysed by flow cytometry (n=4-7 mice/group). **K.** Frequency of T_{regs} as % of total live $CD45^+$ cells in blood of mice bearing orthotopically transplanted KEP tumors treated with control antibody, or anti-PD-1/CTLA4, 1-2 days before mastectomy, as analysed by flow cytometry (n=4-7 mice/group). **L.** Quantification of undivided responder cells ($CD8^+$ and $CD4^+$ T cells) based on flow cytometric assessment of CTV dilution, upon co-culture with CD3/CD28 pre-activated T_{regs} ($CD4^+CD25^+$) isolated from lymph nodes of mice bearing transplanted mammary tumors($225mm^2$). Mice were treated with control antibody or anti-PD-1/CTLA4. Cells were co-cultured at indicated ratios for 96h in presence of CD3/CD28 beads (data pooled from 2 independent *in vitro* experiments, with n=4 biological replicates).
Data in D-F, I-L show mean ± SEM. P-values are determined by Log-rank test (B), Unpaired Students T-test (D-F, I-L). * $P < 0.05$, ** $P < 0.01$, *** $P < 0.001$, **** $P < 0.0001$.

To assess potential changes in $CD8^+$ T cell activation that occur upon treatment with ICB and DT, the expression of CD44, CD62L, PD-1, CD25, CD69 was measured in blood of tumor-bearing mice by flow cytometry. T_{reg} depletion was sufficient to strongly increase the frequency of $CD44^+CD62L^-$ effector cells as compared to ICB and control-treated mice, which is not further increased upon combination of ICB + DT. Only the frequency of PD-1 was further increased on $CD8^+$ T cells upon the combination of ICB and DT compared to DT alone (Fig. 2F). Similar observations were made for $CD4^+$ T cells (S2E). Combined, these data show that T_{reg} depletion is sufficient to induce $CD8^+$ T cell activation in blood, but the combination of ICB + DT is necessary to increase circulating $CD8^+$ T cells and NK cells.

Analysis of the immune landscape in resected tumors showed that none of the treatments altered the frequency of conventional T cells as measured by flow cytometry. Notably, T_{reg} depletion, either with or without ICB, did induce changes in the myeloid compartment (Fig. 2G). In line with previous research, we observed that T_{reg} depletion promoted an increase in eosinophil[32] and a decrease in cDC2 tumor infiltration[33] (Fig. 2G). Thus, in contrast to blood, changes in immune cell composition in resected tumors are mostly dictated by T_{reg} ablation, and are not further changed upon combination of ICB and DT (Fig. 2H). Similarly, the intratumoral accumulation of activated $CD8^+$ and $CD4^+$ T cells is enhanced upon T_{reg} depletion compared to control, and ICB + DT compared to ICB alone (Fig. 2H, S2F). However, besides upregulation of CD69 on $CD8^+$ T cells, the combination of ICB + DT does not further enhance the intratumoral accumulation activated T cells compared to control + DT (Fig. 2H, S2G).

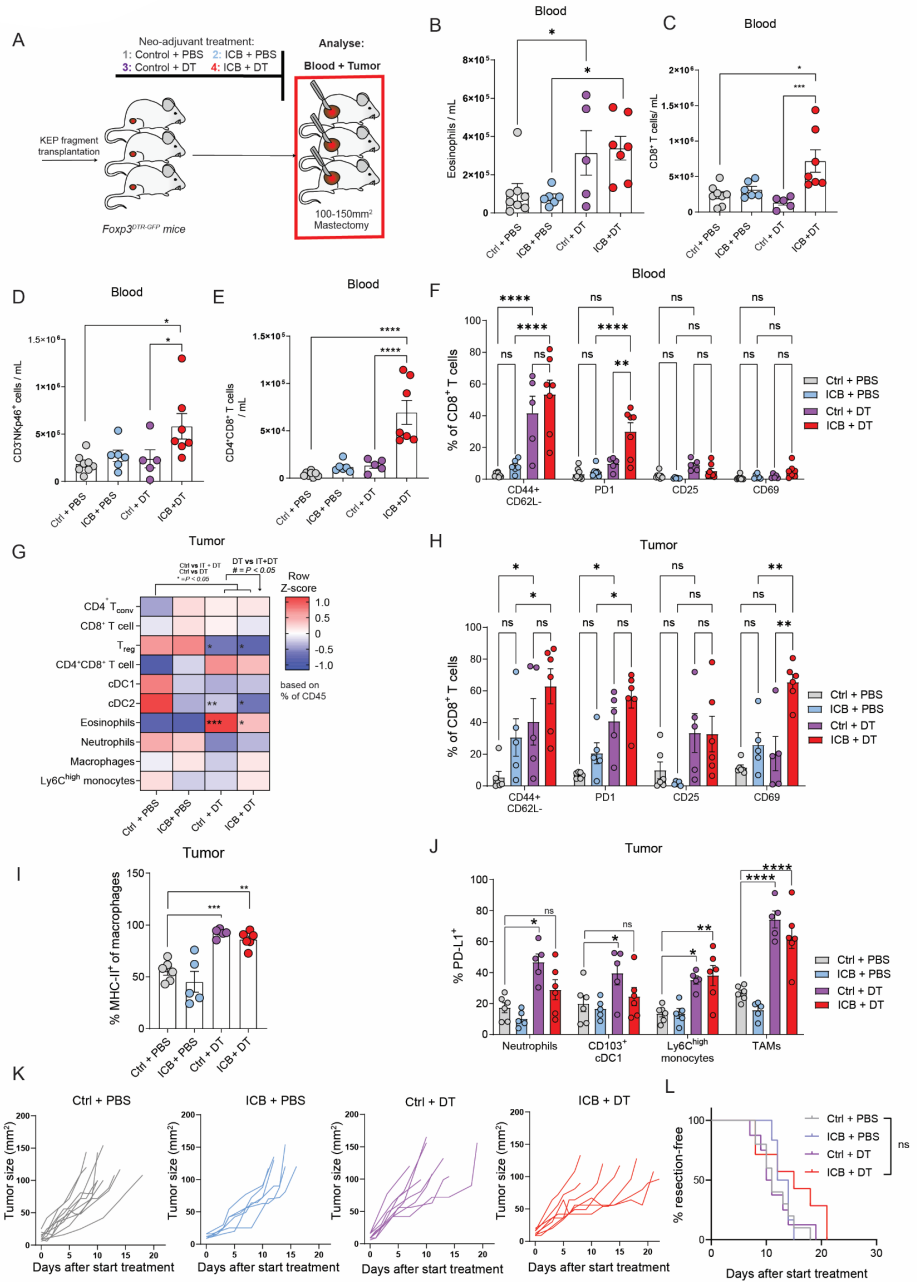

FIGURE 2. Neoadjuvant depletion of T_{regs} changes the systemic and tumor immune landscape, but does not improve ICB response in primary tumors

A. Schematic overview of study. KEP-tumor fragments were orthotopically transplanted, and mice were treated with combinations of ICB, control antibody (rat IgG2a, clone 2A3), DT or PBS (DT vehicle control) as indicated. Ctrl or ICB was started upon presentation of palpable tumors (4-6mm^2), administered twice weekly, and discontinued upon mastectomy. DT or PBS was started at a tumor size of 9-12 mm^2 and administered twice in total (day 0 & 4). At a tumor size of 100-150mm^2, mastectomy

was performed. Blood (taken 1-2 days before mastectomy) and resected tumors were analysed by flow cytometry. **B-E**. Absolute cell counts of eosinophils (B) $CD8^+$ T cells (C), NK cells (D) and $CD4^+CD8^+$ T cells (E) in blood of mice treated with indicated treatments, as determined by flow cytometry, 1-2 days before mastectomy (n=5-8 mice/group). **F.** Frequency of indicated markers (% of positive cells) gated on $CD8^+$ T cells in blood of mice treated with indicated treatments, as determined by flow cytometry, 1-2 days before mastectomy (n=5-8 mice/group). **G.** Heatmap depicting tumor-immune landscape in mastectomized tumors of mice receiving indicated treatments. Row Z-score calculated based on frequency of indicated cell type of total $CD45^+$ cells (n=5-6 mice/group). **H.** Frequency of indicated markers (% of positive cells) gated on $CD8^+$ T cells in mastectomized tumors of mice treated with indicated treatments, as determined by flow cytometry (n=5-6 mice/group). **I.** Frequency of $MHC\text{-}II^+$ cells gated on macrophages ($CD11b^+$ $F4/80^+$) in mastectomized tumors of mice receiving indicated treatments (n=5-6 mice/group). **J.** Frequency of $PD\text{-}L1^+$ cells within indicated immune cell subsets in mastectomized tumors of mice receiving indicated treatments (n=5-6 mice/group). **K.** Tumor growth curves of individual mice receiving indicated treatments (n=6-10 mice/group). **L.** Kaplan-Meier curve of mice bearing orthotopically transplanted KEP tumors treated as indicated. Endpoint was reached when mice underwent mastectomy at ~120mm^2 (n=7-10 mice/group).
Data in B-F,H-J show mean ± SEM. P-values were calculated by One-way ANOVA with Sidak's correction (B-E, G), Tukey's correction, Holm-Sidak correction (G). 2-way ANOVA with Sidak correction (F,H, J), Log-rank test (L). * $P < 0.05$, ** $P < 0.01$, *** $P < 0.001$, **** $P < 0.0001$

In addition to these observations, we found that T_{reg} depletion upregulated PD-L1 expression on neutrophils, conventional dendritic cells (cDC1), $Ly6C^{high}$ monocytes and tumor-associated macrophages (TAMs) (Fig. 2J). Importantly, PD-L1 is a clinical biomarker for response to immune-checkpoint inhibitors, suggesting that T_{reg} depletion may remodel the TME into a state that is favourable for ICB response. We also found a strong increase of MHC-II expression on TAMs, reflective of M1-like polarization based on this single marker, to which anti-tumoral functions have been attributed[34] (Fig. 2I). Importantly, these changes were not further enhanced in the context of ICB. One change in tumors that was associated to the combination of ICB + DT, but not control + DT is an increase in frequency of inflammatory $CD101^+CD62L^-$ eosinophils, as compared to control treatment (Fig. S2). Together, this shows that genetic ablation of T_{regs} drives broad pro-inflammatory changes in intratumoral T- and myeloid cells. These changes are mostly related to T_{reg} depletion and occur independent of ICB, despite the observation that ICB increases the intratumoral accumulation of T_{regs}. Finally, analysis of tumor sizes revealed that none of the treatments significantly delayed tumor growth (Fig. 2K-L), showing that depletion of T_{regs} in the context of ICB does not drive anti-tumor responses. These findings are in line with previous results showing that T_{regs} are not critical for regulation of primary tumor growth in the KEP model [15].

TABLE 1. Histopathological assessment of immune-related pathology in mice receiving neoadjuvant treatment with Ctrl + DT and ICB + DT, as analysed blindly by a trained pathologist, related to figure S2C. Mice were sacrificed at indicated time points after mastectomy due to development of metastasis- or metastasis-unrelated pathology (see Table 2)

Case #	Exp group	Tumor-draining axillary lymph node	Non-draining axillary lymph node	Spleen	Pancreas	Lungs	Liver	Kidneys
21KDV930 *14 days after mastectomy*	Ctrl + DT	Lymphocytic hyperplasia	Marked hyperplasia with lymphocytes and plasma cells	Lymphoid compartment: apopotic lymphocytes, moderate numbers	Marked neutrophilic interstitial pancreatitis, with atrophy/loss of exocrine pancreatic tissue (60% affected)	Moderate inflammation, mostly perivascular lymphocytic Focal small cluster of cells resembling (metastatic) carcinoma	Moderate inflammation, mostly adjacent to central veins and bile ducts / portal areas, with neutrophils, lymphocytes, plasma cells	Mild multifocal interstitial nephritis with neutrophils, macrophages, lymphocytes, plasma cells
21KDV696 *20 days after mastectomy*	Ctrl + DT	Lymphocytic hyperplasia	No abnormalities	Lymphoid compartment: apopotic lymphocytes, moderate numbers	Marked subacute interstitial pancreatitis, with neutrophils, lymphocytes and plasma cells, degeneration and atrophy/loss of exocrine pancreatic tissue (30% affected)	Moderate inflammation, mostly perivascular lymphocytic	Moderate inflammation, mostly adjacent to central veins and bile ducts / portal areas, with neutrophils, lymphocytes, plasma cells	Mild multifocal interstitial nephritis with neutrophils, macrophages, lymphocytes, plasma cells
21VIS010 *50 days after mastectomy*	Ctrl + DT	Minimal lymphocytic hyperplasia	Hyperplastic	Lymphoid compartment: apopotic lymphocytes, low numbers	-	Carcinoma metastases in pleura and lung	Moderate inflammation, mostly adjacent to central veins and bile ducts / portal areas, with neutrophils, lymphocytes, plasma cells	Minimal focal interstitial nephritis
21VIS012 *20 days after mastectomy*	Ctrl + DT	No abnormalities	Hyperplastic, with many apoptotic lymphocytes	Mild lymphocytic hyperplasia, moderate numbers of apoptotic lymphocytes	Marked subacute interstitial pancreatitis, with neutrophils, lymphocytes and plasma cells, degeneration and atrophy/loss of exocrine pancreatic tissue (50% affected)	Mild inflammation, mostly perivascular lymphocytic Focal small cluster of cells resembling (metastatic) carcinoma	Mild inflammation, mostly adjacent to central veins and bile ducts / portal areas, with neutrophils, lymphocytes, plasma cells	Minimal focal interstitial nephritis

TABLE 1 CONTINUED.

Case #	Exp group	Tumor-draining axillary lymph node	Non-draining axillary lymph node	Spleen	Pancreas	Lungs	Liver	Kidneys
21KDV388 *10 days after mastectomy*	ICB + DT	Hyperplastic, many apoptotic cells, multifocal lymphadenitis with neutrophils, macrophages and multinucleated giant cells	Hyperplastic, with many apoptotic lymphocytes	Lymphoid compartment: hyperplasia, many apopotic lymphocytes	Moderate insterstitial pancreatitis, mostly periductal, with neutrophils, lymphocytes and plasma cells (20% affected)	Marked vasculitis and perivsculitis with many lymphocytes, in some places associated with local crystalline macrophage pneumonia	Moderate inflammation, mostly adjacent to central veins and bile ducts / portal areas, with neutrophils, lymphocytes, plasma cells	Mild multifocal interstitial nephritis with neutrophils, macrophages, lymphocytes, plasma cells
21KDV519 *56 days after mastectomy*	ICB + DT	Hyperplastic, moderate numbers of apoptotic cells	No abnormalities	No abnormalities	Moderate periductal inflammation (10% affected)	Mild vasculitis and perivasculitis	Mild inflammation, mostly adjacent to central veins and bile ducts / portal areas, with neutrophils, lymphocytes, plasma cells	Mild interstitial nephritis, mild dilation of pelvis and cortical tubules
21KDV677 *80 days after mastectomy*	ICB + DT	Hyperplastic	Hyperplastic	Increased numbers of megakaryocytes in the hematopoietic compartment	Mild periductal inflammation (5% affected)	Minimal perivascular inflammation	Minimal inflammation, mostly adjacent to central veins and bile ducts / portal areas, with neutrophils, lymphocytes, plasma cells	Minimal focal interstitial nephritis
21KDV678 *80 days after mastectomy*	ICB + DT	Moderate numbers of apoptotic lymphocytes	Hyperplastic, with moderate numbers of apoptotic lymphocytes	Mild lymphoid hyperplasia, few germinal centers	Moderate periductal inflammation (40% affected)	Minimal perivascular inflammation	Mild to moderate inflammation, mostly adjacent to central veins and bile ducts / portal areas, with neutrophils, lymphocytes, plasma cells	Minimal focal interstitial nephritis and tubular degeneration

T_{reg}-depletion during ICB induces durable systemic T cell activation and prolongs metastasis-related survival

Ablation of T_{regs} during ICB mobilised both $CD8^+$ T cells and NK cells in blood of tumor-bearing mice, raising the question whether T_{regs} functionally impair the systemic immune activation necessary to combat metastasis. To investigate whether neoadjuvant T_{reg} depletion in the context of ICB affects metastasis formation, mice were monitored for development of overt metastatic disease after resection of primary tumors (Fig. 3A). In addition, T cell activation was analysed in blood of mice 7 days after mastectomy (post-mastectomy). Of note, mice were only treated before resection of the primary tumor. Despite discontinuation of ICB, T_{regs} were still found to be increased in blood of mice that had been treated with ICB before mastectomy, as measured by flow cytometry 7 days after mastectomy (Fig. 3B). Moreover, these T_{regs} displayed increased expression of the activation markers CD44 and PD-1 compared to control-treated mice, which was not observed in the initial pre-mastectomy characterisation (Fig. 3C, S3A). Interestingly, $CD44^+$ T_{regs} have been described to have strong immunosuppressive potential, and play an important role in curbing auto-immunity[35]. In addition, a recent study showed that $PD\text{-}1^+$ T_{regs} gain increased proliferative and immunosuppressive capacity upon PD-1 blockade *in vitro*[17,18]. Thus, our data suggest that ICB does not only drive the expansion of T_{regs} in blood, but on a longer-term, also induces phenotypical changes that are associated to T_{reg} activation.

To analyse whether neoadjuvant depletion of T_{regs} in the context of ICB induces long-term effects after discontinuation of treatment, we next assessed T cell activation in blood of mice 7 days after mastectomy. At this time point, we found that both the CD8 and CD4 T cell compartment in blood of mice that had been treated with ICB + DT before mastectomy harboured a significantly increased frequency of $CD44^+CD62L^-$ effector cells, compared to control- and monotherapies (Fig. 3D, S3B). In addition, $CD8^+$ T cells in mice previously treated with ICB + DT showed increased expression of PD-1 compared to all monotherapies, and increased CD69 expression compared to control-treated mice. To further asses the kinetics of this observation, we compared $CD8^+$ T cell activation between control + DT and ICB + DT treated mice pre- and post-mastectomy (Fig. 3E). The $CD44^+CD62L^-$ effector CD8 T cell population is maintained in mice that had been treated with ICB + DT before mastectomy, but is decreased in mice previously treated with control + DT (Fig. 3F). Thus, neoadjuvant systemic depletion of T_{regs} in the context of ICB leads to durable T cell activation, at least up until 7 days after discontinuation of treatment, raising the question whether these systemic pro-inflammatory conditions may have anti-metastatic potential. Analysis of metastasis-related survival showed that control antibody-treated mice developed metastatic disease, characterised by respiratory distress and end-stage metastatic tumor burden (>225mm^2) in axillary lymph nodes and intraperitoneal organs (causes of death indicated in Table 2), with a median survival of 28 days. In line with previously published results describing an important role for T_{regs} in the development of lymph node metastasis in the KEP metastasis model[15],

we did not detect any lymph node metastasis in T_{reg}-depleted mice, either with or without ICB. Strikingly, whereas neoadjuvant ICB treatment nor neoadjuvant T_{reg} depletion improved survival, the combined treatment of T_{reg} depletion and ICB treatment significantly prolonged metastasis-related survival (Fig 3G). Combined, these data show that T_{regs} form a barrier for response to ICB in a mouse model for spontaneous breast cancer metastasis.

TABLE 2. Cause of death of mice shown in figure 3G

Case	Treatment	Cause of death
21KDV682	Ctrl + PBS	Respiratory distress
21KDV694	Ctrl + PBS	Respiratory distress
21KDV704	Ctrl + PBS	Tumor burden lymph node metastasis + Respiratory distress
21KDV709	Ctrl + PBS	Respiratory distress
21KDV716	Ctrl + PBS	Tumor burden lymph node metastasis
21KDV722	Ctrl + PBS	Respiratory distress
21KDV773	Ctrl + PBS	Tumor burden lymph node/liver metastasis + Respiratory distress
21KDV839	Ctrl + PBS	Respiratory distress
21KDV917	Ctrl + PBS	Tumor burden intraperitoneal metastasis
21VIS011	Ctrl + PBS	Respiratory distress
21KDV369	ICB + PBS	Respiratory distress
21KDV381	ICB + PBS	Respiratory distress
21KDV391	ICB + PBS	Respiratory distress
21KDV410	ICB + PBS	Tumor burden lymph node metastasis
21KDV430	ICB + PBS	Metastasis-unrelated death
21KDV489	ICB + PBS	Respiratory distress
-	Ctrl + DT	Metastasis-unrelated death
21KDV696	Ctrl + DT	Respiratory distress
21KDV794	Ctrl + DT	Metastasis-unrelated death
21KDV801	Ctrl + DT	Respiratory distress
21KDV930	Ctrl + DT	Respiratory distress
21VIS010	Ctrl + DT	Respiratory distress
21VIS012	Ctrl + DT	Metastasis-unrelated death
22KDV032	Ctrl + DT	Long-term survivor
21KDV388	ICB + DT	Respiratory distress
21KDV443	ICB + DT	Metastasis-unrelated death
21KDV484	ICB + DT	Respiratory distress
21KDV485	ICB + DT	Respiratory distress
21KDV519	ICB + DT	Metastasis-unrelated death
21KDV677	ICB + DT	Long-term survivor
21KDV678	ICB + DT	Long-term survivor

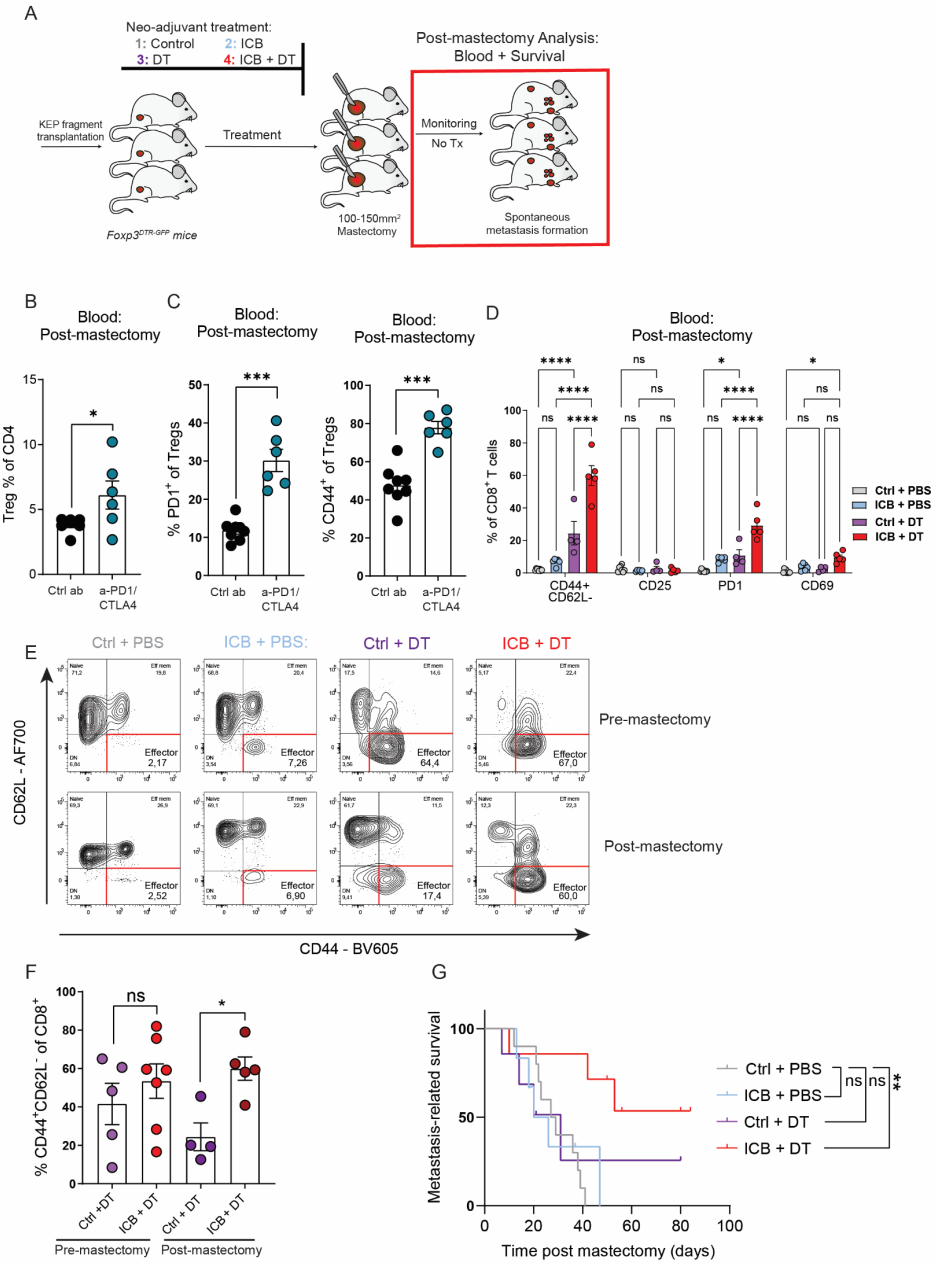

FIGURE 3. ICB combined with T_{reg} depletion induces durable systemic T cell activation and extends metastasis-related survival

Mice were treated as described in figure 2A. After mastectomy, treatments were discontinued, and mice were monitored for the development of metastatic disease. Blood samples were analysed 7-8 days after (post) mastectomy by flow cytometry. **B.** Frequency of T_{regs} ($CD4^+CD25^+$) as % of total live $CD45^+$ cells in blood of mice 7 days after mastectomy, previously treated as indicated (n=6-8 mice group). **C.** Frequency of PD-1 (left) and CD44 (right) expression on gated T_{regs} ($CD4^+CD25^+$) in blood of mice 7 days after mastectomy, previously treated as indicated (n=6-8 mice group). **D.**

Frequency of indicated markers (% of positive cells) gated on $CD8^+$ T cells in blood of mice 7 days after mastectomy, previously treated as indicated (n=6-8 mice group). **E.** Representative dot plots depicting CD44 and CD62L expression gated on $CD8^+$ T cells, in blood of mice receiving indicated neoadjuvant treatments, analysed 1-2 days before mastectomy (pre-mastectomy) and 7 days after mastectomy (post-mastectomy). **F.** Frequency of $CD44^+CD62L^-$ effector cells of $CD8^+$ T cells in blood of mice receiving indicated neoadjuvant treatments, assessed pre- and post-mastectomy (n=4-7 mice/group). **G.** Kaplan-Meier plot showing metastasis-related survival after mastectomy of mice treated as indicated. Censored cases represent mice that were sacrificed due to tumor-unrelated causes (n=7-10 mice/group).
Data in B-D, F show mean ± SEM. P-values were calculated by Student's T-test (B-D,F), log-rank test (G).* $P < 0.05$, ** $P < 0.01$, *** $P < 0.001$, **** $P < 0.0001$.

DISCUSSION

Understanding the hurdles that impair effective anti-tumor immunity upon anti-PD-1/CTLA4 therapy is key to improve responses rates to ICB in breast cancer patients. Here, we used the clinically relevant KEP-based mouse model for spontaneous multi-organ breast cancer metastasis[23], which is unresponsive to combined a-PD-1/a-CTLA4 therapy, to study how T_{regs} impact resistance to ICB. Analysis of mammary tumor-bearing mice showed that ICB increases the accumulation of T_{regs}, but not conventional T cells, in blood and tumors (Fig. 1). Neoadjuvant depletion of T_{regs} during ICB induced the expansion of $CD8^+$ T cells and NK cells in blood of KEP tumor-bearing mice, which was not observed upon T_{reg} depletion without ICB (Fig. 2). T_{reg} depletion by itself strongly induces activation of T cells in the blood compartment, which could be significantly extended upon combination of ICB and T_{reg} depletion (Fig. 3). This likely has consequences for metastasis formation, as the combination of T_{reg} depletion and ICB improves metastasis-related survival compared to control-treated mice, which was not observed in mice treated with either monotherapy. Combined, these findings demonstrate that T_{regs} can form a hurdle for response to ICB in a mouse models for spontaneous breast cancer metastasis formation.

ICB-induced accumulation and activation of T_{regs} in tumor-bearing mice potentially enhances intratumoral and systemic immunosuppression, which may antagonize effective anti-tumor immunity. Based on the findings in our study, we propose several mechanisms that may contribute to improved control of metastases observed upon T_{reg} depletion in the context of ICB. Interestingly, we found that T_{regs} control several parameters that have been associated to therapeutic responses of ICB. In tumors, T_{reg} depletion resulted in the upregulation of PD-1 on $CD8^+$ T cells, and PD-L1 on myeloid cells. Both these observations are linked to response to anti-PD-1 therapy[17,36]. In addition, T_{reg} depletion re-shaped the TME into a more pro-inflammatory anti-tumorigenic environment, most notably characterized by increased infiltration of activated $CD8^+$ T cells, inflammatory eosinophils and M1-like macrophage polarization. These populations have been described to have direct tumor-killing capacities[37–39] and both eosinophils and M1-like macrophages promote $CD8^+$ T cell

activation, via amongst others, expression of T cell recruiting and activation chemokines such as CXCL9 and increased antigen presentation capacity[40,41]. Interestingly, increased systemic and intratumoral eosinophil accumulation has previously been associated with ICB response in melanoma patients[42] and linked to anti-tumorigenic activity in mouse models of breast cancer responsive to ICB[40]. Furthermore, increased recruitment of inflammatory eosinophils to the TME has been linked to anti-tumorigenic activity in a mouse model of breast cancer metastasis[43]. We hypothesize that these pro-inflammatory conditions induced intratumorally by T_{reg} depletion, may have contributed in combination with ICB to the development of a robust anti-metastatic immune response. In line with this hypothesis, we found that the combination of T_{reg} depletion and ICB induced a synergistic effect in the blood compartment on the mobilisation of $CD8^+$ and $CD4^+CD8^+$ T cells, NK cells, and additionally extended T cell activation. We speculate this may confer protection against circulating cancer cells or metastatic formation, leading to improved survival. Which of these anti-cancer mechanisms are most important to curb metastasis, and by which underlying immune cell crosstalk T_{regs} suppress anti-metastatic immunity, remains a topic of future research. Of note, the anti-tumoral effects of ICB + DT were only observed in the metastatic context, and not the primary tumor context. This suggests that additional hurdles for anti-tumor immunity are in place in primary KEP tumors, that are unrelated to T_{regs}. Previous research using the KEP model has shown that primary tumors are abundantly infiltrated by immunosuppressive neutrophils and macrophages[44] which may functionally suppress T cell function in absence of T_{regs}.

Our results concerning the adverse role of T_{regs} in the response to immunotherapy are consistent with clinical data which have revealed correlations between $PD\text{-}1^+$ T_{regs} and therapy response, relapse and hyper progressive disease in NCSLC, melanoma, and gastric cancer respectively[16–18]. Preclinical studies using inoculated B16 and MC38 cell line tumor models have shown that PD-1 blockade reactivates the proliferative and immunosuppressive capacity of $PD\text{-}1^+$ T_{regs}, thereby promoting tumor growth[17,18]. Furthermore, the efficacy of PD-1 blockade was shown to be dependent on high PD-1 expression on $CD8^+$ T cells, but low PD-1 expression on T_{regs}[17]. In our study, we found that after discontinuation of treatment, the frequency of $CD44^+$ and $PD\text{-}1^+$ T_{regs} is strongly increased in blood of mice that received neoadjuvant treatment of anti-PD-1/CTLA4. This suggests that ICB treatment itself plays an important role in the accumulation of $PD\text{-}1^+$ T_{regs}, which can negatively impact anti-tumor immunity as discussed above. It remains to be investigated whether ICB-induced PD-1 expression is caused by increased proliferation of T_{regs} upon anti-CTLA4[19] or anti-PD-1[18], or whether increased PD-1 expression on T_{regs} is potentially a result of chronic TCR stimulation in the context of ICB. Nevertheless, understanding how ICB induces PD-1 expression on T_{regs} may support the development of immune checkpoint inhibitors that selectively activate conventional T cells, but not T_{regs}.

Finally, our data suggest that combining ICB with T_{reg}-targeting strategies is a potential avenue to improve ICB responses in breast cancer. However, due to the critical role of T_{regs} in upholding immune tolerance and thereby prevention of auto-immune related diseases, approaches that partially instead of fully deplete T_{regs} may be more feasible for use in cancer patients including OX-40, CCR4 and CD25[11,18,45]. Promisingly, preliminary histopathological analysis (Fig. S2C, Table 1) in KEP tumor-bearing mice showed that immune-related pathology was not further exacerbated upon combination of ICB + T_{reg} depletion, compared to T_{reg} depletion alone. As this study provides proof-of-principle that T_{regs} impair anti-tumor immunity in the context ICB, it will be crucial to identify how the variety of immunomodulatory drugs that are in clinical development will affect T_{reg} activation beyond anti-PD-1/anti-CTLA4. Looking forward, this may contribute to improved clinical decision making regarding the use of T_{reg}-activating immunomodulatory drugs in cancer patients with abundant intratumoral accumulation of T_{regs}.

MATERIAL AND METHODS

Mice

Mice were kept in individually ventilated cages at the animal laboratory facility of the Netherlands Cancer Institute under specific pathogen free conditions. Food and water were provided *ad libitum.* All animal experiments were approved by the Netherlands Cancer Institute Animal Ethics Committee, and performed in accordance with institutional, national and European guidelines for Animal Care and Use. The study is compliant with all relevant ethical regulations regarding animal research.

The following genetically engineered mice have been used in this study: *Keratin14 (K14)-cre;Cdh1$^{F/F}$;Trp53$^{F/F}$*[22] and *Cdh1$^{F/F}$;Trp53$^{F/F}$;Foxp3$^{GFP\text{-}DTR}$* mice (further referred to as *Foxp3$^{GFP\text{-}DTR}$*) . All mouse models were on FVB/n background, and genotyping was performed by PCR analysis on toe clips DNA as described[22]. Starting at 6-7 weeks of age, female mice were monitored twice weekly for the development of spontaneous mammary tumor development. Upon mammary tumor formation, perpendicular tumor diameters were measured twice weekly using a calliper. End-stage was defined as cumulative tumor burden of 225mm^2, unless indicated otherwise.

Intervention studies

Antibody treatments in tumor-bearing KEP mice were initiated at a tumor size of 50mm^2, and at 2-4mm^2 in KEP transplantation experiments. Mice were randomly allocated to treatment groups upon presentation of palpable tumors, and were intraperitoneally injected twice weekly with ICB; 100 µg of anti-PD-1 (1 mg/mL in PBS, clone RMP1-14, BioXCell) and 100 µg of anti-CTLA4 (1 mg/mL in PBS, clone 9D9, BioXCell) or control; 100 µg rat

IgG2a (1 mg/mL in PBS, clone 2A3, BioXCell). Treatments were discontinued at cumulative tumor burden of 225mm^2 in the KEP model, or upon mastectomy for KEP transplantation experiments at indicated size. For depletion of T_{regs}, DT or PBS (DT vehicle control) treatment was initiated at a tumor size of 6-9mm^2. Mice were treated twice with 25 µg diphtheria toxin (Sigma) or PBS on day 0, and 4.

Flow cytometry analysis and cell sorting

Draining lymph nodes and tumors were collected in ice-cold PBS, and blood was collected in heparin-containing tubes. Draining lymph nodes and tumors were processed as previously described[46]. Blood was obtained via cardiac puncture for end-stage analyses. Erythrocyte lysis for blood was performed in NH_4Cl erythrocyte lysis buffer for 5 minutes. Single cell suspensions were incubated for 20 minutes with anti-CD16/32 (2.4G2, BD Biosciences) to block unspecific Fc receptor binding and fluorochrome conjugated antibodies diluted in FACS buffer (2.5% FBS, 2 mM EDTA in PBS). For analysis of intracellular proteins, cells were fixed and permeabilized after surface and live/dead staining using the FOXP3 Transcription buffer set (Thermofisher), according to manufacturer's instruction. Fixation, permeabilization and intracellular staining was performed for 30 minutes. Cell suspensions were analysed on a BD Symphony SORP or sorted on a FACS ARIA II (4 lasers). Absolute cell counts were determined using 123count eBeads (ThermoFisher) according to manufacturer's instruction. Single cell suspensions for cell sorting were prepared under sterile conditions. Sorting of T_{regs} (Live, $CD45^+CD3^+CD4^+CD25^+$ from indicated tissues and splenic responder cells (Live, $CD45^+CD3^+$ → $CD4^+CD25^-$ or $CD8^+$) performed as previously described[46]. The following fluorochrome-conjugated antibodies were used in this study: CD3- BV421 (1:100), CD3-PECy7 (1:200), CD3-APC (1:400), CD4-APCeF780 (1:200), CD4-BV785 (1:400), CD4-PE (1:200), CD8-APC (1:200), CD8-BUV395 (1:200), CD8-FITC (1:400), CD11c-BUV737 (1:100), CD11b-BV786 (1:400), CD25-PE (1:200), CD25-APC (1:200), CD44-BV605 (1:200), CD45-BUV395 (1:200), CD45-BUV563 (1:400), CD62L-AF700 (1:200), CD62L-APCeF780 (1:200), CD69-BUV737 (1:200), CD101-PECy7 (1:200), CD103-APC (1:200), F4/80-BUV395 (1:200), FOXP3-AF647 (1:100), Ki67-BV786 (1:200), Ly6C-eF450 (1:400), Ly6G-AF700 (1:200), MHC-II-FITC (1:200), NKp46-FITC (1:200), NKp46-PE (1:200), PD1-PECy7 (1:200), PDL1-PE (1:200), SiglecF-BV605 (1:200).Viability dyes: 7AAD (1:20), Fixable viability dye eFluor 780 (1:1000).

KEP metastasis model

The KEP metastasis model has been applied as previously described[23]. Tumors from KEP mice (100mm^2) were fragmented into small pieces (~1 mm^2) and stored at -150 °C in Dulbecco's Modified Eagle's Medium F12 containing 30% fetal calf serum and 10% dimethyl sulfoxide. Selection of mouse invasive lobular carcinomas (mILC) donor tumors was based on high cytokeratin 8 and absence of vimentin and E-cadherin expression as determined by immunohistochemistry. Donor KEP tumor pieces were thawed, washed, and orthotopically transplanted into the 4th mammary fat pad of female recipient 8-16 week old

FOXP3$^{DTR-GFP}$ mice. Upon tumor outgrowth to a size of 100-150mm^2, tumors were surgically removed. Following mastectomy, mice were monitored for development of overt multi-organ metastatic disease by daily palpation and observation of physical health, appearance, and behavior. Lungs, liver, spleen, intestines, kidneys, and tumor-draining (proper axillary and accessory axillary) lymph nodes were collected and analysed microscopically for the presence of metastatic foci by immunohistochemical cytokeratin 8 staining. Mice were excluded from analysis due to following predetermined reasons: No outgrowth of tumors upon transplantation, mice sacrificed due to surgery-related complications, mice sacrificed due to development of end-stage (225mm^2) local recurrent tumors prior to presentation of metastatic disease, mice sacrificed due to metastasis-unrelated pathology.

T_{reg} suppression assays

T_{reg}-T cell suppression assays were performed as previously described[46]. T_{regs} (Live, CD45$^+$, CD3$^+$, CD8$^-$ CD4$^+$, CD25^{high}) sorted from freshly isolated samples were activated overnight in IMDM containing 8% FCS, 100 IU/ml penicillin, 100 µg/ml streptomycin, 0.5% β-mercapto-ethanol, 300U/mL IL-2, 1:5 bead:cell ratio CD3/CD28 coated beads (Thermofisher). Per condition, 2.5*10^4 cells were seeded in 96-wells plate, which were further diluted to appropriate ratios (1:2 – 1:16. Responder cells (Live, CD45$^+$, CD3$^+$, CD4$^+$, CD25$^-$ and Live, CD45$^+$, CD3$^+$, CD8$^+$) were rested overnight. Next, responder cells were labelled with CellTraceViolet, and co-cultured with T_{regs} in cIMDM supplemented with CD3/CD28 beads (1:5 bead cell ratio) for 96 hours (without exogenous IL-2).

Immunohistochemistry

Immunohistochemical analyses were performed by the Animal Pathology facility at the Netherlands Cancer Institute. Formalin-fixed tissues were processed, sectioned and stained as described[23]. In brief, tissues were fixed for 24 h in 10% neutral buffered formalin, embedded in paraffin, sectioned at 4 µm and stained with haematoxylin and eosin (H&E) for inflammation-related histopathological evaluation by a trained animal pathologist. Slides were digitally processed using QuPath. For immunohistochemical analysis, 5-µm paraffin sections were cut, deparaffinized and stained. Brightness and contrast for representative images were adjusted equally among groups.

Statistical analysis

Data analyses were performed using GraphPad Prism (version 8). Data show means ± SEM unless stated otherwise. The statistical tests used are described in figure legends. For comparison of two groups of continuous data, Student's T-test and Mann Whitney's T Test were used as indicated. For comparison of a single variable between multiple groups of normally distributed continuous data, we used one-way ANOVA, followed by indicated post-hoc analyses. For comparison of ≥2 variables between multiple groups, two-way ANOVA was used, followed by indicated post-hoc analyses. Fisher's exact test was used

to assess significant differences between categorical variables obtained from lymph node metastasis incidence. All tests were performed two-tailed. P-values < 0.05 were considered statistically significant. *In vivo* interventions were performed once with indicated sample sizes, unless otherwise indicated. *In vitro* experiments were repeated independently as indicated, Asterisks statistically significant differences. * $P < 0.05$, ** $P < 0.01$, *** $P < 0.001$, **** $P < 0.0001$.

Author contributions

K.Ko, L.S, O.B and K.E.d.V. conceived the ideas and designed the experiments. K.Ko, L.S, O.B performed experiments and data analysis. K.Ko, L.S, O.B, D.K., K.V, C.-S.H., L.R and K.Ke performed animal experiments. K.E.d.V. supervised the study, K.E.d.V and K.K acquired funding, K.K, L.S, O.B and K.E.d.V. wrote the paper and prepared the figures with input from all authors.

Acknowledgements

We thank members of the Tumor Biology & Immunology Department, NKI for their insightful input. We thank the flow cytometry facility, animal laboratory facility, transgenesis facility and animal pathology facility of the Netherlands Cancer Institute for technical assistance. We thank Sjoerd Klaarenbeek for providing histopathological analysis.

Funding

NWO Oncology Graduate School Amsterdam (OOA) Diamond Program (KK)
Netherlands Organization for Scientific Research grant NWO-VICI 91819616 (KdV)
Dutch Cancer Society grant KWF10083; KWF10623; KWF13191 (KdV)
Oncode Institute (KdV)

Competing interests

KdV reports research funding from Roche and is consultant for Macomics, outside the scope of this work.

Data availability

Data are available from the authors on reasonable request.

REFERENCES

1. Blank, C. U. *et al.* Neoadjuvant versus adjuvant ipilimumab plus nivolumab in macroscopic stage III melanoma. *Nature Medicine* vol. 24 1655–1661 (2018).
2. Doroshow, D. B. *et al.* Immunotherapy in Non–Small Cell Lung Cancer: Facts and Hopes. *Clin. Cancer Res.* **25**, 4592–4602 (2019).
3. Chalabi, M. *et al.* Neoadjuvant immunotherapy leads to pathological responses in MMR-proficient and MMR-deficient early-stage colon cancers. *Nat. Med. 2020 264* **26**, 566–576 (2020).
4. Sharma, P., Hu-Lieskovan, S., Wargo, J. A. & Ribas, A. Leading Edge Review Primary, Adaptive, and Acquired Resistance to Cancer Immunotherapy. (2017) doi:10.1016/j.cell.2017.01.017.
5. Adams, S. *et al.* Pembrolizumab monotherapy for previously untreated, PD-L1-positive, metastatic triple-negative breast cancer: Cohort B of the phase II KEYNOTE-086 study. *Ann. Oncol.* **30**, 405–411 (2019).
6. Dirix, L. Y. *et al.* Avelumab, an anti-PD-L1 antibody, in patients with locally advanced or metastatic breast cancer: A phase 1b JAVELIN solid tumor study. *Breast Cancer Res. Treat.* **167**, 671–686 (2018).
7. Chen, D. S. & Mellman, I. Oncology Meets Immunology: The Cancer-Immunity Cycle. *Immunity* **39**, 1–10 (2013).
8. Simon, S. & Labarriere, N. PD-1 expression on tumor-specific T cells: Friend or foe for immunotherapy? *https://doi.org/10.1080/2162402X.2017.1364828* **7**, (2017).
9. Tanaka, A. & Sakaguchi, S. Regulatory T cells in cancer immunotherapy. *Cell Research* vol. 27 109–118 (2017).
10. Sharpe, A. H. & Pauken, K. E. The diverse functions of the PD1 inhibitory pathway. *Nat. Rev. Immunol.* **18**, 153–167 (2018).
11. Plitas, G. & Rudensky, A. Y. Regulatory T Cells in Cancer. *Annu. Rev. Cancer Biol.* **4**, 459–477 (2020).
12. Kos, K. & de Visser, K. E. The Multifaceted Role of Regulatory T Cells in Breast Cancer. *Annu. Rev. Cancer Biol.* **5**, (2021).
13. Bos, P. D., Plitas, G., Rudra, D., Lee, S. Y. & Rudensky, A. Y. Transient regulatory T cell ablation deters oncogene-driven breast cancer and enhances radiotherapy. *J. Exp. Med.* **210**, 2435–2466 (2013).
14. Clark, N. M. *et al.* Regulatory T Cells Support Breast Cancer Progression by Opposing IFN-γ-Dependent Functional Reprogramming of Myeloid Cells. *Cell Rep.* **33**, (2020).
15. Kos, K. *et al.* Tumor-educated Tregs drive organ-specific metastasis in breast cancer by impairing NK cells in the lymph node niche. *Cell Rep.* **38**, 110447 (2022).
16. Huang, A. C. *et al.* A single dose of neoadjuvant PD-1 blockade predicts clinical outcomes in resectable melanoma. *Nat. Med.* **25**, 454–461 (2019).
17. Kumagai, S. *et al.* The PD-1 expression balance between effector and regulatory T cells predicts the clinical efficacy of PD-1 blockade therapies. *Nat. Immunol.* **21**, 1346–1358 (2020).
18. Kamada, T. *et al.* PD-1(+) regulatory T cells amplified by PD-1 blockade promote hyperprogression of cancer. *PNAS* **116**, 9999–10008 (2019).
19. Marangoni, F. *et al.* Expansion of tumor-associated Treg cells upon disruption of a CTLA-4-dependent feedback loop. *Cell* **184**, 3998-4015.e19 (2021).
20. Kavanagh, B. *et al.* CTLA4 blockade expands FoxP3+ regulatory and activated effector CD4+ T cells in a dose-dependent fashion. *Blood* **112**, 1175 (2008).
21. Sharma, A. *et al.* Anti-CTLA-4 immunotherapy does not deplete Foxp3 þ regulatory T cells (Tregs) in human cancers. *Clin. Cancer Res.* **25**, 1233–1238 (2019).
22. Derksen, P. W. B. *et al.* Somatic inactivation of E-cadherin and p53 in mice leads to metastatic lobular mammary carcinoma through induction of anoikis resistance and angiogenesis. *Cancer Cell* **10**, 437–449 (2006).
23. Doornebal, C. W. *et al.* A Preclinical Mouse Model of Invasive Lobular Breast Cancer Metastasis. *Cancer Res.* **73**, 353 LP – 363 (2013).
24. Tavares, M. C. *et al.* A high CD8 to FOXP3 ratio in the tumor stroma and expression of PTEN in tumor cells are associated with improved survival in non-metastatic triple-negative breast carcinoma. *BMC Cancer* **21**, 901 (2021).
25. Kim, J. M., Rasmussen, J. P. & Rudensky, A. Y. Regulatory T cells prevent catastrophic autoimmunity throughout the lifespan of mice. *Nat. Immunol.* **8**, 191–7 (2007).
26. Wang, S., Shen, H., Bai, B., Wu, J. & Wang, J. Increased CD4+CD8+Double-Positive T Cell in Patients with Primary Sjögren's Syndrome Correlated with Disease Activity. *J. Immunol. Res.* **2021**, (2021).
27. Parel, Y. *et al.* Presence of CD4+CD8+ double-positive T cells with very high interleukin-4 production potential in lesional skin of patients with systemic sclerosis. *Arthritis Rheum.* **56**, 3459–3467 (2007).
28. Bohner, P. *et al.* Double positive CD4+CD8+ T cells are enriched in urological cancers and favor T helper-2 polarization. *Front. Immunol.* **10**, 622 (2019).

29. Desfrançois, J. *et al.* Double Positive CD4CD8 αβ T Cells: A New Tumor-Reactive Population in Human Melanomas. *PLoS One* **5**, (2010).
30. Kim, J. M., Rasmussen, J. P. & Rudensky, A. Y. Regulatory T cells prevent catastrophic autoimmunity throughout the lifespan of mice. *Nat. Immunol.* **8**, 191–197 (2007).
31. Liu, J. *et al.* Assessing immune-related adverse events of efficacious combination immunotherapies in preclinical models of cancer. *Cancer Res.* **76**, 5288–5301 (2016).
32. Carretero, R. *et al.* Eosinophils orchestrate cancer rejection by normalizing tumor vessels and enhancing infiltration of CD8 + T cells. *Nat. Immunol.* **16**, 609–617 (2015).
33. Binnewies, M. *et al.* Unleashing Type-2 Dendritic Cells to Drive Protective Antitumor CD4+ T Cell Immunity. *Cell* **177**, 556-571.e16 (2019).
34. Pan, Y., Yu, Y., Wang, X. & Zhang, T. Tumor-Associated Macrophages in Tumor Immunity . *Frontiers in Immunology* vol. 11 3151 (2020).
35. Levine, A. G., Arvey, A., Jin, W. & Rudensky, A. Y. Continuous requirement for the TCR in regulatory T cell function. *Nat. Immunol.* **15**, 1070–1078 (2014).
36. Davis, A. A. & Patel, V. G. The role of PD-L1 expression as a predictive biomarker: an analysis of all US Food and Drug Administration (FDA) approvals of immune checkpoint inhibitors. *J. Immunother. Cancer* **7**, 278 (2019).
37. Hollande, C. *et al.* Inhibition of the dipeptidyl peptidase DPP4 (CD26) reveals IL-33-dependent eosinophil-mediated control of tumor growth. *Nat. Immunol.* **20**, 257–264 (2019).
38. Zhang, F. *et al.* Genetic programming of macrophages to perform anti-tumor functions using targeted mRNA nanocarriers. *Nat. Commun. 2019 101* **10**, 1–16 (2019).
39. Waldman, A. D., Fritz, J. M. & Lenardo, M. J. A guide to cancer immunotherapy: from T cell basic science to clinical practice. *Nat. Rev. Immunol. 2020 2011* **20**, 651–668 (2020).
40. Zheng, X. *et al.* CTLA4 blockade promotes vessel normalization in breast tumors via the accumulation of eosinophils. *Int. J. cancer* **146**, 1730–1740 (2020).
41. Akuthota, P., Wang, H. & Weller, P. F. Eosinophils as Antigen-Presenting Cells in Allergic Upper Airway Disease. *Curr. Opin. Allergy Clin. Immunol.* **10**, 14 (2010).
42. Simon, S. C. S. *et al.* Eosinophil accumulation predicts response to melanoma treatment with immune checkpoint inhibitors. *Oncoimmunology* **9**, (2020).
43. Grisaru-Tal, S. *et al.* Metastasis-Entrained Eosinophils Enhance Lymphocyte-Mediated Antitumor Immunity. *Cancer Res.* **81**, 5555–5571 (2021).
44. Salvagno, C. *et al.* Therapeutic targeting of macrophages enhances chemotherapy efficacy by unleashing type I interferon response. *Nat. Cell Biol.* **21**, 511–521 (2019).
45. Solomon, I. *et al.* CD25-Treg-depleting antibodies preserving IL-2 signaling on effector T cells enhance effector activation and antitumor immunity. *Nat. Cancer 2020 112* **1**, 1153–1166 (2020).
46. Kos, K., van Baalen, M., Meijer, D. A. & de Visser, K. E. Flow cytometry-based isolation of tumor-associated regulatory T cells and assessment of their suppressive potential. in *Methods in Enzymology* (2019). doi:10.1016/bs.mie.2019.07.035.

SUPPLEMENTARY MATERIAL

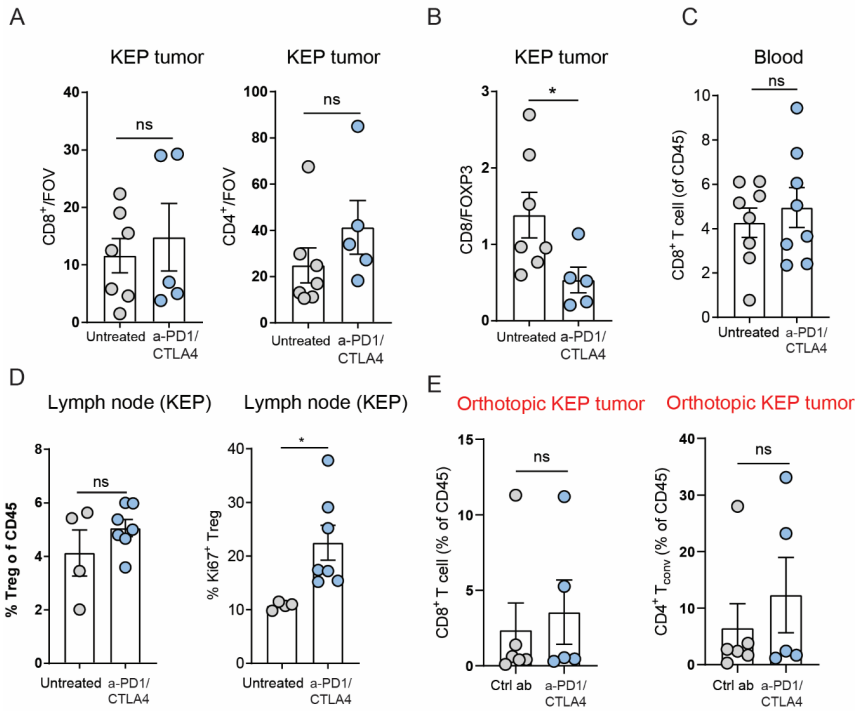

SUPPLEMENTAL FIGURE 1. Effect of ICB on intratumoral and systemic T cell accumulation in tumor-bearing KEP mice

CD8 (left) and CD4 (right) counts in spontaneous mammary tumors (225mm^2) of KEP mice treated as indicated, as determined by immunohistochemical analysis (counts per 40x field of view, average of five randomly selected areas) (n=5-7 mice/group). **B.** Ratio of CD8 and FOXP3 counts shown in Fig. 1D and S1A. **C.** Frequency of CD8$^+$ T cells as % of total live CD45$^+$ cells in blood of KEP mice bearing mammary tumors (225mm^2), treated with control or anti-PD-1/CTLA4 (n=8 mice group). **D.** Quantification of T_{regs} as % of total live CD45$^+$ cells (left) and frequency of Ki-67 expression (right) on T_{regs} (CD4$^+$CD25$^+$), and in lymph nodes isolated from KEP mice bearing mammary tumors (225mm^2), treated as indicated (n=4-7 mice/group). **E.** Frequency of CD8$^+$ (left) and CD4$^+$CD25$^-$ (right) T cells as % of total live CD45$^+$ cells in orthotopically transplanted KEP tumors (100-150mm^2) of mice treated with control antibody, or anti-PD-1/CTLA4, as analysed by flow cytometry (n=4-7 mice/group).

Data in A-E show mean ± SEM. P-values were calculated by Student's T-test. * P < 0.05, ** P < 0.01, *** P < 0.001, **** P < 0.0001.

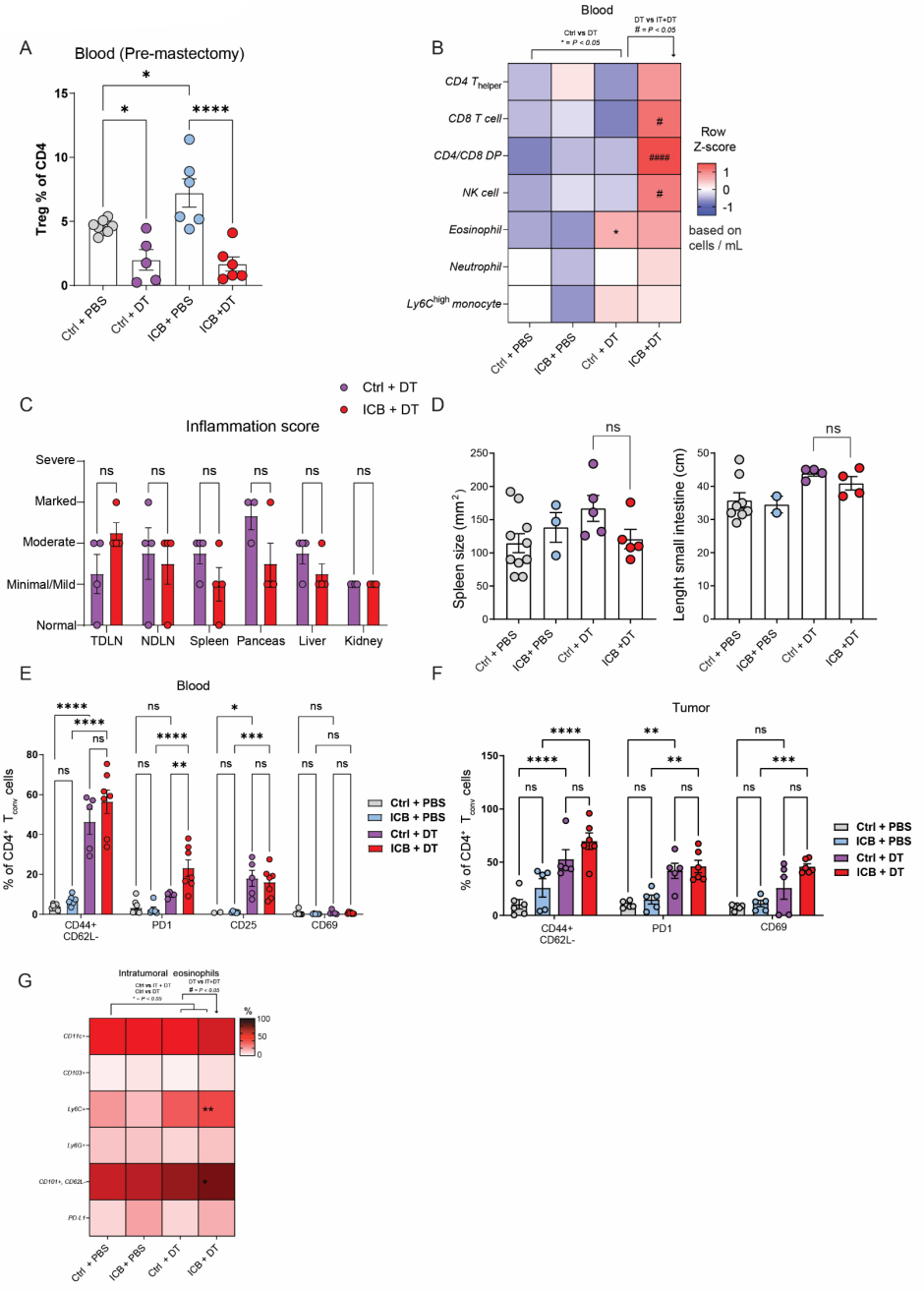
A
Blood (Pre-mastectomy)
Treg % of CD4
Ctrl + PBS
Ctrl + DT
ICB + PBS
ICB +DT
B
Blood
Ctrl vs DT
* = P < 0.05
DT vs IT+DT
= P < 0.05
CD4 T helper
CD8 T cell
CD4/CD8 DP
NK cell
Eosinophil
Neutrophil
Ly6C high monocyte
Row Z-score
based on cells / mL
C
Inflammation score
Ctrl + DT
ICB + DT
Severe
Marked
Moderate
Minimal/Mild
Normal
TDLN
NDLN
Spleen
Panceas
Liver
Kidney
D
Spleen size (mm2)
Lenght small intestine (cm)
E
Blood
% of CD4+ Tconv cells
CD44+ CD62L-
PD1
CD25
CD69
Ctrl + PBS
ICB + PBS
Ctrl + DT
ICB + DT
F
Tumor
G
Intratumoral eosinophils

SUPPLEMENTAL FIGURE 2. Pre-mastectomy analysis of the effect of T_{reg} depletion in the context of ICB on blood and tumors of KEP tumor-bearing mice:
A. Frequency of T_{regs} (defined as $CD4^+GFP^+$ in Ctrl + DT, ICB + PBS, ICB + DT or $CD4^+CD25^+$ in Ctrl + PBS) in blood of mice treated with indicated treatments, as determined by flow cytometry 1-2 days before mastectomy (n=5-8 mice/group). **B.** Heatmap depicting immune landscape in blood of mice receiving indicated treatments, as determined by flow cytometry 1-2 days before mastectomy. Row Z-score calculated based on absolute cell counts of indicated cell type per mL of blood (n=6-8 mice/group). **C.** Histopathological assessment of inflammation-related pathology in various organs of mice treated as indicated as analysed blindly by a trained animal pathologist. Scoring based on data shown in Table 1. **D.** Size of spleen (left) and small intestine (right) of mice treated as indicated. **E.** Frequency of indicated markers gated on $CD4^+$ T_{conv} cells in blood of mice treated as indicated, determined by flow cytometry, pre-mastectomy (n=2-8 mice/group). **F.** Frequency on indicated markers on gated $CD4^+$ T_{conv} cells in mastectomized tumors of mice treated as indicated, determined by flow cytometry, pre-mastectomy (n=5-6 mice/group). **G.** Heatmap depicting expression of indicated markers on eosinophils in mastectomized tumors of mice receiving indicated treatments (n=5-6 mice/group). Data in A,E,F show mean ± SEM. P-values were calculated using One-way ANOVA with Sidak's correction (A,B,D,G), 2-way ANOVA with Sidak's correction (C,E,F).

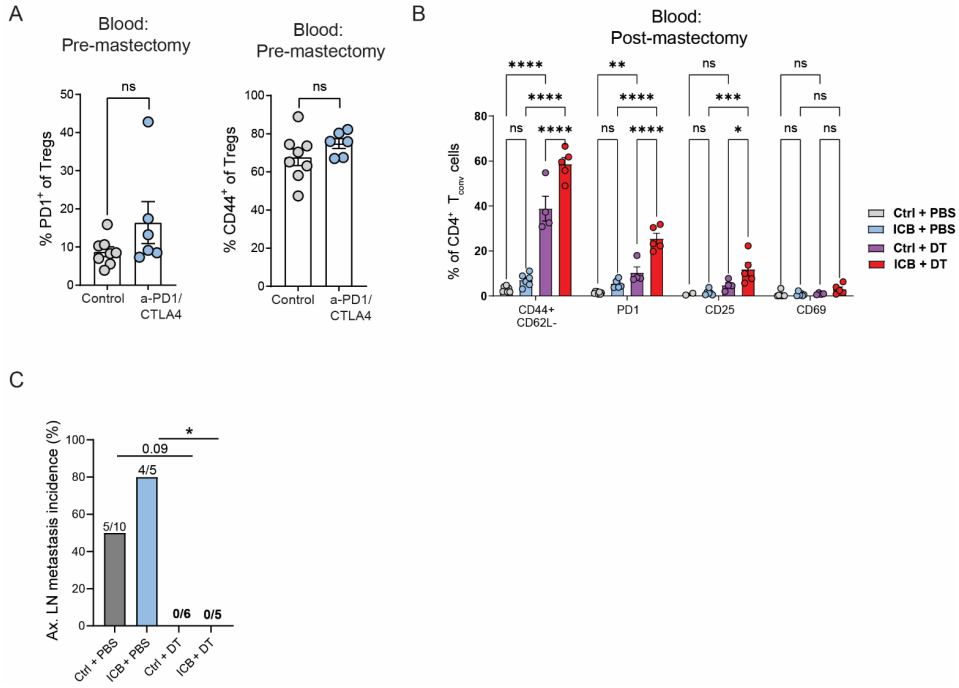

SUPPLEMENTAL FIGURE 3. Post-mastectomy analysis of the effect of T_{reg} depletion in the context of ICB on blood and tumors of KEP tumor-bearing mice:
A. Frequency of PD-1 (left) and CD44 (right) expression on T_{regs} ($CD4^+CD25^+$) in blood of mice 1-2 days before mastectomy, treated as indicated (n=6-8 mice group). **B.** Expression of indicated markers on $CD4^+$ T_{conv} cells in blood of mice 7 days after mastectomy, previously treated as indicated (n=6-8 mice group). **C.** % and number of mice with metastases in axillary TDLNs in mice treated as indicated, as determined by immunohistochemical analysis of keratin 8 staining. Data in A,B show mean ± SEM. P-values were calculated using Student's T-test (A), 2-way ANOVA with Sidak's correction (B), Fisher's Exact Test (C). * $P < 0.05$, ** $P < 0.01$, *** $P < 0.001$, **** $P < 0.0001$.

7

Flow cytometry-based isolation of tumor-associated regulatory T cells and assessment of their suppressive potential

Kevin Kos[1], Martijn van Baalen[2], Denize A. Meijer[1] &
Karin E. de Visser[1*]

Affiliations
[1]Division of Tumor Biology & Immunology, Oncode Institute, Netherlands Cancer Institute, Amsterdam, The Netherlands;
[2] Flow cytometry facility, Netherlands Cancer Institute, Amsterdam, The Netherlands

Methods in Enzymology. 2019, 632:259-281

ABSTRACT

Regulatory T cells (T_{regs}) play a major role in establishing an immunosuppressive tumor microenvironment. In order to fully uncover their role and molecular regulation in tumor-bearing hosts, it is critical to combine phenotypical characterization with functional analyses. A standard method to determine the suppressive potential of T_{regs} is with an *in vitro* suppression assay, in which the impact of freshly isolated T_{regs} on T cell proliferation is assessed. The assay requires the isolation of substantial numbers of T_{regs} from tissues and tumors, which can be challenging due to low yield or cell damage during sample preparation. In this chapter we discuss a flexible suppression assay which can be used to assess the suppressive potential of low numbers of murine T_{regs}, directly isolated from tumors. We describe methods for tissue preparation, flow cytometry based sorting of T_{regs} and optimal conditions to perform a suppression assay, to obtain reliable and reproducible results.

INTRODUCTION

There is a growing appreciation for the influential role of the tumor microenvironment on cancer biology[1]. This has led to the realization that the immune system is not only involved in tumor clearance, but can also support tumor growth and metastasis via different mechanisms, including the induction of intra-tumoral and systemic immunosuppression[2]. One of the key cell types that is involved in exerting immunosuppression in cancer patients is the Foxp3$^+$ CD4$^+$ regulatory T cell (T_{reg})[3].

In mice, regulatory T cells are characterized by high expression of the transcription factor Foxp3, which arms these cells with immunosuppressive properties[4,5]. Other proteins that are highly expressed by T_{regs} include CD25, CTLA-4 and GITR[6]. T_{regs} play a central role in many aspects of immune homeostasis, and are for example critical in resolving inflammation, dampening immunity towards food- and commensal microbial antigens and controlling adipose inflammation[7–9]. Importantly, T_{regs} are the gate keepers of peripheral tolerance and thus responsible for clearing auto-reactive T cells from the periphery[10]. To perform this role, T_{regs} have a wide arsenal of immunosuppressive abilities, including the release of cytokines, inhibition of T cell priming and direct effector cell killing[6]. In a cancer setting, many of these immunosuppressive mechanisms can be directly employed to prevent anti-tumor immunity and promote tumor growth[3]. However, the type of suppressive effector mechanism that is used in a certain setting depends on many factors, such as signals from the local environment, and the activation status of the T_{reg} or the target cell. Therefore, when investigating T_{regs}, it is important to combine a comprehensive phenotypical analysis with functional assays that assess their suppressive potential.

The suppressive potential of T_{regs} is best assessed with a suppression assay. For this assay, T_{regs} are isolated from a source of interest and subsequently co-cultured with activated conventional CD4$^+$ and CD8$^+$ T cells (responder cells) in several ratios. These responder cells are labeled with a fluorescent proliferation dye prior to the start of the co-culture. By analyzing the intensity of the proliferation dye after several days, one can assess to what extent T_{regs} from a source of interest can suppress responder cell proliferation (Figure 1). Although the focus of this six day protocol is on testing the suppressive potential of tumor-derived T_{regs}, the assay is applicable to murine T_{regs} obtained from virtually any tissue, disease model, or genetically manipulated context. In addition, the protocol allows modifications to fit the user's research question. This includes changing the type of responder cells, or supplementing the co-culture with blocking/stimulating agents, e.g. antibodies or cytokines of choice.

Satisfactory execution of a suppression assay can be quite tedious due to many different variables that have to be taken into account. For example, results can be influenced by the

chosen isolation method, choice of stimulatory signals and responder cells, and culture conditions. This chapter describes a protocol for the isolation of T_{regs} from murine mammary tumors, spleens and lymph nodes by flow cytometry-based cell sorting and analysis of their suppressive potential on splenic $CD4^+$ and $CD8^+$ T lymphocytes. We provide detailed descriptions of optimal sample preparation, sorting strategies, co-culture conditions, execution and analysis of the suppression assay.

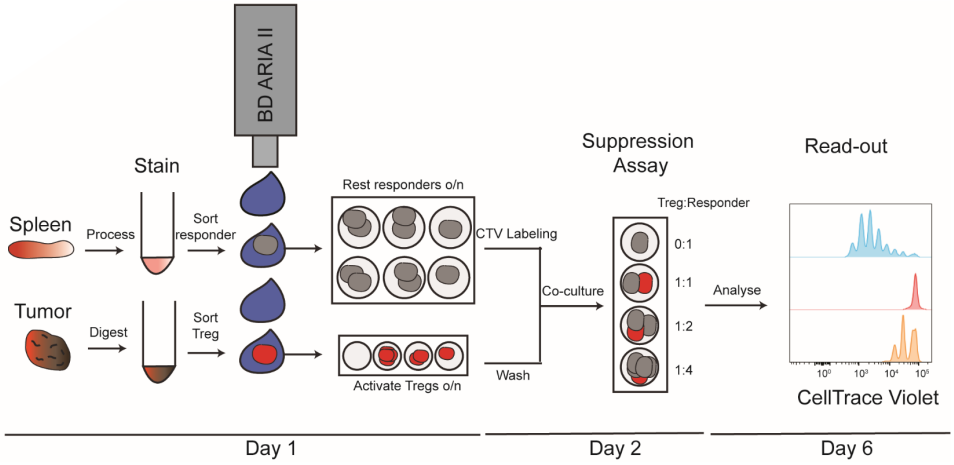

FIGURE 1. Schematic overview of the 6-day suppression assay described in this protocol.

EQUIPMENT AND MATERIALS

Preparation of single-cell suspensions from freshly isolated murine tissues

1. Freshly isolated murine tissues of interest in PBS on ice
2. McIlwain Tissue Chopper (Ted Pella Inc.) including chopping discs, blades and scalpel
3. Plunger of a 2mL syringe
4. Cell strainer, mesh size 70µm (Falcon)
5. Shaking waterbath or shaker
6. Red Blood Cell (RBC) lysis buffer: 155mM NH_4Cl, 10mM $KHCO_3$, 0.1mM EDTA in H_2O, pH 7.2–7.4 (Note 1).
7. Freshly prepared tumor digestion mix: 3mg/mL Collagenase A (Roche) in serum free DMEM (Dulbecco), Deoxyribonuclease I from bovine pancreas (DNAse) 25µg/mL (Sigma Aldrich)
8. Inactivation buffer: DMEM medium supplemented with 10% vol/vol FCS
9. Sorting buffer: 1x PBS, 0.5 % BSA, 2mM EDTA

Antibody staining & cell sorting

1. Freshly prepared single cell suspensions from tissues of interest on ice
2. Fluorescently labeled anti-mouse antibodies (Table 1)
3. LIVE/DEAD™ Fixable Aqua Dead Cell Stain Kit (Thermofisher)
4. 7-AAD Viability Staining Solution (Thermofisher)
5. Fc block: purified anti-mouse CD16/32 antibody (BD Biosciences)
6. 1.4ml Push Cap U-bottom tubes (Micronic)
7. 5mL polypropylene round-bottom tubes, 12x75mm (Falcon)
8. 5mL polypropylene tubes with 35µm cell strainer snap cap (Falcon)
9. Collection/Culture buffer: IMDM (Dulbecco) , 9% FCS, 100IU/mL penicillin, 100µg/mL streptomycin, β-mercapto-ethanol 0.2% (Merck), GlutaMAX 1% (Thermofisher)
10. A 3-laser flow cytometry based cell sorter, with the ability to detect at least 5 different fluorescent labels

TABLE 1. Recommended fluorochrome-conjugated antibody panel for optimized T_{reg}/responder cell sorting from murine tumor tissues.

Antigen	Fluorochrome	Clone	Concentration	Marker	Manufacturer
CD3	APC-eF780	145-2C11	1:400	T lymphocytes	BioLegend
CD4	PE	GK1.5	1:200	$CD4^+$ T lymphocytes	Thermofisher
CD25	APC	PC61	1:400	Regulatory T cells	Thermofisher
CD8	FITC	53-6.7	1:400	$CD8^+$ T lymphocytes	BD Biosciences

Suppression assay

1. Freshly sorted T_{regs} and responder cells on ice
2. Recombinant murine IL-2 (Peprotech)
3. Dynabeads™ Mouse T-Activator CD3/CD28 (Thermofisher)
4. CellTrace™ Violet Cell Proliferation dye (Thermofisher)
5. A 3-laser analytical flow cytometer, with the ability to detect at least 5 different fluorescent labels

Essential laboratory materials

1. 1x sterile phosphate buffered saline (PBS)
2. 12-multichannel pipette
3. Tissue culture-treated 96-well U-bottom plates (Greiner bio one)
4. Tissue culture-treated 6-well plates (Greiner bio one)
5. Sterile filter tips
6. 15 and 50mL polypropylene tubes (Falcon)
7. 1.5mL Eppendorf tubes (Eppendorf)
8. Refrigerated (plate) centrifuge

9. Cell counting equipment (manual/automated)
10. Ice bucket

PREPARATION OF SINGLE-CELL SUSPENSIONS FROM FRESHLY ISOLATED MURINE TISSUES

The suppression assay can be performed with T_{regs} obtained from any tissue, dependent on the research question of the experiment. It is important to realize that the number of T_{regs} that can be obtained will greatly vary between different tissues or stages of disease. T_{regs} can be quite easily isolated from spleen and lymph nodes and are therefore commonly used for standard assays. In contrast, murine tumors may harbor few intra-tumoral T cells, and accordingly yield a low number of T_{regs}. Isolating sufficient numbers of T_{regs} from tumors can therefore be challenging, but is essential for high quality results. T_{regs} and responder cells are isolated from single cell suspensions of murine tissues via flow cytometry based sorting. Typically, each murine tissue requires a specific approach for optimal preparation of single cell suspensions. In this protocol, we will describe the isolation of T_{regs} from murine spleen, lymph nodes and mammary tumors.

Keep cells sterile, on ice and protected from light, unless otherwise stated throughout the protocol. Before starting processing of tissues, cool PBS and sorting buffer on ice and warm the tumor digestion mix to 37°C (10mL in a 15mL tube per tumor)

Spleen and lymph nodes

1. Remove fat attached to the spleen/lymph nodes and place organ of interest on a (separate) 70µm cell strainer, inserted into a 50mL tube.
2. Gently mash the tissue with the plunger through the filter, while adding ~15mL cold sterile PBS until cells have passed through the cell strainer.
3. Centrifuge the cells at 300g, 4°C for 5 minutes and aspirate supernatant.
4. Incubate the spleen cell pellet (skip this step for the lymph node cells) in 1mL of sterile RBC lysis buffer for 2 minutes at room temperature. Stop RBC lysis with 10mL of cold sorting buffer and subsequently pellet the cells.
5. Resuspend the cells in 1mL (spleen) or 500 µL (lymph nodes) of sorting buffer on ice and count (manually/automated) the number of cells in suspension.

Mouse mammary tumors

The following protocol applies to tumors that measure up to a maximum of 1500mm^3 (Note 2).

1. Place the tumor on a chopping disc cleaned with 70% ethanol. Remove non-tumor tissue such as fat tissue. Make sure the tumor is free of lymph nodes, to prevent

contamination with lymph node-derived T_{regs}. Pre-cut the tumor in small pieces using a clean scalpel.

2. Place the disc under the tissue chopper and chop the tumor at least 3x, to a homogenous sample. Use maximum cutting speed and blade force, 5–10µm blade travel. Alternatively, other cutting instruments can be used to fragment the tumor.
3. Scrape the chopped tumor from the disc with a scalpel and carefully insert into a tube with 10ml of warmed digestion mix. Incubate at 37ºC for 1 hour with gentle agitation. This can be done in a shaking water bath, or with a shaker placed in an incubator.
4. After incubation, pass the cells using a plunger through a 70µm cell strainer capped into a 50mL tube and add 15mL of cooled inactivation buffer to stop the enzymatic digestion.
5. Centrifuge the cells at 300g, 4°C for 5 minutes and aspirate supernatant. Resuspend the cells in 1mL of sorting buffer on ice and count the cells.

The suppression assay requires the co-culture of T_{reg} and responder cells. Here, the responder cells are of a combination of splenic $CD4^+CD25^-$ and $CD8^+$ T cells, which are co-cultured with T_{regs} in five different ratios for 96 hours.

In order to estimate the portion of the single cell suspensions that should be stained and sorted to obtain sufficient cells to perform the assay, it is important to calculate the required number of cells first. Testing a single condition in five T_{reg}:responder ratios requires a total input of 125.000 responder cells and 50.000 T_{regs}. Per ratio, 25.000 responder cells are plated. To obtain a T_{reg}:responder ratio of 1:1, 25.000 T_{regs} are co-cultured with 25.000 responder cells. The remaining 25.000 T_{regs} are serially diluted, with linearly fewer T_{regs} for each ratio. When testing T_{regs} from multiple conditions, multiply the number of required responder cells accordingly. This suppression assay has been optimized for an input of 50.000 T_{regs} but can be downscaled to an input of 10.000 T_{reg} cells.

As each tissue yields a different number of T_{regs}, we have summarized our typical sorting yields here. From a spleen of a naïve adult wild-type FVB mouse, $0.8*10^6$ $CD4^+CD25^+$ T_{regs}, $3.0*10^6$ $CD8^+$ T cells and $10*10^6$ $CD4^+$ $CD25^-$ T cells can be recovered. The number of T_{regs} that can be obtained from a tumor is size and model dependent. From a tumor sized 1500mm^3, we generally recover between 50.000 and 100.000 T_{regs}.

Estimate the portion of single cell suspension that should be fluorescently labeled and sorted accordingly, and proceed with the antibody staining procedure (Note 3).

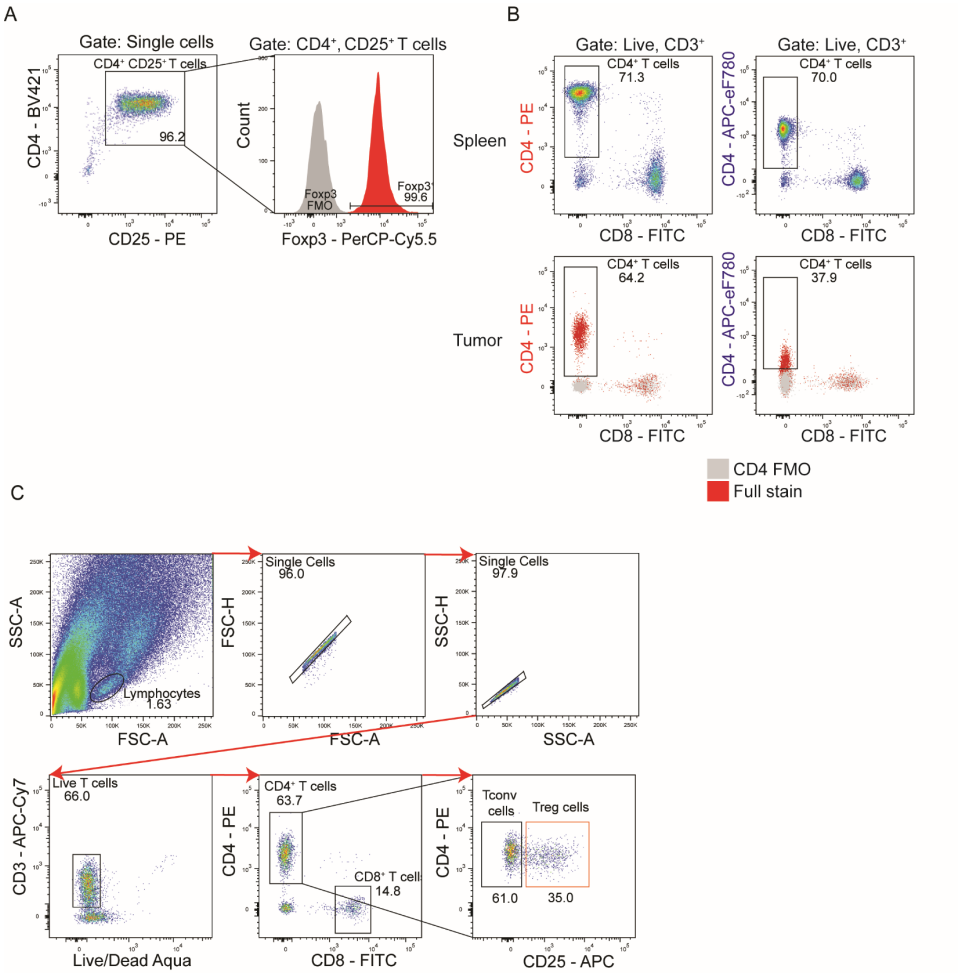

FIGURE 2. Flow cytometry-based sorting of regulatory T cells.
A. Splenic CD4+CD25+ cells were sorted as described and intracellularly stained for FOXP3 to confirm T_{reg} identity. **B**. Single cell suspensions from spleen and tumor were fluorescently labeled according to Table0 1, or an alternative panel using a relatively dim antibody for CD4. CD4 expression on live $CD3^+$ T cells is shown. **C.** Recommended gating strategy to sort T_{regs} from fluorescently labeled single cell suspensions. Tumor tissue is shown.

FLUORESCENT ANTIBODY STAINING & CELL SORTING

After the preparation of single cell suspensions, cells are fluorescently labeled in order to identify and sort T_{regs} and responder cells from the samples. Here, a thoroughly tested and optimized approach for the fluorescent staining and sorting of T_{regs} is presented. The choice of antibody-fluorochrome conjugate combination dictates the purity of the isolated T_{reg} population. $CD4^+$ T_{regs} in mice are characterized by high expression of the transcription

factor Foxp3. However, unless Foxp3-reporter mice are used, it is not possible to sort live T_{regs} based on this marker, because detection of intracellular Foxp3 requires fixation and permeabilization. To circumvent this, it is widely accepted to sort T_{regs} based on surface expression of CD4 and CD25 (IL2-receptor α-chain) [11]. Since CD25 can also be transiently expressed on conventional T cells upon TCR stimulation, it is important to confirm T_{reg} identity of sorted $CD4^+$ $CD25^{high}$ cells by intracellular Foxp3 staining, as shown in Figure 2A (Note 4). Additionally, tumor tissue-derived T_{regs} express relatively lower levels of CD4 as compared to T_{regs} derived from other tissues due to enzymatic treatment. Therefore, a relatively bright anti-CD4 fluorochrome-antibody conjugate must be used to discriminate these cells from the CD4 negative fraction, as illustrated in Figure 2B. Using the following protocol, T_{regs} can be directly sorted from the single cell suspensions without the need for additional purification steps.

Cell suspensions are first incubated with Fc receptor block solution (Note 5), followed by incubation with fluorescently labeled antibodies (Table 1). Finally, cells are stained with a viability dye to distinguish viable from dead cells. To compensate for spectral overlap, single fluorochrome stained samples should be prepared for each fluorochrome (Note 6). To determine positive populations for CD4-PE and CD25-APC, fluorescence minus one (FMO) controls should be included for each tissue that is sorted.

1. Plate the previously calculated number of cells from each single cell suspension in a 96-well plate. Plate a maximum of $6*10^6$ cells per well. Keep the plate on ice.
2. In the same 96-well plate, plate cells in 6 additional wells for each single fluorochrome sample and an unstained sample. For splenocytes, plate ~$1*10^6$ cells/well. When sorting tumor samples, plate compensation beads instead of cells to save sample for sorting.
3. Plate 2 extra wells for each tissue sample for CD4-PE and CD25-APC FMO controls. Plate same number of cells/well as determined in 3.1. The plate now contains cells for sorting, single fluorochrome controls, and FMO controls.
4. Prepare the following solutions in cold sterile sorting buffer (viability dye in PBS), 50µL per well.

Solutions for fluorescent labeling of single cell suspensions

1. Antibody mix (Note 7)
    1. Prepare the mix using the antibodies and concentrations described in table 1. Prepare 50µL antibody mix per well. For example, if $60*10^6$ splenocytes are sorted, calculate for 10 wells. Prepare 50µL extra. (10 wells * 50µL) + 50µL = 550µL antibody mix.
2. Viability dye
    1. Fixable LIVE/DEAD Aqua cell stain kit (1:1000 in PBS)
3. Fc receptor block solution.

1. Dilute purified anti-mouse CD16/32 antibody (1:100)

Control solutions for flow-based sorting

4. CD4-PE and CD25-APC FMO controls.
   Prepare FMO controls for each tissue that will be sorted.
   1. Prepare the antibody mix as in a. but without the CD4-PE antibody.
   2. Prepare the antibody mix as in a. but without the CD25-APC antibody.
5. Single fluorochrome controls (Note 6)
   1. Prepare single fluorochrome controls by diluting each fluorochrome (including the viability dye) from table 1 separately. Use the indicated concentration.

5. Centrifuge the 96-well plate for 2 minutes at 380g after preparation of the solutions. Flick off the supernatant in a waste bin in the flow hood and gently press the plate upside down on a tissue.
6. Resuspend cell samples (all, except single fluorochrome controls) in 50µL of Fc receptor block solution and incubate 5 minutes on ice. After incubation, centrifuge the plate and discard supernatant.
7. During this incubation, add 50µL of single fluorochrome controls to designated wells.
8. Resuspend the fluorescent antibody mix and FMO controls and add 50µL to the designated wells. Gently mix with a pipette and incubate the plate for 20 minutes protected from light at 4°C.
9. After incubation, wash the plate 1x with PBS (Note 8)
10. Stain cells with viability dye according to manufacturer's instructions. After incubation, wash the cells 1x with sorting buffer.
11. Resuspend samples for single fluorochrome- and FMO controls in 200µL sorting buffer and collect in 1.4mL U-bottom tubes.
12. Resuspend each sample for sorting in 200µL sorting buffer. Filter the sample through a 35µm cell strainer into a 5mL polypropylene tube. Combine all samples from matching tissue in a single tube. Replace the cell strainer cap if clogged to enhance cell recovery. T_{regs}/responders will be sorted directly from this tube. Keep tubes sterile, on ice and protected from light.
13. Adjust sample volume to an appropriate cell concentration with sorting buffer, to increase sorting efficiency (Note 9). Guidelines:
    1. 70µm nozzle: $14*10^6$ - $21*10^6$ cells/mL
    2. 85µm nozzle: $10*10^6$ - $15*10^6$ cells/mL
    3. 100µm nozzle $4*10^6$ - $6*10^6$ cells/mL
14. Prepare 5mL polypropylene collection tubes with 1mL collection medium for collection of T_{reg}/responders (Note 10 & 11).
15. Sort cells in an aseptic fashion. Keep samples cooled at all times during the sorting process. Keep the collected cells on ice.
16. Apply the following gating strategy on single cells that are negative for the viability dye.

See Figure 2C for gating T_{regs} in tumor tissue (Note 12).

1. Regulatory T cells:
    1. $CD3^+$, $CD8^-$, $CD4^+$, $CD25^+$
2. SPLEEN RESPONDERS - Conventional $CD4^+$ T cells:
    1. $CD3^+$, $CD8^-$, $CD4^+$, $CD25^-$
3. SPLEEN RESPONDERS - $CD8^+$ T cells:
    1. $CD3^+$, $CD4^-$, $CD8^+$, $CD25^{+/-}$

17. Sort both $CD4^+$ and $CD8^+$ responder cells simultaneously in the same collection tube. (Note 13)
18. Sort T_{regs} from each tissue in a separate collection tube (Note 14).
19. Perform a purity check on collected cells after sorting (Note 15):
    1. Resuspend 20µL of the collected cell suspension in 180µL PBS
        1. Run ddH_2O at high differential pressure until sample line is clean
        2. Record 500 to 1.000 events in the gate of the sorted subset.
    2. Mix 20µL of collection buffer with 180µL PBS.
        1. Run ddH_2O at high differential pressure until sample line is clean
        2. Record for the same amount of time to determine background signal
    3. Determine the percentage of the population of interest from total events (Note 16).
20. Immediately proceed with the suppression assay. (Note 17)

SUPPRESSION ASSAY

A schematic representation of the assay is shown in Figure 3. Freshly sorted T_{regs} and responder cells are first cultured separately overnight to allow for activation and resting respectively. The following morning, responder cells are labeled with CellTrace™ Violet Proliferation (CTV) Dye (Note 18) and co-cultured with T_{regs} at different ratios for 96 hours. Finally, responder cell proliferation is analyzed by flow cytometry to determine the suppressive potential of the T_{regs}. This protocol is optimized for the analysis of low numbers of T_{regs}, and has been validated for an input as low as 10.000 T_{regs} per condition. However, if T_{reg} yield is sufficient, for robustness we strongly recommend performing the assay with 50.000 T_{regs}, and technical replicates for test conditions and controls.

Controls

In order to adequately determine how T_{regs} affect responder cell proliferation, it is essential to include appropriate controls during the co-culture of T_{regs} and responder cells.

1. To determine the maximum proliferative potential of responder cells in a given time period, responder cells should be cultured with stimulatory signals in the absence of T_{regs}. This is essential to verify that responder cells have the capacity to proliferate, allowing for a window of T_{reg} mediated inhibition of proliferation.

2. To determine the background proliferative activity of unstimulated responder cells in a given time period, responder cells should be cultured in the absence of both T_{regs} and stimulatory signals. This is an essential control to verify that responder cells do not proliferate in the absence of stimulation. Additionally, the cells from this control are used to set up CTV signal for data acquisition.

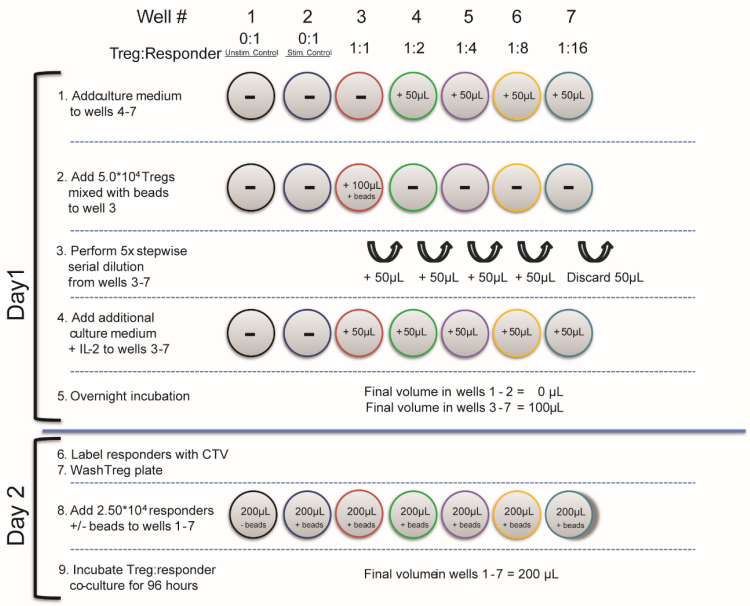

FIGURE 3. Schematic plate layout for the suppression assay.
Follow stepwise instructions to co-culture T_{regs} and responder cells in five T_{reg}:Responder ratios in seven wells, per T_{reg} condition. Repeat for other conditions if necessary.

Additional considerations have to be taken into account in order to draw reliable conclusions from the assay. Although cell isolation by flow sorting allows for near 100% purity of the target populations, this method of cell sorting is performed under relatively high pressure conditions. As a result, shear stress may damage cells and alterations may occur in the redox state and metabolic profile [12]. This procedure may therefore directly impact the performance of cells in this assay. It is essential that after sorting, cells are first cultured separately overnight, to allow cells to recover from sorting induced stress as shown in Figure 4A (Note 19).

Another consideration is the method of responder cell stimulation, as there is a fine balance between excessive and inadequate stimulation. In this assay, responder T cells

are stimulated with anti-CD3 and anti-CD28 antibodies covalently bound to magnetic beads, leading to both TCR activation and co-stimulation. Although beads are simple and extremely reproducible in use, these beads do not fully mimic true antigen-presenting cells (APCs) and bypass any inhibitory effect on proliferation and priming mediated by T_{reg} signaling to APCs. If APCs are required, the user can exchange beads with APCs of choice. It is important to titrate bead:responder ratios because excessive stimulation of responder cells can lead to loss of T_{reg} mediated suppression, whereas inadequate activation may prevent responder cell proliferation. We have found that a ratio of bead:responder of 1:5 provides a window for suppression while simultaneously activating responder cells.

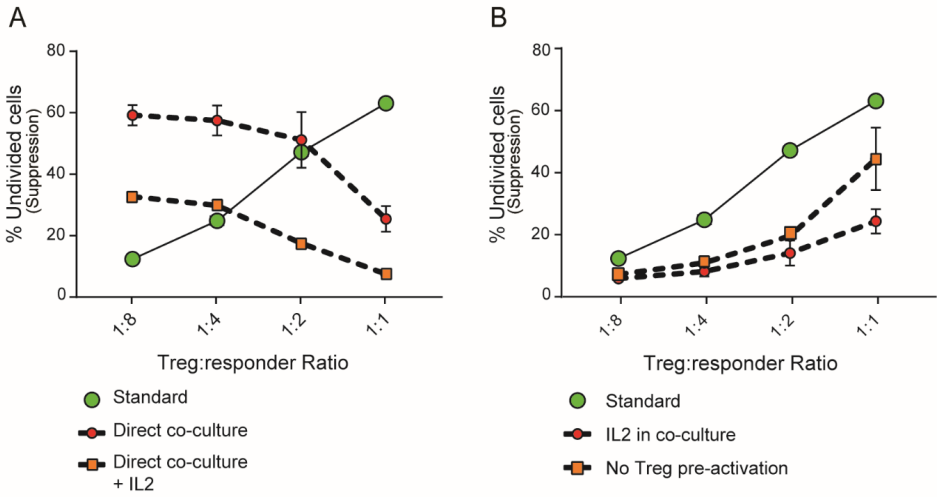

FIGURE 4. Impact of culture conditions on responder cell proliferation.
The percentage of undivided responder cells is plotted for T_{reg}:Responder ratios following suppression assays with various conditions. Standard data: Assay was performed as recommended, including overnight resting, resulting in ratio-dependent proliferation. **A.** When a resting period is omitted and cells are directly co-cultured, ratio-dependent proliferation is lost. **B.** Adding IL-2 (300U/mL) to the co-culture, or omitting T_{reg} pre-activation reduces assay sensitivity. Two technical replicates were used per condition, mean ± SEM is shown from two independent biological replicates.

Additional to responder cell activation, overnight activation of T_{regs} prior to responder cell co-culture greatly enhances suppressive potential. T_{reg} pre-activation may be essential when sorting from homeostatic conditions (Figure 4B) (Note 20).

Finally, T cell proliferation protocols typically include supplementation of IL-2 to culture medium. However, supplementing the co-culture medium with IL-2 highly increases

responder cell proliferation in the presence of T_{regs}, thus severely reducing the window of T_{reg} suppression. It is therefore strongly recommended to perform the assay in the absence of IL-2. (Note 21) (Figure 4B)

Day 1 – T_{reg} pre-activation & Responder resting - See figure 3

Responder cells

1. Determine the number of responder T cells and centrifuge the cells for 5 minutes, 250g at 4°C. Discard supernatant and resuspend the cells in culture medium at a concentration of $1.0*10^6$ cells/mL. Do not add beads or recombinant IL-2.
2. Plate 2mL of the cell suspension per well in a tissue culture-treated 6-wells plate.
3. Incubate the cells overnight at 37°C, 5% CO_2.

T_{regs}

4. Accurately determine the number of T_{regs} and subsequently centrifuge the cells for 5 minutes, 250g at 4°C. Discard supernatant and resuspend the cells in culture medium at a concentration of $5.0*10^5$ cells/mL.
5. T_{reg} and responder cells will be co-cultured in the T_{reg}:responder ratios 1:1, 1:2, 1:4, 1:8 and 1:16. The following protocol applies to an input of 50.000 T_{regs} for each condition, which are all seeded into the "1:1" well.
6. Add CD3/CD28 coated Dynabeads™ in a 1:5 bead:cell ratio to the T_{reg} cell suspension and mix. (Note 22)
7. In a tissue culture-treated round bottom 96-wells plate, add 50 µL of culture medium to wells 4-7; add 100 µL of the T_{reg} cell suspension to well 3 (Figure 3).
8. Transfer 50µL of T_{reg} cell suspension to the well designated for the 1:2 ratio. Mix thoroughly, but avoid bubble formation. This will result in a two-fold dilution of both T_{regs} and beads.
9. Repeat step 8 in consecutive wells to serially dilute 1:4, 1:8 and 1:16 T_{reg}:responder ratios. Discard the leftover 50µL of T_{reg} suspension.
10. Finally, add 50µL of culture buffer + murine recombinant IL-2 (600U/mL) to all wells that now contain T_{regs}. Final volume per well is 100 µL.
11. Incubate the 96-well plate overnight at 37 °C, 5% CO_2.

Day 2 – T_{reg}:Responder co-culture

1. Harvest responder cells from the 6-well plate by thorough resuspension. Collect the cells in a 15mL tube and centrifuge the tube 5 minutes, 250g. Keep an aliquot of cells apart for step 4.3.2 (~25K cells)
2. Label responder cells with CellTrace™ Violet according to manufacturer's instructions.
3. After labeling, accurately determine the cell number. Recovery rate after sorting, overnight culture and labeling is typically ~40%.
4. Discard the supernatant and resuspend the responder cells at $1.25*10^5$ cells/mL in

culture medium.

5. Remove at least 200µL from the suspension ($2.5*10^4$ cells) and reserve for unstimulated controls.
6. Add CD3/CD28 coated Dynabeads™ in a 1:5 bead cell ratio to the responder cell suspension and mix.
7. Wash the 96-well plate containing the activated T_{regs} with culture medium.
8. Start T_{reg}:responder co-culture by adding 200µL of the responder cell suspension to all ratios and mix by pipette. Also add 200µL of responder cells to the stimulation control condition in well 2. Add cells from step 4.2.5 (unstimulated control condition) to well 1.
9. Incubate the cells at 37°C, 5% CO_2 for 96 hours (Note 23)

Day 6 - Analysis

The suppressive potential of T_{regs} will be determined by measuring the proliferation of responder cells on day 6 (Note 24). As both CD4 and CD8 T cells are used as responder cells, proliferation can be assessed for each cell type separately. Cells will again be fluorescently labeled according to Table 1, with the exception of LIVE/DEAD Aqua as this channel is now reserved for CTV. Instead of LIVE/DEAD Aqua, we recommend using 7-AAD viability staining solution to detect dead cells (Note 25).

1. After incubation, wash cells 1x in sorting buffer
2. Re-stain cells according to step 3.2-3.10, omit FMO controls. Use beads for single fluorochrome controls.
    1. A small sample of the stimulated control cells can be used as a single fluorochrome control for CTV.
    2. A small sample of unstained stimulated control cells are spiked into the CTV sample to obtain a negative population.
    3. A small sample of unstained stimulated control cells are stained with 7-AAD
3. Resuspend cells in 100µL sorting buffer + 7-AAD (1:100) and proceed with cell analysis on a flow cytometer.
4. Prior to compensation, acquire an unstimulated responder cell sample and adjust detector gain of the channel used for CTV. Set the signal of the undivided peak to an intensity of 10^5.
5. Run compensation controls and set up gates. Gate Live, single, $CD3^+$ CTV^+ cells to exclude T_{regs} from the analysis (Note 26).

Record sufficient CTV^+ cells to perform descriptive and analytical statistics with the predetermined level of confidence. Ideally, a minimum number of 2.000 CTV^+ events is recorded.

Data analysis

To assess the suppressive potential of T_{regs}, perform fluorescence compensation on recorded

samples and gate: Single, Live, $CD3^+$, CTV^+ cells. The first peak (intensity 10^5) indicates the undivided population. Each subsequent peak indicates consecutive cell division. The CTV^- fraction represents the T_{regs}. At this point, it is not possible to discriminate T_{regs} from responder cells based on CD25 expression, as responder cells will have upregulated CD25 in response to strong TCR stimulation. Confirm stimulation-dependent proliferation in controls. Draw gates to determine the percentage of divided/undivided fraction of the cells (Figure 5). For each sample, determine the percentage of the undivided population, and plot this according to T_{reg}:responder ratios (See graph type in Figure 4). The impact of T_{regs} from different conditions on responder cell proliferation can now be assessed (Note 27). An appropriate statistical test can be applied using the mean of the variable "% of undivided cells".

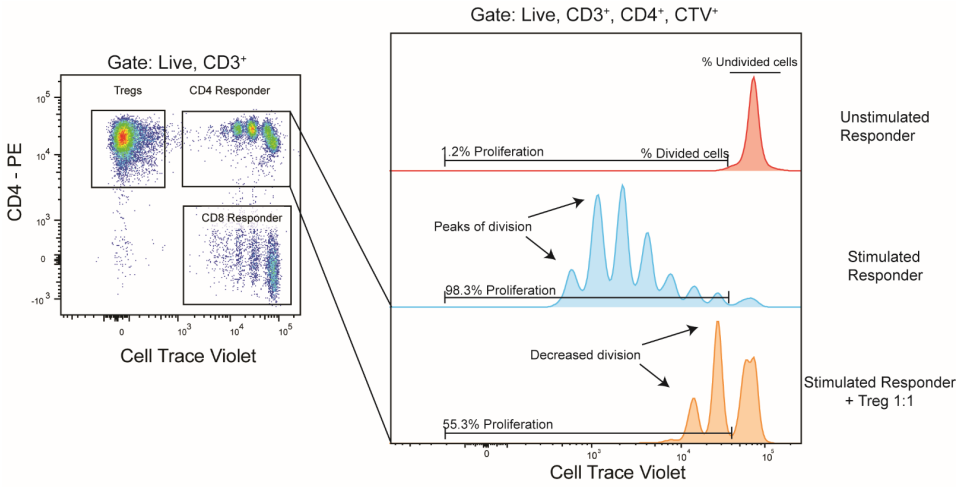

FIGURE 5. Recommended analysis of the suppression assay.
A suppression assay was performed as described with splenic T_{regs} and analyzed 96 hours after co-culture (day 6 of the assay). Responder cells do not proliferate in the absence of stimulation, but strongly divide when stimulated. T_{regs} potently suppress responder cell proliferation. T_{reg}:Responder ratio of 1:1 is shown.

NOTES

1. Commercially available RBC lysis buffers can contain fixation solutions. These should be avoided to maintain viability and cell function.
2. Mechanical disruption and enzymatic digestion is used to dissociate tumor tissue into a single cell suspension. Both treatments can result in cell damage and subsequent cell death. Additionally, enzymatic digestion can lead to a reduction of the available recognizable epitopes of cell surface markers. Preparation of single cell suspensions from tumor tissue should be optimized, *i.e.* duration and force of mechanical disruption,

enzyme choice, concentration and incubation time should be determined empirically per tumor type[13,14]. The described digestion method is optimized for mammary tumors[15].

3. The abundance of T_{regs} varies per tissue type. To sort sufficient cells to perform the assay, it is important to fluorescently label an adequate proportion of single cell suspensions. For tumor samples, we recommend to use 100% of the available tissue for sorting. For responder cells, sort at least 2-3 times the required number of cells to compensate for cells lost during washing and labeling steps.
4. Contamination of activated T-helper cells within the $CD25^{high}$ T_{reg} population may depend on mouse strain, genotype, tissue and homeostatic conditions of mice within the animal housing facility.
5. Murine myeloid- and B cells have high expression of Fc receptors, that specifically bind the Fc domain of fluorescently labeled antibodies. This may lead to false interpretation of positive signal, and could lead to sorting of a contaminated population. Therefore, incubate single cell suspensions in αCD16/32 Fc blocking reagent.
6. Guidelines for single fluorochrome controls
    1. The compensation matrix is determined with an algorithm that is embedded in the cell sorter software. To calculate the compensation values, the algorithm requires an accurate determination of the median fluorescent intensities (MFI) from the negative population and positive fluorochrome carrier population for each channel. An accurate estimate of the median is dependent on the variance, and the minimal number of negative and positive events required is between 2.000 and 5.000 for each.
    2. The median fluorescent intensity of the positive population must be at least as high as the highest median fluorescent intensity of an experimental sample. It is recommended to perform compensation on cells obtained from tissue that will be used for sorting T_{regs}. When sample is limited, the use of antibody-binding beads is recommended.
    3. The median fluorescent intensities of the negative and positive populations must be within the linear range of the detectors that are used.
    4. The antibody-fluorochrome conjugates used to prepare the single stains must be the same as those used in the experimental samples.
7. When the recommended antibody panel is modified, we advise to titrate antibody concentrations to determine the stain index and effect on data spread in secondary channels. The goal is to maintain optimal discrimination between negative and positive cell populations.
8. Washing entails the process of centrifuging the plate for 2 minutes at 380g, subsequently flicking off the supernatant and resuspending all samples in PBS followed by centrifugation. Lastly, flick of the supernatant and continue.
9. Nozzle diameter is determined as follows: average diameter of cells of interest * 6. For lymphocytes, the 70µm nozzle is acceptable. It also allows for acceptable duration of the sort. Using larger nozzles results in higher recovery and increased cell function, but

samples may require pre-enrichment to ensure acceptable sort times.

10. Sorting charged droplets that contain cells of interest can lead to accumulation of electrostatic charge inside a tube made of insulating polymers. Therefore, polypropylene tubes should be used to avoid build-up of electrostatic charge. Additionally, sorting into polypropylene tubes results in lower cell adherence to the tube walls, as compared to polystyrene tubes.
11. Addition of at least 1-2% FCS to the collection buffer has been shown to strongly reduce negative effects of cell sorting on cell viability, redox and metabolic perturbations. [12,16]
12. $CD8^+$ and $CD4^+$ T cell proliferation can be mitigated by multiple cell types, especially in the tumor microenvironment. To investigate the specific role of regulatory T cells on the suppression of cytotoxic T cells, the isolated T_{reg} fraction must be free from contamination of other cell types. In this specific assay, CD3 is used to uniquely identify cells of interest, and exclude other cell types that may bias the results. For example, DCs and B lymphocytes.
13. Sorting both CD4 and CD8 responder cells allows for investigating T cell-specific suppression. In this assay, cells are sorted in physiological ratios (CD4:CD8 = ~3:1 in spleen), but this can be adjusted to the user's preference, including sorting CD4 and CD8 T cells separately. Investigating suppression of CD4 and CD8 T cells provides a general method of assessing suppression of T_{regs}. Alternatively, it is possible to use virtually any other cell type of interest as responders.
14. Sorting T_{regs} and responder cells from spleen samples can be performed relatively fast, and takes approximately ~20-30 minutes per conditions in our experience. In contrast, sorting tumor samples can take up to multiple hours due to high cell concentration and a low T_{reg} fraction. In case of insufficient T_{reg} yield from tumors, an optional pre-enrichment of tumor samples may be performed. Sterile isolation of $CD45^+$ cells from the tumor sample via positive magnetic selection may increase yield and does not interfere with surface staining. Alternatively, percoll gradient separation may increase yield, although we have not tested this in this assay.
15. Doublets with $CD3^+$ cells and incorrect determination of charge delay timing (drop delay) may result in contamination or insufficient isolation of the cells of interest. A post-sort (purity) check can be performed to evaluate the collected samples.
16. The median fluorescent intensity may be slightly lower after sorting. Adjustment of the gates may be required to estimate to percentage correctly.
17. In our experience, storing cells on ice for up to one hour after sorting does not impact cell viability.
18. CellTrace™ Violet, is a fluorescent dye which covalently binds free amines on the surface and the inside of cells. When cells divide, the dye is equally divided over daughter cells, resulting in a 50% reduction of signal intensity per division. This allows for the visualization of proliferation in the responder cell pool. Alternatively, responder cells can be labeled with fluorescent proliferation dyes such as CFSE. This does require

modification of recommended antibody panels.

19. For cell sorting, we used a FACSAria II (BD Biosciences) with a 70µm nozzle and 70psi. Likely, the observed negative effect on proliferation when cells are co-cultured directly after cell sorting is due to shear stress from the cuvette-based cell sorter. If a resting period is undesired, this effect may be minimized by using a jet-in-air based cell sorter at lower sheath pressure, e.g. with a 100µm nozzle and 20psi. When omitting sorting-induced stress is not required (If using magnetic-based cell isolation for example), alternative assays exist as discussed here[17].
20. In our experience, T_{reg} pre-activation does not impact pre-existing differences in suppressive potential between T_{reg} populations.
21. Conventional CD4 T cells produce high levels of IL-2, whereas T_{regs} do not, although essential for survival of both. Accordingly, a proposed mechanism of T_{reg} suppression is CD25-mediated depletion of IL-2 from the local microenvironment[18].
22. Beads added for T_{reg} activation on day 0 will not induce responder cell proliferation during co-culture, for which additional beads are added.
23. Co-culture time may be adjusted as preferred, but should be minimally 72 hours.
24. Further in-depth analysis may include flow-cytometric analysis of responder cells and T_{regs} focused on the expression of cell surface receptors, intracellular cytokine production and cell-death. Culture medium can be collected after co-culture for cytokine analysis.
25. For analysis, an LSR II SORP (BD Biosciences) was used. The configurations are provided in table 2.
26. Divided $CD4^+$ responder cells may lose CTV to such an extent that these cells become indistinguishable from T_{regs} during analysis. In case of prolonged co-culture, it is advisable to additionally label the T_{reg} cells. This could be done by using alternative fluorescent proliferation labels, congenic markers, or including Foxp3 in the analysis panel.
27. Additional methods for analyzing T cell proliferation that may provide higher sensitivity are reviewed here[19]. Alternatively, specialized software to analyse proliferation data can be used (ModFit LT™, Flowjo LLC).

TABLE 2. LSR II Configurations for suppression assay analysis.

Antigen	Fluorochrome	Configuration FACSAria II	Configuration LSR II SORP
CD3	APC-Cy7	633nm laser (20mW); 750LP, 780/60	638nm laser (40mW); 750LP, 780/60
CD4	PE	488nm laser (20mW); 565LP, 585/42	561nm laser (40mW); 565LP, 585/42
CD8	FITC	488nm laser (20mW); 502LP, 530/30	488nm laser (50mW); 505LP, 525/50
CD25	APC	633nm laser (20mW); 660/20	638nm laser (40mW); 670/14
Free amines	L/D Aqua	405nm laser (25mW); 502LP, 530/30	
Free amines	CTV		405nm laser (40mW); 450/50
dsDNA	7-AAD		561nm laser (40mW); 600LP, 610/20

REFERENCES

1. Binnewies, M. *et al.* Understanding the tumor immune microenvironment (TIME) for effective therapy. *Nature Medicine* **24**, 541–550 (2018).
2. Kitamura, T., Qian, B. Z. & Pollard, J. W. Immune cell promotion of metastasis. *Nature Reviews Immunology* **15**, 73–86 (2015).
3. Togashi, Y., Shitara, K. & Nishikawa, H. Regulatory T cells in cancer immunosuppression — implications for anticancer therapy. *Nature Reviews Clinical Oncology* (2019) doi:10.1038/s41571-019-0175-7.
4. Li, Z., Li, D., Tsun, A. & Li, B. FOXP3+ regulatory T cells and their functional regulation. *Cellular and Molecular Immunology* **12**, 558–565 (2015).
5. Fontenot, J. D., Gavin, M. A. & Rudensky, A. Y. Foxp3 programs the development and function of CD4+CD25+ regulatory T cells. *Nature Immunology* **4**, 330 (2003).
6. Vignali, D. A. A., Collison, L. W. & Workman, C. J. How regulatory T cells work. *Nature Reviews Immunology* **8**, 523–532 (2008).
7. Josefowicz, S. Z. *et al.* Extrathymically generated regulatory T cells control mucosal TH2 inflammation. *Nature* **482**, 395–399 (2012).
8. Littman, D. R. & Rudensky, A. Y. Th17 and Regulatory T Cells in Mediating and Restraining Inflammation. *Cell* **140**, 845–858 (2010).
9. Sharma, A. & Rudra, D. Emerging Functions of Regulatory T Cells in Tissue Homeostasis. *Frontiers in Immunology* **9**, 883 (2018).
10. Chang, X., Zheng, P. & Liu, Y. Selective elimination of autoreactive T cells in vivo by the regulatory T cells. *Clinical immunology (Orlando, Fla.)* **130**, 61–73 (2009).
11. Thornton, A. M. & Shevach, E. M. CD4+CD25+ Immunoregulatory T Cells Suppress Polyclonal T Cell Activation In Vitro by Inhibiting Interleukin 2 Production. *The Journal of Experimental Medicine* **188**, 287 LP – 296 (1998).
12. Llufrio, E. M., Wang, L., Naser, F. J. & Patti, G. J. Sorting cells alters their redox state and cellular metabolome. *Redox Biology* **16**, 381–387 (2018).
13. Abuzakouk, M., Feighery, C. & O'Farrelly, C. Collagenase and Dispase enzymes disrupt lymphocyte surface molecules. *Journal of Immunological Methods* **194**, 211–216 (1996).
14. Autengruber, A., Gereke, M., Hansen, G., Hennig, C. & Bruder, D. Impact of enzymatic tissue disintegration on the level of surface molecule expression and immune cell function. *European journal of microbiology & immunology* **2**, 112–120 (2012).
15. Salvagno, C. & de Visser, K. E. Purification of Immune Cell Populations from Freshly Isolated Murine Tumors and Organs by Consecutive Magnetic Cell Sorting and Multi-parameter Flow Cytometry-Based Sorting BT - The Tumor Microenvironment: Methods and Protocols. in (eds. Ursini-Siegel, J. & Beauchemin, N.) 125–135 (Springer New York, 2016). doi:10.1007/978-1-4939-3801-8_10.
16. Brennan, J. K., Mansky, J., Roberts, G. & Lichtman, M. A. Improved methods for reducing calcium and magnesium concentrations in tissue culture medium: application to studies of lymphoblast proliferation in vitro. *In vitro* **11**, 354–360 (1975).
17. Collison, L. W. & Vignali, D. A. A. In vitro Treg suppression assays. *Methods in molecular biology (Clifton, N.J.)* **707**, 21–37 (2011).
18. Chen, X. & Oppenheim, J. J. Resolving the identity myth: key markers of functional CD4+FoxP3+ regulatory T cells. *International immunopharmacology* **11**, 1489–1496 (2011).
19. McMurchy, A. N. & Levings, M. K. Suppression assays with human T regulatory cells: A technical guide. *European Journal of Immunology* **42**, 27–34 (2012).

8

Discussion

The work described in this thesis sprouted from my fascination for the tumor-supportive role that the immune system can play in cancer progression, and studies this concept mainly from the angle of regulatory FOXP3$^+$CD4$^+$ T cells in breast cancer. First, the current knowledge and open questions regarding T_{reg} biology in breast cancer are reviewed in **chapter 2. Chapter 3** focusses on T_{regs} in the primary tumor context, and demonstrates the importance of macrophages for the intratumoral conversion of conventional CD4$^+$ T cells into T_{regs}. In **chapters 4** and **5**, the focus shifts to tissue-specific mechanisms of breast cancer metastasis. Specifically, research in **chapter 4** reveals a mechanism by which T_{regs} selectively promote lymph node metastasis, and **chapter 5** discusses how neutrophils enhance lung metastasis. **Chapter 6** lifts a corner of the veil regarding the potential detrimental role of T_{regs} in immunotherapy response in primary and metastatic breast cancer. Together, the work in this thesis aims to contribute to improved understanding of immunoregulatory mechanisms at play during diverse stages of breast cancer progression and immunotherapy response. Below, I detail how insights gained in this thesis:

1) fit within the current research literature.
2) may spark new research questions that when answered help improve our fundamental understanding of immune regulation in cancer metastasis.
3) may have therapeutic relevance in the form of T_{reg}-based clinical applications.

BYSTANDER OR ARCHITECT? T_{REGS} & BREAST CANCER PATHOGENESIS

T_{regs} abundantly populate primary breast tumors and metastases, as demonstrated in both patient tumor samples and preclinical mouse models. Over the past decade, this has raised significant interest to understand their functional role for disease progression. Based on the outcome of these studies (**chapter 2**), T_{regs} are often portrayed as undisputed benefactors of primary tumor growth. Based on findings in this thesis, I would like to suggest a nuance to this interpretation. So far, the link between T_{regs} and tumor progression stems from observations that show that targeting T_{regs} in mice bearing inoculated (GEMM-derived) cancer cell lines slows tumor growth by unleashing anti-tumor immunity[1–4]. However, these cell line-inoculated tumor models have key weaknesses that complicate the translation to human breast cancer. One issue is that syngeneic cell line-based tumors do typically not resemble the immunogenicity of human tumors from the same origin[5], thereby potentially setting unrealistic expectations for the efficacy of immune therapies in cold, non-inflamed tumor types. To illustrate this, human breast tumors are generally poorly immunogenic[6], have typically only modest infiltration of T cells[7] and score rather low in terms of mutational load[8]. On average, breast cancers harbour one somatic mutation per Mb: ten times less than what is considered sufficient to mount anti-tumoral T cell responses[9]. In contrast, two of the go-to murine tumor cell lines for breast cancer research which are classified as

triple-negative breast cancer (TNBC), E0771 and 4T1, have a similar mutational burden of 1-5 mutations per Mb[10,11], but are characterized by high intratumoral infiltration of T cells, expression of co-stimulatory receptors and neo-antigens[5,10–12]. In line, E0771 and 4T1 tumors are responsive to anti-PD-1 immune checkpoint blockade (ICB)[1,13], while the efficacy of PD-1/PD-L1 blockade in patients with TNBC is considered to be low[14]. Furthermore, T_{reg} depletion in 4T1 and E0771 tumors is sufficient to unleash anti-tumor immunity, suggesting T_{regs} are a key barrier to effective immunity in immunogenic breast tumor types[1,2,10,15]. In humans, TNBC is considered to have the relatively highest immunogenicity of all breast cancer subtypes, as TNBC harbours the highest frequency of neo-antigens and cancer germline antigens[16]. Counterintuitively, high T_{reg} infiltration is correlated to a favourable prognosis in TNBC (**chapter 2**), contrasting with the pro-tumoral role of T_{regs} in 4T1 and E0771 tumors.

Apart from disparities with human cancers, studying T_{reg} function in highly immunogenic models poses another complication. It was recently reported that the reduction in lung metastasis that is seen upon Treg depletion in 4T1-bearing mice is in fact a consequence of the primary tumor responding to Treg depletion, and not a direct effect of T_{regs} on metastatic colonies in the lung niche[2]. Thus, by using tumor models that are responsive to T_{reg} depletion such as 4T1, the effect of T_{reg} depletion on metastasis formation is obscured by its effect on the primary tumor. Together, this illustrates that insights into T_{reg} function deduced from popular cancer cell line-based mouse models may inaccurately reflect, and potentially overestimate, the importance of T_{regs} in human breast cancer.

In this thesis, we aimed to examine T_{regs} in a context that is more true-to-nature using genetically engineered mouse models (GEMMs) for mammary tumorigenesis. The use of GEMMs enables the study of tissue-specific, *de novo* tumor formation and progression of malignancies driven by clinically relevant mutations in an immune-proficient environment. Dependent on underlying genetic modifications, GEMMs can reflect the poorly immunogenic and chronic inflammatory state of human breast cancer, albeit with a lower mutational burden as observed in human tumors. The trade-off for superior cancer modelling is that the use of GEMMs is generally expensive, time-consuming and laborious due to extensive breeding costs, long-term tumor latencies and associated monitoring of animals. To circumvent the practical disadvantages of GEMMs, syngeneic cell lines derived from PyMT-MMTV and Pdx1-Cre;LSL-$Kras^{G12D}$;$Trp53^{F/F}$ GEMMs have been used to study T_{reg} function[3,17,18]. Despite producing rapid and reproducible results and the potential to easily introduce further genetic modifications, GEMM-derived cancer cell lines can show key differences in their immune landscape, with increased frequencies of T_{regs}, $CD8^+$ T cells and NK cells, as compared to *de novo* tumors[19]. As this may critically impact the outcome of immunological studies and thereby still reduce their clinical value as compared to GEMM-based models, this approach has been limited in this thesis.

In our studies in **chapter 3, 4 and 6**, we interrogated the impact of T_{regs} on breast cancer pathogenesis, utilising the lowly immunogenic *K14Cre;Cdh1$^{F/F}$;Trp53$^{F/F}$* (KEP) model for mammary tumorigenesis, reflective of human invasive lobular carcinoma[20]. To do so, we employed three different strategies to target T_{regs} in mice bearing spontaneous and orthotopically transplanted primary tumors.

1) Antibody-based depletion using an anti-CD25 antibody with enhanced binding to activating FcγRs for optimal intratumoral depletion[21].
2) Inducible ablation of FOXP3$^+$ cells by diphtheria toxin in *Foxp3$^{GFP\text{-}DTR}$* mice.
3) Indirect blockade of intratumoral T_{reg} accumulation via targeting of macrophages using anti-CSF1R.

Despite efficient intratumoral depletion of T_{regs}, none of the strategies affected primary tumor growth, thus contrasting with previous literature (**chapter 2**). Intriguingly, we did find intratumoral T_{regs} to be immunosuppressive *in vitro* and highly functional *in vivo*, as T_{reg} depletion increased the expression of inflammatory markers on myeloid cells, and strongly activated both CD4$^+$ and CD8$^+$ T cells (**chapter 4 and 6**). These functional results are consistent with previous observations in breast cancer models[1,3,15], and emphasize that T_{regs} are key orchestrators of the immunosuppressive tumor niche. Furthermore, T_{regs} in KEP tumors were validated to be enriched for a Tumor T_{reg} gene signature[22] that is conserved across species and tumor types, indicating T_{regs} in the KEP model do not display an atypical phenotype. Combined, these data suggest that highly immunosuppressive T_{regs} are not by definition indispensable for orchestrating immune escape of primary tumors in poorly immunogenic GEMMs. Instead, these findings are in line with the concept that different immunosuppressive cells including T_{regs}, tumor-associated macrophages, neutrophils, other suppressor cells of myeloid origin, cancer-associated fibroblasts, cancer cells and co-opted tissue-resident cells together construct an intricate immunoregulatory multi-layered network. Critically, this network is not breached by targeting single actors, as the multiple layers appear to be non-redundant, and can adapt to challenges through compensatory influx of immunosuppressive cells[23], or phenotypic adaptations (**chapter 3**). By dissecting separate layers of immunosuppression, like work in this thesis has aimed to do from the angle of T_{regs}, fundamental insights are gained that lay the foundation for the design of therapeutics which may, in the form of personalized combinations, dismantle cancer-associated immune suppression, and thereby set an important step towards anti-tumor immunity.

ONE OF THE GUYS: THE CLINICAL SIGNIFICANCE OF T_{REGS} AMONG THE SUPPRESSIVE TME

Keeping in mind T_{regs} are part of a greater immunosuppressive network, do they, as individual cell type, have a clearly defined clinical significance in the context of breast cancer? As described in **chapter 2**, high intratumoral T_{reg} infiltration correlates either with a poor or a favourable prognosis, dependent on the breast cancer subtype. Correlation with a favourable prognosis is observed in hormone (estrogen, progesterone) receptor negative, and triple-negative breast cancers (TNBC). High T_{reg} density strongly correlates with concurrent stromal and intratumoral $CD8^+$ T-, $CD4^+$ T- and B cell TILs[24,25], and the expression of inflammatory and immune-response related genes in TNBC[26], suggesting the favourable association of T_{regs} in TNBC is reflective of a broader lymphocyte-inflamed environment. This might be linked to the observation that TNBC tumors are relatively immunogenic[16], potentially driving T cell infiltration. As this observation contrasts with the immunosuppressive nature of T_{regs}, it would be of interest to test the functionality of T_{regs} isolated from these TNBC tumors, as chronic inflammatory conditions have been shown to induce IFN-γ-mediated T_{reg} dysfunction, and loss of suppressive phenotype[27]. Thus, sustained pro-inflammatory challenges like T cell responses to tumor-associated antigens, or therapeutic activation of innate cGAS-STING and inflammasome pathways may have the potential to relieve T_{reg} suppression in the TME. In hormone receptor positive tumors, the clinical significance of T_{regs} is more aligned with preclinical data: High T_{reg} density correlates with poor disease outcome (**chapter 2**). However, there is a catch in interpretation of these studies. The likelihood of finding high T_{reg} numbers is strongly associated to high tumor grade and incidence of lymph node metastasis, which are both negative prognostic indicators in itself, raising the question: Is the mere presence of T_{regs} sufficient to predict disease outcome? Several studies have shown that T_{regs} are a prognostic factor for disease outcome in univariate analyses, but not in multivariate analyses that include above-mentioned clinical variables, thereby showing that T_{regs} are likely not independently predictive of disease outcome (**chapter 2**). Even the discovery that the chemokine receptor CCR8 is uniquely expressed on tumor-associated T_{regs}, and detrimental for disease outcome in breast cancer, could not be substantiated in multivariate analysis[28]. A few studies have assessed the clinical relevance of T_{regs} in the context of the broader immunosuppressive TME. Interestingly, in patients with invasive ductal carcinoma, low T_{reg} infiltration was found to independently correlate with an increased overall survival in multivariate analysis with $CD8^+$ T cells, B cells and macrophages[29]. By assessing the predictive value of individual immune cell types using the deconvolution algorithm CIBERSORT on mixed breast cancer gene expression datasets, both M2-like macrophages and T_{regs} were associated with poor disease outcome[30]. A similar study using CIBERSORT showed that immune infiltrates are heterogeneous, and strongly differ per breast cancer subtype, but still identified T_{regs}, macrophages and mast cells to be amongst most detrimental immune cells[31]. The negative disease outcome associated to both macrophage and T_{reg} abundance is

reminiscent of work shown in **chapter 3**, which reveals that macrophages play an important role in the maintenance of T_{regs} in the breast TME. Notably, both these CIBERSORT-based studies found T_{regs} to be significantly associated to poor disease outcome in multivariate analysis, suggesting that measuring T_{reg} abundance relative to the immune infiltrate as a whole is potentially a more informative metric as opposed to single immunohistological assessment of absolute FOXP3 counts, which ignores other immunosuppressive cells within the TME. Currently, CIBERSORT on bulk RNAseq data classifies a biased number of cell types, and disregards (tissue-specific) cell phenotypes. Future use of deconvolution algorithms on single cell datasets of breast tumors may provide deeper insights into specific T_{reg} phenotypes that are associated with disease progression.

In addition to analyses that interrogate each cell type individually, another study performed a comprehensive analysis from the TME as a whole using CIBERSORT on breast cancer gene expression datasets, and analysed whether particular immune cell clusters are enriched in patients with poor disease outcome[32]. A pro-tumorigenic immune cluster was discovered, that correlated to poor prognosis across breast cancer subtypes. This cluster consisted of M2-like macrophages, resting mast cells, resting memory $CD4^+$ T cells, and γδ T cells. T_{regs} were not assigned to this cluster, potentially due to their contrasting roles in different breast cancer subtypes.

Taken together, the clinical significance of T_{regs} is influenced by a multitude of factors. While these factors include breast cancer subtype, and the broader immune infiltrate, the importance of tissue-specific T_{reg} phenotypes, or their spatial organisation within stroma or tertiary lymphoid structures, and cellular crosstalk is currently unclear. Looking forward, the emerging appreciation for breast cancer diversity in terms of ecotypes that take cancer- and immune cell heterogeneity into account, may further define the clinical significance of T_{regs} beyond traditional subtypes in the near future[33].

STOCKHOLM SYNDROME: T_{REGS} AND LYMPH NODE METASTASIS

Whereas the clinical significance of $FOXP3^+$ TILs on disease outcome is often conflicting and subtype dependent, one histopathological feature is consistently correlated to high intratumoral T_{reg} density: the presence of lymph node metastases[34]. From a clinical viewpoint, assessing lymph node involvement is paramount for evaluating prognosis and therapeutic follow-up, as regional lymph nodes are often the first site of metastasis[35]. Since breast cancer patients with lymph node metastasis have up to 40% lower five-year survival rate compared to node-negative patients[35–40], insights into this hallmark event that bridges local and metastatic disease are imperative to halt early-stage tumor spread. The correlation

between T_{regs} and lymph node metastasis has been validated in multiple independent meta-analyses that have probed the prognostic value of T_{reg} infiltration in breast cancer[34,41,42], which has triggered more in-depth assessments of T_{regs} in sentinel lymph nodes of breast cancer patients. On a quantitative level, T_{regs} were found to be increased in tumor-infiltrated lymph nodes compared to non-infiltrated lymph nodes of breast cancer patients[43], which associated with decreased maturation of dendritic cells[44]. Strikingly, others showed that T_{reg} accumulation and suppression of dendritic cells precedes detectable tumor-infiltration in lymph nodes[45,46], suggesting that T_{regs} might play a role in preparing the lymph node niche for tumor arrival. In line with this hypothesis, tumor-draining lymph nodes become heavily immune-suppressed during tumor progression, and switch from an inflammatory- to an inhibitory state, characterized by T cell exhaustion, reduced expression of IFN-γ, IL-17 and loss of T cell activation[44,45,47–49]. Moreover, qualitative assessment of breast cancer sentinel lymph nodes by flow cytometry revealed that functionally suppressive effector T_{regs}^{50} increase in invaded compared to non-invaded lymph nodes, and have increased expression of PD-1 and ICOS[51]. In a similar study, T_{regs} in metastatic lymph nodes were found to have increased expression of HLA-DR, PD-1, CD38, TIGIT and $CD45^{RO}$ and co-localised with $CD8^{+}$ T cells[49].

Despite the wealth of clinical data that point towards a role for T_{regs} in lymph node metastasis, mechanistic data are lacking. One study revealed that T_{regs} within tumor-draining lymph nodes potentiate distant cancer spread[52], but their role in loco-regional metastasis to lymph nodes has remained elusive. We addressed this open question in **chapter 4** and uncover a causal role for T_{regs} in the formation of lymph node metastasis. While we show that T_{regs} impair the function of anti-metastatic NK cells, we did not fully elucidate the mechanistic basis for this inhibitory interaction that occurs specifically in the lymph node niche. One possibility is that T_{regs} impair NK cell cytotoxicity by limiting the availability of IL-2, which is critical for NK cell function[53,54], plays a role in the expansion of T_{regs}^{55}, and is particularly abundant in lymph nodes[56]. Secondly, there are indications that T_{regs} restrain NK cell activation through suppression of lymph node dendritic cells[57,58], which would align with clinical data showing dendritic cells are suppressed in breast cancer sentinel lymph nodes[45]. Interestingly, LAG-3 expression by T_{regs} can limit dendritic cell activation via MHC-II engagement[59], and we observed *Lag3* to be uniquely upregulated in KEP T_{regs} in lymph nodes (**chapter 4**). Finally, emerging data show that tumor-draining lymph nodes turn acidic during cancer progression, which can impair T- and NK cell function[60,61]. In contrast, T_{regs} maintain their suppressive function in acidic conditions[62], and form a barrier for PD-1 blockade through upregulation of PD-1[63].

Besides breast cancer, there are indications that T_{regs} are associated with lymph node metastasis in other cancer types[48,64]. T_{regs} were found to be elevated in tumor-invaded, compared to non-invaded lymph nodes of patients with lung adenocarcinoma[65], melanoma[66],

cervical[67]- and gastric cancer[68], either in absolute numbers or as a ratio compared to conventional T cells. In patients with colon cancer, high T_{reg} density in lymph nodes was predictive of disease progession[69]. While still rather limited, these studies support the notion that T_{regs} are perhaps central regulators of lymph node metastasis in a multitude of cancer types. Again, mechanistic data are still lacking to substantiate this hypothesis, but there is a clear basis for future research to address this research question, thereby guiding the development of new therapeutic strategies to limit early metastatic spread. As an example: it was recently discovered in a GEMM for spontaneous lung adenocarcinoma that anergic $CD4^+$ T cells can differentiate into suppressive T_{regs} in tumor-draining lymph nodes[70], and it would be of interest to test the effect of T_{reg} depletion on lymph node metastasis in this model.

SUPPRESSED SOIL: THE ROLE OF IMMUNOSUPPRESSION IN ORGANOTROPISM OF METASTASIS

Chapter 4 of this thesis describes a mechanism by which tumor-educated T_{regs} promote metastasis to lymph nodes, but not lungs, surfacing a complex question about metastasis. Why are some tissues more prone to colonisation than others? Cancer cell-intrinsic mechanisms like subtype, gene-, and protein expression determine how compatible metastasizing cancer cells are with their new environment[71]. However, the destined local tissue and vasculature are not passive bystanders as cues from specialised resident cells can support metastatic outgrowth[72–74]. It is clear that highly specialised tissue-resident cells like brain astrocytes[75], lung fibroblasts[76] and hepatic stellate cells[77] engage in tissue-specific mechanisms to modulate metastasis formation in their own tissue, but how the immune system is involved in tissue-tropism of metastasis is only beginning to be understood.

Based on the findings in **chapter 4**, I propose that immunosuppressive pathways that support metastasis, have an important tissue-specific component. Across different organs, unique local cues dictate tissue-specific gene programs in resident and patrolling immune cell subsets. These tissue-specific adaptations may differentially impact immune crosstalk in response to tumor-derived signals, likely resulting in niche-specific immunoregulatory mechanisms[64,78,79] (**chapter 4**). In line with this concept, recent evidence shows that the systemic immune landscape is distinctly remodelled in a tissue-dependent fashion during primary tumor development in mice, causing systemic immune dysfunction[80]. Furthermore, metastases of breast and ovarian cancer were found to have distinct infiltrates of immunosuppressive cells in different tissues[81,82], and it is becoming increasingly clear that tissue-specific factors play an important role in shaping local tumor microenvironments and accompanying immunosuppressive features[74,83].

To add to this complexity, each tumor is unique, and primary tumors from different cell lines differentially impact the systemic immune landscape[80], suggesting cancer cell-intrinsic mechanisms can also affect distant immune suppression[84]. Tumor-secreted factors, acting in the TME or beyond can induce systemic immunosuppressive conditions, that allow distant metastasis formation (**chapter 4 & 5**). In particular the systemic mobilisation of myeloid cells in response to tumor-derived factors can support the preparation of a pre-metastatic niche, or a distant immunosuppressive environment[85]. For instance, research in our lab has shown that loss of the tumor suppressor gene p53 in mammary tumors kick-starts a cascade of CCL2 - TAM - Il-1β - γδ T cell – IL17 that drives the systemic accumulation of immunosuppressive neutrophils, which promote metastasis to lung and lymph nodes[86–88]. In addition, breast cancer-derived CCL2 has also been shown to enhance bone metastasis via the local recruitment and polarisation of monocyte-derived macrophages[89]. Although less well studied, tumor-derived factors can also engage systemic immune suppression mediated by the adaptive immune system, most prominently through activation of T_{regs} (**chapter 4**). While we did not identify which factors underlie systemic T_{reg} expansion and activation, others have identified galectin-1[90], IL-2[55,91] and IL-33[92,93] as potential candidates. Importantly, activated T_{regs} in the blood of breast cancer patients are predictive for poor disease outcome[94], highlighting the relevance of understanding how T_{regs} mediate systemic immune suppression during metastasis formation.

Another aspect of how cancer cell-intrinsic features may be intertwined with immunosuppression and organotropism relates to the finding that metastases in different tissues have a distinct genetic make-up[95]. Interestingly, lymph node metastases of colorectal cancer patients were found to be more polyclonal compared to distant metastases, potentially reflective of weaker evolutionary selection in nodular metastases[96]. As it has been shown that evolution of metastatic clones is in part shaped by immune pressure[97], two immune-related explanations for this phenomenon can be formulated. Either there is limited immune pressure in lymph nodes which would allow polyclonal, immunogenic metastatic clones to survive, or, as supported by preclinical and clinical data (**chapter 4**), there are strong immunosuppressive conditions that may limit immune editing in tumor-draining lymph nodes. This second hypothesis suggests that the adaptation of metastatic cells to a distant organ is, besides other determinants[34], dependent on the level of immunosuppression in the destined tissue. Weakly immunosuppressive conditions require cancer-cell intrinsic adaptations to evade immune recognition. In contrast, a high level of (tumor-induced) immunosuppression protects immunogenic metastatic clones from eradication by the immune system, and metastases are therefore not pressured to evolve poor immunogenicity. Thus, the immunogenicity of metastasizing cancer cells may be in part shaped by the potential of tumors to induce systemic immunoregulation, for example through co-option of neutrophils, TAMs and T_{regs}. From a therapeutic viewpoint, this suggests that tumors which succeed in creating systemic immunosuppressive conditions,

may have immunogenic metastatic clones, and may therefore be vulnerable to T cell-based immunotherapeutics, when combined with strategies that overcome immunosuppression. As we found in **chapter 4** that lymph node metastases, but not lung metastases were prone to NK cell-mediated killing, it would be of interest to analyse whether lymph node metastases express NK cell activating ligands, and whether the expression of these ligands is lost in lung metastatic clones.

Next to tissue-specific cues and cancer cell-intrinsic mechanisms, the homeostatic immune composition varies greatly across different organs[98], which has several consequences for local cancer-associated immunosuppression and organotropism of metastasis. Firstly, unique tissue-resident cell types may be prone to co-option by tumors, as demonstrated for lung-resident innate lymphoid type 2 cells and neutrophils (**chapter 5**), pulmonary alveolar macrophages, and central nervous system resident myeloid cells[99–101], which can locally suppress anti-metastatic immune responses in lungs and brain respectively. Secondly, tumor-associated immune suppression is typically not dependent on a single cell or pathway, but instead consists of multiple layers of interconnected and functionally redundant immunosuppressive mechanisms, that are also shaped by the local immune landscape[78,79], and can affect local effector cell function. To illustrate this, we demonstrate in **chapter 4** that NK cells in the lungs, but not the lymph nodes undergo a shift towards a more immature phenotype in tumor-bearing mice, that is independent of T_{regs}, reflective of a different immunosuppressive network.

Combined, organotropism of metastasis can be influenced by immunosuppression through tissue-specific cues, resident cells and immune composition, and cancer cell-intrinsic mechanisms in the form of genetic make-up and tumor-derived factors. Moreover, tissue-specific micro- and mycobiomes may further modulate local immunosuppression in the context of metastasis[102,103]. From the perspective of cytotoxic, anti-tumoral immune cells, getting effectively around distinct regulatory hurdles in different organs seems a daunting challenge. As such, in my view, overcoming tumor-associated immunosuppression will require a more tissue-focussed approach. Broader appreciation for tissue-specific mechanisms of immunoregulation may inspire novel approaches that selectively interfere with metastatic tropism to certain organs. Ultimately, combining these approaches may prove helpful to peel away the different layers of immunosuppression, allowing for anti-tumor immunity.

Going forward, as we are increasingly confronted with the complexity of metastatic disease, it will be important to develop sophisticated models that adequately recapitulate this complexity. This is not only important to increase our fundamental understanding of immunoregulatory mechanisms in cancer, but more so to improve the translation of promising preclinical findings into clinical success. This is an urgent need, as currently

only 0.1% of pre-clinical drug targets are ultimately approved for human use[104]. At the time of writing, a limited number of immunological studies have been performed in models that realistically recapitulate the metastatic cascade and spectrum as it occurs in patients. Experimental metastasis models based on intra-cardiac, intra-venous or intra-portal injections can reflect dissemination to clinically relevant organs (bone, brain, lung and liver), but by no means model the complexity related to heterogeneity, evolution and selection of highly metastatic clones[105]. On the other hand, popular model systems based on orthotopic inoculation of cancer cell lines such as 4T1, EO771 and GEMM-derived MMTV-PyMT more adequately model local tumor cell invasion and intravasation, but fail to recapitulate tissue-tropism of metastasis seen in the clinical setting, intratumoral heterogeneity, and the chronic and systemic inflammation that underlies *de novo* tumor development, progression and metastasis[106]. Because of this, most of current knowledge regarding the role of pro-metastatic, immunosuppressive immune cells and the formation of a pre-metastatic niche in breast cancer comes from single-organ metastasis systems like breast-to-lung[85]. While breast cancer in patients indeed often spreads to lungs, other important niches like lymph nodes, bone, brain and liver are heavily understudied, and it is unclear how interchangeable lung-specific mechanisms are to other tissues, or between different types of cancer. Therefore, more comprehensive models of systemic immunosuppression in the context of cancer are necessary to achieve clinical translation.

The development of *in vivo* somatic gene editing approaches through local delivery of viral vectors provides a cutting-edge approach to model tumorigenesis[107,108]. Excitingly, by replacing orthotopic transplantations of tumor fragments with somatic induction of *de novo* tumors, current spontaneous metastasis models can be updated to additionally reflect progression from initial neoplastic transformation to overt disseminated disease. Such a complete model of metastasis formation may also better reflect the full metastatic spectrum as it is observed in patients, which is still a caveat of GEMMs[105]. Interestingly, the *Cdh1$^{f/f}$Trp53$^{f/f}$;Foxp3$^{GFP\text{-}DTR}$* model described in **chapter 4** and **6** could potentially be used for this approach, and could be combined with genetic ablation of FOXP3^{+} cells to study their function in the progression of invasive breast cancer.

SUPRESSING SUPPRESSION: MANIPULATING T_{REGS} TO THE BENEFIT OF CANCER PATIENTS

The fundamental insights gained into T_{reg} biology in the context of cancer are moving towards clinical practice[109,110]. Importantly, therapeutic targeting of T_{regs} will always be a fine balance between mitigating immunoregulation to unleash anti-tumor immunity, and preserving peripheral tolerance to limit autoimmune-related toxicity. In order to limit toxicity related to the manipulation of T_{regs}, one approach that has been studied in cynomolgus monkeys

is to only partially deplete T_{regs} using anti-CD25, which is sufficient to enhance effector cell activation[111] but does not lead to catastrophic auto-immunity, as is observed upon sustained depletion of T_{regs} in $FOXP3^{DTR\text{-}GFP}$ mice[4,112]. Besides depleting T_{regs}, other approaches are possible that target specific aspects of T_{reg} biology, and can be fine-tuned to specific niches, such as targeting of chemokine receptors, cytokines or immunomodulatory proteins that are important for tumor-educated T_{regs}. The work described in this thesis may provide novel insights into therapeutic targeting of T_{regs} in the following three different contexts:

1) Primary breast cancer (**chapter 3**)
2) Lymph node metastasis (**chapter 4**)
3) Immune checkpoint blockade (**chapter 6**)

Primary breast cancer

In **chapter 3** we show that tumor-associated macrophages control two important independent facets regarding the conversion of $CD4^+$ T_{convs} into $FOXP3^+$ T_{regs}: release of TGF-β, and upregulation of PD-1 expression on $CD4^+$ T_{convs}. Thus, targeting macrophages using anti-CSF1R has the attractive collateral effect of reducing the intratumoral accumulation of peripherally induced T_{regs}, which have been implicated in suppressing antigen-specific anti-tumor immunity[70,113]. The benefit of such an indirect anti-T_{reg} approaches is that the reduction in T_{regs} is limited to the TME whereas systemic, indiscriminate targeting of T_{regs} may trigger severe widespread auto-immunity, due to their elemental role in immune tolerance[112]. Apart from the role of PD-1 in T_{reg} conversion, PD-1 expression is a hallmark of functionally exhausted intratumoral $CD4^+$ T_{helper} cells[114]. As our data show that macrophages promote PD-1 signalling on intratumoral $CD4^+$ T cells, it can be envisioned that macrophages thereby contribute to dysfunction of intratumoral $CD4^+$ T cells, which might be reversed upon macrophage depletion. However, evidence for this hypothesis and how exactly macrophages enhance PD-1 expression on $CD4^+$ T cells would require further study. Another benefit is that anti-CSF1R seems to hit two birds with one stone by reducing both immunosuppressive TAMs and T_{regs}. However, how many birds remain? Previous research using the KEP model has shown that targeting macrophages is not sufficient to induce anti-tumoral effects, due to the compensatory influx of immunosuppressive neutrophils in tumors upon anti-CSF1R, which suppress $CD8^+$ T cell function[23]. As such, targeting T_{regs}, whether these are of thymic- or peripheral origin **(chapter 3)**, is likely only part of the equation to achieve anti-tumor immunity in tumors with dominant immunosuppression. Excitingly, this realisation has already inspired interesting treatment combinations, and it has been shown that targeting multiple facets of this network simultaneously, combined with a T cell-activating treatment, can induce anti-tumor immunity against primary tumors in the KEP model ([23], Blomberg *et al;* personal communication).

Lymph node metastasis

In **chapter 4**, we demonstrate that targeting of T_{regs} impairs metastasis to tumor-draining lymph nodes, raising the question whether this may be therapeutically exploited in breast cancer patients. Our preclinical data show that immunosuppressive T_{regs} arise early during mammary tumorigenesis, indicating that T_{reg}-targeting strategies might be most beneficial to reduce cancer spread to lymph nodes in the neoadjuvant context. In support of this, the disappearance of lymph node metastasis in breast cancer patients treated with diverse neoadjuvant chemotherapy regimens was strongly associated with decreased intratumoral *CTLA4* gene expression and increased activity of peripheral NK cells[115]. Interestingly, there are early indications that neoadjuvant administration of ICB can drive major pathological responses in multiple patients groups[116–119], suggesting the pre-operative window might also be an attractive context to target T_{regs}. Below, I detail some exciting targets that may have relevance in the context of lymph node metastasis.

Most famously, the development of antibodies designed to block the co-inhibitory receptor CTLA-4 in patients has pioneered ICB for the treatment of cancer. CTLA-4 is highly expressed by tumor-educated T_{regs} in lymph nodes (**chapter 4**) and plays a key role in suppressing DC maturation and T cell priming by binding CD80/86 on DC's[109]. While there is ongoing controversy whether anti-CTLA4 antibodies deplete intratumoral T_{regs}[120–122], part of its efficacy is contributed to its inhibitory effect on T_{reg} function[123], which might be valuable to restrain T_{reg} activity in tumor-draining lymph nodes. As data in **chapter 6** show that anti-CTLA4 (combined with anti-PD1) increases the proliferation of T_{regs}, it will still be important to assess the net effect of blocking T_{reg} CTLA4 activity versus increased T_{reg} proliferation on lymph node metastasis formation.

A particularly promising target is the chemokine receptor CCR8. In breast cancer patients, CCR8 is selectively expressed on a clinically relevant population of highly suppressive T_{regs} found both in tumor[28] and blood[94]. In mice, single cell TCR clonotype analysis revealed that CCR8 is specifically expressed on clonally expanded T_{regs} in both tumor and tumor-draining lymph nodes, which are likely reactive to tumor-associated antigen[124]. Several groups have demonstrated that ablation of CCR8 selectively depletes intratumoral T_{regs} without induction of systemic toxicity, and improves tumor control of inoculated cancer cell lines[124–126], demonstrating the anti-tumor potential of this approach. Others showed that T_{regs} isolated from metastatic lymph nodes and tumors share expression of a gene signature consisting of *CCR8*, *CD80* and *HAVCR3*, which correlates to disease outcome in breast cancer patients[51]. Interestingly, both *Cd80* and *Havcr3* are part of the tissue-independent KEP T_{reg} gene signature described in **chapter 4**, indicating that the KEP model might be relevant to study the therapeutic potential of targeting these immunomodulatory receptors during metastasis formation. Finally, T_{reg}-derived TGF-β1 in tumor-draining lymph nodes potentiates distant metastatic spread[52], and blocking TGF-β might therefore be another

attractive approach. However, due to the pleiotropic and context-dependent role of TGF-β in cancer metastasis and immune regulation, clinical targeting of TGF-β has not yet matured[127]. Collectively, several exciting targets have been identified that, likely in combination with an approach that sustains T cell activation within tumors, may subvert immunosuppression by tumor-educated T_{regs} in breast cancer patients in the future.

Immune checkpoint blockade

Research in **chapter 6** describes how ICB inadvertently activates T_{regs}, thereby limiting its therapeutic benefit. Among the rapid development of novel therapeutics aimed at engaging T cells, this surfaces an important notion: T_{regs} are T cells. In fact, T_{regs} have been shown to express most, if not all, co-signalling receptors described to modulate the function of effector $CD8^+$ and conventional $CD4^+$ T cells in tumors. This includes proteins that widely attract clinical interest such as: PD-1, CTLA-4, TIGIT[128], ICOS[129], 4-1BB[130], CD27[131,132] and OX-40[133], for which antagonistic or agonistic monoclonal antibodies are in development. To optimally exploit these targets for anti-cancer benefit, it is critical to understand the net effect on immune activation of simultaneously engaging co-signalling receptors on T_{regs} and conventional $CD4^+$ and $CD8^+$ T cells. As observed in **chapter 6**, blockade of co-inhibitory receptors can increase T_{reg} proliferation and activation. These activated T_{regs} likely limit the intended activation of effector cells, since depletion of T_{regs} in the context of ICB mobilises $CD8^+$ T- and NK cells in blood. In line with this notion, it has been shown that anti-PD-1 reactivates dysfunctional $PD\text{-}1^+$ T_{regs}, which subsequently restrains concurrent $CD8^+$ T cell activation and negatively impacts immunotherapy response in patients with gastric cancer and non-small cell lung cancer[134,135]. Furthermore, CTLA-4 on T_{regs} inhibits the proliferation of effector cells by engaging CD28 on dendritic cells, but this same mechanism inhibits the proliferation of T_{regs} themselves[136]. Indeed, anti-CTLA-4 has been shown to expand T_{regs} in cancer patients[120,137], but it is unknown whether this impacts therapeutic benefit. Promisingly, blockade of so-called "second-tier"[128] co-inhibitory proteins TIGIT and TIM-3, but not LAG-3[138], does not appear to provoke T_{reg} activation, but instead reduces the suppressive activity of T_{regs}[139,140]. Therefore, in tumors that are abundantly populated by $PD\text{-}1^+$ or $CTLA\text{-}4^+$ $T_{regs,}$ an alternative approach to anti-PD-1/CTLA-4 therapy might be blockade of TIGIT and TIM-3.
On the other side of the co-signalling spectrum, therapeutic engagement of co-stimulatory receptors can also induce T_{reg} activation. Ligation of co-stimulatory receptor 4-1BB has been shown to activate both $CD8^+$ T cells[141] and T_{regs}[142]. In addition, CD27 co-stimulation expands T_{regs} in hyperlipidaemic mice[143], and ablation of CD27 on T_{regs} synergizes with anti-PD-1 therapy in mice bearing MC38 cell line tumors[144]. Finally, in mice, the co-stimulatory receptor ICOS has been shown to mark highly suppressive T_{regs}[129], and $ICOS^{KO}$ mice have impaired Th1 and Th2 responses, but also reduced T_{regs} in models for allergy and infection[145]. Combined, these findings indicate that pulling the brakes on co-inhibitory signalling does not only evoke (re)activation of beneficial effector cells, but engages immunosuppressive T_{regs} via the same mechanisms. Likewise, various co-stimulatory agonists appear to activate

both regulatory and conventional T cells. The intrinsic similarity in response to modulation of co-signalling between T_{regs} and conventional T cells on a cellular level, simultaneously activates opposing pro- and anti-inflammatory effector mechanisms. This may be a valuable built-in brake that limits excessive immune activation, but may also offset the benefit of therapeutic modulation of co-signalling receptors. Ultimately, this conundrum raises the question: which response takes the upper hand? As has been shown in the context of PD-1, this is likely dependent on the balance between cell types that express the receptor of interest, and the intensity of expression of both the receptor and its ligand[135], which might greatly differ in distinct niches. Indeed, different metastases within the same patient can have distinct expression of co-signalling molecules[81], demonstrating the relevance of this concept in cancer patients. Another consideration is that cells in distinct differentiation states of the same lineage can respond differently to immunomodulatory drugs. As we show in **chapter 3** and **6**, PD-1 plays a dual role on $CD4^+$ T cells. PD-1 signalling in intratumoral conventional $CD4^+$ T promotes their conversion into T_{regs}, and PD-1 blockade has been shown to inhibit this process in CT26 colorectal tumors[146]. On T_{regs}, PD-1 signalling has not been described to impact their differentiation, but is primarily linked to dysfunction[147]. It is possible that other co-signalling molecules also differently impact $CD4^+$ T cell plasticity, but this remains a topic of future research.

Going forward, a more comprehensive understanding of how therapeutic interference with co-signalling impacts regulatory and conventional T cells and its resulting effect on anti-tumor immunity may be key to improve clinical responses of these approaches. Promisingly, innovative treatment strategies could be employed that selectively activate conventional T cells, but not T_{regs}. As an example, anti-PD1-IL2 fusion proteins, consisting of a high affinity PD-1 antibody coupled to a non-T_{reg} binding IL-2 variant, have been shown to selectively expand tumor-specific T cells, but not T_{regs}, and are moving towards clinical development[91,148]. Another approach could be to develop bispecific antibodies which direct co-inhibitory agonists, or co-stimulatory antagonists to T_{regs}, using proteins abundantly expressed on T_{regs} like CD25 and GITR. Besides the detrimental role of T_{regs} in the context of ICB, little is known about the impact of T_{regs} on other T cell-based immunotherapy approaches, like adoptive T cell transfer using engineered chimeric antigen receptor (CAR) T cells or expanded TILs[149]. It would be of interest to investigate whether T_{regs} are present in these products, and antagonize the function of co-transferred conventional T cells. Combined, it is clear that T_{regs} are direct targets of immunomodulatory drugs, and should be regarded as such, in the design, validation, and clinical rollout of novel avenues of immunotherapy.

REFERENCES

1. Liu, J. *et al.* Improved efficacy of neoadjuvant compared to adjuvant immunotherapy to eradicate metastatic disease. *Cancer Discov.* **6**, 1382–1399 (2016).
2. Hughes, E. *et al.* Primary breast tumours but not lung metastases induce protective anti-tumour immune responses after Treg-depletion. *Cancer Immunol. Immunother.* 1–11 (2020) doi:10.1007/s00262-020-02603-x.
3. Bos, P. D., Plitas, G., Rudra, D., Lee, S. Y. & Rudensky, A. Y. Transient regulatory T cell ablation deters oncogene-driven breast cancer and enhances radiotherapy. *J. Exp. Med.* **210**, 2435–2466 (2013).
4. Liu, J. *et al.* Assessing immune-related adverse events of efficacious combination immunotherapies in preclinical models of cancer. *Cancer Res.* **76**, 5288–5301 (2016).
5. Zhong, W. *et al.* Comparison of the molecular and cellular phenotypes of common mouse syngeneic models with human tumors. *BMC Genomics* **21**, 2 (2020).
6. Gatti-Mays, M. E. *et al.* If we build it they will come: targeting the immune response to breast cancer. *npj Breast Cancer 2019 51* **5**, 1–13 (2019).
7. Vonderheide, R. H., Domchek, S. M. & Clark, A. S. Immunotherapy for breast cancer: What are we missing? *Clin. Cancer Res.* **23**, 2640–2646 (2017).
8. Alexandrov, L. B. *et al.* Signatures of mutational processes in human cancer. *Nature* **500**, 415–421 (2013).
9. Schumacher, T. N. & Schreiber, R. D. Neoantigens in cancer immunotherapy. *Science* **348**, 69–74 (2015).
10. Crosby, E. J. *et al.* Complimentary mechanisms of dual checkpoint blockade expand unique T-cell repertoires and activate adaptive anti-tumor immunity in triple-negative breast tumors. *Oncoimmunology* **7**, (2018).
11. Schrörs, B. *et al.* Multi-Omics Characterization of the 4T1 Murine Mammary Gland Tumor Model. *Front. Oncol.* **10**, 1195 (2020).
12. Lechner, M. G. *et al.* Immunogenicity of murine solid tumor models as a defining feature of in vivo behavior and response to immunotherapy. *J. Immunother.* **36**, 477–489 (2013).
13. Kasikara, C. *et al.* Pan-TAM tyrosine kinase inhibitor BMS-777607 Enhances Anti-PD-1 mAb efficacy in a murine model of triple-negative breast cancer. *Cancer Res.* **79**, 2669–2683 (2019).
14. Adams, S. *et al.* Pembrolizumab monotherapy for previously treated metastatic triple-negative breast cancer: Cohort A of the phase II KEYNOTE-086 study. *Ann. Oncol.* **30**, 397–404 (2019).
15. Clark, N. M. *et al.* Regulatory T Cells Support Breast Cancer Progression by Opposing IFN-γ-Dependent Functional Reprogramming of Myeloid Cells. *Cell Rep.* **33**, (2020).
16. Hammerl, D. *et al.* Breast cancer genomics and immuno-oncological markers to guide immune therapies. *Semin. Cancer Biol.* **52**, 178–188 (2018).
17. Jang, J. E. *et al.* Crosstalk between Regulatory T Cells and Tumor-Associated Dendritic Cells Negates Anti-tumor Immunity in Pancreatic Cancer. *Cell Rep.* **20**, 558–571 (2017).
18. Loyher, P. L. *et al.* CCR2 influences T regulatory cell migration to tumors and serves as a biomarker of cyclophosphamide sensitivity. *Cancer Res.* **76**, 6483–6494 (2016).
19. Gutierrez, W. R. *et al.* Divergent immune landscapes of primary and syngeneic Kras-driven mouse tumor models. *Sci. Rep.* **11**, 1098 (2021).
20. Derksen, P. W. B. *et al.* Somatic inactivation of E-cadherin and p53 in mice leads to metastatic lobular mammary carcinoma through induction of anoikis resistance and angiogenesis. *Cancer Cell* **10**, 437–449 (2006).
21. Arce Vargas, F. *et al.* Fc-Optimized Anti-CD25 Depletes Tumor-Infiltrating Regulatory T Cells and Synergizes with PD-1 Blockade to Eradicate Established Tumors. *Immunity* **46**, 577–586 (2017).
22. Magnuson, A. M. *et al.* Identification and validation of a tumor-infiltrating Treg transcriptional signature conserved across species and tumor types. *PNAS* **115**, E10672–E10681 (2018).
23. Salvagno, C. *et al.* Therapeutic targeting of macrophages enhances chemotherapy efficacy by unleashing type I interferon response. *Nat. Cell Biol.* **21**, 511–521 (2019).
24. West, N. R. *et al.* Tumour-infiltrating FOXP3 + lymphocytes are associated with cytotoxic immune responses and good clinical outcome in oestrogen receptor-negative breast cancer. *Br. J. Cancer* **108**, 155–162 (2013).
25. Liu, S. *et al.* Prognostic significance of FOXP3+ tumor-infiltrating lymphocytes in breast cancer depends on estrogen receptor and human epidermal growth factor receptor-2 expression status and concurrent cytotoxic T-cell infiltration. *Breast Cancer Res.* **16**, (2014).
26. Yeong, J. *et al.* Higher densities of Foxp3 + regulatory T cells are associated with better prognosis in triple-negative breast cancer. *Breast Cancer Res. Treat.* **163**, 21–35 (2017).
27. Overacre-Delgoffe, A. E. *et al.* Interferon-γ Drives Treg Fragility to Promote Anti-tumor Immunity. *Cell* **169**,

1130-1141.e11 (2017).
28. Plitas, G. *et al.* Regulatory T Cells Exhibit Distinct Features in Human Breast Cancer. *Immunity* **45**, 1122–1134 (2016).
29. Xu, Y., Lan, S. & Zheng, Q. Prognostic significance of infiltrating immune cell subtypes in invasive ductal carcinoma of the breast. *Tumori* **104**, 196–201 (2018).
30. Ali, H. R., Chlon, L., Pharoah, P. D. P., Markowetz, F. & Caldas, C. Patterns of Immune Infiltration in Breast Cancer and Their Clinical Implications: A Gene-Expression-Based Retrospective Study. *PLoS Med.* **13**, (2016).
31. Bense, R. D. *et al.* Relevance of Tumor-Infiltrating Immune Cell Composition and Functionality for Disease Outcome in Breast Cancer. *JNCI J. Natl. Cancer Inst.* **109**, (2017).
32. Tekpli, X. *et al.* An independent poor-prognosis subtype of breast cancer defined by a distinct tumor immune microenvironment. *Nat. Commun. 2019 101* **10**, 1–14 (2019).
33. Wu, S. Z. *et al.* A single-cell and spatially resolved atlas of human breast cancers. *Nat. Genet.* **53**, 1334–1347 (2021).
34. Jiang, D., Gao, Z., Cai, Z., Wang, M. & He, J. Clinicopathological and prognostic significance of FOXP3+ tumor infiltrating lymphocytes in patients with breast cancer: a meta-analysis. *BMC Cancer* **15**, 727 (2015).
35. Dings, P. J. M., Elferink, M. A. G., Strobbe, L. J. A. & de Wilt, J. H. W. The Prognostic Value of Lymph Node Ratio in Node-Positive Breast Cancer: A Dutch Nationwide Population-Based Study. *Ann. Surg. Oncol.* **20**, 2607–2614 (2013).
36. Vinh-Hung, V., Burzykowski, T., Cserni, G., Voordeckers, M. & Steene, J. Van De. Functional form of the effect of the numbers of axillary nodes on survival in early breast cancer. *Int J Oncol* **22**, (2003).
37. Vinh-Hung, V., Cserni, G., Burzykowski, T., Steene, J. van de & Voordeckers, M. Effect of the number of uninvolved nodes on survival in early breast cancer. *Oncol Rep* **10**, (2003).
38. Beenken, S. W. *et al.* Axillary Lymph Node Status, But Not Tumor Size, Predicts Locoregional Recurrence and Overall Survival After Mastectomy for Breast Cancer. *Ann. Surg.* **237**, 732–739 (2003).
39. Carter, C., Allen, C. & Henson, D. Relation of tumor size, lymph node status, and survival in 24,740 breast cancer cases. *Cancer* **63**, (1989).
40. Wu, S. G. *et al.* Prognostic Value of Metastatic Axillary Lymph Node Ratio for Chinese Breast Cancer Patients. *PLoS One* **8**, e61410 (2013).
41. Wang, Y., Sun, J. & Qu, X. Regulatory T cells are an important prognostic factor in breast cancer: a systematic review and meta-analysis. *Neoplasma* **63**, 789–798 (2016).
42. Zhou, Y. *et al.* Prognostic value of tumor-infiltrating Foxp3+ regulatory T cells in patients with breast cancer: a meta-analysis. *J. Cancer* **8**, 4098–4105 (2017).
43. Mansfield, A. S. *et al.* Simultaneous Foxp3 and IDO expression is associated with sentinel lymph node metastases in breast cancer. *BMC Cancer* **9**, (2009).
44. Mansfield, A. S., Heikkila, P., Von Smitten, K., Vakkila, J. & Leidenius, M. Metastasis to sentinel lymph nodes in breast cancer is associated with maturation arrest of dendritic cells and poor co-localization of dendritic cells and CD8+ T cells. *Virchows Arch.* **459**, 391–398 (2011).
45. van Pul, K. M. *et al.* Selectively hampered activation of lymph node-resident dendritic cells precedes profound T cell suppression and metastatic spread in the breast cancer sentinel lymph node. *J. Immunother. Cancer* **7**, 133 (2019).
46. Nakamura, R. *et al.* Accumulation of regulatory T cells in sentinel lymph nodes is a prognostic predictor in patients with node-negative breast cancer. *Eur. J. Cancer* **45**, 2123–2131 (2009).
47. Faghih, Z. *et al.* Immune profiles of CD4+ lymphocyte subsets in breast cancer tumor draining lymph nodes. *Immunol. Lett.* **158**, 57–65 (2014).
48. Rotman, J., Koster, B. D., Jordanova, E. S., Heeren, A. M. & de Gruijl, T. D. Unlocking the therapeutic potential of primary tumor-draining lymph nodes. *Cancer Immunol. Immunother.* **68**, 1681 (2019).
49. Rye, I. H. *et al.* Breast cancer metastasis: immune profiling of lymph nodes reveals exhaustion of effector T cells and immunosuppression. *Mol. Oncol.* **16**, 88–103 (2022).
50. Miyara, M. *et al.* Functional Delineation and Differentiation Dynamics of Human CD4+ T Cells Expressing the FoxP3 Transcription Factor. *Immunity* **30**, 899–911 (2009).
51. Núñez, N. G. *et al.* Tumor invasion in draining lymph nodes is associated with Treg accumulation in breast cancer patients. *Nat. Commun.* **11**, 1–15 (2020).
52. Huang, S. *et al.* TGF-β1 secreted by Tregs in lymph nodes promotes breast cancer malignancy via up-regulation of IL-17RB. *EMBO Mol. Med.* **9**, 1660–1680 (2017).
53. Gasteiger, G. *et al.* IL-2–dependent tuning of NK cell sensitivity for target cells is controlled by regulatory T cells. *J. Exp. Med.* **210**, 1167–1178 (2013).
54. Littwitz-Salomon, E. *et al.* Activated regulatory T cells suppress effector NK cell responses by an IL-2-mediated mechanism during an acute retroviral infection. *Retrovirology* **12**, 1–13 (2015).
55. Sim, G. C. *et al.* IL-2 therapy promotes suppressive ICOS+ Treg expansion in melanoma patients. *J. Clin.*

Invest. **124**, 99–110 (2014).
56. Owen, D. L. *et al.* Identification of Cellular Sources of IL-2 Needed for Regulatory T Cell Development and Homeostasis. *J. Immunol.* **200**, 3926–3933 (2018).
57. Terme, M. *et al.* Regulatory T cells control dendritic cell/NK cell cross-talk in lymph nodes at the steady state by inhibiting CD4+ self-reactive T cells. *J. Immunol.* **180**, 4679–4686 (2008).
58. Ghiringhelli, F. *et al.* CD4+CD25+ regulatory T cells inhibit natural killer cell functions in a transforming growth factor-β-dependent manner. *J. Exp. Med.* **202**, 1075–1085 (2005).
59. Liang, B. *et al.* Regulatory T cells inhibit dendritic cells by lymphocyte activation gene-3 engagement of MHC class II. *J. Immunol.* **180**, 5916–5926 (2008).
60. Wu, H. *et al.* T-cells produce acidic niches in lymph nodes to suppress their own effector functions. *Nat. Commun. 2020 111* **11**, 1–13 (2020).
61. Brand, A. *et al.* LDHA-Associated Lactic Acid Production Blunts Tumor Immunosurveillance by T and NK Cells. *Cell Metab.* **24**, 657–671 (2016).
62. Watson, M. L. J. *et al.* Metabolic support of tumour-infiltrating regulatory T cells by lactic acid. *Nat. 2021 5917851* **591**, 645–651 (2021).
63. Kumagai, S. *et al.* Lactic acid promotes PD-1 expression in regulatory T cells in highly glycolytic tumor microenvironments. *Cancer Cell* **40**, 201-218.e9 (2022).
64. Huppert, L. A. *et al.* Tissue-specific Tregs in cancer metastasis: opportunities for precision immunotherapy. *Cell. Mol. Immunol. 2021 191* **19**, 33–45 (2021).
65. Schneider, T. *et al.* Foxp3+ Regulatory T Cells and Natural Killer Cells Distinctly Infiltrate Primary Tumors and Draining Lymph Nodes in Pulmonary Adenocarcinoma. (2011) doi:10.1097/JTO.0b013e31820b80ca.
66. Van Den Hout, M. F. C. M. *et al.* Melanoma sequentially suppresses different DC subsets in the sentinel lymph node, affecting disease spread and recurrence. *Cancer Immunol. Res.* **5**, 969–977 (2017).
67. Heeren, A. M. *et al.* Nodal metastasis in cervical cancer occurs in clearly delineated fields of immune suppression in the pelvic lymph catchment area. *Oncotarget* **6**, 32484–32493 (2015).
68. Lee, H. E., Park, D. J., Kim, W. H., Kim, H. H. & Lee, H. S. High FOXP3+ regulatory T-cell density in the sentinel lymph node is associated with downstream non-sentinel lymph-node metastasis in gastric cancer. *Br. J. Cancer* **105**, 413 (2011).
69. Deng, L. *et al.* Accumulation of Foxp3+ T regulatory cells in draining lymph nodes correlates with disease progression and immune suppression in colorectal cancer patients. *Clin. Cancer Res.* **16**, 4105–4112 (2010).
70. Alonso, R. *et al.* Induction of anergic or regulatory tumor-specific CD4+ T cells in the tumor-draining lymph node. *Nat. Commun.* **9**, 1–17 (2018).
71. Chen, W., Hoffmann, A. D., Liu, H. & Liu, X. Organotropism: new insights into molecular mechanisms of breast cancer metastasis. *npj Precis. Oncol. 2018 21* **2**, 1–12 (2018).
72. Zhang, L. *et al.* Microenvironment-induced PTEN loss by exosomal microRNA primes brain metastasis outgrowth. *Nature* **527**, 100–104 (2015).
73. Hoshino, A. *et al.* Tumour exosome integrins determine organotropic metastasis. *Nature* **527**, 329–335 (2015).
74. Salmon, H., Remark, R., Gnjatic, S. & Merad, M. Host tissue determinants of tumour immunity. *Nat. Rev. Cancer* **19**, 215 (2019).
75. Wasilewski, D., Priego, N., Fustero-Torre, C. & Valiente, M. Reactive astrocytes in brain metastasis. *Front. Oncol.* **7**, 298 (2017).
76. Liu, G. *et al.* Lung fibroblasts promote metastatic colonization through upregulation of stearoyl-CoA desaturase 1 in tumor cells. *Oncogene 2018 3711* **37**, 1519–1533 (2018).
77. Kang, N., Gores, G. J. & Shah, V. H. Hepatic Stellate Cells: Partners in Crime for Liver Metastases? *Hepatology* **54**, 707 (2011).
78. Devaud, C. *et al.* Tissues in Different Anatomical Sites Can Sculpt and Vary the Tumor Microenvironment to Affect Responses to Therapy. *Mol. Ther.* **22**, 18–27 (2014).
79. Oliver, A. J. *et al.* Tissue-Dependent Tumor Microenvironments and Their Impact on Immunotherapy Responses. *Front. Immunol.* **9**, 1 (2018).
80. Allen, B. M. *et al.* Systemic dysfunction and plasticity of the immune macroenvironment in cancer models. *Nat. Med.* **26**, 1125–1134 (2020).
81. De Mattos-Arruda, L. *et al.* The Genomic and Immune Landscapes of Lethal Metastatic Breast Cancer. *Cell Rep.* **27**, 2690-2708.e10 (2019).
82. Jiménez-Sánchez, A. *et al.* Heterogeneous Tumor-Immune Microenvironments among Differentially Growing Metastases in an Ovarian Cancer Patient. *Cell* **170**, 927 (2017).
83. Thorsson, V. *et al.* The Immune Landscape of Cancer. *Immunity* **48**, 812 (2018).
84. Spranger, S. & Gajewski, T. F. Impact of oncogenic pathways on evasion of antitumour immune responses. *Nat. Rev. Cancer* **18**, 139–147 (2018).
85. Kitamura, T., Qian, B. Z. & Pollard, J. W. Immune cell promotion of metastasis. *Nat. Rev. Immunol.* **15**,

73–86 (2015).
86. Coffelt, S. B. *et al.* IL-17-producing γδ T cells and neutrophils conspire to promote breast cancer metastasis. *Nature* **522**, 345–348 (2015).
87. Kersten, K. *et al.* Mammary tumor-derived CCL2 enhances pro-metastatic systemic inflammation through upregulation of IL1β in tumor-associated macrophages. *Oncoimmunology* **6**, (2017).
88. Wellenstein, M. D. *et al.* Loss of p53 triggers WNT-dependent systemic inflammation to drive breast cancer metastasis. *Nature* **572**, 538–542 (2019).
89. Ma, R. Y. *et al.* Monocyte-derived macrophages promote breast cancer bone metastasis outgrowth. *J. Exp. Med.* **217**, (2020).
90. Dalotto-Moreno, T. *et al.* Targeting Galectin-1 Overcomes Breast Cancer-Associated Immunosuppression and Prevents Metastatic Disease. *Cancer Res.* **73**, 1107–1117 (2013).
91. Ren, Z. *et al.* Selective delivery of low-affinity IL-2 to PD-1+ T cells rejuvenates antitumor immunity with reduced toxicity. *J. Clin. Invest.* **132**, (2022).
92. Matta, B. M. *et al.* Peri-alloHCT IL-33 administration expands recipient T-regulatory cells that protect mice against acute GVHD. *Blood* **128**, 427–439 (2016).
93. Matta, B. M. & Turnquist, H. R. Expansion of regulatory T cells in vitro and in vivo by IL-33. in *Methods in Molecular Biology* vol. 1371 29–41 (Humana Press Inc., 2016).
94. Wang, L. *et al.* Connecting blood and intratumoral Treg cell activity in predicting future relapse in breast cancer. *Nat. Immunol.* **20**, 1220–1230 (2019).
95. Angus, L. *et al.* The genomic landscape of metastatic breast cancer highlights changes in mutation and signature frequencies. *Nat. Genet. 2019 5110* **51**, 1450–1458 (2019).
96. Reiter, J. G. *et al.* Lymph node metastases develop through a wider evolutionary bottleneck than distant metastases. *Nat. Genet.* **52**, 692–700 (2020).
97. Angelova, M. *et al.* Evolution of Metastases in Space and Time under Immune Selection. *Cell* **175**, 751-765.e16 (2018).
98. Chen, Z. *et al.* Inference of immune cell composition on the expression profiles of mouse tissue. *Sci. Reports 2017 71* **7**, 1–11 (2017).
99. Schuijs, M. J. *et al.* ILC2-driven innate immune checkpoint mechanism antagonizes NK cell antimetastatic function in the lung. *Nat. Immunol.* **21**, 998–1009 (2020).
100. Guldner, I. H. *et al.* CNS-Native Myeloid Cells Drive Immune Suppression in the Brain Metastatic Niche through Cxcl10. *Cell* **183**, 1234-1248.e25 (2020).
101. Sharma, S. K. *et al.* Pulmonary alveolar macrophages contribute to the premetastatic niche by suppressing antitumor T cell responses in the lungs. *J. Immunol.* **194**, 5529–5538 (2015).
102. Ingman, W. V. The Gut Microbiome: A New Player in Breast Cancer Metastasis. *Cancer Res.* **79**, 3539–3541 (2019).
103. Alam, A. *et al.* Fungal mycobiome drives IL-33 secretion and type 2 immunity in pancreatic cancer. *Cancer Cell* **40**, 153-167.e11 (2022).
104. Seyhan, A. A. Lost in translation: the valley of death across preclinical and clinical divide – identification of problems and overcoming obstacles. *Transl. Med. Commun. 2019 41* **4**, 1–19 (2019).
105. Gómez-Cuadrado, L., Tracey, N., Ma, R., Qian, B. & Brunton, V. G. Mouse models of metastasis: progress and prospects. *Dis. Model. Mech.* **10**, 1061–1074 (2017).
106. Kersten, K., de Visser, K. E., van Miltenburg, M. H. & Jonkers, J. Genetically engineered mouse models in oncology research and cancer medicine. *EMBO Mol. Med.* **9**, 137–153 (2017).
107. Annunziato, S. *et al.* Modeling invasive lobular breast carcinoma by CRISPR / Cas9-mediated somatic genome editing of the mammary gland. *Genes Dev.* **30**, 1470–1480 (2016).
108. Annunziato, S. *et al.* Comparative oncogenomics identifies combinations of driver genes and drug targets in BRCA1-mutated breast cancer. *Nat. Commun.* **10**, (2019).
109. Togashi, Y., Shitara, K. & Nishikawa, H. Regulatory T cells in cancer immunosuppression — implications for anticancer therapy. *Nat. Rev. Clin. Oncol.* **16**, 356–371 (2019).
110. Plitas, G. & Rudensky, A. Y. Regulatory T Cells in Cancer. *Annu. Rev. Cancer Biol.* **4**, 459–477 (2020).
111. Solomon, I. *et al.* CD25-Treg-depleting antibodies preserving IL-2 signaling on effector T cells enhance effector activation and antitumor immunity. *Nat. Cancer 2020 112* **1**, 1153–1166 (2020).
112. Kim, J. M., Rasmussen, J. P. & Rudensky, A. Y. Regulatory T cells prevent catastrophic autoimmunity throughout the lifespan of mice. *Nat. Immunol.* **8**, 191–197 (2007).
113. Su, S. *et al.* Blocking the recruitment of naive CD4+ T cells reverses immunosuppression in breast cancer. *Cell Res.* **27**, 461–482 (2017).
114. Balança, C. C. *et al.* PD-1 blockade restores helper activity of tumor-infiltrating, exhausted PD-1hiCD39+ CD4 T cells. *JCI Insight* **6**, (2021).
115. Kim, R. *et al.* A potential role for peripheral natural killer cell activity induced by preoperative chemotherapy in breast cancer patients. *Cancer Immunol. Immunother.* **68**, 577–585 (2019).
116. Blank, C. U. *et al.* Neoadjuvant versus adjuvant ipilimumab plus nivolumab in macroscopic stage III

melanoma. *Nat. Med.* **24**, 1655–1661 (2018).
117. Vos, J. L. *et al.* Neoadjuvant immunotherapy with nivolumab and ipilimumab induces major pathological responses in patients with head and neck squamous cell carcinoma. *Nat. Commun. 2021 121* **12**, 1–13 (2021).
118. Chalabi, M. *et al.* Neoadjuvant immunotherapy leads to pathological responses in MMR-proficient and MMR-deficient early-stage colon cancers. *Nat. Med. 2020 264* **26**, 566–576 (2020).
119. van Dijk, N. *et al.* Preoperative ipilimumab plus nivolumab in locoregionally advanced urothelial cancer: the NABUCCO trial. *Nat. Med. 2020 2612* **26**, 1839–1844 (2020).
120. Sharma, A. *et al.* Anti-CTLA-4 immunotherapy does not deplete Foxp3 þ regulatory T cells (Tregs) in human cancers. *Clin. Cancer Res.* **25**, 1233–1238 (2019).
121. Quezada, S. A. & Peggs, K. S. Lost in translation: Deciphering the mechanism of action of anti-human CTLA-4. *Clin. Cancer Res.* **25**, 1130–1132 (2019).
122. Vargas, F. A. *et al.* Fc Effector Function Contributes to the Activity of Human Anti-CTLA-4 Antibodies. *Cancer Cell* **33**, 649-663.e4 (2018).
123. Peggs, K. S., Quezada, S. A., Chambers, C. A., Korman, A. J. & Allison, J. P. Blockade of CTLA-4 on both effector and regulatory T cell compartments contributes to the antitumor activity of anti-CTLA-4 antibodies. *J. Exp. Med.* **206**, 1717–1725 (2009).
124. Kidani, Y. *et al.* CCR8-targeted specific depletion of clonally expanded Treg cells in tumor tissues evokes potent tumor immunity with long-lasting memory. *Proc. Natl. Acad. Sci. U. S. A.* **119**, (2022).
125. Wang, T. *et al.* CCR8 blockade primes anti-tumor immunity through intratumoral regulatory T cells destabilization in muscle-invasive bladder cancer. *Cancer Immunol. Immunother.* **69**, 1855–1867 (2020).
126. Campbell, J. R. *et al.* Fc-optimized anti-CCR8 antibody depletes regulatory t cells in human tumor models. *Cancer Res.* **81**, 2983–2994 (2021).
127. Teixeira, A. F., ten Dijke, P. & Zhu, H. J. On-Target Anti-TGF-β Therapies Are Not Succeeding in Clinical Cancer Treatments: What Are Remaining Challenges? *Front. Cell Dev. Biol.* **8**, 605 (2020).
128. Anderson, A. C., Joller, N. & Kuchroo, V. K. Lag-3, Tim-3, and TIGIT: Co-inhibitory Receptors with Specialized Functions in Immune Regulation. *Immunity* **44**, 989–1004 (2016).
129. Vocanson, M. *et al.* Inducible costimulator (ICOS) is a marker for highly suppressive antigen-specific T cells sharing features of TH17/TH1 and regulatory T cells. *J. Allergy Clin. Immunol.* **126**, (2010).
130. Chester, C., Sanmamed, M. F., Wang, J. & Melero, I. Immunotherapy targeting 4-1BB: mechanistic rationale, clinical results, and future strategies. *Blood* **131**, 49–57 (2018).
131. Buchan, S. L., Rogel, A. & Al-Shamkhani, A. The immunobiology of CD27 and OX40 and their potential as targets for cancer immunotherapy. *Blood* **131**, 39–48 (2018).
132. Van De Ven, K. & Borst, J. Targeting the T-cell co-stimulatory CD27/CD70 pathway in cancer immunotherapy: Rationale and potential. *Immunotherapy* **7**, 655–667 (2015).
133. De Simone, M. *et al.* Transcriptional Landscape of Human Tissue Lymphocytes Unveils Uniqueness of Tumor-Infiltrating T Regulatory Cells. *Immunity* **45**, 1135–1147 (2016).
134. Kamada, T. *et al.* PD-1(+) regulatory T cells amplified by PD-1 blockade promote hyperprogression of cancer. *PNAS* **116**, 9999–10008 (2019).
135. Kumagai, S. *et al.* The PD-1 expression balance between effector and regulatory T cells predicts the clinical efficacy of PD-1 blockade therapies. *Nat. Immunol.* **21**, 1346–1358 (2020).
136. Marangoni, F. *et al.* Expansion of tumor-associated Treg cells upon disruption of a CTLA-4-dependent feedback loop. *Cell* **184**, 3998-4015.e19 (2021).
137. Kavanagh, B. *et al.* CTLA4 blockade expands FoxP3+ regulatory and activated effector CD4+ T cells in a dose-dependent fashion. *Blood* **112**, 1175 (2008).
138. Zhang, Q. *et al.* LAG-3 limits regulatory T cell proliferation and function in autoimmune diabetes. *Sci. Immunol.* **2**, (2017).
139. Banerjee, H. *et al.* Expression of Tim-3 drives phenotypic and functional changes in Treg cells in secondary lymphoid organs and the tumor microenvironment. *Cell Rep.* **36**, 109699 (2021).
140. Ge, Z., Peppelenbosch, M. P., Sprengers, D. & Kwekkeboom, J. TIGIT, the Next Step Towards Successful Combination Immune Checkpoint Therapy in Cancer. *Front. Immunol.* **12**, 2987 (2021).
141. Wen, T., Bukczynski, J. & Watts, T. H. 4-1BB ligand-mediated costimulation of human T cells induces CD4 and CD8 T cell expansion, cytokine production, and the development of cytolytic effector function. *J. Immunol.* **168**, 4897–4906 (2002).
142. Zhang, P. *et al.* Agonistic anti-4-1BB antibody promotes the expansion of natural regulatory T cells while maintaining Foxp3 expression. *Scand. J. Immunol.* **66**, 435–440 (2007).
143. Winkels, H. *et al.* CD27 co-stimulation increases the abundance of regulatory T cells and reduces atherosclerosis in hyperlipidaemic mice. *Eur. Heart J.* **38**, 3590–3599 (2017).
144. Muth, S., Klaric, A., Radsak, M., Schild, H. & Probst, H. C. CD27 expression on Treg cells limits immune responses against tumors. *J. Mol. Med.* **100**, 439–449 (2022).
145. Wikenheiser, D. J. & Stumhofer, J. S. ICOS co-stimulation: Friend or foe? *Front. Immunol.* **7**, 304 (2016).

146. Dyck, L. *et al.* Anti-PD-1 inhibits Foxp3 + Treg cell conversion and unleashes intratumoural effector T cells thereby enhancing the efficacy of a cancer vaccine in a mouse model. *Cancer Immunol. Immunother. 2016 6512* **65**, 1491–1498 (2016).
147. Lowther, D. E. *et al.* PD-1 marks dysfunctional regulatory T cells in malignant gliomas. *JCI Insight* **1**, 1–15 (2016).
148. Umana, P. Abstract ND03: PD1-IL2v: A next generation, PD-1-targeted cytokine. *Cancer Res.* **81**, ND03–ND03 (2021).
149. Rohaan, M. W., Wilgenhof, S. & Haanen, J. B. A. G. Adoptive cellular therapies: the current landscape. *Virchows Arch.* **474**, 449–461 (2019).

English Summary
Nederlandse samenvatting
Curriculum Vitae
Acknowledgements
List of publications
PhD portfolio

ENGLISH SUMMARY

The human immune system is equipped with powerful cellular mechanisms that provide protection against threats which may compromise tissue function and homeostasis. These mechanisms can be used to deal with external threats like pathogenic micro-organisms, but are also suitable as a counter to the internal threat of cancer. However, the manifestation of cancer in today's society as a leading global health challenge demonstrates this counter is not waterproof, and tumors are able to evade immune pressure. An important reason for this observation is that cancer cells are in essence not foreign cells, but have acquired characteristics, as a result of continuous accumulation of mutations, that distinguishes them from healthy cells. Thus, cancer cells balance on the edge of self- and non-self. This complicates detection by the immune system, which requires a threat to be clearly identifiable to be of foreign nature (i.e. immunogenic), to become fully activated. On top of being poorly recognisable, tumors actively employ other means to evade immune-mediated eradication. In general, immune effector mechanisms have to be carefully regulated to prevent self-inflicted tissue damage and auto-immune-related pathology which can result from excessive or misguided immune activation. However, mounting evidence shows that tumors can co-opt immunoregulatory mechanisms to limit immune responses against primary tumors and metastases. In cancer types like breast cancer, tumor-derived signals can guide the infiltration and anti-inflammatory polarisation of myeloid- and adaptive immune cells which, together with local stromal- and tumor cells, construct a dense network of immunosuppression. These immunosuppressive conditions are characterised by abundant expression of immune inhibitory receptors, anti-inflammatory cytokines and other immune-modulatory factors that can turn the tumor microenvironment (TME) into a hostile milieu for effector cells, thereby blunting anti-cancer mechanisms. Moreover, it is becoming increasingly clear that tumor-associated immunosuppression takes on systemic forms, and thereby helps cancer to spread beyond the primary tumor. By increasing our understanding of the immunoregulatory mechanisms that are hijacked in the context of breast cancer, existing immune-based therapeutic approaches can be improved to overcome immunosuppression, while new insights may also inspire novel avenues of immunotherapy.

An important cell type that is broadly involved in controlling immune activation is the regulatory FOXP3^{+}CD4^{+} T cell (T_{regs}). T_{regs} are equipped with a diverse arsenal of immunosuppressive mechanisms, and T_{reg} dysfunction stands at the basis of a wide range of auto-immune-related diseases. In cancer, T_{regs} are thought to be important allies of tumors, as the immunosuppressive function of T_{regs} can be directed against anti-tumor immunity. The work described in this thesis explores the intricate relationship of T_{regs} with primary and metastatic breast cancer, and T cell based immunotherapeutic approaches, using sophisticated mouse models that recapitulate the development and progression of poorly immunogenic breast tumors.

Chapter 2 reviews the exciting progress of the past years regarding our understanding of T_{regs} in (human) breast cancer, and discusses the future prospects of T_{reg}-targeting strategies. $FOXP3^+$ T_{regs} mainly develop in the thymus, but can also arise in the periphery through TGF- β mediated differentiation of conventional $CD4^+$ T cells. These peripheral T_{regs} (pT_{regs}) acquire FOXP3 expression and immunosuppressive activity, in a process called 'peripheral conversion'. However, if, and by which mechanisms , pT_{regs} accumulate in mammary tumors is largely unknown. Research in **Chapter 3** identifies that tumor-associated macrophages (TAMs), which are the most abundant immune cell type in spontaneously arising murine mammary tumors, play a key role in the accumulation of pT_{regs} in tumors. In part, this is mediated by TGF-β released by TAMs. We also show that TAMs induce PD-1 expression on intratumoral conventional $CD4^+$ T cells, which additionally "prepares" these cells for intratumoral conversion into pT_{regs}.

The local TME dictates the phenotype and function of intratumoral immune cells, but the systemic inflammation that accompanies tumor development and progression affects immune cell function far beyond the borders of the primary tumor. In **chapter 4**, we studied how mammary tumor development affects the phenotype, transcriptome and function of T_{regs} in tumors, blood and distant organs. During tumorigenesis, T_{regs} become systemically activated and acquire enhanced immunosuppressive potential. Interestingly, RNAseq analysis of T_{regs} in distant organs of tumor-bearing mice revealed that T_{regs} in different organs uniquely adapt to mammary tumorigenesis. Targeting these tumor-educated T_{regs} limits metastatic spread to lymph nodes but not to lungs, demonstrating that T_{regs} support metastasis formation in a tissue-specific manner. Mechanistically, tumor-educated T_{regs} that reside in the lymph node niche, but not those of the lungs, can limit the activation of anti-metastatic NK cells. In line, we show that T_{regs} increase, while NK cells decrease, in sentinel lymph nodes of breast cancer patients compared with healthy controls. This study identifies T_{regs} as key regulators of lymph node metastasis in breast cancer, and reveals that neo-adjuvant targeting of T_{regs} in breast cancer may have therapeutic benefit. **Chapter 5** further highlights the importance of immune regulation in tissue tropism of metastasis from the angle of neutrophils, by discussing how cancer-cell derived Cathepsin C drives neutrophil accumulation in lungs, thereby promoting metastasis.

Therapeutic strategies aimed at engaging T cell-mediated anti-cancer immunity, such as immune checkpoint blockade (ICB) are transforming the treatment landscape of cancer. Because T_{regs} can highly express immune checkpoint molecules, it is important to understand how ICB influences T_{reg} biology, which is the focus of **Chapter 6**. As spontaneous mammary KEP tumors are therapeutically unresponsive towards the combination of anti-PD1/anti-CTLA4, this model allows the study of immunotherapy resistance mechanisms. ICB-treated mice are characterized by expansion of immunosuppressive T_{regs} in blood and tumors, while effector T cells remain unchanged. Depletion of T_{regs} in the context of ICB remodels the tumor

immune landscape into a more pro-inflammatory state, and unleashes the accumulation of activated $CD8^+$ T cells and NK cells in blood. Moreover, T_{reg} depletion during ICB extends metastasis-related survival, showing T_{regs} form a hurdle for the response to ICB.

Besides phenotypic characterisation, functional assays are helpful to study how cancer, tissue-context, or therapeutics impact the immunosuppressive potential of T_{regs}. **Chapter 7** details an experimental protocol that has been used throughout the thesis, which enables quantitative and reproducible assessment of T_{reg} function isolated from tumors and other organs.

Finally, **chapter 8** discusses the insights from this thesis in a broader perspective, and provides my thoughts on how to further advance our fundamental understanding of T_{reg} biology in cancer. Ultimately, this may contribute to the development of therapeutic applications aimed at bypassing tumor-supportive immunoregulatory mechanisms in breast cancer.

NEDERLANDSE SAMENVATTING

Het menselijk immuunsysteem is uitgerust met krachtige mechanismes die bescherming bieden tegen ziekteverwekkers, met het doel schade aan weefsels en organen te voorkomen. Deze mechanismes kunnen ingezet worden als verdediging tegen bedreigingen van buitenaf, zoals pathogene micro-organismen, maar ze bieden ook bescherming tegen een bedreiging die van binnenuit komt: kanker ontwikkeling. Kijkend naar de incidentie van kanker in onze huidige samenleving toont echter aan dat deze bescherming niet waterdicht is. Tumoren kunnen namelijk onder de druk van het immuunsysteem ontkomen. Een belangrijke reden hiervoor is dat kankercellen in essentie geen lichaamsvreemde cellen zijn. Wel hebben kankercellen, als gevolg van continue accumulatie van mutaties, eigenschappen verkregen die ze onderscheidt van gezonde cellen. Kankercellen balanceren daardoor op het randje van lichaamseigen en lichaamsvreemd. Dit bemoeilijkt de herkenning van kankercellen door het immuunsysteem, waarvoor een dreiging duidelijk geïdentificeerd moet kunnen worden als lichaamsvreemd (of immunogeen) om geactiveerd te kunnen raken. Naast dat tumoren slecht herkenbaar zijn, gebruiken ze ook actief andere middelen om immuun-gemedieerde uitroeiing te omzeilen. In het geval van overmatige of misplaatste activering van het immuunsysteem, treden regulatoire mechanismen in werking, die schade aan lichaamseigen weefsels en auto-immuun gerelateerde pathologie voorkomen. Steeds meer bewijs toont echter aan dat tumoren in staat zijn om deze immunoregulerende mechanismen te kapen, en daarmee anti-tumor immuunresponsen tegen primaire en gemetastaseerde kankers kunnen beperken.

Bij kankersoorten zoals borstkanker, kunnen signalen afkomstig van de tumor de infiltratie en ontstekingsremmende polarisatie van myeloïde en adaptieve immuuncellen teweeg brengen. Samen met lokale stromale- en tumorcellen, wordt zo een compact netwerk van immunosuppressie gevormd. Deze intratumorale immunosuppressie wordt gekenmerkt door expressie van immuunremmende receptoren, ontstekingsremmende cytokinen en andere immuunmodulerende factoren die het milieu van de tumor kunnen veranderen in een vijandige omgeving voor effectorcellen. Hiermee worden anti-tumor mechanismen geremd. Bovendien wordt het steeds duidelijker dat deze tumor-geassocieerde immunosuppressie niet beperkt is tot de primaire tumor zelf, maar ook buiten de grenzen van de tumor aanwezig is, wat de verspreiding van kankercellen faciliteert. Door ons begrip van immunoregulerende mechanismen die in borstkanker een rol spelen te vergroten, kunnen bestaande immunotherapieën worden verbeterd om immunosuppressie te omzeilen. Daarnaast kunnen nieuwe inzichten ook de ontwikkeling van nieuwe immunotherapieën stimuleren.

Een belangrijk celtype dat breed betrokken is bij het in goede banen leiden van immuun activatie zijn de regulatoire $FOXP3^{+}CD4^{+}$ T-cellen (T_{regs}). T_{regs} zijn uitgerust met een divers

arsenaal aan immunosuppressieve mechanismen. Een vermindering in aantal- of functie van T_{regs} in het lichaam staat aan de basis van een breed scala aan auto-immuunziekten, terwijl T_{regs} tijdens kanker belangrijke bondgenoten zijn van tumoren, omdat de immunosuppressieve functie van T_{regs} kan worden gericht tegen anti-tumorimmuniteit. Het werk beschreven in dit proefschrift onderzoekt de complexe relatie van T_{regs} met primaire en gemetastaseerde borstkanker, met behulp van geavanceerde muismodellen die de ontwikkeling en progressie van slecht immunogene tumoren nabootsen. **Hoofdstuk 2** geeft eerst overzicht van de vooruitgang van de afgelopen jaren over ons begrip van T_{regs} in (menselijke) borstkanker, en bespreekt vanuit welke therapeutische invalshoek T_{regs} nuttig kunnen zijn.

$FOXP3^+$ T_{regs} ontwikkelen zich voornamelijk in de thymus, maar kunnen ook in andere weefsels ontstaan door TGF-β-gemedieerde differentiatie van conventionele $CD4^+$ T-cellen. Deze perifere T_{regs} (pT_{regs}) verwerven FOXP3 expressie en immunosuppressieve activiteit, in een proces dat 'perifere conversie' wordt genoemd. Of, en door welke mechanismen, pT_{regs} accumuleren in borsttumoren is echter grotendeels onbekend. Onderzoek in **hoofdstuk 3** toont aan dat de tumor-geassocieerde macrofagen (TAMs), dit zijn de meeste voorkomende immuuncellen in spontane borsttumoren, een sleutelrol spelen in de accumulatie van pT_{regs} in tumoren. Dit wordt gedeeltelijk gemedieerd door TGF-β dat wordt afgegeven door TAMs. Daarnaast laten we zien dat zien TAMs PD-1-expressie induceren op intratumorale conventionele $CD4^+$ T-cellen, wat als voorbereiding dient op de intratumorale differentiatie in pT_{regs}.

Het lokale milieu van de tumor heeft een belangrijke invloed op het fenotype en de functie van intratumorale immuuncellen. Daarnaast kan de systemische ontsteking die gepaard gaat met tumorontwikkeling en -progressie de functie van immuuncellen tot ver buiten de grenzen van de primaire tumor beïnvloeden. In **hoofdstuk 4** hebben we onderzocht hoe de ontwikkeling van borsttumoren het fenotype, de genexpressie, en de functie van T_{regs} kan beïnvloeden. Naast tumoren, hebben we dit onderzocht in bloed en organen die vatbaar zijn voor metastase ontwikkeling. Dit toonde aan dat T_{regs} tijdens de ontwikkeling van borsttumoren systemisch worden geactiveerd, en daarmee nog immunosuppresiever. Daarnaast onthulde RNAseq-analyse dat T_{regs} in verschillende organen zich op unieke wijze aanpassen aan borsttumor ontwikkeling. Het depleteren van deze tumor-opgeleide T_{regs} beperkte de uitzaaiing van kankercellen specifiek naar lymfeklieren, maar niet naar longen. Hiermee werd duidelijk dat de rol van T_{regs} voor metastasevorming per weefsel kan verschillen. Mechanistisch onderzoek toonde aan dat tumor-opgeleide T_{regs} die zich in de lymfeklieren bevinden de activering van anti-tumor NK cellen kunnen remmen, terwijl T_{regs} in longen geen functionele invloed uitoefenen op NK cellen. Consistent met onze pre-klinische data ontdekten we dat T_{regs} toenemen in de schildwachtklier van borstkanker patiënten, terwijl NK cellen afnemen, in vergelijking met lymfeknopen van gezonde personen. Deze studie laat zien dat T_{regs} een belangrijke rol spelen bij de ontwikkeling van lymfekliermetastase bij

borstkanker, en onthult dat neoadjuvante targeting van T_{regs} bij borstkanker therapeutisch voordeel kan hebben. Het belang van immuunregulatie voor de uitzaaiing van kanker naar verschillende organen wordt verder benadrukt in **hoofdstuk 5**. Hier wordt beschreven dat borstkankercellen Cathepsine C aanmaken. Dit veroorzaakt de accumulatie van neutrofielen in de longen van tumor-dragende muizen, wat lokaal de vorming van metastasen bevordert. Therapeutische strategieën die gericht zijn op het activeren van T-cellen tegen kanker, zoals immuuncheckpoint blokkade (ICB), revolutioneren de behandeling van kanker. Omdat T_{regs} immuuncheckpoint-moleculen in hoge mate tot expressie kunnen brengen, is het ook belangrijk om te begrijpen hoe ICB T_{regs} beïnvloed. Dit is de focus van **hoofdstuk 6**. Omdat spontane tumoren van het KEP model niet reageren op de combinatie van anti-PD1/anti-CTLA4, is het mogelijk dit model te gebruiken om onderzoeken hoe resistentie tegen ICB ontstaat. We ontdekten dat muizen behandeld met ICB worden gekenmerkt door expansie van immunosuppressieve T_{regs} in bloed en tumoren, terwijl effector-T-cellen onveranderd blijven. Depletie van T_{regs} tijdens ICB induceert inflammatie in tumoren, en ontketent de accumulatie van geactiveerde $CD8^+$ T-cellen en NK-cellen in het bloed. Bovendien verlengt de depletie van T_{regs} tijdens ICB de overleving van muizen met metastase ontwikkeling, wat aantoont dat T_{regs} een hindernis vormen voor een gewenste reactie op ICB.

Naast fenotypische karakterisering, zijn functionele testen nuttig om te bestuderen hoe kanker, weefselcontext of therapieën het immunosuppressieve karakter van T_{regs} beïnvloeden. **Hoofdstuk 7** beschrijft een experimenteel protocol dat in het proefschrift is gebruikt. Dit protocol maakt het mogelijk om kwantitatief en reproduceerbaar de functie van tumor-geassocieerde T_{regs} te beoordelen.

Ten slotte worden in **hoofdstuk 8** de inzichten uit dit proefschrift in een breder perspectief besproken en geef ik mijn gedachten over hoe we ons fundamentele begrip van T_{reg}-biologie bij kanker nog verder kunnen vergroten. Uiteindelijk kan dit bijdragen aan de ontwikkeling van therapeutische toepassingen die gericht zijn op het omzeilen van immuunregulerende mechanismen bij borstkanker.

CURRICULUM VITAE

Kevin Kos was born in Blaricum on the 12th of February, 1993. In 2011, he obtained his university preparatory education degree, majoring Nature & Health at Ergooiers College Huizen. The same year, he started the bachelor Biomedical Sciences at Vrije Universiteit Amsterdam. He graduated in 2014 with a research thesis describing the impact of a fungal-microbial interaction on caries development, performed in the laboratory of Dr. Bastiaan Krom, department of Preventive Dentistry, ACTA, Amsterdam. In 2014 he enrolled in the Oncology reseach Master's Programme, VUmc, Amsterdam, from which he graduated *cum laude* in 2016. During this track, he performed his minor research internship in the lab of Prof. Dr. Emile Voest, looking into mechanisms of fatty-acid mediated chemoresistance, under supervision of Dr. Julia Houthuijzen. Research for his master Thesis was performed in the laboratory of Prof. Dr. Mark Smyth in the QIMR Berghofer research institute, Brisbane, Australia. Under supervision of Dr. Eva Putz, he studied the importance of heparanase for the tumor invasion of NK cells. In preparation for his PhD research starting in 2016, he wrote a research proposal in collaboration with (the lab of) Prof. Dr. Karin de Visser, Department of Immunology and Tumor Biology, Netherlands Cancer Institute, Amsterdam, on the elusive role of regulatory T cells in breast cancer. The proposal was awarded with the NWO-OOA Diamond Grant, enabling him to fund and carry out his designed research proposal under supervision of Prof. Dr. Karin de Visser. The major findings of this project are described in this Thesis.

ACKNOWLEDGMENTS

Research is teamwork, and can only progress through discoveries that build on previous discoveries: metaphorically known as standing on the shoulders of giants. Throughout my PhD, I was very fortunate to stand on the shoulders of many such giants, who have been of critical importance in the making of this thesis, and to whom I would like to express my gratitude.

Karin, although T_{regs} may have been the odd one out in your lab at first, I could not have imagined a better mentor or environment, due to your endless support, enthusiasm and positivity. Your mentality of putting sound, thorough and relevant science above everything have shaped me as a scientist for which I am very grateful, and I will not forget: the data are the data.

Jannie, I feel honoured to have you as my co-promotor, and to have learnt from your inspiring views on immunology.

My paranymphs: Max, the spindoctor of immunology: good data is fantastic data, and bad data are opportunities. To say I enjoyed our (scientific) discussions is an understatement, but most importantly: thank you for the gentle nudges to actually put the ideas into practice. Danique: science is serious business but your bubbly presence makes it a lot more fun: I very much enjoyed working and laughing side by side to you in the lab. I'm looking forward to visit you in Limburg.

The (post-covid) north office: Tisee & Kim: If it wasn't for your help, I think I would still be doing transplantations at T2 today. Thank you for all the help, laughs and inevitable baby talk over the years: I am much better prepared now. Hannah: Anyone who thinks they are an immunologist should have a chat with you to verify that first. Thank you for letting me pick your razorsharp mind, and introducing me into the weird world of yolk-sac macrophages.

My PhD-student contemporaries: Mark, with whom I could share the pleasures and troubles of working on T_{regs}, you are a fantastic scientist and let no one tell you otherwise. Elselien, thank you for your mental support during the project: you are also almost there! Aldo: I think the B3/H3 merge was a great success, and am happy to have worked alongside you. I hope your aspiration of becoming a USA postdoc come true. Olga: we've brainstormed a lot of immunology (experiments) together, which was very inspiring and helpful. Thank you very much for collaborating on the T_{reg}-project.

My fantastic K-Fish colleagues, old and new: Camilla & Riccardo (yes), Anni, Lisanne, Daphne, Claudia, Antoinette, Noor, Quinte, Denize, Ewald, and all other colleagues who

have made the NKI a place to remember: Daniel, Alessandra, Ronak, Frank, Thomas, Bente, Chantal, Marleen, Camiel, Karin, Serena, Luuk, Marnix, Shanna, Christel, Jeremi, Leonie, Nika, Ziva, Salo, Julia, Lisette, Henri, Krijn, Maarten, Anne, Mirjam, Kaspar, Maaike & Sjoerd. It was a pleasure to work with all of you. Thank you for all the good times.

A big thanks to members of the B3, C2 and B6 departments, for exciting work discussions on immunology and breast cancer research, and all the inspiring PI's I had the pleasure to learn from: Leila, Hein, Heinz, Jacco, Emile, Marleen & Jos.

Lorenzo: my apologies for disturbing your valuable night's rest. Thank you for keeping me sane until the end.

Muhammad: Thank you for your valuable contributions to the project(s), I very much enjoyed our collaboration.

Sander: the T_{reg} master: Your tips and ideas have been very valuable to the early days of the project.

Paul: thank you for being a fantastic lab manager, and introducing me into the amazing world of birding.

Martijn, Frank, Anita, Debajit & Guido: you guys make flow cytometry look easy: thank you for all the help.

Q, Reinier, Knaag (the pinnacle of relaxation), Jort & Marnix: you taught me there is a time for science, and a time for anything else. Thank you for your dear friendships.

Papa, Mama & Danielle: bedankt voor jullie nuchtere kijk op de zaak, oprechte interesse en onvoorwaardelijke steun. De microscoop als cadeau heeft z'n vruchten afgeworpen. Opa, je hebt er even op moeten wachten, maar eindelijk is het dan zover. Nu kunnen we de S echt schrappen. Hans & Ria, Vera & Xander, naast een dochter/zus, ook nog een schoonzoon/zwager in een PhD traject. Gelukkig houden jullie altijd het hoofd koel. Veel dank voor alle support.

Mona: has sido un gran apoyo durante todo el proyecto. Te traeré una lata de atún.

Wietske: mijn lieve bloem. Partners in science en in de liefde. Woorden schieten (letterlijk) tekort om het geluk dat ik op B3 met jou heb gevonden hier te omschrijven. Ik ben er heel dankbaar voor, en kijk uit naar de toekomst samen.

PUBLICATIONS

Macrophages promote intratumoral conversion of conventional CD4⁺ T cells into regulatory T cells via PD-1 signalling.
Kevin Kos, Camilla Salvagno, Max D. Wellenstein, Denize A. Meijer, Cheei-Sing Hau, Kim Vrijland, Daphne Kaldenbach, Elisabeth A.M. Raeven, Martina Schmittnaegel, Carola Ries, Karin E. de Visser.
Oncoimmunology, Apr 2022, 11(1)

Tumor-educated T_{regs} drive organ-specific metastasis in breast cancer by impairing NK cells in the lymph node niche.
Kevin Kos, Muhammad Aslam, Rieneke van de Ven, Max D. Wellenstein, Wietske Pieters, Antoinette van Weverwijk, Danique E.M Duits, Kim van Pul, Cheei-Sing Hau, Kim Vrijland, Daphne Kaldenbach, Elisabeth A.M. Raeven, Sergio A. Quezada, Rudi Beyaert, Heinz Jacobs, Tanja D. de Gruijl, Karin E. de Visser.
Cell Reports 2022 Mar 1;38(9):110447

Pro-mutagenic Effects of the Gut Microbiota in a Lynch syndrome Mouse Model
Wietske Pieters, Floor Hugenholtz, Kevin Kos, Maxime Cammeraat, Teddy C. Moliej, Daphne Kaldenbach, Sjoerd Klarenbeek, Mark Davids, Lisa Drost, Charlotte de Konink, Elly Delzenne-Goette, Karin de Visser, Hein te Riele.
Gut Microbes, Jan-Dec 2022;14(1):2035660.

Neutrophils create a fertile soil for metastasis.
Kevin Kos, Karin E. de Visser.
Cancer Cell, 2021 Mar 8;39(3):301-303

The Multifaceted Role of Regulatory T Cells in Breast Cancer.
Kevin Kos**,** Karin E. de Visser.
Annual Review of Cancer Biology. 2021 Mar;5:291-310

Flow cytometry-based isolation of tumor-associated regulatory T cells and assessment of their suppressive potential.
Kevin Kos, Martijn van Baalen, Denize A. Meijer, Karin E. de Visser.
Methods in Enzymology. 2020;632:259-281.

Therapeutic targeting of macrophages enhances chemotherapy efficacy by unleashing type I interferon response.
Camilla Salvagno, Metamia Ciampricotti, Sander Tuit, Cheei-Sing Hau, Antoinette van Weverwijk, Seth Coffelt, Kelly Kersten, Kim Vrijland, Kevin Kos, Thomas Ulas, Ji-Ying Song, Chia-Huey Ooi, Dominik Rüttinger, Philippe A. Cassier, Jos Jonkers, Joachim L. Schultze, Carola Ries, Karin E. de Visser.
Nature Cell Biology. 2019 Apr;21(4):511-521.

NK cell heparanase controls tumor invasion and immune surveillance.
Eva M. Putz, Alyce J. Mayfosh, Kevin Kos, Deborah S. Barkauskas, Kyohei Nakamura, Liam Town, Katharine J. Goodall, Dean Y. Yee, Ivan K. Poon, Nikola Baschuk, Fernando Souza-Fonseca-Guimaraes, Mark D. Hulett, Mark J. Smyth.
Journal of Clinical Investigation. 2017 Jun 30;127(7):2777-2788.

Targeting cytokine signaling checkpoint CIS activates NK cells to protect from tumor initiation and metastasis.
Eva M. Putz, Camille Guillerey, Kevin Kos, Kimberley Stannard, Kim Miles, Rebecca B. Delconte, Kazuyoshi Takeda, Sandra E. Nicholson, Nicholas D. Huntington, Mark J. Smyth
Oncoimmunology. 2017 Feb 7;6(2):e1267892.

***Candida albicans* in oral biofilms could prevent caries.**
Hubertine M. Willems*, Kevin Kos*, Mary Ann Jabra-Rizk, Bastiaan P. Krom.
*These authors contributed equally
Pathogens and Disease, 2016, 74.

PHD PORTFOLIO

Courses and Workshops

2016 Basic Course on R, Erasmus MC, Rotterdam, The Netherlands

2017 Ethics and Integrity in Science, NKI, The Netherlands

2018 How to be(come) a successful grant applicant, VUmc, Amsterdam, The Netherlands

2019 Clinical Internship, NKI, Amsterdam, The Netherlands

2019 Qlucore hands on training, VUmc Amsterdam, The Netherlands

2021 Digital Career Event workshops Amsterdam UMC
- The science of job searching
- Welcome to the outside world

2021 BCF Career Event Workshops
- How to Present Your Best Self for Interviews or Promotions
- Job application tips
- CV building

Conferences attended

2016 'The complexity of tumor-host immune interactions', LUMC TIMMC symposium, Leiden, The Netherlands

2017 Understanding Tumour Immunology', **Poster**, Beatson Institute, Glasgow, Scotland

2017 'New Horizons in Cancer Research', CGC annual meeting KIT, Amsterdam, The Netherlands

2018 Oncode Institute Launch, Amsterdam, The Netherlands

2018 International PhD Student Cancer Conference, **Poster,** Francis Crick Institute, London, UK

2018 25th Biennial Congress of the EACR, **Poster**, Amsterdam, The Netherlands

2018 'Horizons of Cancer Biology', **Poster**, ISREC-SCCL Symposium, Lausanne, Switzerland

2019 Oncode Annual Scientific meeting, Amsterdam, The Netherlands

2019 'Uncovering Mechanisms of Immune-Based Therapy in Cancer and Autoimmunity', **Poster**,
Keystone Symposium, Breckenridge, USA

2019 International PhD Student Cancer Conference, **Chair,** NKI Amsterdam, The Netherlands

2020 Oncode Tumour microenvironment and Immunology meeting, **Speaker**, Veenendaal, The Netherlands

2021 'Defense is the best Attack: EACR Immuno-Oncology Breakthroughs', **Speaker**, online event

2021 Oncode-CGC Annual Scientific Meeting, Speaker, Utrecht, The Netherlands

Retreat participation

2017-2018 Annual OOA graduate student retreat, **Poster/Speaker/Chair**, Renesse, The Netherlands

2016-2019 C2 department Retreat, **Poster/Speaker**, Egmond, The Netherlands

2018 KDV Lab retreat, **Speaker**, Middelburg, The Netherlands

Organising Committee

2019 International PhD Student Cancer Conference, NKI Amsterdam, The Netherlands

2017-2022 B3 'Happiness' Committee

Supervision of Students

2019 Supervision 2nd year master student Biomedical Sciences UvA, Denize A. Meijer